

Universiteit
Leiden
The Netherlands

# Diagnostic and intraoperative targeted molecular imaging for pancreatic cancer

Tummers, W.S.F.J.

**Citation**
Tummers, W. S. F. J. (2018, November 13). *Diagnostic and intraoperative targeted molecular imaging for pancreatic cancer*. Retrieved from https://hdl.handle.net/1887/66717

| | |
|---|---|
| Version: | Not Applicable (or Unknown) |
| License: | Licence agreement concerning inclusion of doctoral thesis in the Institutional Repository of the University of Leiden |
| Downloaded from: | https://hdl.handle.net/1887/66717 |

**Note:** To cite this publication please use the final published version (if applicable).

Cover Page



Universiteit Leiden




The handle http://hdl.handle.net/1887/66717 holds various files of this Leiden University dissertation.

**Author**: Tummers, W.S.F.J.
**Title**: Diagnostic and intraoperative targeted molecular imaging for pancreatic cancer
**Issue Date**: 2018-11-13

# Diagnostic and Intraoperative Targeted Molecular Imaging for Pancreatic Cancer

Willemieke Tummers

# Diagnostic and Intraoperative Targeted Molecular Imaging for Pancreatic Cancer

Willemieke Tummers

© W.S.F.J. Tummers 2018

ISBN: 978-94-6332-404-5

Lay-out: Selma Hoitink, persoonlijkproefschrift.nl
Printing: GVO Drukkers & Vormgevers

All rights reserved. No parts of this thesis may be reproduced, distributed, stored in a retrieval system or transmitted in any form or by any means, without prior written permission of the author.

The research in this thesis was financially supported by Dutch Cancer Society, Stanford Cancer Institute Translational Research Grant, Intuitive Surgical Clinical Robotics Research Grant. Michaël-van Vloten Fonds, Lisa Waller Hayes Foundation, Jo Kolk Studiefonds, McKinsey Grant, and Ketel1 Studiefonds.

Financial support by Intuitive Surgical, Inc. LI-COR Biosciences, Surgvision, Quest Medical Imaging, LUMC, MSB Gouda, Chipsoft, Curadel, Groene Hart Ziekenhuis for the printing of this thesis is gratefully acknowledged.

# Diagnostic and Intraoperative Targeted Molecular Imaging for Pancreatic Cancer

Proefschrift

ter verkrijging van
de graad van Doctor aan de Universiteit Leiden,
op gezag van Rector Magnificus prof.mr. C.J.J.M. Stolker,
volgens besluit van het College voor Promoties
te verdedigen op dinsdag 13 november 2018
klokke 15:00 uur

door

Willemieke Suzanne Fokje Josephine Tummers

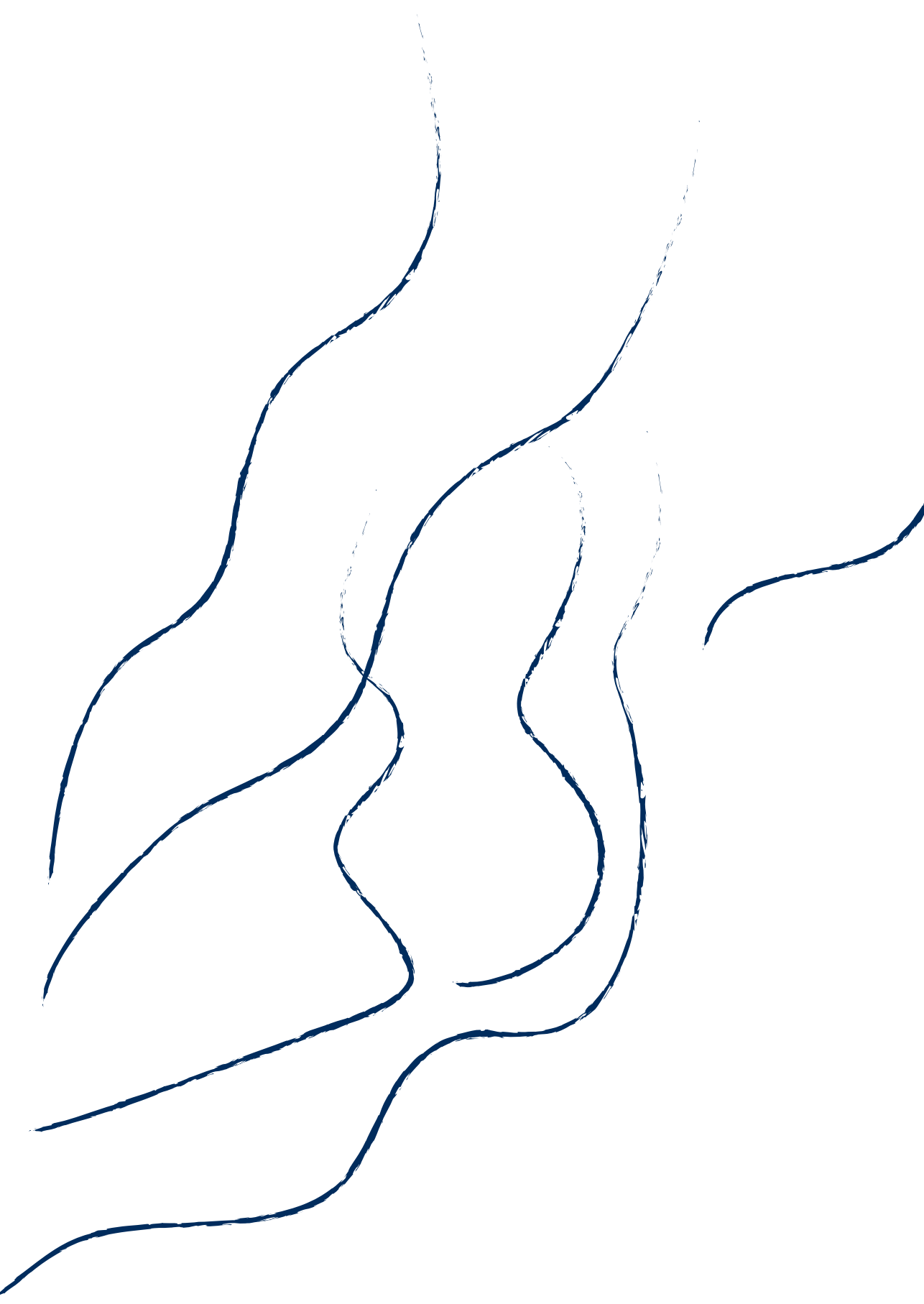
geboren te Enschede

in 1989

| | |
|---|---|
| **Promotor** | Prof. dr. C.J.H. van de Velde |
| **Co-promotores** | Dr. A.L. Vahrmeijer<br>Dr. R.J. Swijnenburg |
| **Leden promotiecommissie** | Prof. dr. J. Burggraaf<br>Prof. dr. L.F. de Geus-Oei<br>Prof. dr. C.H.J. van Eijck (Erasmus MC, Rotterdam)<br>Prof. dr. S.S. Gambhir (Stanford University, United States) |

# TABLE OF CONTENTS


| | | |
|---|---|---|
| **Chapter 1** | Introduction and thesis outline | *7* |
| **Part I: Development of Targeted Molecular Imaging for Pancreatic Cancer** | | |
| **Chapter 2** | Advances in Diagnostic and Intraoperative Molecular Imaging of Pancreatic Cancer | *19* |
| **Chapter 3** | Tumor characteristics and surgical technical aspects of R1 in pancreatic cancer surgery | *55* |
| **Chapter 4** | Selection of optimal molecular targets for tumor-specific imaging in pancreatic ductal adenocarcinoma | *77* |
| **Part II: Validation of Targeted Molecular Imaging for Pancreatic Cancer** | | |
| **Chapter 5** | Preclinical development and validation of multimodal probe for the tumor-specific imaging of pancreatic cancer | *103* |
| **Chapter 6** | On-target probes for early detection | *127* |
| **Part III: Clinical Translation of Targeted Molecular Imaging** | | |
| **Chapter 7** | Regulatory Aspects of Optical Methods and Exogenous Targets for Cancer Detection | *137* |
| **Chapter 8** | Guide for Successful Clinical Translation of Optical Imaging Agents for Molecular Imaging | *167* |
| **Part IV: Clinical Application of Targeted Molecular Imaging for Pancreatic Cancer** | | |
| **Chapter 9** | Clinical Translation of Integrin αvβ6 Cystine Knot Positron Emission Tomography (PET) Tracers | *203* |
| **Chapter 10** | Intraoperative Pancreatic Cancer Detection Using Tumor-Specific Multimodality Molecular Imaging | *219* |
| **Chapter 11** | Detection of Visually Occult Metastatic Lymph Nodes Using Molecularly Targeted Fluorescent Imaging During Surgical Resection of Pancreatic Cancer | *237* |
| **Part V: Future Directions for Targeted Molecular Imaging** | | |
| **Chapter 12** | Recommendations for reporting on emerging optical imaging agents to promote clinical approval | *257* |
| **Chapter 13** | General discussion and future perspectives | *283* |
| **Appendices** | Summary<br>Nederlandse samenvatting<br>List of publications<br>Curriculum Vitae<br>Dankwoord | *295* |



Chapter | 1

# Introduction and thesis outline

# INTRODUCTION AND THESIS OUTLINE

## General

The treatment of disease has changed over the last decennia from population-based treatments to personalized medicine, with no exception to cancer therapy. The focus on personalized treatment in oncology is mainly based on our growing understanding of the pathophysiology of cancer. Molecular imaging has played a major role in this. Molecular imaging can be defined by the noninvasive, real-time visualization of biochemical events at the cellular and molecular level within living cells, tissues, and/or intact subjects.[1] Molecular imaging can be performed in patients during the entire treatment process, with the potential to provide a movie of the patient's disease instead of separate snap-shots. In the diseased state, one can choose to image chemical processes in the body or a target of interest, such as a cell surface receptor. The form of molecular imaging that is currently widely applied, is positron emission tomography using fluor-18-deoxyglucose (FDG-PET), where areas of the body with increased uptake of glucose are highlighted.

The use of molecular imaging could potentially improve the accuracy of cancer detection especially when combined with conventional imaging modalities such as ultrasound and CT, by improving sensitivity and specificity. When performing tissue-specific molecular imaging with a highly specific target and a sensitive imaging system, one should be able to see all involved lesions, even micrometastases. One of the cancer types that is in great need of improved detection and treatment is pancreatic cancer. Pancreatic cancer has a dismal prognosis due to late onset of symptoms and therefore most patients present with advanced stage of disease, resulting in less than 30% of patients to undergo a potentially curative surgical resection. Of those patients, the rate of irradical resections is high, mainly due to invisible tumor boundaries due to the perineural and perivascular growth pattern of the tumor. The most commonly performed surgical procedure for pancreatic cancer is the pylorus-preserving pancreatico-duodenectomy or the classic Whipple procedure. This surgery has a high morbidity with a long recovery period. Since the life expectancy of this disease is low, even after surgery, there is a high need to select only those patients for surgery that will actually benefit from a resection. This highlights the need for a tool able to detect this disease earlier, to properly stratify patients for the optimal primary treatment modality, either surgery

or neoadjuvant chemo- and/or radiotherapy, and in addition, improve results during the actual surgical resection. Tumor-specific molecular imaging has the potential do to this.

## Molecular imaging techniques



Molecular imaging can be done in the diagnostic process in the form of tumor-specific PET imaging, or during surgery using near-infrared fluorescence (NIRF) and photoacoustics. Fluorescence imaging is based on adding an exogenous contrast agent (a fluorophore) into the patient that can create contrast to the dark background, and permits detection of the desired tissue of interest in the surgical field.[2] Fluorescence light in the near-infrared window (NIR) (700-900 nm) has the advantage over visible light in several ways. First, there is an increased depth penetration and decreased autofluorescence compared to light in the visible range since NIR light is impaired by absorbance and scatter. This results in a depth penetration of around 5-8 mm in tissue. Second, since tissue has almost no light excitation in the NIR range, the signal-to-background contrast can be maximized in this range. Lastly, NIR light is invisible for the human eye, and therefore, it will not change the surgical field.[3] This requires specialized cameras that can make the light visible for the surgeon on a screen.[4] The advantage of fluorescence imaging is that it can be used during open and minimally invasive surgery, such as laparoscopy and robotic surgery, depending on the used camera. Currently, there are several cameras that can be used for this purpose. The difficulty of developing a camera is the high dependency on an available imaging agent and vice versa. Choosing the right combination will determine the success of both the agent and the camera, since the failure of an agent to identify tumor in a specific manner could be due to agent failure of because the camera was not sensitive enough to detect the signal.[5]

As described above, NIRF imaging is superior for the detection of superficial lesions < 8 mm of depth. However, to improve the rate of radical resections in pancreatic cancer surgery, a depth of around 5 cm needs to be achieved, since the deep vascular margin is mainly affected. Photoacoustic imaging is based on ultrasound and uses the “light in, sound out”- principle. This technique can image at clinically relevant depths (up to 5 cm). The conversion of light to sound is called the photoacoustic effect, being introduced first by Alexander Graham Bell in 1881.[6] In photoacoustic imaging, tissue absorbs pulsed laser light and emanates ultrasound waves as a result of transient thermoelastic expansion.

Because photoacoustic imaging relies on light only one-way and detection is based on sound waves, deeper tissue penetration is possible. Resulting in two to three orders of magnitude weaker ultrasound scattering than optical scattering in tissue.[7] The key strengths of PAI are its ability to collect functional and molecular information from most tissues, and the high spatial resolution, without the use of non-ionizing radiation.[8]

## Imaging agents

Both for NIRF imaging and photoacoustic imaging, fluorescent dyes are needed to enhance the optical signal. Currently, extensive experience is obtained with the non-specific fluorescent dyes indocyanine green (ICG) and methylene blue (MB). These dyes are approved by the U.S. Food and Drug Administration (FDA) for perfusion imaging, and are proven safe. Therefore, these agents were prefect candidates for off-label use in the first fluorescent imaging studies. When injected intravenously these agents migrate to the tumor using the enhanced permeability and retention (EPR) effect of neovasculature. The dye leaks to the tumor due to low interstitial pressure in the tumor microenvironment and is retained there. This method works well for hypervascular tumors, but it is well-known that pancreatic cancer is hypovascular, has minimal leaky vessels and almost no EPR effect. This is also shown in a study of Hutteman et al. were ICG was used to image pancreatic cancer, without successful tumor demarcation.[9]

Based on the variable results obtained with the non-specific agents, the field changed to developing tumor-specific agents, targeting a specific feature of the tumor or it's microenvironment. These targeted agents consist of a targeting ligand and a signalling moiety. This signalling moiety can either be a fluorescent or photoacoustic dye, or a radionuclide in case of PET imaging. Over the last years, tremendous amounts of literature have been published describing the development and preclinical validation of these novel agents. However, only a few of these agents make it into clinical trials and show successful results. This is mainly due to the extensive approval process to perform clinical trials with new agents, and because preclinical results are hard to translate to the human situation. Currently, a few successful first-in-human trials are conducted for tumor-specific intraoperative imaging with targeted agents in ovarian, and colon cancer.[10-13]

Potentially, molecular imaging in pancreatic cancer could be successful when using a tumor-specific targeted agent, in contrast to the unsuccessful attempt seen with the non-specific ICG. There has been scepsis in the field on whether or not this imaging technique would work for pancreatic cancer. Pancreatic carcinomas have a the dense stroma surrounding the tumor, which could potentially prevent imaging tracers from actually reaching their tumor cell targets. This has been put forward as an explanation for the unpromising results with targeted antibody therapy in pancreatic cancer.[14] In this thesis, we describe the first results and show proof of tumor penetration by tumor-specific imaging agents.

There is a large range of potential targeting ligands, such as small molecules, peptides, aptamers, antibodies, engineered protein fragments, nanoparticles, or micro-sized contrast agent. Each of these types of agents are different in size and thus possesses different pharmacokinetic characteristics. In this thesis, tumor-specific imaging of pancreatic cancer is performed using both an antibody and a peptide, showing the different characteristics of these agents, and their respective advantages.

### Imaging targets for pancreatic cancer imaging

For molecular imaging to be of an additional value in detection and treatment of pancreatic cancer, a highly specific imaging signal is needed. In the case of pancreatic cancer, in order to achieve a high tumor-to-background ratio, one needs to identify a target that is only present on pancreatic cancer, and not or in minimal amount on chronic pancreatitis and/or the surrounding unaffected pancreatic tissue For imaging purposes, the ideal target is a cellular-membrane receptor that is also present in tumor-positive lymph nodes and retains expression in vital tumor cells after neoadjuvant therapy. In this thesis several targets for pancreatic cancer are described, together with the advantages and disadvantages. Important to notice is that, at least, at this point there is no optimal biomarker for pancreatic cancer imaging which also ensures all of the above described features. An agent, or multiple agents, directed against more targets, also known as multiplexing, would probably be ideal. However, at this point the process to receive FDA approval for one novel agent is challenging, since no precedent is available yet. Therefore, a situation where one can inject multiple novel imaging agents into one patient will probably not be realized in the near future.

The experimental parts of this thesis focus on two targets, namely integrin alpha$_v$beta$_6$ (αvβ6) and the epidermal growth factor receptor (EGFR). For now, integrin αvβ6 seems to be the most promising target of the two, due to the low expression in chronic pancreatitis, and the high and homogenous expression in tumor, tumor-positive lymph nodes, and retained expression after neoadjuvant therapy. A disadvantage of this target is that expression in chronic pancreatitis and normal pancreatic tissue is not completely absent, due to very low expression in the normal ductal tissue. Other promising targets that are mentioned in this thesis, but not further studied are CEA,[12,13] and uPAR. The advantage of uPAR is that it is not only present on the tumor tissue, but also on the tumor microenvironment, which is abundantly expressed in pancreatic cancer. A disadvantage is that abundant stroma is also present on chronic pancreatitis, making it harder to differentiate between the two entities.

## Translation from molecule to man

As described above, one of the most challenging aspect of this research is the translation of results generated in the preclinical setting to the clinic. A large amount of the conducted research will not even make it to this stage and will therefore not directly benefit the patient. For this thesis, a unique collaboration was put into place between Stanford University Medical School, the LUMC and the Center for Human Drug Research (CHDR), to ensure an optimal roadmap for promising preclinical agents to make it into the clinic. All of the partners have their unique knowledge and experience, providing the possibility to develop a roadmap from molecule to man. The Gambhir Lab at Stanford University is world-leader in the development and preclinical validation of novel targeted imaging agents. The CHDR on the other hand has the unique position to perform first-in-human studies in a safe and controlled environment, and the Image-Guided Surgery Group at LUMC has the most experience in conducting oncologic trials with fluorescence guided surgery.

## Regulatory aspects

One of the main struggles to get a novel imaging agent into the clinic in the USA are the regulatory aspects set by the FDA. To be able to request for a new drug application (NDA), large clinical trials are needed, and patient benefit needs to be shown. These trials are costly, and clinically relevant and objective endpoints are hard to reach with imaging studies. Especially the costs of these large trials make it impossible for an academic partner to pursue this alone. In addition,

industry partners are less willing to participate since the expected profit of imaging agents is minimal, compared to the development of pharmaceuticals. Another problem is that the FDA sees these agents as diagnostics agents, which means that no adverse events are allowed. However, the field argues that some minor grade I-II adverse events should be allowed, since these agents are used in oncologic patients that generally have a worst prognosis compared to the general population. Another challenge for approval is that at this point no real precedence exists for the products used in tumor-specific optical imaging (e.g. camera's and imaging agents). For optical imaging systems this is challenging, because this makes it hard to get 510(k) approval based on equal performances compared to predicate devices.

## THESIS OUTLINE

The thesis consists of five parts describing the entire process from development of tumor-specific molecular imaging for pancreatic cancer to the clinical application and future directions of this novel method for cancer detection in general and in specific for pancreatic cancer. **Part 1** focuses on the development of targeted molecular imaging for pancreatic cancer. **Part 2** describes the validation of this technique in preclinical setting. **Part 3** focusses on the clinical translation of targeted molecular imaging in general, and **part 4** describes the first-in-human clinical use of tumor-specific imaging agents in pancreatic cancer patients. **Part 5** provides an introduction into the future directions of targeted molecular imaging in general and for pancreatic cancer specific.

**Chapter 2** introduces tumor-specific molecular imaging to improve both diagnostics and intra-operative management of pancreatic cancer. It summarizes the current data available, explains the need to push this field forward, and describes promising novel studies. **Chapter 3** shows the results of a retrospective study on the outcome of pancreatic cancer patients, especially focusing on the effect of tumor margin-positive (R1) resection, and indicates where tumor-specific imaging can make a difference. **Chapter 4** summarizes on optimal molecular targets to detect pancreatic cancer, based on an immunohistochemistry study. In part 2, the achieved results of part 1 are used to translate the use of targeted imaging from *ex vivo* experiments to preclinical setting. **Chapter 5** shows the preclinical validation of a novel fluorescent imaging agent, targeting αvβ6, in

preclinical pancreatic cancer models. **Chapter 6** focusses on different targeted imaging agents and methods to enhance imaging signal for early detection of cancer. In part two the possibility to use targeted imaging in pancreatic cancer in preclinical setting is shown. To be able to translate these promising preclinical results into humans, several crucial steps need to be taken, which are discussed in part 3. **Chapter 7** describes the regulatory aspects to achieve approval for the use of both imaging systems and imaging agents. **Chapter 8** provides an overview for the successful clinical translation of optical imaging agents. In part 4, the clinical use of targeted molecular imaging in pancreatic cancer patients is shown for the first time describing several first-in-human studies. **Chapter 9** describes the results of the clinical translation of targeted PET tracers for pancreatic cancer imaging. **Chapter 10** shows the results of intra-operative identification of pancreatic cancer using fluorescently labelled cetuximab. **Chapter 11** focuses on the detection of visually occult tumor-positive lymph nodes using molecularly targeted fluorescent imaging during surgical resection. Lastly, part 5 provides an insight into the future of this technique and discusses the steps needed to make this a widely used technique in the future. **Chapter 12** describes the need to develop a standardized method in assessing agents for fluorescence-guided surgery. And in **Chapter 13**, a general discussion is provided and the future perspectives are discussed.

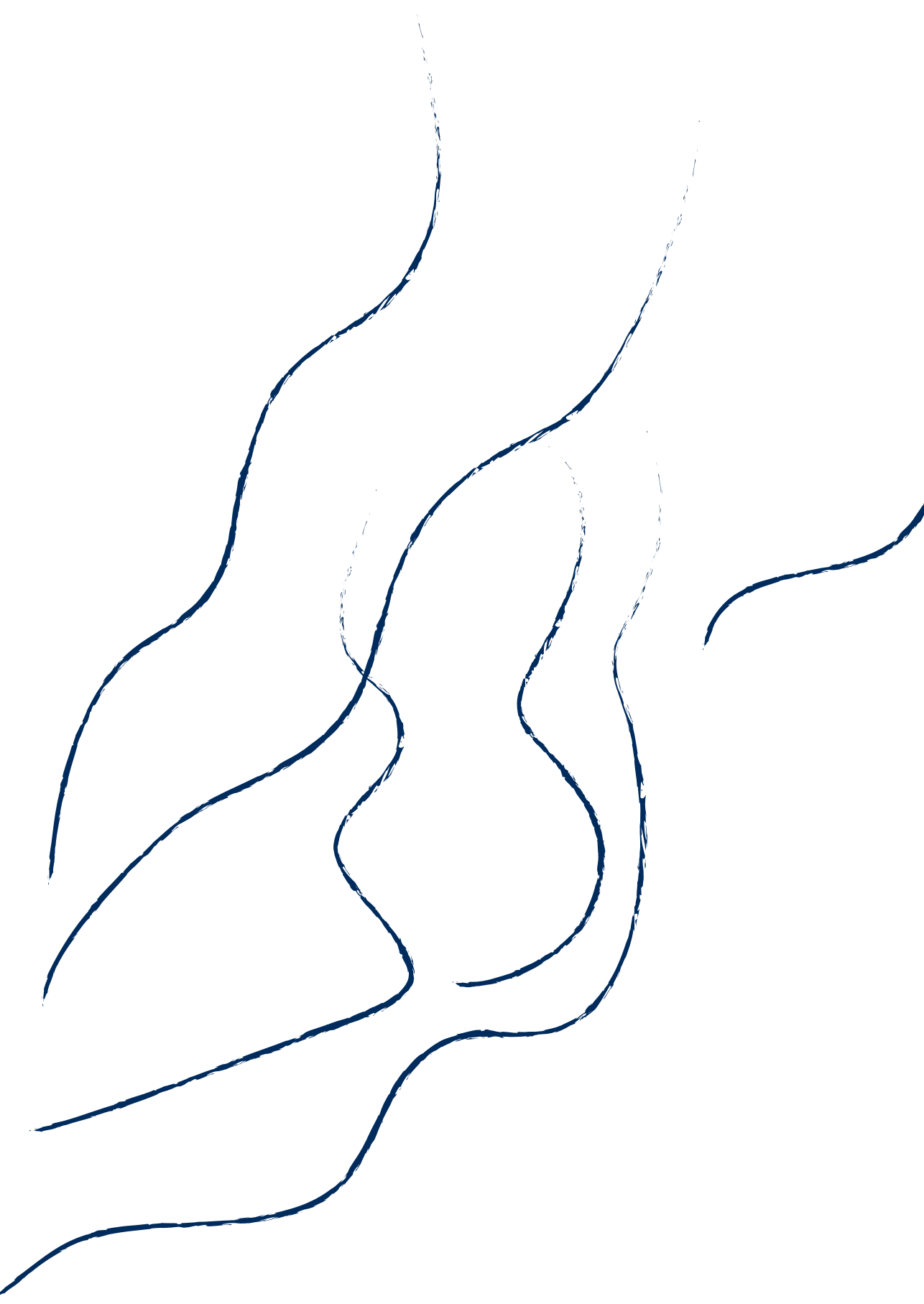
# REFERENCES


1. James, M.L. and S.S. Gambhir, A molecular imaging primer: modalities, imaging agents, and applications. Physiol Rev, 2012. 92(2): p. 897-965.
2. Frangioni, J.V., In vivo near-infrared fluorescence imaging. Curr Opin Chem Biol, 2003. 7(5): p. 626-34.
3. Cilliers, C., J. Liao, L. Atangcho, et al., Residualization Rates of Near-Infrared Dyes for the Rational Design of Molecular Imaging Agents. Mol Imaging Biol, 2015. 17(6): p. 757-62.
4. Vahrmeijer, A.L., M. Hutteman, J.R. van der Vorst, et al., Image-guided cancer surgery using near-infrared fluorescence. Nat Rev Clin Oncol, 2013. 10(9): p. 507-18.
5. Zhu, B. and E.M. Sevick-Muraca, A review of performance of near-infrared fluorescence imaging devices used in clinical studies. Br J Radiol, 2015. 88(1045): p. 20140547.
6. Bell, A.G., The production of sound by radiant energy. Science, 1881. 2(49): p. 242-53.
7. Xua, M., Wang, L. V., Photoacoustic imaging in biomedicine. Review of Scientific Instruments, 2006. 77(041101).
8. Zackrisson, S., S.M. van de Ven, and S.S. Gambhir, Light in and sound out: emerging translational strategies for photoacoustic imaging. Cancer Res, 2014. 74(4): p. 979-1004.
9. Hutteman, M., J.R. van der Vorst, J.S. Mieog, et al., Near-infrared fluorescence imaging in patients undergoing pancreaticoduodenectomy. Eur Surg Res, 2011. 47(2): p. 90-7.
10. Burggraaf, J., I.M. Kamerling, P.B. Gordon, et al., Detection of colorectal polyps in humans using an intravenously administered fluorescent peptide targeted against c-Met. Nat Med, 2015.
11. van Dam, G.M., G. Themelis, L.M. Crane, et al., Intraoperative tumor-specific fluorescence imaging in ovarian cancer by folate receptor-alpha targeting: first in-human results. Nat Med, 2011. 17(10): p. 1315-9.
12. Hoogstins, C.E., Q.R. Tummers, K.N. Gaarenstroom, et al., A Novel Tumor-Specific Agent for Intraoperative Near-Infrared Fluorescence Imaging: A Translational Study in Healthy Volunteers and Patients with Ovarian Cancer. Clin Cancer Res, 2016. 22(12): p. 2929-38.
13. Boogerd, L.S.F., C.E.S. Hoogstins, D.P. Schaap, et al., Safety and effectiveness of SGM-101, a fluorescent antibody targeting carcinoembryonic antigen, for intraoperative detection of colorectal cancer: a dose-escalation pilot study. Lancet Gastroenterol Hepatol, 2018.
14. Adiseshaiah, P.P., R.M. Crist, S.S. Hook, et al., Nanomedicine strategies to overcome the pathophysiological barriers of pancreatic cancer. Nat Rev Clin Oncol, 2016. 13(12): p. 750-765.



Part | I

# Development of Targeted Molecular Imaging for Pancreatic Cancer



Chapter | 2

# Advances in Diagnostic and Intraoperative Molecular Imaging of Pancreatic Cancer

Willemieke S Tummers [1 2], Juergen K Willmann [1 †], Bert A Bonsing [2], Alexander L Vahrmeijer [2], Sanjiv S Gambhir [3], Rutger-Jan Swijnenburg [2]

[1] Department of Radiology, Molecular Imaging Program at Stanford, Stanford University, Stanford, CA, 94305, USA.
[2] Department of Surgery, Leiden University Medical Center, Albinusdreef 2, 2300 RC, Leiden, The Netherlands.
[3] Departments of Radiology, Bioengineering, and Materials Science & Engineering, Molecular Imaging Program at Stanford, Canary Center at Stanford for Cancer Early Detection. Stanford University, Stanford, CA, 94305, USA.

*Pancreas. 2018 Jul;47(6):675-689*

## ABSTRACT

Pancreatic ductal adenocarcinoma (PDAC) has a dismal prognosis. In order to improve outcomes, there is a critical need for improved tools for detection, accurate staging and resectability assessment. This could improve patient stratification for the most optimal primary treatment modality. Molecular imaging, used in combination with tumor-specific imaging agents, can improve established imaging methods for PDAC. These novel, tumor-specific imaging agents developed to target specific biomarkers have the potential to specifically differentiate between malignant and benign diseases, such as pancreatitis. When these agents are coupled to various types of labels, this type of molecular imaging can provide integrated diagnostic, non-invasive imaging of PDAC as well as image-guided pancreatic surgery. This review provides a detailed overview of the current clinical imaging applications, upcoming molecular imaging strategies for PDAC, and potential targets for imaging, with an emphasis on intraoperative imaging applications.

## INTRODUCTION

Pancreatic ductal adenocarcinoma (PDAC) accounts for about 90% of all pancreatic neoplasms and is the fourth most common cause of cancer-related deaths in developed countries.[1] PDAC has a dismal prognosis, with a five-year survival rate of less than 5%. Pain, jaundice and weight loss are the most common presenting symptoms but in the early stages of the disease, these symptoms may be subtle which often leads to delayed diagnoses.[2] The median size of PDAC at the time of diagnosis is ~3.1 cm, and these statistics have not changed in the past three decades despite advances in imaging technologies, as well as in vitro diagnostic testing methods.[3] Resection of tumors while they are small, well-defined and localized results in a higher chance of complete tumor clearance which translates into greater patient survival rates.[3, 4]

Only 15% to 25% of patients are eligible for curative resection at their initial diagnosis, due to locoregional spread and metastasis.[5, 6] More precise detection methods can lead to improved patient stratification for the most optimal primary treatment modality; either surgery or systemic (neoadjuvant) therapy. This selection can prevent patients from undergoing resections without any oncologic benefit. Another advantage of precise visualization of the tumor could be a more radical resection. Tumor margin-positive (R1) resections occur in up to 70% of PDAC cases, leading to a high number of locoregional recurrence.[7, 8] This means that for all patients diagnosed with PDAC, only 15% of these patients will receive a radical, tumor-margin negative resection and have a chance for prolonged survival. Therefore, improved tools for diagnosis, accurate staging, and more effective, tumor-margin negative pancreatic surgeries are crucial for improving patient outcomes.[9]

Imaging techniques play an important role in the diagnosis of PDAC. Current clinical imaging protocols include transabdominal ultrasound, computed tomography (CT) and/or magnetic resonance imaging (MRI) for disease staging and prediction of resectability.[1] Endoscopic ultrasound (EUS) can complement these imaging methods with valuable staging information as well as the opportunity of tissue diagnosis by fine-needle aspiration.[10]

Molecular functional imaging has the potential to play an important role in PDAC management and be of complementary value to these conventional imaging techniques. It could be used for earlier tumor detection, and improved characterization, staging, and response assessment to neoadjuvant therapy. It could also serve as a guide for surgery during diagnostic laparoscopy and tumor resection. Possible imaging modalities for molecular imaging include molecularly-targeted contrast-enhanced transabdominal (CEUS) and EUS, CT, MRI, positron emission tomography (PET), photoacoustic imaging (PAI), fluorescence molecular imaging, and Raman optical imaging (figure 1).

Recently, Laeseke et al. published a review focused on the role of molecular imaging in early detection of PDAC.[11] The current review gives an overview of the status of clinical imaging applications, the advances of molecular imaging strategies, and most optimal imaging targets for PDAC, with a special emphasis on intraoperative applications.

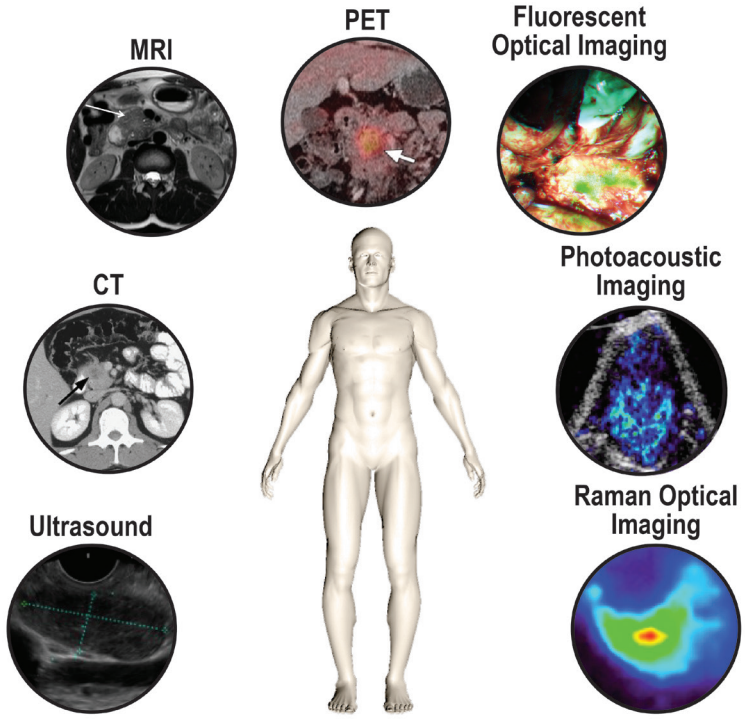



**Figure 1.** Schematic illustration of the key imaging modalities used for the diagnostics and potential intraoperative modalities for pancreatic cancer. Ultrasound, (endoscopic) ultrasound; CT, computed tomography; MRI, magnetic resonance imaging; PET, positron emission tomography. Representative images are shown of pancreatic cancer with the displayed modalities, expect for photoacoustic and raman optical imaging.

# CURRENT DIAGNOSTIC IMAGING TOOLS FOR PDAC



## Transabdominal and endoscopic ultrasound

Ultrasound (US) is often the initial diagnostic assessment used in patients presenting with jaundice, weight loss, and abdominal pain. US is a relatively inexpensive, portable, noninvasive, and widely available tool. However, the sensitivity and accuracy of US is highly dependent on the operator's skills, degree of disease progression and body habitus of the patient. Therefore, sensitivity of conventional US for detecting PDAC varies widely and ranges from 95% in tumors > 3 cm to 50% in tumors < 1 cm.[12] In addition, it is difficult to differentiate between PDAC and inflammatory diseases such as pancreatitis using US technology.

EUS has become a valuable diagnostic tool for PDAC since it allows for tissue sampling and cytological evaluation, both of which can provide a definitive diagnosis.[13, 14] For the evaluation of solid pancreatic tumors, EUS detects lesions <2 cm with greater sensitivity (98%) than CT (86%). On the other hand, EUS also has important limitations in the evaluation of solid pancreatic lesions. First, there is substantial operator-dependence, resulting in variable sensitivity ranging from 57% to 81%.[15, 16] Second, the sensitivity is relatively poor (80%) when detecting PDAC in patients with pancreatitis.[17] And finally, the invasive nature of EUS is a significant disadvantage of this technique.

## Computed Tomography

Multiphase multi-detector row CT (MDCT) with intravenous contrast is the diagnostic test of choice for suspected pancreatic lesions. MDCT has the highest accuracy in determining the extent of primary tumor, locoregional extension, vascular invasion, distant metastases and resectability.[14] MDCT is used to predict resectability of PDAC with a positive predictive value (PPV), sensitivity and specificity of 89%, 96% and 33-72%, respectively.[18, 19] An additional advantage of MDCT imaging is the possibility to detect extrapancreatic spread by perineural invasion.[20] This is of great importance since these patients have significantly reduced survival after pancreaticoduodenectomy.[21] CT perfusion can be used to differentiate between low and high grade PDAC, by using peak enhancement intensity values and blood volume parameters.[22] Despite its sensitivity, MDCT

cannot reliably detect small lesions (<1cm), differentiate between malignant lesions and benign conditions, or detect isoattenuating primary tumors.[23]

## Magnetic Resonance Imaging

MRI has a reported sensitivity and specificity for diagnosis of PDAC of 85-93% and 72-79%, respectively.[24, 25] MRI has advantages over CT regarding improved soft tissue contrast resolution and the absence of ionizing radiation. This leads to several situations were MRI is preferred above CT; such as with small tumors, isoattenuating lesions, and fatty infiltration in the pancreatic head.[26] In addition, there are alternative sequences when using MRI, such as magnetic resonance cholangiopancreaticography (MRCP) which can be used to image the biliary and pancreatic ducts in detail. MRCP has comparable sensitivity to the more invasive endoscopic retrograde cholangiopancreaticography (ERCP) in diagnosing PDAC.[27] Another potential sequence is diffusion-weighted images (DWI), with this technique the difference in diffusion of water molecules is visualized by using the apparent diffusion coefficient (ADC). PDAC tends to have low ADC values due to high levels of fibrosis. This methods is helpful for the identification of subtle lesions with diffusion restriction.[26] Due to its high soft tissue contrast MRI is the preferred modality for assessing cystic lesions in the pancreas.[28] Another important advantage of MRI over CT is the more precise detection of enlarged lymph nodes and distant metastases.[28] A disadvantage of both CT and MRI, is that neither can reliably distinguish residual or necrotic tumor from fibrosis and radiation changes after treatment.

## PET Imaging

Currently, PET is the only molecular imaging technique used for PDAC. It enables whole body imaging to allow staging of diseases, similar to CT and MRI. [$^{18}$F]-2-fluoro-2-deoxy-glucose ($^{18}$F-FDG)-PET has an established role in the work-up of various malignancies. The normal pancreas has low glucose usage compared to PDAC, so areas with increased uptake can be visualized and point towards potential lesions. Because the metabolic activity of a tumor is expressed by the degree of $^{18}$F-FDG uptake it is possible to predict tumor aggressiveness and even survival in patients by the degree of uptake.[29, 30] The average sensitivity and specificity of $^{18}$F-FDG for PDAC are 94% and 90% respectively, compared to 82% and 75% for CT.[31] Choi et al. reported the use of $^{18}$F-FDG-PET to detect biologically active tumor volumes and therefore to assess treatment

effectiveness.[32] A recent multi-center trial in the UK with 550 patients looking at the diagnosis of PDAC showed a sensitivity of 92.7% for FDG PET/CT compared to 88.5% for MDCT (p=0.010) and a specificity of 75.8% compared to 70.6% (p=0.023).[33] A problem of using $^{18}$F-FDG uptake, is that glucose metabolism is not specific for malignant processes, and physiologic uptake can be found in normal tissues as well as in inflammatory tissue which might lead to false-positive findings, causing a similar appearance for pancreatitis and PDAC.[34]



## CURRENT INTRA-OPERATIVE IMAGING TOOLS

A major limitation of the aforementioned imaging techniques, such as CT, MRI or PET is the fact that these techniques cannot be applied as intraoperative imaging tools due to altered positioning of the body, and tissue manipulation by the surgeon.[35] For brain cancer surgery, the use of MRI-guided resection has almost become standard practice.[36] Unfortunately, this method is time-consuming, costly. Therefore, chances are low that MRI-guided resection will be widely-implemented outside the field of brain cancer surgery. Currently, the only tools available for a pancreatic surgeon to ensure complete tumor resection are visual and tactile information, frozen-section analysis by a pathologist, and intra-operative ultrasound.

Intra-operative frozen-section analysis (IFSA) is commonly performed to determine resectability when unanticipated locoregional spread is identified during surgery and to ensure negative final margins after resection.[37] Although frozen section analysis is commonly used to determine successful ablation, it is time-consuming,and only samples a small fraction of the wound bed which could lead to false-negative results. During surgery, if the IFSA of the resection margin turns out to be positive, additional pancreatic tissue is often removed in an effort to clear the margin. Only a few single institutional studies have assessed the value of this surgical maneuver so far and it is shown that there is actually no improved overall survival when additional IFSA-guided resection is performed.[38-40] IFSA has a reported low incidence of false-positive results, but the amount of false-negative results has ranged widely from 1.2% to 75%.[41, 42] This relatively high incidence of false-negative results could indicate that

preoperative imaging and possibly even surgical judgement are more reliable than a negative IFSA.

### Intra-operative Ultrasound

Currently, the only intra-operative imaging technique to help the surgeon delineate PDAC from its surrounding structures is anatomical intraoperative ultrasound. The ability to provide high resolution real-time imaging, along with accurate lesion detection, has established the role of intraoperative ultrasound (IOUS) in PDAC surgery. IOUS can be used for intraoperative guidance and localization of lesions, for determining resectability, surgical planning, differentiation between cystic and non-cystic lesions, and metastatic survey.[43, 44] IOUS also has disadvantages since it is less reliable for detecting superficial and small lesions compared to visual and tactile methods.[45] Another disadvantage is its operator dependence; substantial training and experience are essential for generating and interpreting useful images for intra-operative surgical decision-making.[12, 46]

## THE NEED FOR ADVANCED MOLECULAR IMAGING IN PDAC

To be able to improve detection and patient stratification for treatment, there is a critical need to develop and improve imaging methods that specifically recognize cancer.[47] In current practice, the accurate identification of tumors is mainly subjective and relies heavily on the surgeon's experience leading to a significant variability in surgical outcomes.[48] This inability to exactly identify tumors intraoperatively could result in: 1) Incomplete resection of tumors that could otherwise have been resected completely; 2) Attempt to resect tumors which should have been identified as locally advanced tumors; 3) Incomplete lymph node clearance due to lack of knowledge of the involved or potentially involved lymph nodes, and 4) Resection of the primary tumor in the presence of visually occult micrometastasis. In each of these situations, patients undergo operations with little or no oncological benefit, but with a high risk of deterioration of quality of life due to surgery in their end stage of life. There are two other challenges a surgeon faces when resecting PDAC. First, both the benign pancreatitis and malignant PDAC have abundant stroma, and

therefore both entities are difficult to distinguish using conventional imaging techniques. Second, the introduction of neoadjuvant treatment regimens such as FOLFIRINOX, leading to a 51% increase in tumors becoming resectable after 4 months of neoadjuvant treatment.[49] One of the major drawbacks after neoadjuvant treatment is that conventional imaging modalities, such as CT and MRI, are often not able to differentiate between viable tumor and chemoradiation-induced tumor necrosis and fibrosis, and, therefore, prediction of resectability is limited.[50] Neoadjuvant treatment effects make differentiation between (vital) tumor and fibrotic pancreatic tissue even harder for surgeons during the operation.



Tumor-targeted molecular imaging could provide crucial information in these situations. Molecular imaging can either be performed by using conventional imaging techniques in combination with tumor-specific imaging agents, or by the development of novel imaging techniques, such as fluorescent, photoacoustic and Raman optical imaging. Currently, several first-in-human clinical trials are conducted using these techniques in pancreatic cancer patients.

## TUMOR-TARGETED MOLECULAR IMAGING STRATEGIES FOR PDAC

A molecular imaging approach using imaging agents that target molecular features of cancer could lead to more precise diagnoses.[13] The common consensus is that PDAC evolves from precursor lesions that transform into invasive carcinoma through a multistep process, that involves the progression from pancreatic intraepithelial neoplasia (PanIN) into PDAC.[51] Genetic alterations, such as mutations in the KRAS oncogene or p53, DPC4, and BRCA2 tumor suppressor genes affect a core group of signaling pathways. The processes that are altered in PDAC lead to the expression of specific biomarkers, and these changed biomarkers may serve as targets for tumor-specific imaging.[52] Potential biomarkers for tumor-specific targeting must possess certain characteristics such as diffuse upregulation through tumor tissue, strong upregulation compared to the expression in normal and surrounding tissue, and localization on the cellular membrane.[53, 54] An effective molecular imaging agent needs to

demonstrate a high ratio of specific to non-specific binding to make sure the signal truly reflects the molecular imaging target.

There are numerous categories of available molecular imaging agents including small molecules, peptides, aptamers, antibodies, engineered protein fragments, nanoparticles, or micro-sized contrast agent. Each of these types of agents is different in size and thus possesses different pharmacokinetic characteristics (Table 1). It goes beyond the scope of this review to describe all the different molecular imaging agents in detail; however, please refer to the following review for further details.[55]

**Table 1.** Available Molecular Imaging Ligands with an Example, and the Main Advantages and Disadvantages.

| Type | Small molecule | Peptide | Aptamer | Monoclonal antibody | Protein fragment (diabody) | Nanoparticle | Microbubble |
|---|---|---|---|---|---|---|---|
| **Size** | <0.5 kDa | 0.5-2 kDa | 5-15 kDa | 150 kDa | 55 kDa | 10-100 nm | 1-4 μm |
| **Example** | $^{18}$F-FDG | Cyclic RGD peptide | [$^{99}$Tc]-TTA-1 | Cetuximab-IRDye800 | [$^{18}$F]FB-T84.66 | EGFR antibody-gold nanoparticle | VEGFR2-targeted microbubble |
| **Advantage** | Easy escape vasculature. | Easily modified. Superior selectivity. | Inexpensive production. High diversity. | High affinity and specificity. | Superior tumor penetration. High tumor- to blood ratio. | Effective delivery of signaling and therapeutic payload. | Good safety, wide availability of contrast mode ultrasound scanner |
| **Drawback** | Costly development. Limited size for the signaling component. | Rapid degradation. | Low in vivo stability. Poor membrane passage. | Slow clearance. Restricted in passing biological barriers. | Accumulation in kidneys. | Difficult extravasation due to size. | Imaging limited to molecular targeted differentially expressed on tumor vasculature |

The most important groups of targeted imaging agents that are currently being explored are based on targeting specific receptors that are upregulated during the progress of PDAC development. For example, global expression analysis of PDAC has revealed that claudin 4 and prostate stem cell antigen (PSCA) are upregulated in the vast majority of PDACs.[56, 57] Given the membrane localization and the presence of an extracellular domain, these proteins are attractive candidates for targeted imaging. Additionally, claudin 4 has a high expression in high grade PanIN lesions, indicating the potential to detect lesions before development into an invasive carcinoma.[58] Other targets employed for tumor-specific imaging of different cancer types are not applicable for PDAC due to co-expression of these receptors on normal pancreatic tissue (somatostatin, secretin, bombesin, cholecystokinin, vasoactive intestinal peptide).[59-62] Another possibility for PDAC would be the use of a combined target, against both tumor and surrounding stroma, which can be of significant advantage because of the abundance of stroma in PDAC, such as the target uPAR.[63] Since several potential imaging targets have been identified for normal pancreatic tissue, an alternative strategy could be to visualize normal tissue while abnormal/cancerous would be visualized by a lack of imaging signal. For example by targeting the bombesin receptor, PDAC would appear by a lack of contrast agent uptake.[64] However, specificity of those potential molecular imaging targets compared to pancreatitis is still to be determined.

## MOLECULARLY TARGETED IMAGING AGENTS FOR CURRENT CLINICAL IMAGING MODALITIES

### Molecularly targeted (intra-operative) ultrasound

Contrast-enhanced US (CEUS) involves the use of targeted microbubble imaging agents and specialized imaging techniques. For the diagnosis and differentiation of pancreatic malignancies, transabdominal CEUS has generated test characteristics comparable to, or better than other diagnostic modalities such as conventional ultrasound and CT.[65] CEUS with a non-specific agent showed similar sensitivity to contrast-enhanced CT for the detection of PDAC (91.7% and 97.2%, respectively) and of pancreatitis (82.1% and 67.9%, respectively).[66] Intra-operative CEUS is well established in liver surgery, but it has not yet found its place in PDAC. However, CEUS provides a potential for the detection of small

tumors, since it shows improved sensitivity and specificity compared to multi-detector CT (MDCT) for pancreatic lesions <2 cm; 91% vs 71% and 94% vs 92%, respectively.[67]

Ultrasound using molecularly targeted microbubbles would be a tool to increase sensitivity and specificity even further.[68] Targeted imaging agents differ from those initially developed by the presence of a targeting moiety able to link the microbubble to the selected biomarker.[68-72] A disadvantage of microbubbles is their relatively large diameter. Therefore, they remain within the vascular compartment after intravascular administration, which limits targeting to molecules that are overexpressed on the surface of endothelial cells of the tumor vasculature (Figure 2).[73]

### *Molecular-targeted agents for ultrasound imaging*

The formation of new blood vessels is a fundamental process during tumor progression. Under hypoxic conditions, which are required for effective tumor angiogenesis, expression of hypoxia-inducible factors is induced in endothelial vessels resulting in vascular endothelial growth factor receptor (VEGFR) expression.[74] VEGFR is a receptor tyrosine kinase that mediates most of the proangiogenic activity of VEGF. Our group has previously shown that VEGFR2 is a promising target for detection of PDAC. In a cohort of 129 patients, VEGFR2 was abundantly expressed in up to 72% of all PDAC cases.[75] Microbubbles developed to recognize VEGFR2, integrin and endoglin were used to visualize tumor angiogenesis by ultrasound imaging in PDAC of genetically engineered mouse models.[76, 77] Recently, first-in-human clinical trials using a VEGFR2-targeted agent have been performed.[72] and shown great potential in detecting breast and ovarian cancer.[78] Foygel et al discovered and validated thymocyte antigen 1 (Thy1) as a new PDAC imaging target.[79] Thy1 is a marker expressed on the neovasculature of PDAC and shown to be differentially expressed in PDAC versus pancreatitis and normal pancreatic tissue in humans.[79] *In vivo* imaging studies with a genetically engineered mouse model of PDAC showed a 4-5.5-fold increased signal in PDAC compared to normal parenchyma when using a novel Thy1-targeted microbubble.[79] Clinical trials with these agents in PDAC patients have not yet been performed, but are planned for the future.

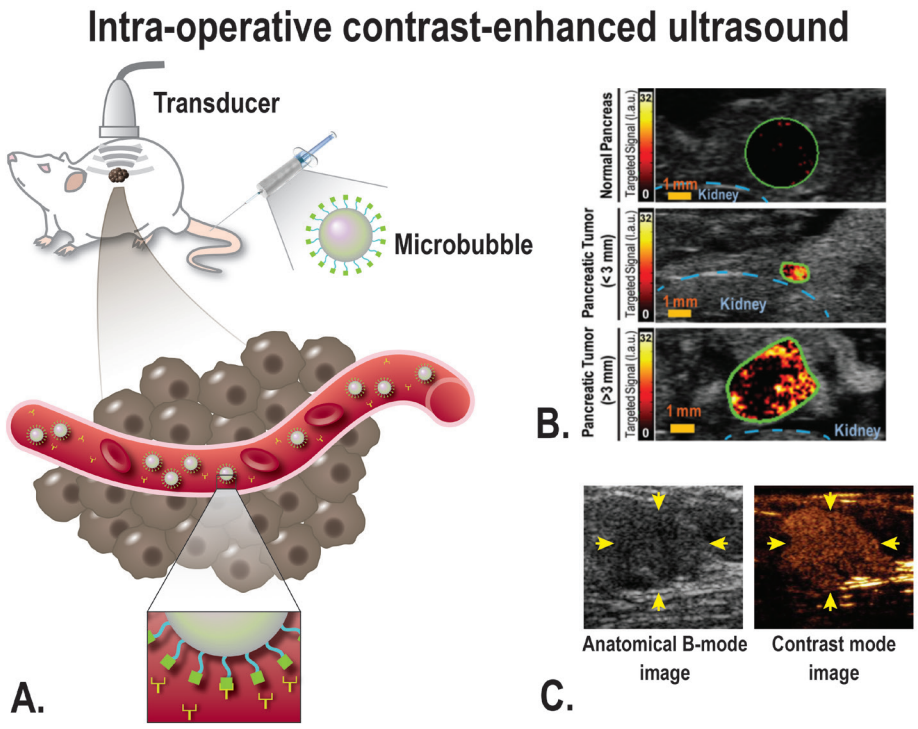



**Figure 2. A.** Schematic overview of the principle of ultrasound molecular imaging. A molecularly-targeted contrast agent (microbubble) is administered intravenously into the subject (in this case a mouse). Sound waves are transmitted into the subject by the transducer, the sound wave reflections are recorded and converted into images. Because of the size of microbubbles of several micrometers, the contrast agent remains intravascular and attaches to the target of choice (for example VEGFR2). Examples of in vivo molecular ultrasound images with microbubbles in **B.** transgenic mouse model of PDAC, showing a strong signal when targeting VEGFR2 in focus of PDAC compared to normal pancreatic tissue, even in small PDAC lesions [From Pysz MA et al. Radiology. 2015 Mar;274(3):790-9], and **C.** in human with breast cancer using microbubbles targeting kinase insert domain receptor ($MB_{KDR}$). Left panel: the anatomical image for reference, right panel: $MB_{KDR}$ accumulation in breast cancer lesion [Willmann JK et al. J Clin Oncol. 2017 Mar 14:JCO2016708594]

## Molecularly targeted MRI

MRI has a fairly high sensitivity as described above, but increased sensitivity could be realized by increased enhancement of the tumors using molecularly-targeted contrast agents. Pirollo et al. described a way to systemically deliver the imaging agent gadolinium in a tumor-targeted nanocomplex leading to better tissue penetration, and therefore better visualization of PDAC in an orthotopic animal model.[80]

### *Molecular-targeted agents for MRI*

Studies using targeted MR imaging against biomarkers, such as plectin-1 and EGFR, showed tumor targeting both *ex vivo* and *in vivo*.[81, 82] ScFvEGFR-IO injection lead to 4.8 fold specific decrease in MRI signal in the tumor area, compared to a non-targeted particle.[81] Mucin-1 is a tumor-specific antigen that is one of the early hallmarks of carcinogenesis in a broad range of tumors, including PDAC.[83] Medarova et al. developed a dual-modality imaging agent targeting Mucin-1 in an orthotopic PDAC model for both MRI and NIRF imaging.[83, 84] A potential drawback for clinical use of mucin-1 as imaging target is that this antigen expression is down-regulated after neoadjuvant gemcitabine therapy.[85]

## Molecularly targeted PET

The specificity of PET imaging could be improved by using a more disease-specific imaging agent compared to FDG-PET (Figure 3). There are several preclinical examples of disease-specific PET imaging in PDAC, and recently, for the first time a first-in-human trial is performed by Kimura et al. using a tumor-specific peptide targeting integrin αvβ6, [18F]FP-R01-MG-F2, for the detection of PDAC. This study shows proof even in this cancer type with dense stroma, an imaging agent can penetrate the tumor [Kimura RH, et al. under review].

### *Molecularly targeted agents for PET imaging*

In preclinical setting, several targets are explored. Aung et al described the use of $^{64}$Cu-RAFT-RGD, targeting αvβ3, for imaging an orthotopic pancreatic tumor-bearing mouse model showing higher detectability of cancer cells as compared to $^{18}$F-FDG-PET.[86] Carbohydrate antigen 19-9 (CA19-9) is widely used as a serum marker of PDAC, and it is known to be presented on the tumor cells of approximately 90% of all PDAC patients.[87, 88] A dual-modal probe targeting CA19-9 using PET and near-infrared fluorescence imaging was developed by Houghton et al. This probe identified metastases and map sentinel lymph nodes in an orthotopic PDAC mouse model via both PET-computed tomography (PET/CT) and NIRF imaging.[89] Unfortunately, CA19-9 is also presented on pancreatitis and therefore, this agent will be of limited value in the clinic.[90] The earlier mentioned cell surface receptor integrin αvβ6 is a well-known

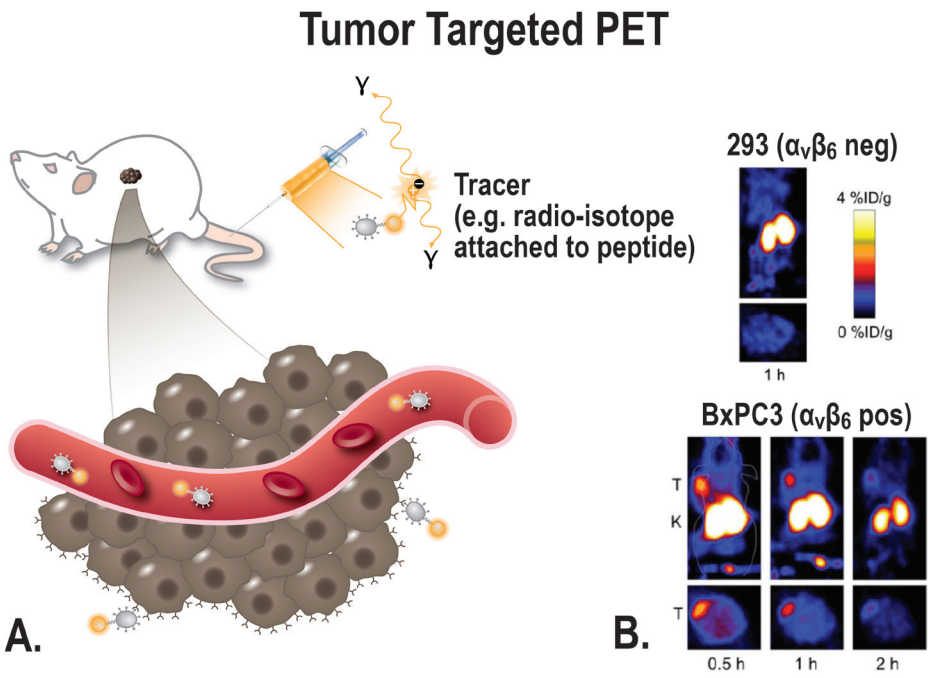



**Figure 3. A.** Schematic overview of the principle of tumor-targeted PET imaging, a suitable tracer will be administered into the subject (in this case a mouse). Depending on the size of the tracer, the tracer can target the cancer at multiple locations; e.g. intravascular, receptors on the cell membrane, or intracellular. **B.** Small-animal PET imaging. BxPC-3 (integrin $\alpha_v\beta_6$ pos) and 293 (integrin $\alpha_v\beta_6$ negative) cells were xenografted in nude mice. PET images were acquired in tumor-bearing mice using a $\alpha_v\beta_6$-targeted cysteine knot ($^{18}$F-fluorobenzoate-$R_0$1) [From Hackel, et al. J Nucl Med 2013; 54:1101–1105].

target for molecular imaging of PDAC since over 90% of human PDAC cases overexpress αvβ6.[91-96] Hackel et al. used two version of an $^{18}$F-labeled integrin αvβ6–targeted cystine knot peptide for successful PET-imaging of PDAC xenografted tumors in mice.[91] Tissue factor (TF), a transmembrane glycoprotein, is also known to be upregulated during tumor growth and metastasis. There is a strong correlation between the aberrant expression of TF, staging and overall survival in PDAC, making TF an attractive imaging target.[97, 98] Hong et al. developed a PET tracer, $^{64}$Cu-NOTA-ALT-836, for imaging TF expression using the chimeric antihuman TF monoclonal antibody, ALT-836. Serial PET revealed that the uptake of (64)Cu-NOTA-ALT-836 was significantly higher in TF positive tumors compared to negative tumors.[99] Activated leukocyte cell adhesion molecule (ALCAM) homotypic interactions promote primary tumor growth, and this cell-surface glycoprotein is upregulated on cancer cells relative to normal

cells.[100] McCabe et al. imaged ALCAM expression by using a cysteine-modified diabody, CysDb, which binds specifically to ALCAM-positive cells with a binding affinity of 1-3 nM and microPET images showed specific targeting of positive tumors.[101] Clinical translation of this probe seems unlikely due to its relatively short half-life and potential nephrotoxicity due to high renal exposure of the beta-emitting radionuclide. Alternatively, this agent could be labeled with 18F, which would overcome these limitations. Lastly, the transferrin receptor (TfR) was investigated as a possible target for PET imaging in PDAC. TfR is a cell-surface receptor involved in iron uptake. It is overexpressed on cells with high proliferation rates, and about 80% of all PDAC patients show high TfR expression.[102] Sugyo et al. developed a PET probe targeting TfR, with a mean tumor-to-muscle ratio of 9.8 at day 6 in a subcutaneous PDAC model. However, a major disadvantage of this probe is its high accumulation in the liver, which could hinder detection of tumor tissue in close proximity to the liver.[103]

## INTRAOPERATIVE MOLECULAR IMAGING TECHNIQUES: POTENTIAL FOR IMPROVED INTRA-OPERATIVE PERFORMANCE

### Fluorescence molecular imaging

Over the last few years, intraoperative imaging technologies using near-infrared (NIR) fluorescence have made enormous progress. The volume of publications in this field has increased eightfold in the literature in the last 10 years.[104] Benefits of Fluorescence imaging using NIR fluorescent light include the ability to image in real time using an NIR fluorescence camera system without impeding the current clinical workflow. If surgeons were able to resect tumors and preserve normal structures more easily, time of surgery could be shortened, thereby reducing anesthesia time and its associated risks. Furthermore, this could subsequently lower rates of recurrence and complications, which would improve patient outcomes and even drive down costs.[35] Fluorescence imaging using NIR fluorescent light has already been established as a powerful tool for guiding precise intra-operative positioning in other types of cancer such as liver metastases.[105], breast cancer.[106, 107], ovarian cancer.[108], melanoma.[109], vulvar cancer.[110, 111], and cervical cancer.[112, 113]. Currently, only the non-specific dyes methylene blue (MB) and indocyanine green (ICG) are approved for clinical use

by the FDA and in order to determine the true clinical benefit of tumor-specific fluorescent imaging, developing and clinically assessing tumor-specific imaging agents will be essential (Figure 4). Recently, two first-in-human clinical studies are performed by our research groups using tumor-specific intra-operative imaging in PDAC, targeting CEA with SGM-101 [Hoogstins CE et al. under review] and EGFR with cetuximab-IRDye800.[114] Hoogstins et al. performed a phase 1 clinical trial targeting CEA, with a 700nm fluorescent agent [Hoogstins CE et al. under review]. Tummers et al. conducted a clinical trial using both NIR and PA imaging for the tumor-specific detection of PDAC with cetuximab-IRDye800.[114] In both trials successful PDAC imaging could be performed, however interfering autofluorescence was seen with the fluorescent agent at 700 nm. These trials show the first proof that this imaging technique is possible in PDAC, despite the idea that the dense stroma of PDAC will restrict targeted-imaging and therapy. Tummers et al. even show proof of drug penetration into the a single tumor duct.[114]

### *Molecular-targeted agents for fluorescent molecular imaging*

As described above, until now only agents targeting the CEA and EGFR receptor are used in clinical trials for NIR fluorescent imaging of PDAC. With cetuximab-IRDye800, it was even possible to establish a significantly different fluorescent signal in PDAC compared to peritumoral inflammation.[114] Furthermore, only preclinical work is performed for the identification of intraoperative imaging agents and targets. As mentioned before, αvβ6 seems to be a reliable target for PDAC. Gao et al. synthesized an integrin αvβ6-targeted near-infrared phthalocyanine dye-labeled agent, termed Dye-SA-B-HK, and investigated it for possible targeted theranostics. Dye-SA-B-HK specifically bound to integrin αvβ6 in vitro and *in vivo* with high receptor binding affinity, and when used for surgical guidance, the tumors were successfully removed completely.[93] The main advantage of this agent compared to nanoparticles is the size of this agent, which gives the ability to extravasate, and faster excretion. Zhang et al. recently developed an optical imaging agent, suitable for both fluorescent and photoacoustic imaging. This imaging agents consists of a cysteine knottin targeting αvβ6 conjugated to the dye Atto-740, A740-R01. The agent was able to successfully detect integrin αvβ6 both in vitro and *in vivo* by photoacoustic and fluorescence imaging.[115]

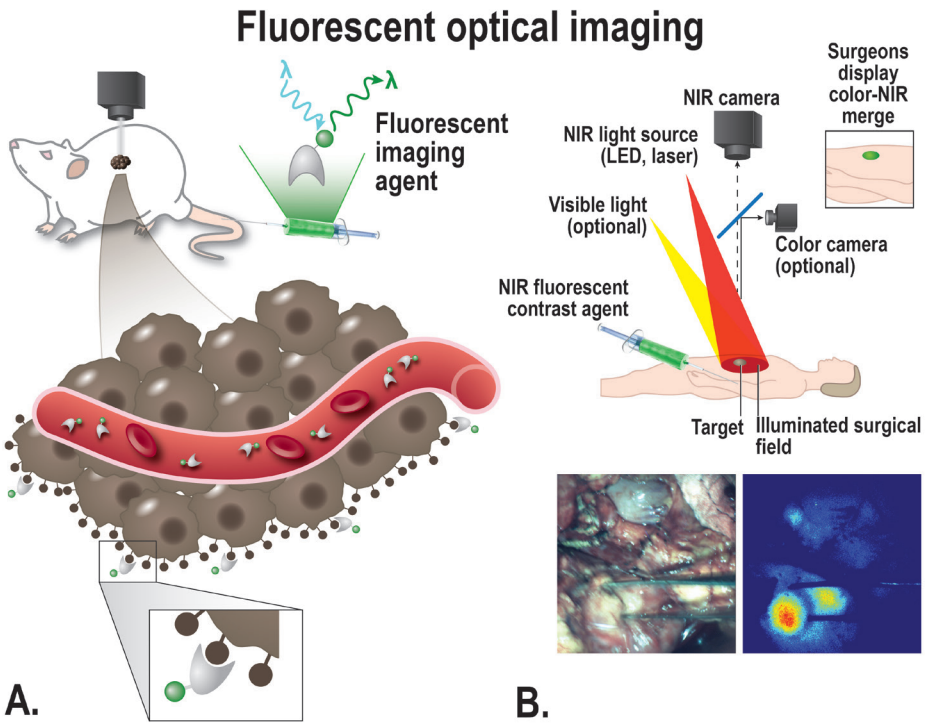



**Figure 4. A.** Schematic overview of the principle of fluorescent imaging, a suitable targeted imaging agent with a fluorescent dye will be administered into the subject (in this case a mouse). The agent is visualized using a fluorescence imaging system, with an adequate excitation laser and camera able to detect the emitted light. The targeted agents migrate to the cellular targets to visualize the tumor in a target-specific manner, the imaging agent can target the cancer at multiple locations depending on the size; e.g. intravascular, receptors on the cell membrane, or intracellular. **B.** Top: schematic overview showing the principle of fluorescent imaging. Bottom: Intraoperative image showing the use of tumor-targeted fluorescent guided imaging during pancreatic cancer surgery.

Cathepsin E (Cath E) is a tumor-associated intracellular non-lysosomal aspartic proteolytic enzyme. In normal physiology Cath E is expressed in immune cells. In the pancreas, Cath E is present in PanIN lesions and PDAC, but not in normal pancreatic tissue.[116] Targeting Cath E can be done by Cath E-activatable imaging probes. These agents are nonfluorescent or produce low-fluorescence in their unactivated state, but become fluorescent after activation as a result of binding to their molecular target such as a tumor-specific enzyme.[35, 116, 117] Using an activatable imaging probe has several advantages. First, in its native state the quenched probe is optically silent, thereby minimizing background fluorescence and enhancing tumor-to-background ratios. Second, protease recognition sites allow for specific activation of probes. Finally, probes can

be designed to be activated by different proteases, thus permitting specific detection of tumors with different protease expression profiles.[118, 119] Recently, Whitley et al. published results of the first-in-human trial using a protease-activated fluorescent imaging probe, LUM015, to detect soft tissue sarcoma or breast cancer. This study demonstrated the probe's safety in humans and also its tumor-specific fluorescence.[120]



Despite improved tissue penetration as compared to visible light, an essential limitation of the use of NIR fluorescence imaging intraoperatively is its inability to visualize structures deeper than approximately 5 – 8 mm below the surface.[35, 121] As a result of this limitation, the field has been shifting towards developing a combination of different forms of imaging modalities, such as PAI, as described in the clinical trial of Tummers et al.[114]

### Photoacoustic imaging

Photoacoustic imaging (PAI), also referred to as optoacoustic imaging, is a relatively new imaging technique with significant promise. PAI provides real-time, noninvasive imaging of the optical absorption properties of tissues. PAI relies on the photoacoustic effect; a pulsed nanosecond-long red-shifted laser beam that is used to stimulate localized thermoplastic expansion of the tissues. This expansion generates pressure waves, synonymous with those produced in ultrasound, which can be detected by a transducer and converted into images.[121] The combined use of light and sound gives PAI an important advantage over other imaging modalities including CT, PET or ultrasound because it provides unique scalability of its spatial resolution. The penetration up to clinically relevant depths, namely from 6 mm to 5 cm, is an important factor for its potential intraoperative use during PDAC surgery (Figure 5).[121-124]

PAI can be performed based on two methods: by relying on the differences in the optical absorption properties of endogenous tissue or by using exogenous imaging agents targeting a specific molecular process of interest. Exogenous imaging agents have the ability to greatly enhance the contrast generated by PAI. The selection of an imaging agent will depend on the application for which it will be used. Design considerations and requirements for a PAI imaging agent include: (1) ease of synthesis, (2) overall size on the nano-scale or smaller in order to extravasate the vascular compartment, (3) a large absorption cross-

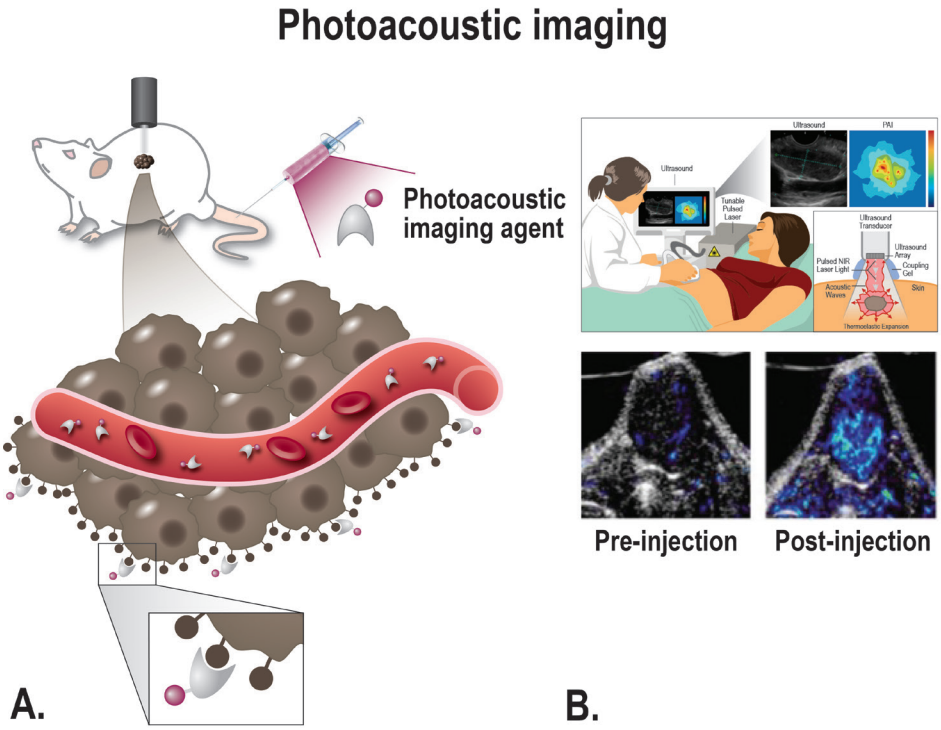



**Figure 5. A.** Schematic overview of photoacoustic imaging principle; after injection of a tumor-targeting agent the imaging agent will target tumor cells and produces an enhanced photoacoustic signal, after excitation with a laser. The agent can target the cancer at multiple locations depending on the size; e.g. intravascular, receptors on the cell membrane, or intracellular. **B.** Top: Schematic overview showing the principle of photoacoustic imaging; the thermo-elastic expansion caused by heating of the tissue due to the laser will lead to acoustic waves that can be converted into both ultrasound and molecular images. Bottom: Tumor-targeted photoacoustic imaging. Mice bearing FTC133 tumors were photoacoustically imaged using 680 and 750 nm light before and after the injection of a MMP-targeting probe [From: Levi, et al. Clin Cancer Res. 2013 Mar 15;19(6):1494-502].

section of light in the NIR wavelength region where light penetration into tissue is maximized, (4) a surface chemistry that allows simple bioconjugation of targeting moieties, (5) proven safety profile, and (6) a structural and molecular biostability in biological fluids.[125] Photostability is also very important for these agents as they often suffer from loss of optical absorption (photobleaching) due to exposure to prolonged pulsed laser irradiation.[126] Nanoparticles are the most commonly used types PAI agents, and especially gold nanoparticles, single-walled carbon nanotubes (SWNT), and quantum dots.[121, 125, 127, 128] Gold nanoparticles have an advantage in that their optical properties are highly tunable over the NIR spectrum by varying their size and shape. However, they

have major disadvantages since they consist of gold, which is not approved for human use, and they can become deformed after extended exposure to laser radiation.[129] SWNTs absorb light over a broad spectrum, and targeting agents can easily be conjugated for molecular imaging. Quantum dots are strongly fluorescent and have been shown in multiple studies to be successful PAI agents in PDAC.[130, 131] Other important disadvantages of gold nanoparticles, SWNTs, and quantum dots are their inability to sufficiently extravasate and the potential long term effects due to retention in the reticuloendothelial system which are not an issue for small particles.[132, 133]



As previously stated, the strengths of PAI include its clinically relevant depth penetration compared to fluorescence imaging and the potential to visualize extravascular molecular imaging targeted compared to molecular CEUS. The main disadvantages of PAI are its inability to image through bone or air-filled structures, and the fact that no commercial intra-operative systems are available for now.[55] Clinical applications for molecular photoacoustic imaging are still being explored. For diagnostics in PDAC, PAI could potentially be used during EUS in order to improve the sensitivity of the procedure. Studies investigating the intraoperative use of PAI are limited, and only described by Tummers et al.[114] By targeting the EGFR receptor, a significant difference was shown in PA signal in the tumor and surrounding pancreatic tissue. This indicates that intraoperatively PAI could potentially help determining the extent of the tumor infiltration before removal, tumor delineation, and the completeness of removal following resection and also play an important role in the assessment of metastases and lymph node status.[121]

### *Molecular-targeted agents for photoacoustic molecular imaging*

In preclinical studies, the first use of targeted photoacoustic imaging using SWNT was described by De La Zerda et al. in 2008. Intravenous administration of SWNT conjugated to cyclic Arg-Gly-Asp (RGD) peptides in mice bearing tumors showed eight times greater photoacoustic signal compared to mice injected with non-targeted nanotubes.[128] Levi et al. developed and validated both tumor-specific PAI agents for prostate cancer, against gastrin-releasing peptide receptor.[134], and for follicular thyroid carcinoma, against MMP-9.[135] Both agents showed increased PAI signal compared to a control agent. Conjugated polymers (CPs) are upcoming optical imaging agents that have unique chemical

and optical properties thus allowing them to be used as imaging agents for PAI among other technologies.[136] Balasundaram et al. used folate-CP dots for the molecular imaging of breast cancer and showed a strong PA signal compared to non-specific CP dots.137 Promising PAI agents are activatable agents, as firstly described by Levi et al. targeting a proteolytic enzyme, e.g. MMP-2, which is photoacoustically silent before cleavage and leads to PAI signal after activation by the target.[138]

To tackle the abovementioned limitation fluorescence guided surgery is facing with limited depth penetration, PAI could help determining the extent of tumor before removal, and the completeness of the resection intraoperatively. On the other hand, fluorescent imaging has a superior sensitivity for superficial lesions. By combining the two modalities, the strengths of both NIR fluorescence imaging and PAI have the potential to overcome the limitations of the individual techniques in a combinatorial fashion.

### Raman optical imaging

Raman optical imaging is based on the Raman effect, a process discovered by Chandrasekhara Venkata Raman in 1928 that is based on the inelastic scattering of light. Objects made of different molecular compositions will scatter light differently and produce unique spectra that are a function of the chemical bonds contained in the molecule of interest. Unfortunately, Raman scatter is very weak, with less than one in a million incident photons experiencing this effect.[121, 139, 140] When the scattering molecule is placed on a surface of a roughened plasmonic substrate, the signal is increased by many log orders and is known as surface-enhanced Raman scattering (SERS).[141, 142] A major advantage of Raman optical imaging is the potential to detect multiple SERS nanoparticles simultaneously (a process called multiplexing), by modifying the Raman active layer that is absorbed onto the metal surface.[139] Raman spectroscopy is recently tested *ex vivo* on human colon tissue. Zavaleta et al developed a Raman spectroscope in combination with a multiplexed panel of tumor-targeting Raman nanoparticles, to rapidly distinguish between normal and precancerous tissues and to identify flat lesions in the colon.[143] This technology could be used for helping endoscopists or surgeons to delineate tumors while performing procedures.[144, 145] Additionally, Jermyn et al. developed a handheld contact Raman spectroscopy probe for the detection of cancer cells in the human brain. Intra-operatively, they were able to

differentiate normal brain from cancer and normal brain invaded by cancer with a cellular resolution with sensitivity of 93% and specificity of 91% in humans.[146] Kircher et al. described a MRI-PAI-Raman imaging nanoparticle to delineate the margins of brain tumors. This triple-modality-nanoparticle approach combines the strengths of the three modalities and leads to more accurate brain tumor imaging and resection in mouse models.[147] A variation on Raman spectroscopy, transmission Raman spectroscopy, has enabled identification of calcifications at depths of up to 2.7 cm in breast tissue.[148] This technique could potentially be used in the differentiation between PDAC and pancreatitis, since the latter is known for containing abundant calcifications. However, continued development of Raman spectroscopic instrumentation is needed in order to perform at the level necessary for intraoperative clinical use, including the design of a probe and the complete hardware which will need to be compact and easily integrated into the clinical OR.[149]



## SUMMARY AND CHALLENGES FOR THE FUTURE

Despite great efforts to improve treatment for patients with PDAC in recent years, the disease still has the worst prognosis of all major solid cancers. Molecular imaging using tumor-targeting agents and various modalities has shown great potential, both clinically and preclinically, in order to bridge the gap between diagnostic and intraoperative imaging for PDAC treatment, and for monitoring response to perioperative chemo- and or radiotherapy. Multimodal imaging modalities also have significant potential when used as an integrated diagnostic and intraoperative technology, since this can overcome limitations of the individual modalities. At this point, feasibility of tumor-specific PET and fluorescence is shown in PDAC patients, and as soon as the other modalities are translated into the clinic the full potential of tumor-specific molecular can be assessed (Figure 6).

The discovery of the perfect target (Table 2) and translation of molecular-targeted imaging to the clinic remains challenging due to the need for specific exogenous imaging agents in order to image the biochemical process of interest. The discovery and validation of such imaging targets is time-consuming and expensive, and rarely results in a clinically useful agent. Many of the imaging

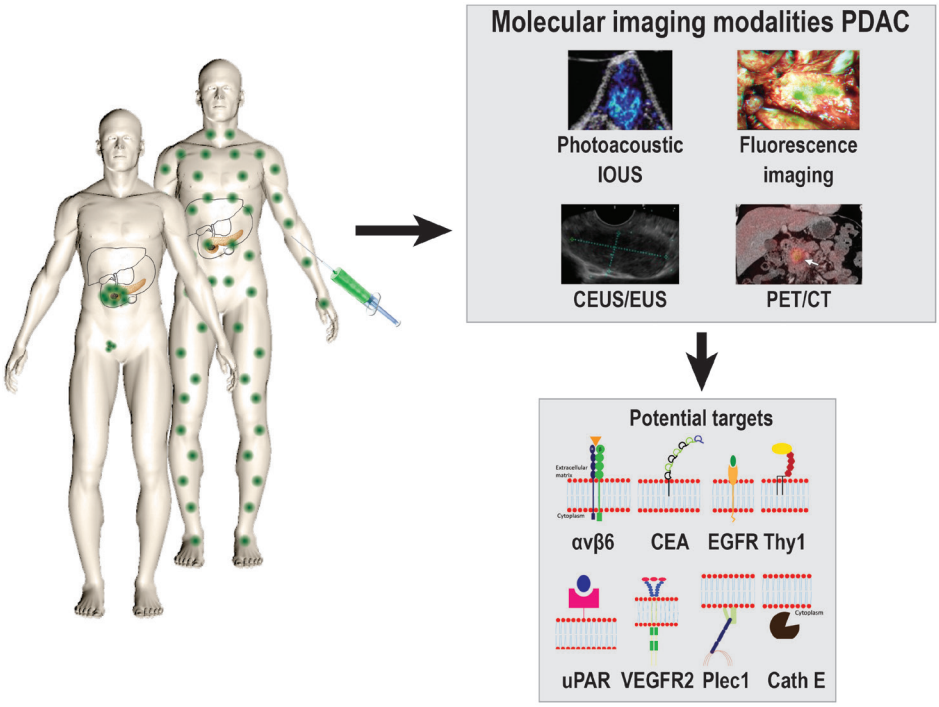



**Figure 6.** A schematic overview of the principle of tumor-targeted imaging in pancreatic cancer, showing the most promising imaging modalities for early diagnosis and improved surgical treatment, and most promising targets for this purpose. Avβ6; Integrin αvβ6, CEA; Carcinoembryonic Antigen, EGFR; Epidermal growth factor receptor, Thy1; Thy-1 cell surface antigen, uPAR; Urokinase receptor, VEGFR2; Vascular endothelial growth factor receptor 2, Plec1; Plectin 1, Cath E; Cathepsin E.

probes reported in animal models have failed to reach the clinic and are still in the investigational stage. Unfortunately, the extensive approval process of the FDA makes it impossible to quickly test imaging probes in a clinical pilot study in order to determine effectiveness in humans and thus save resources and concentrate on more promising probes.[150] In addition, the added value of molecularly-targeted imaging to patient benefit still needs to be proven before wide-spread use of this technique is expected. This needs to be accomplished by increasing the number of human trials using a standardized technique to demonstrate safety and effectiveness. Although this is still far from current reality, the bulk of preclinical studies and the first successful clinical studies outlined in this review, show that more wide-spread clinical use is on the horizon.

**Table 2**. Summary of Potential Targets Molecular Imaging Purposes for PDAC with Main Advantages and Disadvantages.

| Target | Type | Localization | Main advantage | Main disadvantage | References |
|---|---|---|---|---|---|
| **ALCAM (CD166)** | Glycoprotein in immunoglobulin family | Cell membrane | Expression in PDAC 2.5x higher compared to normal pancreatic tissue. | Expression on activated immune cells and the expression of ALCAM in pancreatitis is unknown. | 100, 101 |
| **αvβ6** | Integrin | Cell membrane | Diffuse, strong expression in PDAC. | Mild expression on normal ductal tissue. | 75, 150 |
| **CA19-9** | Glycosylation product presented on cell surface proteins | Cell membrane | Expressed in up to 90% of all pancreatic cancers. | Expression on pancreatitis and normal ductal tissue. | 87, 88, 90, 151 |
| **Cath E** | Proteolytic enzyme | Intracellular | Ideal for imaging purposes due to potential use of activatable probes and differentiation between PDAC, normal pancreatic tissue, and pancreatitis. | Intracellular location of target makes internalization of probe required. | 53, 115, 152 |
| **Claudin 4** | Integral membrane protein | Tight junctions | Upregulation in metastasis and expression in PanIN 3. | Ability to discriminate between PDAC and pancreatitis is unknown. Overexpression in PanIN 1 and 2. | 58, 153 |
| **EGFR** | Receptor tyrosine kinase | Cell membrane | EGFR-mediated cellular internalization of targeted particles. | EGFR is expressed in pancreatitis and on duodenal tissue, which could potentially interfere with the surgical field. | 75, 81, 154 |

**Table 2**. Summary of Potential Targets Molecular Imaging Purposes for PDAC with Main Advantages and Disadvantages.

| Target | Type | Localization | Main advantage | Main disadvantage | References |
|---|---|---|---|---|---|
| **Endoglin (CD105)** | Type 1 membrane glycoprotein | Cell membrane | Expression levels vary throughout tumor growth, and overexpression is related to poor prognosis. | Expression is restricted to vascular endothelial cells undergoing active angiogenesis. Expression in pancreatitis is unknown. | 77, 155 |
| **Mesothelin** | GPI-anchored glycoprotein | Cell membrane | Expressed in PDAC and not in normal pancreatic tissue or in pancreatitis. | Mesothelin is released into the bloodstream what could reduce the signal at tumor site. | 156, 157 |
| **Mucin-1** | O-glycosylated proteins | Cell membrane | Expression on apical surface in normal tissue. Expression is correlated with more aggressive biological behavior. | Possible down-regulation of expression after neoadjuvant therapy. Present in the RNA of pancreatitis patients. | 85, 158, 159 |
| **NGAL** | Secreted protein | Extracellular | Potential biomarker for early detection, can also differentiate between PDAC and pancreatitis in urine and bile. | Not bound on tumor cell membrane, which could complicate imaging specificity. | 160, 161 |
| **PCSA** | GPI-anchored glycoprotein | Cell membrane | Upregulation in PDAC compared to pancreatitis and normal pancreatic tissue. | Overexpressed in only 60% of pancreatic cancers. | 56, 162 |
| **Plectin-1** | Protein for linkage in cytoskeleton | Cytoplasm | Overexpressed in PDAC compared to normal pancreatic tissue and pancreatitis. Also expressed in PanIN 3 and is therefore a potential marker for early detection. | Target is expressed in the cytoplasm as opposed to on the cell membrane. | 82 |

**Table 2**. Summary of Potential Targets Molecular Imaging Purposes for PDAC with Main Advantages and Disadvantages.

| Target | Type | Localization | Main advantage | Main disadvantage | References |
|---|---|---|---|---|---|
| **TF** | Glycoprotein | Cell membrane | TF is used in staging and is correlated with incidence of metastases and with overall survival. | The expression of TF in pancreatitis in humans in unknown. | 98, 163 |
| **TfR** | Glycoprotein | Cell membrane | Upregulation is induced by hypoxia, a known feature of PDAC. | Receptors are highly expressed in the liver. Expression of TfR in pancreatitis is unknown. | 102, 103, 164 |
| **Thy1** | GPI-anchored glycoprotein | Cell membrane | Marker for cancer-associated fibroblasts; also expressed on tumor vasculature but not in pancreatitis. | Thy1 is present on stromal cells, which is also upregulated in pancreatitis. | 79, 165 |
| **uPAR** | GPI-anchored glycoprotein | Cell membrane | Expression on both tumor cells and stromal cells in the tumor microenvironment. | High uPAR staining in negative lymph nodes due to staining of tumor microenvironment. | 75, 166, 167 |
| **VEGFR2** | Receptor tyrosine kinase | Cell membrane | Upregulated in 72% of all PDAC cases. | Restricted to vascular endothelium. VEGFR2 expression is increased in pancreatitis. | 75, 154, 168, 169 |

# REFERENCES


1. Vincent A, Herman J, Schulick R, et al. Pancreatic cancer. Lancet, 2011;378:607-20.
2. Jang JY, Kang MJ, Heo JS, et al. A prospective randomized controlled study comparing outcomes of standard resection and extended resection, including dissection of the nerve plexus and various lymph nodes, in patients with pancreatic head cancer. Ann Surg, 2014;259:656-64.
3. Tummala P, Junaidi O,Agarwal B Imaging of pancreatic cancer: An overview. J Gastrointest Oncol, 2011;2:168-74.
4. Agarwal B, Correa AM,Ho L Survival in pancreatic carcinoma based on tumor size. Pancreas, 2008;36:e15-20.
5. Stathis A,Moore MJ Advanced pancreatic carcinoma: current treatment and future challenges. Nat Rev Clin Oncol, 2010;7:163-72.
6. Barugola G, Partelli S, Marcucci S, et al. Resectable pancreatic cancer: who really benefits from resection? Ann Surg Oncol, 2009;16:3316-22.
7. Verbeke CS Resection margins and R1 rates in pancreatic cancer--are we there yet? Histopathology, 2008;52:787-96.
8. Verbeke CS, Leitch D, Menon KV, et al. Redefining the R1 resection in pancreatic cancer. Br J Surg, 2006;93:1232-7.
9. Gao D, Gao L, Zhang C, et al. A near-infrared phthalocyanine dye-labeled agent for integrin alphavbeta6-targeted theranostics of pancreatic cancer. Biomaterials, 2015;53:229-38.
10. Hartwig W, Werner J, Jager D, et al. Improvement of surgical results for pancreatic cancer. Lancet Oncol, 2013;14:e476-85.
11. Laeseke PF, Chen R, Jeffrey RB, et al. Combining in Vitro Diagnostics with in Vivo Imaging for Earlier Detection of Pancreatic Ductal Adenocarcinoma: Challenges and Solutions. Radiology, 2015;277:644-61.
12. Balci NC,Semelka RC Radiologic diagnosis and staging of pancreatic ductal adenocarcinoma. Eur J Radiol, 2001;38:105-12.
13. Cote GA, Smith J, Sherman S, et al. Technologies for imaging the normal and diseased pancreas. Gastroenterology, 2013;144:1262-1271.
14. Kramer-Marek G, Gore J,Korc M Molecular imaging in pancreatic cancer--a roadmap for therapeutic decisions. Cancer Lett, 2013;341:132-138.
15. Haycox A, Lombard M, Neoptolemos J, et al. Review article: current practice and future perspectives in detection and diagnosis of pancreatic cancer. Aliment Pharmacol Ther, 1998;12:937-48.
16. Ahmad NA, Kochman ML, Brensinger C, et al. Interobserver agreement among endosonographers for the diagnosis of neoplastic versus non-neoplastic pancreatic cystic lesions. Gastrointest Endosc, 2003;58:59-64.
17. DeWitt J, Devereaux B, Chriswell M, et al. Comparison of endoscopic ultrasonography and multidetector computed tomography for detecting and staging pancreatic cancer. Ann Intern Med, 2004;141:753-63.
18. Ellsmere J, Mortele K, Sahani D, et al. Does multidetector-row CT eliminate the role of diagnostic laparoscopy in assessing the resectability of pancreatic head adenocarcinoma? Surg Endosc, 2005;19:369-73.
19. Zamboni GA, Kruskal JB, Vollmer CM, et al. Pancreatic adenocarcinoma: value of multidetector CT angiography in preoperative evaluation. Radiology, 2007;245:770-8.
20. Deshmukh SD, Willmann JK,Jeffrey RB Pathways of extrapancreatic perineural invasion by pancreatic adenocarcinoma: evaluation with 3D volume-rendered MDCT imaging. AJR Am J Roentgenol, 2010;194:668-74.
21. Chang ST, Jeffrey RB, Patel BN, et al. Preoperative Multidetector CT Diagnosis of Extrapancreatic Perineural or Duodenal Invasion Is Associated with Reduced Postoperative Survival after Pancreaticoduodenectomy for Pancreatic Adenocarcinoma: Preliminary Experience and Implications for Patient Care. Radiology, 2016;281:816-825.
22. D'Onofrio M, Gallotti A, Mantovani W, et al. Perfusion CT can predict tumoral grading of pancreatic adenocarcinoma. Eur J Radiol, 2013;82:227-33.

23. Prokesch RW, Chow LC, Beaulieu CF, et al. Isoattenuating pancreatic adenocarcinoma at multi-detector row CT: secondary signs. Radiology, 2002;224:764-8.
24. Kauhanen SP, Komar G, Seppanen MP, et al. A prospective diagnostic accuracy study of 18F-fluorodeoxyglucose positron emission tomography/computed tomography, multidetector row computed tomography, and magnetic resonance imaging in primary diagnosis and staging of pancreatic cancer. Ann Surg, 2009;250:957-63.
25. Bipat S, Phoa SS, van Delden OM, et al. Ultrasonography, computed tomography and magnetic resonance imaging for diagnosis and determining resectability of pancreatic adenocarcinoma: a meta-analysis. J Comput Assist Tomogr, 2005;29:438-45.
26. Raman SP, Horton KM,Fishman EK Multimodality imaging of pancreatic cancer-computed tomography, magnetic resonance imaging, and positron emission tomography. Cancer J, 2012;18:511-22.
27. Adamek HE, Albert J, Breer H, et al. Pancreatic cancer detection with magnetic resonance cholangiopancreatography and endoscopic retrograde cholangiopancreatography: a prospective controlled study. Lancet, 2000;356:190-3.
28. Vachiranubhap B, Kim YH, Balci NC, et al. Magnetic resonance imaging of adenocarcinoma of the pancreas. Top Magn Reson Imaging, 2009;20:3-9.
29. Epelbaum R, Frenkel A, Haddad R, et al. Tumor aggressiveness and patient outcome in cancer of the pancreas assessed by dynamic18F-FDG PET/CT. Journal of Nuclear Medicine, 2013;54:12-18.
30. Lee JW, Kang CM, Choi HJ, et al. Prognostic value of metabolic tumor volume and total lesion glycolysis on preoperative18f-fdg pet/ct in patients with pancreatic cancer. Journal of Nuclear Medicine, 2014;55:898-904.
31. Gambhir SS, Czernin J, Schwimmer J, et al. A tabulated summary of the FDG PET literature. J Nucl Med, 2001;42:1S-93S.
32. Choi M, Heilbrun LK, Venkatramanamoorthy R, et al. Using 18F-fluorodeoxyglucose positron emission tomography to monitor clinical outcomes in patients treated with neoadjuvant chemo-radiotherapy for locally advanced pancreatic cancer. Am J Clin Oncol, 2010;33:257-261.
33. Paula Ghaneh WLW, Andrew Titman, Catrin Plumpton, et al. PET-PANC: Multi-centre prospective diagnostic accuracy and clinical value trial of FDG PET/CT in the diagnosis and management of suspected pancreatic cancer. J Clin Oncol, 2016;34:(suppl; abstr 4008).
34. Yokoyama Y, Nagino M, Hiromatsu T, et al. Intense PET signal in the degenerative necrosis superimposed on chronic pancreatitis. Pancreas, 2005;31:192-4.
35. Vahrmeijer AL, Hutteman M, van der Vorst JR, et al. Image-guided cancer surgery using near-infrared fluorescence. Nat Rev Clin Oncol, 2013;10:507-18.
36. Olubiyi OI, Ozdemir A, Incekara F, et al. Intraoperative Magnetic Resonance Imaging in Intracranial Glioma Resection: A Single-Center, Retrospective Blinded Volumetric Study. World Neurosurg, 2015;84:528-36.
37. Nelson DW, Blanchard TH, Causey MW, et al. Examining the accuracy and clinical usefulness of intraoperative frozen section analysis in the management of pancreatic lesions. Am J Surg, 2013;205:613-7; discussion 617.
38. Kooby DA, Lad NL, Squires MH, 3rd, et al. Value of intraoperative neck margin analysis during Whipple for pancreatic adenocarcinoma: a multicenter analysis of 1399 patients. Ann Surg, 2014;260:494-501; discussion 501-3.
39. Lad NL, Squires MH, Maithel SK, et al. Is it time to stop checking frozen section neck margins during pancreaticoduodenectomy? Ann Surg Oncol, 2013;20:3626-33.
40. Dillhoff M, Yates R, Wall K, et al. Intraoperative assessment of pancreatic neck margin at the time of pancreaticoduodenectomy increases likelihood of margin-negative resection in patients with pancreatic cancer. J Gastrointest Surg, 2009;13:825-30.
41. Harris PL, Rumley TO, Lineaweaver WC, et al. Pancreatic cancer: unreliability of frozen section in diagnosis. South Med J, 1985;78:1053-6.

42. Witz M, Shkolnik Z,Dinbar A Intraoperative pancreatic biopsy--a diagnostic dilemma. J Surg Oncol, 1989;42:117-9.
43. Kruskal JB,Kane RA Intraoperative ultrasonography of the pancreas: techniques and clinical applications. Surg Technol Int, 1997;6:49-57.
44. Sun MR, Brennan DD, Kruskal JB, et al. Intraoperative ultrasonography of the pancreas. Radiographics, 2010;30:1935-53.
45. Hata S, Imamura H, Aoki T, et al. Value of visual inspection, bimanual palpation, and intraoperative ultrasonography during hepatic resection for liver metastases of colorectal carcinoma. World J Surg, 2011;35:2779-87.
46. Handgraaf HJ, Boonstra MC, Van Erkel AR, et al. Current and future intraoperative imaging strategies to increase radical resection rates in pancreatic cancer surgery. Biomed Res Int, 2014;2014:890230.
47. Bussom S,Saif MW Methods and rationale for the early detection of pancreatic cancer. Highlights from the "2010 ASCO Gastrointestinal Cancers Symposium". Orlando, FL, USA. January 22-24, 2010. Jop, 2010;11:128-30.
48. Mondal SB, Gao S, Zhu N, et al. Real-time fluorescence image-guided oncologic surgery. Adv Cancer Res, 2014;124:171-211.
49. Conroy T, Desseigne F, Ychou M, et al. FOLFIRINOX versus gemcitabine for metastatic pancreatic cancer. N Engl J Med, 2011;364:1817-25.
50. Ferrone CR, Marchegiani G, Hong TS, et al. Radiological and surgical implications of neoadjuvant treatment with FOLFIRINOX for locally advanced and borderline resectable pancreatic cancer. Ann Surg, 2015;261:12-7.
51. Wang YY,Cui QC [Recent advances in gene change of pancreatic cancer]. Zhongguo Yi Xue Ke Xue Yuan Xue Bao, 2004;26:79-82.
52. Jones S, Zhang X, Parsons DW, et al. Core signaling pathways in human pancreatic cancers revealed by global genomic analyses. Science, 2008;321:1801-6.
53. Harsha HC, Kandasamy K, Ranganathan P, et al. A compendium of potential biomarkers of pancreatic cancer. PLoS Med, 2009;6:e1000046.
54. van Oosten M, Crane LM, Bart J, et al. Selecting Potential Targetable Biomarkers for Imaging Purposes in Colorectal Cancer Using TArget Selection Criteria (TASC): A Novel Target Identification Tool. Transl Oncol, 2011;4:71-82.
55. James ML,Gambhir SS A molecular imaging primer: modalities, imaging agents, and applications. Physiol Rev, 2012;92:897-965.
56. Argani P, Rosty C, Reiter RE, et al. Discovery of new markers of cancer through serial analysis of gene expression: prostate stem cell antigen is overexpressed in pancreatic adenocarcinoma. Cancer Res, 2001;61:4320-4.
57. Iacobuzio-Donahue CA, Ashfaq R, Maitra A, et al. Highly expressed genes in pancreatic ductal adenocarcinomas: a comprehensive characterization and comparison of the transcription profiles obtained from three major technologies. Cancer Res, 2003;63:8614-22.
58. Nichols LS, Ashfaq R,Iacobuzio-Donahue CA Claudin 4 protein expression in primary and metastatic pancreatic cancer: support for use as a therapeutic target. Am J Clin Pathol, 2004;121:226-30.
59. Korner M, Hayes GM, Rehmann R, et al. Secretin receptors in normal and diseased human pancreas: marked reduction of receptor binding in ductal neoplasia. Am J Pathol, 2005;167:959-68.
60. Jensen RT, Wank SA, Rowley WH, et al. Interaction of CCK with pancreatic acinar cells. Trends Pharmacol Sci, 1989;10:418-23.
61. Reubi JC In vitro evaluation of VIP/PACAP receptors in healthy and diseased human tissues. Clinical implications. Ann N Y Acad Sci, 2000;921:1-25.
62. Nock B, Nikolopoulou A, Chiotellis E, et al. [99mTc]Demobesin 1, a novel potent bombesin analogue for GRP receptor-targeted tumour imaging. Eur J Nucl Med Mol Imaging, 2003;30:247-58.
63. Yang L, Mao H, Cao Z, et al. Molecular imaging of pancreatic cancer in an animal model using targeted multifunctional nanoparticles. Gastroenterology, 2009;136:1514-1525.
64. Montet X, Weissleder R,Josephson L Imaging pancreatic cancer with a peptide-nanoparticle conjugate targeted to normal pancreas. Bioconjug.Chem, 2006;17:905-911.

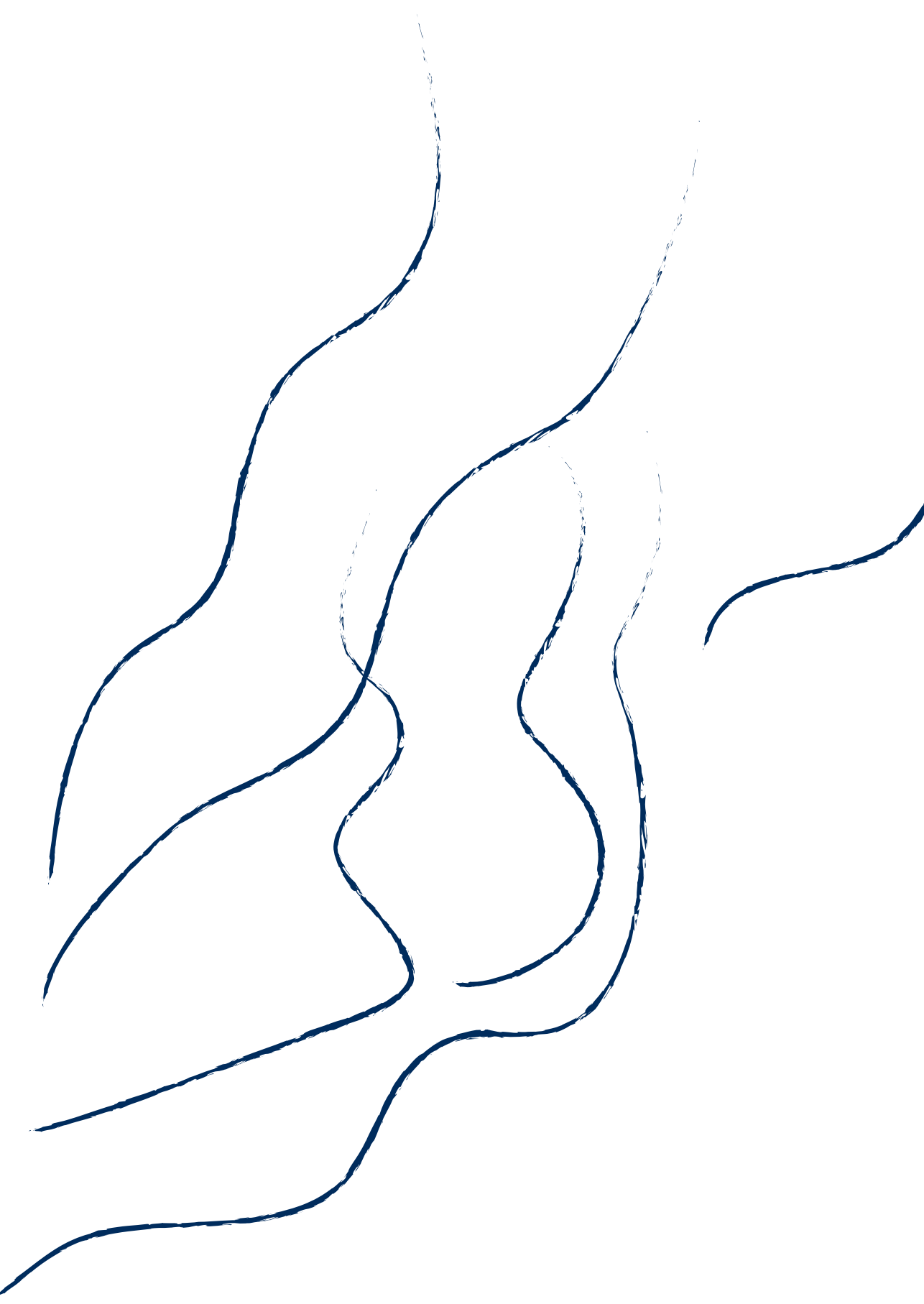
65. Sofuni A, Iijima H, Moriyasu F, et al. Differential diagnosis of pancreatic tumors using ultrasound contrast imaging. J Gastroenterol, 2005;40:518-25.
66. Fan Z, Li Y, Yan K, et al. Application of contrast-enhanced ultrasound in the diagnosis of solid pancreatic lesions--a comparison of conventional ultrasound and contrast-enhanced CT. Eur J Radiol, 2013;82:1385-90.
67. Kitano M, Kudo M, Yamao K, et al. Characterization of small solid tumors in the pancreas: the value of contrast-enhanced harmonic endoscopic ultrasonography. Am J Gastroenterol, 2012;107:303-10.
68. Pysz MA,Willmann JK Targeted contrast-enhanced ultrasound: an emerging technology in abdominal and pelvic imaging. Gastroenterology, 2011;140:785-90.
69. Deshpande N, Needles A,Willmann JK Molecular ultrasound imaging: current status and future directions. Clin Radiol, 2010;65:567-81.
70. Kircher MF,Willmann JK Molecular body imaging: MR imaging, CT, and US. part I. principles. Radiology, 2012;263:633-43.
71. Kircher MF,Willmann JK Molecular body imaging: MR imaging, CT, and US. Part II. Applications. Radiology, 2012;264:349-68.
72. Abou-Elkacem L, Bachawal SV,Willmann JK Ultrasound molecular imaging: Moving toward clinical translation. Eur J Radiol, 2015;84:1685-93.
73. Tranquart F, Arditi M, Bettinger T, et al. Ultrasound Contrast Agents For Ultrasound Molecular Imaging. Zeitschrift fur Gastroenterologie, 2014;52:1268-1276.
74. Bergers G,Benjamin LE Tumorigenesis and the angiogenic switch. Nat Rev Cancer, 2003;3:401-10.
75. de Geus SW, Boogerd LS, Swijnenburg RJ, et al. Selecting Tumor-Specific Molecular Targets in Pancreatic Adenocarcinoma: Paving the Way for Image-Guided Pancreatic Surgery. Mol Imaging Biol, 2016.
76. Pysz MA, Machtaler SB, Seeley ES, et al. Vascular endothelial growth factor receptor type 2-targeted contrast-enhanced US of pancreatic cancer neovasculature in a genetically engineered mouse model: potential for earlier detection. Radiology, 2015;274:790-799.
77. Deshpande N, Ren Y, Foygel K, et al. Tumor angiogenic marker expression levels during tumor growth: longitudinal assessment with molecularly targeted microbubbles and US imaging. Radiology, 2011;258:804-811.
78. Willmann JK BL, Testa A, Rinaldi P, Rindi G, Valluru KS, Petrone G, Martini M, Lutz AM, Gambhir SS Ultrasound Molecular Imaging in Patients with Breast and Ovarian Lesions: First-In-Human Results. Journal of Clinical Oncology, 2017;in press.
79. Foygel K, Wang H, Machtaler S, et al. Detection of pancreatic ductal adenocarcinoma in mice by ultrasound imaging of thymocyte differentiation antigen 1. Gastroenterology, 2013;145:885-894.
80. Pirollo KF, Dagata J, Wang P, et al. A tumor-targeted nanodelivery system to improve early MRI detection of cancer. Mol Imaging, 2006;5:41-52.
81. Yang L, Mao H, Wang YA, et al. Single chain epidermal growth factor receptor antibody conjugated nanoparticles for in vivo tumor targeting and imaging. Small, 2009;5:235-43.
82. Bausch D, Thomas S, Mino-Kenudson M, et al. Plectin-1 as a novel biomarker for pancreatic cancer. Clin Cancer Res, 2011;17:302-9.
83. Medarova Z, Pham W, Kim Y, et al. In vivo imaging of tumor response to therapy using a dual-modality imaging strategy. Int J Cancer, 2006;118:2796-2802.
84. Moore A, Medarova Z, Potthast A, et al. In vivo targeting of underglycosylated MUC-1 tumor antigen using a multimodal imaging probe. Cancer Res, 2004;64:1821-7.
85. Dorn DC, Harnack U,Pecher G Down-regulation of the human tumor antigen mucin by gemcitabine on the pancreatic cancer cell line capan-2. Anticancer Res, 2004;24:821-5.
86. Aung W, Jin ZH, Furukawa T, et al. Micro-positron emission tomography/contrast-enhanced computed tomography imaging of orthotopic pancreatic tumor-bearing mice using the alphavbeta(3) integrin tracer (6)(4) Cu-labeled cyclam-RAFT-c(-RGDfK-)(4). Mol Imaging, 2013;12:376-387.
87. Haglund C, Lindgren J, Roberts PJ, et al. Gastrointestinal cancer-associated antigen CA 19-9 in histological specimens of pancreatic tumours and pancreatitis. Br J Cancer, 1986;53:189-95.

88. Loy TS, Sharp SC, Andershock CJ, et al. Distribution of CA 19-9 in adenocarcinomas and transitional cell carcinomas. An immunohistochemical study of 527 cases. Am J Clin Pathol, 1993;99:726-8.
89. Houghton JL, Zeglis BM, Abdel-Atti D, et al. Site-specifically labeled CA19.9-targeted immunoconjugates for the PET, NIRF, and multimodal PET/NIRF imaging of pancreatic cancer. Proc Natl Acad Sci U S A, 2015;112:15850-5.
90. Makovitzky J The distribution and localization of the monoclonal antibody-defined antigen 19-9 (CA19-9) in chronic pancreatitis and pancreatic carcinoma. An immunohistochemical study. Virchows Arch B Cell Pathol Incl Mol Pathol, 1986;51:535-44.
91. Hackel BJ, Kimura RH, Miao Z, et al. 18F-fluorobenzoate-labeled cystine knot peptides for PET imaging of integrin alphavbeta6. J Nucl.Med, 2013;54:1101-1105.
92. Hausner SH, Abbey CK, Bold RJ, et al. Targeted in vivo imaging of integrin alphavbeta6 with an improved radiotracer and its relevance in a pancreatic tumor model. Cancer Research, 2009;69:5843-5850.
93. Gao D, Gao L, Zhang C, et al. A near-infrared phthalocyanine dye-labeled agent for integrin alphavbeta6-targeted theranostics of pancreatic cancer. Biomaterials, 2015;53:229-238.
94. Kimura RH, Teed R, Hackel BJ, et al. Pharmacokinetically stabilized cystine knot peptides that bind alpha-v-beta-6 integrin with single-digit nanomolar affinities for detection of pancreatic cancer. Clin Cancer Res, 2012;18:839-849.
95. Liu Z, Liu H, Ma T, et al. Integrin alphavbeta6-Targeted SPECT Imaging for Pancreatic Cancer Detection. J Nucl.Med, 2014;55:989-994.
96. Zhu X, Li J, Hong Y, et al. 99mTc-labeled cystine knot peptide targeting integrin alphavbeta6 for tumor SPECT imaging. Mol Pharm, 2014;11:1208-1217.
97. van den Berg YW, Osanto S, Reitsma PH, et al. The relationship between tissue factor and cancer progression: insights from bench and bedside. Blood, 2012;119:924-32.
98. Nitori N, Ino Y, Nakanishi Y, et al. Prognostic significance of tissue factor in pancreatic ductal adenocarcinoma. Clin Cancer Res, 2005;11:2531-9.
99. Hong H, Zhang Y, Nayak TR, et al. Immuno-PET of tissue factor in pancreatic cancer. Journal of Nuclear Medicine, 2012;53:1748-1754.
100. Chen R, Yi EC, Donohoe S, et al. Pancreatic cancer proteome: the proteins that underlie invasion, metastasis, and immunologic escape. Gastroenterology, 2005;129:1187-97.
101. McCabe KE, Liu B, Marks JD, et al. An engineered cysteine-modified diabody for imaging activated leukocyte cell adhesion molecule (ALCAM)-positive tumors. Mol Imaging Biol, 2012;14:336-347.
102. Ryschich E, Huszty G, Knaebel HP, et al. Transferrin receptor is a marker of malignant phenotype in human pancreatic cancer and in neuroendocrine carcinoma of the pancreas. Eur J Cancer, 2004;40:1418-22.
103. Sugyo A, Tsuji AB, Sudo H, et al. Preclinical evaluation of (8)(9)Zr-labeled human antitransferrin receptor monoclonal antibody as a PET probe using a pancreatic cancer mouse model. Nucl.Med Commun, 2015;36:286-294.
104. de Boer E, Harlaar NJ, Taruttis A, et al. Optical innovations in surgery. Br J Surg, 2015;102:e56-72.
105. van der Vorst JR, Schaafsma BE, Hutteman M, et al. Near-infrared fluorescence-guided resection of colorectal liver metastases. Cancer, 2013;119:3411-8.
106. Troyan SL, Kianzad V, Gibbs-Strauss SL, et al. The FLARE intraoperative near-infrared fluorescence imaging system: a first-in-human clinical trial in breast cancer sentinel lymph node mapping. Ann Surg Oncol, 2009;16:2943-52.
107. Mieog JS, Troyan SL, Hutteman M, et al. Toward optimization of imaging system and lymphatic tracer for near-infrared fluorescent sentinel lymph node mapping in breast cancer. Ann Surg Oncol, 2011;18:2483-91.
108. van Dam GM, Themelis G, Crane LM, et al. Intraoperative tumor-specific fluorescence imaging in ovarian cancer by folate receptor-alpha targeting: first in-human results. Nat Med, 2011;17:1315-9.
109. van der Vorst JR, Schaafsma BE, Verbeek FP, et al. Dose optimization for near-infrared fluorescence sentinel lymph node mapping in patients with melanoma. Br J Dermatol, 2013;168:93-8.

110. Crane LM, Themelis G, Arts HJ, et al. Intraoperative near-infrared fluorescence imaging for sentinel lymph node detection in vulvar cancer: first clinical results. Gynecol Oncol, 2011;120:291-5.
111. Hutteman M, van der Vorst JR, Gaarenstroom KN, et al. Optimization of near-infrared fluorescent sentinel lymph node mapping for vulvar cancer. Am J Obstet Gynecol, 2012;206:89 e1-5.
112. van der Vorst JR, Hutteman M, Gaarenstroom KN, et al. Optimization of near-infrared fluorescent sentinel lymph node mapping in cervical cancer patients. Int J Gynecol Cancer, 2011;21:1472-8.
113. Crane LM, Themelis G, Pleijhuis RG, et al. Intraoperative multispectral fluorescence imaging for the detection of the sentinel lymph node in cervical cancer: a novel concept. Mol Imaging Biol, 2011;13:1043-9.
114. Tummers WS, Miller SE, Teraphongphom NT, et al. Intraoperative Pancreatic Cancer Detection using Tumor-Specific Multimodality Molecular Imaging. Ann Surg Oncol, 2018;25:1880-1888.
115. Zhang C, Kimura R, Abou-Elkacem L, et al. A Cystine Knot Peptide Targeting Integrin alphavbeta6 for Photoacoustic and Fluorescence Imaging of Tumors in Living Subjects. J Nucl Med, 2016.
116. Cruz-Monserrate Z, Abd-Elgaliel WR, Grote T, et al. Detection of pancreatic cancer tumours and precursor lesions by cathepsin E activity in mouse models. Gut, 2012;61:1315-22.
117. Abd-Elgaliel WR, Cruz-Monserrate Z, Logsdon CD, et al. Molecular imaging of Cathepsin E-positive tumors in mice using a novel protease-activatable fluorescent probe. Molecular Biosystems, 2011;7:3207-3213.
118. Weissleder R, Tung CH, Mahmood U, et al. In vivo imaging of tumors with protease-activated near-infrared fluorescent probes. Nat Biotechnol, 1999;17:375-8.
119. Hellebust A,Richards-Kortum R Advances in molecular imaging: targeted optical contrast agents for cancer diagnostics. Nanomedicine (Lond), 2012;7:429-45.
120. Whitley MJ, Cardona DM, Lazarides AL, et al. A mouse-human phase 1 co-clinical trial of a protease-activated fluorescent probe for imaging cancer. Sci Transl Med, 2016;8:320ra4.
121. Zackrisson S, van de Ven SM,Gambhir SS Light in and sound out: emerging translational strategies for photoacoustic imaging. Cancer Res, 2014;74:979-1004.
122. Wilson KE, Wang TY,Willmann JK Acoustic and photoacoustic molecular imaging of cancer. J Nucl Med, 2013;54:1851-4.
123. Valluru KS, Wilson KE,Willmann JK Photoacoustic Imaging in Oncology: Translational Preclinical and Early Clinical Experience. Radiology, 2016;280:332-49.
124. Valluru KS,Willmann JK Clinical photoacoustic imaging of cancer. Ultrasonography, 2016;35:267-80.
125. Homan KA, Souza M, Truby R, et al. Silver nanoplate contrast agents for in vivo molecular photoacoustic imaging. ACS nano, 2012;6:641-650.
126. Kim G, Huang SW, Day KC, et al. Indocyanine-green-embedded PEBBLEs as a contrast agent for photoacoustic imaging. J Biomed Opt, 2007;12:044020.
127. Brakmane G, Madani SY,Seifalian A Cancer antibody enhanced real time imaging cell probes--a novel theranostic tool using polymer linked carbon nanotubes and quantum dots. Anticancer Agents Med Chem, 2013;13:821-832.
128. De la Zerda A, Zavaleta C, Keren S, et al. Carbon nanotubes as photoacoustic molecular imaging agents in living mice. Nat Nanotechnol, 2008;3:557-62.
129. Erogbogbo F, Liu X, May JL, et al. Plasmonic gold and luminescent silicon nanoplatforms for multimode imaging of cancer cells. Integrative Biology (United Kingdom), 2013;5:144-150.
130. Shashkov EV, Everts M, Galanzha EI, et al. Quantum dots as multimodal photoacoustic and photothermal contrast agents. Nano Lett, 2008;8:3953-8.
131. Zaman MB, Baral TN, Jakubek ZJ, et al. Single-domain antibody bioconjugated near-IR quantum dots for targeted cellular imaging of pancreatic cancer. J Nanosci.Nanotechnol., 2011;11:3757-3763.
132. Jain RK Delivery of molecular medicine to solid tumors: lessons from in vivo imaging of gene expression and function. J Control Release, 2001;74:7-25.

133. Wilson KE BS, Abou-Elkacem L, Jensen K, Machtaler S, Tian L, Willmann JK. Spectroscopic Photoacoustic Molecular Imaging of Breast Cancer using a B7-H3-targeted ICG contrast agent. Theranostics, 2017;(in press).
134. Levi J, Sathirachinda A,Gambhir SS A high-affinity, high-stability photoacoustic agent for imaging gastrin-releasing peptide receptor in prostate cancer. Clin Cancer Res, 2014;20:3721-9.
135. Levi J, Kothapalli SR, Bohndiek S, et al. Molecular photoacoustic imaging of follicular thyroid carcinoma. Clin Cancer Res, 2013;19:1494-502.
136. Li J, Liu J, Wei CW, et al. Emerging applications of conjugated polymers in molecular imaging. Phys Chem Chem Phys, 2013;15:17006-15.
137. Balasundaram G, Ho CJ, Li K, et al. Molecular photoacoustic imaging of breast cancer using an actively targeted conjugated polymer. Int J Nanomedicine, 2015;10:387-97.
138. Levi J, Kothapalli SR, Ma TJ, et al. Design, synthesis, and imaging of an activatable photoacoustic probe. J Am Chem Soc, 2010;132:11264-9.
139. Zavaleta CL, Kircher MF,Gambhir SS Raman's "effect" on molecular imaging. J Nucl Med, 2011;52:1839-44.
140. Jokerst JV, Pohling C,Gambhir SS Molecular imaging with surface-enhanced Raman spectroscopy nanoparticle reporters. MRS Bull, 2013;38.
141. D.L. Jeanmaire RPVD Surface Raman Spectroelectrochemistry Part I. Heterocyclic, Aromatic, and Aliphatic Amines Adsorbed on the Anodized Silver Electrode. J. Electroanal. Chem., 1977;84:1-20.
142. Fleischmann MH, P. J.; McQuillan, A. J. Raman spectra of pyridine adsorbed at a silver electrode. Chemical Physics Letters, 1974;26:163-166.
143. Zavaleta CL, Garai E, Liu JT, et al. A Raman-based endoscopic strategy for multiplexed molecular imaging. Proc Natl Acad Sci U S A, 2013;110:E2288-97.
144. Zavaleta CL, Hartman KB, Miao Z, et al. Preclinical evaluation of Raman nanoparticle biodistribution for their potential use in clinical endoscopy imaging. Small, 2011;7:2232-40.
145. Garai E, Sensarn S, Zavaleta CL, et al. A real-time clinical endoscopic system for intraluminal, multiplexed imaging of surface-enhanced Raman scattering nanoparticles. PLoS One, 2015;10:e0123185.
146. Jermyn M, Mok K, Mercier J, et al. Intraoperative brain cancer detection with Raman spectroscopy in humans. Sci Transl Med, 2015;7:274ra19.
147. Kircher MF, de la Zerda A, Jokerst JV, et al. A brain tumor molecular imaging strategy using a new triple-modality MRI-photoacoustic-Raman nanoparticle. Nat Med, 2012;18:829-34.
148. Stone N,Matousek P Advanced transmission Raman spectroscopy: a promising tool for breast disease diagnosis. Cancer Res, 2008;68:4424-30.
149. Michael B. Fenn PX, Georgios Pyrgiotakis, Stephen R. Grobmyer, Panos M. Pardalos, and Larry L. Hench Raman Spectroscopy for Clinical Oncology. Advances in Optical Technologies, 2011;2011:20.
150. Tummers WS, Warram JM, Tipirneni KE, et al. Regulatory Aspects of Optical Methods and Exogenous Targets for Cancer Detection. Cancer Res, 2017;77:2197-2206.
151. Sipos B, Hahn D, Carceller A, et al. Immunohistochemical screening for beta6-integrin subunit expression in adenocarcinomas using a novel monoclonal antibody reveals strong up-regulation in pancreatic ductal adenocarcinomas in vivo and in vitro. Histopathology, 2004;45:226-36.
152. Girgis MD, Kenanova V, Olafsen T, et al. Anti-CA19-9 diabody as a PET imaging probe for pancreas cancer. J Surg Res, 2011;170:169-78.
153. Azuma T, Yamada M, Murakita H, et al. Cathepsin E expressed in pancreatic cancer. Adv Exp Med Biol, 1995;362:363-6.
154. Michl P, Buchholz M, Rolke M, et al. Claudin-4: a new target for pancreatic cancer treatment using Clostridium perfringens enterotoxin. Gastroenterology, 2001;121:678-84.
155. Angelescu R, Burada F, Angelescu C, et al. Expression of vascular endothelial growth factor and epidermal growth factor receptor in pancreatic ductal adenocarcinomas, neuroendocrine tumours and chronic pancreatitis. Endosc Ultrasound, 2013;2:86-91.

156. Zhou L, Yu L, Ding G, et al. Overexpressions of DLL4 and CD105 are Associated with Poor Prognosis of Patients with Pancreatic Ductal Adenocarcinoma. Pathol Oncol Res, 2015;21:1141-7.
157. Argani P, Iacobuzio-Donahue C, Ryu B, et al. Mesothelin is overexpressed in the vast majority of ductal adenocarcinomas of the pancreas: identification of a new pancreatic cancer marker by serial analysis of gene expression (SAGE). Clin Cancer Res, 2001;7:3862-8.
158. Hassan R, Laszik ZG, Lerner M, et al. Mesothelin is overexpressed in pancreaticobiliary adenocarcinomas but not in normal pancreas and chronic pancreatitis. Am J Clin Pathol, 2005;124:838-45.
159. Matsuyama M, Kondo F, Ishihara T, et al. Evaluation of pancreatic intraepithelial neoplasia and mucin expression in normal pancreata. J Hepatobiliary Pancreat Sci, 2012;19:242-8.
160. Andrianifahanana M, Moniaux N, Schmied BM, et al. Mucin (MUC) gene expression in human pancreatic adenocarcinoma and chronic pancreatitis: a potential role of MUC4 as a tumor marker of diagnostic significance. Clin Cancer Res, 2001;7:4033-40.
161. Moniaux N, Chakraborty S, Yalniz M, et al. Early diagnosis of pancreatic cancer: neutrophil gelatinase-associated lipocalin as a marker of pancreatic intraepithelial neoplasia. Br J Cancer, 2008;98:1540-7.
162. Hogendorf P, Durczynski A, Skulimowski A, et al. Neutrophil Gelatinase-Associated Lipocalin (NGAL) concentration in urine is superior to CA19-9 and Ca 125 in differentiation of pancreatic mass: Preliminary report. Cancer Biomark, 2016;16:537-43.
163. Wente MN, Jain A, Kono E, et al. Prostate stem cell antigen is a putative target for immunotherapy in pancreatic cancer. Pancreas, 2005;31:119-25.
164. Kakkar AK, Lemoine NR, Scully MF, et al. Tissue factor expression correlates with histological grade in human pancreatic cancer. Br J Surg, 1995;82:1101-4.
165. Jeong SM, Hwang S,Seong RH Transferrin receptor regulates pancreatic cancer growth by modulating mitochondrial respiration and ROS generation. Biochem Biophys Res Commun, 2016;471:373-9.
166. Zhu J, Thakolwiboon S, Liu X, et al. Overexpression of CD90 (Thy-1) in pancreatic adenocarcinoma present in the tumor microenvironment. PLoS One, 2014;9:e115507.
167. Cantero D, Friess H, Deflorin J, et al. Enhanced expression of urokinase plasminogen activator and its receptor in pancreatic carcinoma. Br J Cancer, 1997;75:388-95.
168. Boonstra MC, Verspaget HW, Ganesh S, et al. Clinical applications of the urokinase receptor (uPAR) for cancer patients. Curr Pharm Des, 2011;17:1890-910.
169. Pochon S, Tardy I, Bussat P, et al. BR55: a lipopeptide-based VEGFR2-targeted ultrasound contrast agent for molecular imaging of angiogenesis. Invest Radiol, 2010;45:89-95.
170. Hicklin DJ,Ellis LM Role of the vascular endothelial growth factor pathway in tumor growth and angiogenesis. J Clin Oncol, 2005;23:1011-27.



Chapter | 3

# Tumor Characteristics and surgical technical aspects of R1 in pancreatic cancer surgery

Willemieke S Tummers, MD [1], Jesse V Groen, MD [1], Babs G Sibinga Mulder, B.S.[1], Arantza Farina-Sarasqueta, MD, PhD [2], Johannes Morreau, MD, PhD [2], Hein Putter, PhD [3], Cornelis J van de Velde, MD, PhD [1], Alexander L Vahrmeijer, MD, PhD [1], Bert A Bonsing, MD, PhD [1], J Sven Mieog, MD, PhD [1], Rutger-Jan Swijnenburg, MD, PhD [1]

[1]Department of Surgery, [2]Department of Pathology, and [3]Department of Medical Statistics, Leiden University Medical Center, Albinusdreef 2, 2300 RC, Leiden, The Netherlands

## ABSTRACT

**Background**: The prognosis of patients with PDAC remains poor and selection of patients for potentially curative surgery is challenging. Here, we examined the impact of margin-positive (R1) resection on locoregional recurrence and overall survival (OS), tumor characteristics and/or surgical technical factors that determine R1 resection in PDAC surgery, and how these factors affect outcome.

**Methods:** This retrospective study included 470 patients who underwent surgery for PDAC. The effect of tumor margin status, patient characteristics, and tumor characteristics on locoregional recurrence, distant recurrence, and OS were assessed.

**Results:** R1 resection was associated with decreased OS ($p<0.001$) and reduced time until locoregional recurrence ($p<0.005$). In contrast, disease recurrence patterns were similar between R1 and R0 patients. The main risk factors for early recurrence were tumor stage, tumor-positive lymph nodes (N1), and perineural invasion. Among patients with tumor-negative lymph nodes (N0), those with R1 resections had significantly reduced OS compared to patients who underwent R0 (radical) resection.

**Conclusion:** For pancreatic cancer surgery, R1 status is determined largely by the tumor characteristics. Although R1 resection is a major contributor to reduced survival and early recurrence, overall recurrence patterns are similar between R0 and R1 patients. Finally, in N0 patients, surgical factors affect R1 status.

# INTRODUCTION

The incidence of pancreatic ductal adenocarcinoma (PDAC) is increasing. Despite recent advances in cancer therapy, including improved chemotherapy regimens, overall survival (OS) among patients with PDAC remains poor.[1] Currently, radical surgical resection, combined with (neo)adjuvant chemotherapy, is the only potentially curative treatment. Unfortunately, among patients who undergo surgical resection, margin-positive resections (R1) and rate of recurrence are high.[2, 3] Several factors have been identified as potentially affecting outcome among patients who undergo surgical resection; these factors include resection margin status, tumor size, the presence of perineural and/or lymphangioinvasion, and lymph node status. Among these factors, margin status receives the most attention in literature, yet remains the most controversial and debatable factor.[4] More than two decades ago, Yeo et al. reported that patients who underwent a radical (R0) pancreatoduodenectomy had a 5-year survival rate of 26%, whereas patients who underwent an R1 resection had a 5-year survival rate of only 8%.[5] In addition, Ghaneh et al. recently reported the results of a large multicenter, randomized controlled trial in which they found a significant difference in median survival between R0 resection (24.9 months) and R1 direct positive margin resection (18.7 months).[6]



In contrast, a growing body of data has become available showing that resection margin status is not an independent risk factor for survival. [7-10] One reason suggested to explain this finding is the lack of a standard, international consensus for pathological evaluation and assessment, as well as the lack of a uniform definition of microscopic margin involvement.[11, 12] In addition to this lack of a clear definition, geographical differences have been observed. For example, in the US, a resection margin is considered to be positive if the tumor cells have reached the inked margin;[5, 13] in contrast, in Europe a resection is defined as R1 if the tumor is present within 1 mm of the resection margin.[11, 14, 15] This discrepancy has led to a wide range of reported rates of microscopic resection margin involvement (R1) from less than 20% to more than 75% of cases.[14, 16-20]

When using the R0 definition “absence of tumor tissue at the ink margin”, 50-80% of these patients will develop local recurrence.[21, 22] This finding indicates that this definition does not accurately represent clinically relevant outcomes such as disease-free survival (DFS). Recently, Osipov et al. reported an improved DFS when defining a R0 resection as tumor cells >2 mm from the margin; specifically, increasing the margin from 0.5 mm to 2 mm increased both OS and DFS, whereas further increasing the margin >2 mm did not significantly improve clinical outcome.[23] These results support reports by Chang et al.[24] and Gebauer et al.,[25] who recommend a resection margin definition of 1.5 mm or 2 mm. An alternative hypothesis suggests that recurrence following R1 resection is not due to residual tumor cells, but rather a more aggressive biology of the original tumor.[26, 27] This hypothesis is based on the finding that among patients with a recurrence, an isolated recurrence without distant metastases is relatively rare, occurring in only 10-25% of these patients.[7, 28]

In addition to a high rate of R1 resections, another major problem is the significant prevalence of early recurrence, either locoregional or at distant site, within six months following surgery. Although these patients underwent an extensive surgical procedure with high morbidity and a high risk of reduced quality of life, they received no oncologic benefit.

Here, we investigated a relatively large cohort of pancreatic cancer patients at a tertiary referral center in order to correlate microscopic margin status to survival, local control, and distance metastasis. In addition, we performed a subset analysis in order to investigate the impact of tumor biology characteristics and surgical technical aspects.

# MATERIALS AND METHODS

## Study design

This retrospective database study was approved by the Institutional Medical Ethics Committee at Leiden University Medical Center (LUMC) in Leiden, the Netherlands. Data were retrieved from the electronic patient records of all patients who underwent pancreatic cancer resection at LUMC from January 2006 through December 2016, and follow-up data were collected through October 2017. Patients were included in the study if the diagnosis of pancreaticobiliairy adenocarcinoma was confirmed by pathological examination; patients with any other histopathological diagnosis were excluded. The demographic information and patient characteristics collected in the database included the patient's age at the time of surgery, sex, and type of surgery. The tumor characteristics included pTNM stage, grade, histopathological diagnosis, lymph node involvement, and lymphangio- and/or perineural invasion.



For detailed information on the indications for surgery, adjuant therapy and follow-up plan, please see supplementary methods. Recurrence was defined as evidence of disease on an imaging scan. Local recurrence was defined as the presence of disease in the surgical bed. Regional recurrence was defined as presence in the mesentery, periaortic soft tissue, the pancreatojejunal anastomosis, or in the intracaval, periceliac, and/or retroperitoneal lymph nodes. Distant metastases were defined as the presence of disease in the omentum, peritoneum, solid organs, and/or pelvic lymph nodes. We defined early recurrence as recurrence that occurred within six months following surgery, based on the published definition.[29, 30]

## Pathological assessment

Macroscopic and microscopic examination of the pancreatoduodenectomy specimen was performed using standardized methods in accordance with the guidelines established by the Dutch Pancreatic Cancer Group (DPCG), which followed the recommendations reported by Verbeke and colleagues.[11, 14] Before 2010, examination was performed by bi-valving of the specimen in accordance to Rosai and Ackerman's surgical pathology and Adsay et al. After the specimen is resected, the surgeon attaches colored beads to specific resection margins. Upon receiving the specimen, the pathologist then uses multicolor inking of the

specimen in order to clearly identify the margins. The following terms were used to define the margins: posterior margin, vascular margin (superior mesenteric vein or superior mesenteric artery), common bile duct margin, anterior margin, pancreatic neck margin, caudal margin, and circumferential margin.

Histological findings were reviewed to confirm the diagnosis, tumor characteristics, and R1 status of the margins. Staging was determined using the TNM cancer staging system, 7$^{th}$ edition (2010). For this study, we used the following definition for R1 resection in accordance with Dutch guidelines: a surgical margin with malignant cells identified ⩽1 mm from the inked margin was considered positive, per the guidelines of the British Royal College of Pathology (RCPath).

### Statistical analyses

Data were analyzed using SPSS Statistics for Windows, version 23.0 (IBM Corp., Armonk, NY). For a detailed statistical plan, please see supplementary methods. Kaplan-Meier analysis and the log-rank test were used to analyze differences in survival between groups. Characteristics that were found to be correlated with either recurrence status or survival were included in a Cox proportional hazards regression analysis. Differences were considered statistically significant at $p<0.05$.

## RESULTS

From January 2006 through December 2016, a total of 470 patients underwent surgery for pancreaticobiliairy adenocarcinoma at our center. Among these 470 patients, 322 patients underwent resection (68.5%); the remaining 148 patients (31.5%) underwent exploratory surgery only, either with or without palliative bypass surgery due to distant metastases or non-resectable disease. Of the resected patients, 299 underwent Whipple surgery or pylorus-preserving pancreaticoduodenectomy (PPPD), 35 patients distal pancreatectomy, and 12 total pancreatectomy. Among the 322 resected patients, 193 (59.9%) had an R0 resection, and 129 patients (40.1%) had an R1 resection; 161 of these 322 patients were men, and 161 were women, the mean age was 65.4 years, and the median survival time following resection was 18.0 months. Compared to the

R0 group, more patients in the R1 group received adjuvant therapy (49.2% vs. 59.7%, respectively; p=0.065). Prior to adopting the so-called Verbeke protocol for grossing of pancreas specimens (i.e., from 2006 through 2009), the R1 resection rate was 32.4%; in 2010 and later, the R1 resection was 42.1%; these rates did not differ significantly (p=0.144). Compared to the patients in the R0 group, the patients who underwent an R1 resection (Table 1) had significantly larger tumors (p<0.001), more tumor-positive lymph nodes (p=0.001), and a higher prevalence of perineural invasion (p<0.001).



### *Patients with R1 resection have increased risk of recurrence*

Of all resected patients 60.9% of patients developed a form of recurrence at follow up after resection: 32.6% developed locoregional recurrence, 46.9% developed distant metastases. Time until locoregional recurrence was significantly shorter in the R1 resection group (median: 16 months; 95% CI: 12.5–19.5) compared to the R0 group (median: 36 months; 95% CI: 5.3–66.7; p<0.005) (Figure 1A). Interestingly, in the first 6 months following resection, the prevalence of locoregional recurrence was similar between the R1 and R0 groups (~8%) (Figure 1A). Time until distant metastases was also significantly shorter in the R1 group (median: 15 months; 95% CI: 10.6–19.4) compared to the R0 group (median: 20 months; 95% CI: 13.4–26.6; p<0.05) (Figure 1B). Among the patients who developed metastases, metastases developed more rapidly in the liver (median: 8 months; 95% CI: 6.8–9.2) compared to extrahepatic distant metastases (median: 13 months; 95% CI: 10.6–15.4; p<0.001) (Figure 1C). Finally, time until overall recurrence was significantly shorter in the R1 resection group (median: 13 months; 95% CI: 9.9–16.1) compared to the R0 resection group (median: 15 months; 95% CI: 12.2–17.9; p<0.001) (Figure 1D). Locoregional recurrence was significantly correlated with perineural invasion (HR: 1.62; p<0.04), and the only significant predictor of distant metastases was lymph node status (HR: 1.96; p<0.005) (Table S1).

### *R1 status of the vascular margin negatively influences outcome*

Next, an in-depth analysis was performed of the technical aspects of pancreatic cancer surgery and found that among the various surgical margins, the vascular margin was affected in 46.5% of patients who underwent an R1 resection (Supplementary Table S2). The location of the R1 margin had little effect on surgical outcome. Among the various margins, only the vascular margin

**Table 1.** Patient characteristics categorized by R0 and R1 resection.

| Variable | R0 (N=193) | R1 (N=129) | *p*-value |
|---|---|---|---|
| **Age in years, mean SD)** | 66 (10) | 64 (9) | 0.172 |
| **Sex, M/F** | 95/98 | 66/63 | 0.733 |
| **Death, N (%)** | 130 (67.4) | 101 (78.3) | 0.033 |
| **Median survival in months (95% CI)** | 22 (17.2-26.8) | 15 (12.6-17.4) | <0.001 |
| **Tumor size in mm, mean (SD)** | 26 (15) | 33 (15) | <0.001 |
| **Adjuvant therapy, N (%)** | 95 (49.2%) | 77 (59.7%) | 0.065 |
| **Tumor differentiation, N (%)** | | | 0.564 |
| **Well** | 40 (20.7) | 23 (17.8) | |
| **Moderate** | 80 (41.5) | 53 (41.1) | |
| **Poor** | 71 (36.8) | 53 (41.1) | |
| **Undifferentiated** | 2 (1.0) | 0 (0.0) | |
| **Lymph node status positive, N (%)** | 122 (63.2) | 100 (77.5) | 0.007 |
| **Median number of positive lymph nodes (IQR)** | 1 (0-3) | 3 (1-5) | 0.001 |
| **Tumor stage, N (%)** | | | <0.001 |
| **IA** | 23 (11.9) | 4 (3.1) | |
| **IB** | 9 (4.7) | 2 (1.6) | |
| **IIA** | 40 (20.7) | 19 (14.7) | |
| **IIB** | 118 (60.6) | 89 (69.0) | |
| **III** | 2 (1.0) | 13 (10.1) | |
| **IV** | 1 (0.5) | 2 (1.6) | |
| **Perineural invasion, N (%)** | 104 (53.9) | 97 (75.2) | <0.001 |
| **Lymphangioinvasion, N (%)** | 35 (18.1) | 35 (27.1) | 0.055 |

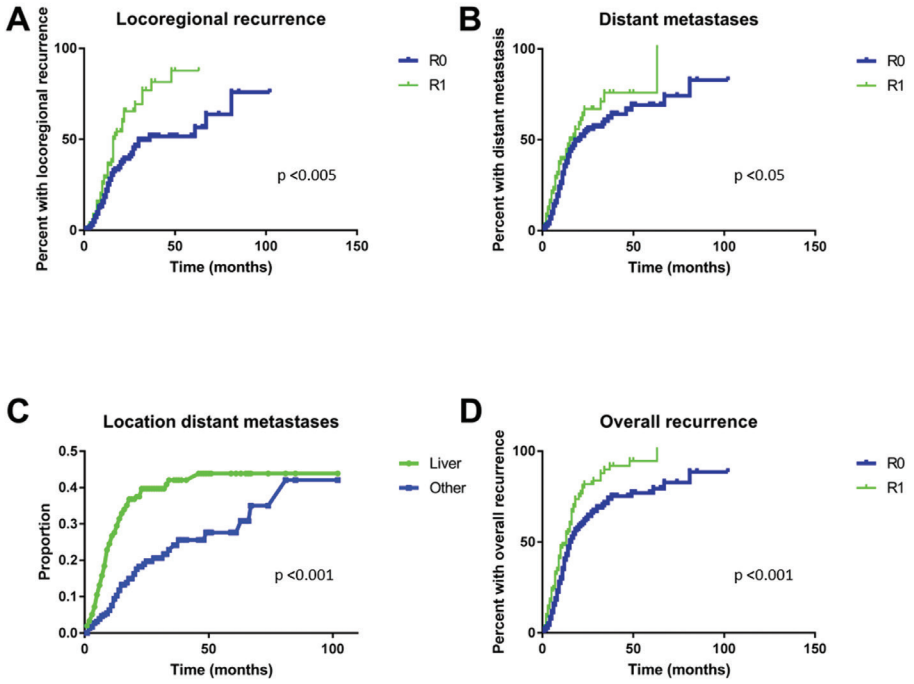



**Figure 1.** (A-B) Locoregional recurrence (A), and distant metastases (B) in patients who underwent R0 or R1 resection. (C) Time course of distant metastases in the liver or other locations. (D) Overall recurrence in patients who underwent R0 or R1 resection.



appeared to affect the clinically relevant outcome measures. Although the vascular margin did not affect OS (Figure S1A), performing an R1 resection at this margin increased the risk of local recurrence compared to other R1 margins, with a shorter amount of time until recurrence (median: 16 months; 95% CI: 14.5–17.5 vs. 28 months; 95% CI: 17.6–38.5; respectively; p=0.07) (Figure S1B). Other margins did not affect the time until local recurrence (Figure S1C). Lastly, distant metastases were not affected by the location of the R1 margin.

Among the 196 patients who had a recurrence, 55 (28.1%) had a recurrence within 6 months following surgery. The patients with early recurrence had a higher tumor stage, more tumor-positive lymph nodes, and a higher prevalence of perineural invasion compared to all other patients without a recurrence within 6 months following their resection, however none of these differences were significant (Table 2). Finally, among the patients who developed distant metastases, liver metastases were significantly more common in the early recurrence group compared to the patients in the late recurrence group (70.9% vs 22.5%, respectively; p<0.001).

**Table 2**. Patient characteristics categorized by time until recurrence.

| Variable | <6 months recurrence (N=55) | All other patients (N=267) | *p*-value |
|---|---|---|---|
| **Age in years, mean (SD)** | 64 (10) | 66(10) | 0.150 |
| **Sex, M/F** | 29/26 | 132/135 | 0.657 |
| **Death, N (%)** | 53 (96.4) | 185 (64.5) | <0.001 |
| **Median survival in months** | 8 | 23 | <0.001 |
| **Tumor size in mm, mean (SD)** | 32 (14) | 28 (16) | 0.083 |
| **Adjuvant therapy, N (%)** | 23 (41.8%) | 149 (55.8%) | 0.058 |
| **Tumor differentiation, N (%)** | | | 0.078 |
| **Well** | 6 (10.9) | 57 (21.3) | |
| **Moderate** | 20 (36.4) | 113 (42.3) | |
| **Poor** | 29 (52.7) | 95 (35.6) | |
| **Undifferentiated** | 0 (0.0) | 2 (0.7) | |
| **Lymph node status positive, N (%)** | 43 (78.2) | 179 (67.0) | 0.104 |
| **Median number of positive lymph nodes (IQR)** | 2 (0-4) | 2 (1-5) | 0.125 |
| **Tumor stage, N (%)** | | | 0.192 |
| **IA** | 2 (3.6) | 25 (9.4) | |
| **IB** | 1 (1.8) | 10 (3.7) | |
| **IIA** | 9 (16.4) | 50 (18.7) | |
| **IIB** | 38 (69.1) | 169 (63.3) | |
| **III** | 3 (5.5) | 12 (4.5) | |
| **IV** | 2 (3.6) | 1 (0.4) | |
| **Perineural invasion, N (%)** | 40 (72.7) | 161 (60.3) | 0.083 |
| **Lymphangio invasion, N (%)** | 15 (27.3) | 55 (20.6) | 0.275 |
| **Resection margin, N (%)** | | | 0.071 |
| **R0** | 27 (49.1) | 166 (62.2) | |
| **R1** | 28 (50.9) | 101 (37.8) | |

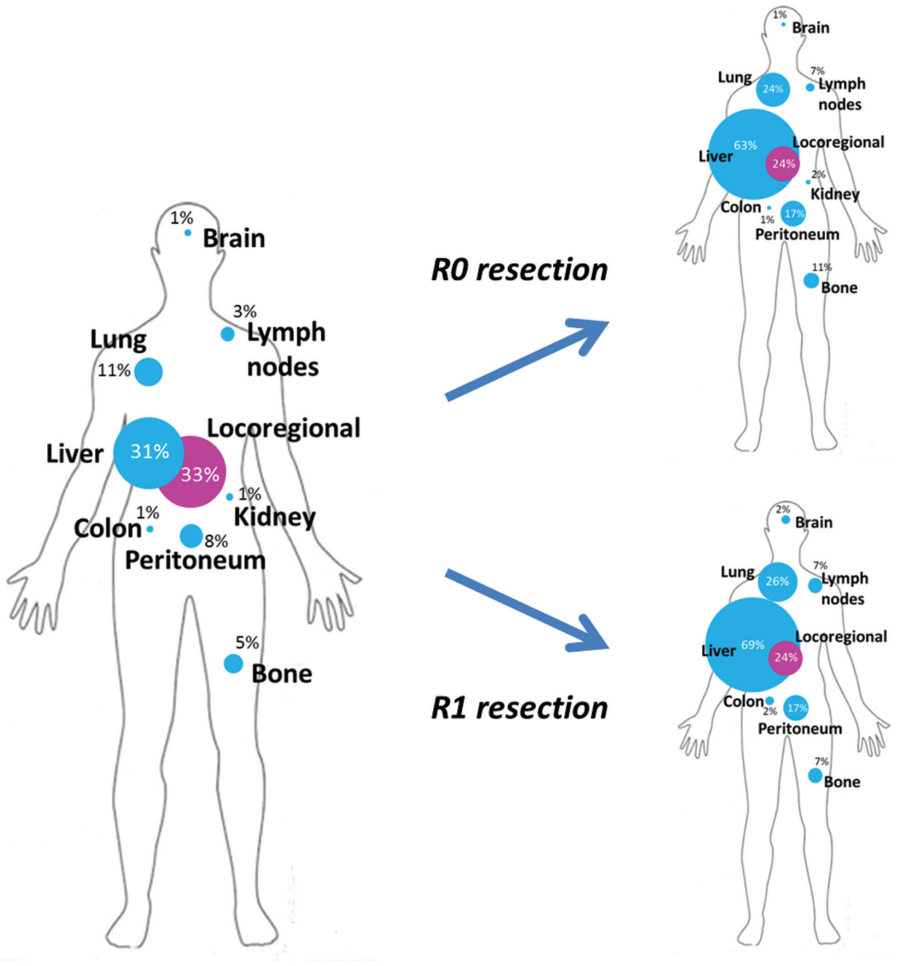



**Figure 2.** Spatial distribution of local recurrence (purple) and distant metastases (blue) following resection, for all patients (left) and only the patients with distant metastases sorted by R0 and R1 status (right).

### *Margin status does not affect long term patterns of recurrence*

Among the patients who developed metastases, the majority of these patients (n = 99) developed liver metastases as the first site of distant spread, compared to only 52 patients with other distant metastases (primarily lung metastases). However, we found no difference in the pattern of metastases between the R0 and R1 resection groups (Figure 2). Interestingly, among our entire patient cohort, 14% presented with distant metastases within 5 months, and of the

patients who develop distant metastases, 26.3% of patients had liver metastases within 6 months after resection.

### *R1 resection reflects poor tumor characteristics and leads to decreased overall survival*

The patients in the R1 resection group had significantly decreased OS time ($p<0.001$), with median survival of 15 months (95% CI: 12.6–17.4) compared to the patients in the R0 group (median OS: 22 months; 95% CI: 17.2–26.8) (Figure 3). Overall, the prognosis among the 55 patients with early recurrence was extremely poor, with overall survival similar to patients who underwent exploratory surgery without resection ($p=0.408$); the median survival time of these two groups was 8 and 5 months, respectively. Multivariable analyses revealed that perineural invasion, tumor-positive lymph node status (N1), and an R1 resection were significant predictors of OS, with hazard ratios (HR) of 1.44 ($p<0.02$), 2.15 ($p<0.001$), and 1.37 ($p<0.05$), respectively. Adjuvant chemotherapy had a protective effect on OS, with HR of 0.70 ($p<0.02$) (Table S3).

### *In node-negative (N0) patients surgical factors play a major role*

Locoregional recurrence occurred significant earlier in the patients with R1 N0 (median: 17 months; 95% CI: 8.7–25.3) or R1 N1 status (median: 16 months; 95% CI: 12.3–19.8) compared to the patients with R0 N0 (median: 67 months) or R0 N1 (median: 27 months; 95% CI: 14.7–39.3) (Figure 4A). Finally, the patients with R0 N0 status had significantly longer interval until the development of distant metastases (median: 67 months; 95% CI: 17.0–117.0) compared to the patients in the R0 N1 (median: 14 months; 95% CI: 10.6–17.4), R1 N0 (median: 13 months; 95% CI: 6.1–19.9), and R1 N1 (median: 17 months; 95% CI: 12.7–21.3) groups (Figure 4B).

On average, the patients with R0 N0 status had significantly longer survival (median: 45 months; 95% CI: 0.00–95.3) compared to the patients with R0 N1 (median: 17 months; 95% CI: 14.7–19.3; $p<0.001$), the patients with R1 N0 status (median: 17 months; 95% CI: 10.4–23.6; $p<0.001$), and the patients with R1 N1 status (median: 14 months; 95% CI: 11.7–16.3; $p<0.001$). Moreover, the patients with R1 N1 status also had significantly longer survival than the patients who underwent exploratory surgery without resection (median: 5 months; 95% CI: 3.9–6.1; $p<0.001$ vs. the R1 N1 group) (Figure 4C). As discussed above, in the

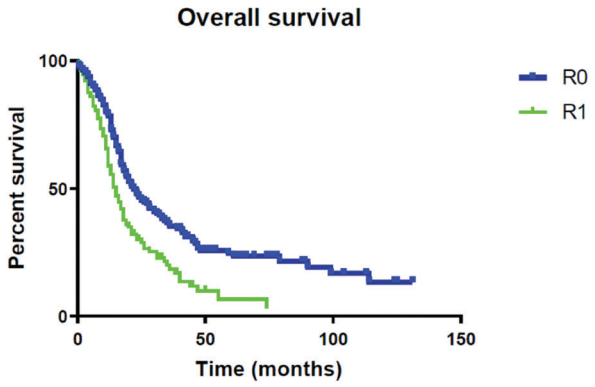



**Figure 3.** Subset analysis of the effect on overall survival of margin status



overall patient population tumor characteristics appears to affect outcome and local control more than performing an R1 resection. However, when we performed a subset analysis based on lymph node status, we found that survival was significantly worse in the N0 patients with an R1 resection, while tumor characteristics were similar (Table 3). Finally, we assessed the effect of adjuvant therapy on OS in node-negative and -positive patients (Figure 4D and 4E). All patient groups with adjuvant therapy show an improved OS, especially node-negative patients with R0 resection (figure 4D). Thus, for the node-negative patients performing a radical surgical resection will make a difference and, primary treatment should focus on getting the patient in an optimal condition to received adjuvant chemotherapy, to improve outcome.

**Table 3**. Effect of tumor biology.

| | **Lymph node status Negative (N0)** | | | **Lymph node status Positive (N1)** | | |
|---|---|---|---|---|---|---|
| | **R0 N0** | **R1 N0** | ***p*-value** | **R0 N1** | **R1 N1** | ***p*-value** |
| **Perineural invasion, Y (%)** | 47.9% | 55.2% | 0.509 | 57.4% | 81.0% | <0.001 |
| **Lymphangioinvasion, Y (%)** | 11.3% | 20.7% | 0.218 | 22.1% | 29.0% | 0.241 |
| **Tumor differentiation, N (%)** | | | 0.802 | | | 0.741 |
| **Well** | 22.5% | 20.7% | | 19.7% | 17.0% | |
| **Moderate** | 35.2% | 34.5% | | 45.1% | 43.0% | |
| **Poor** | 39.4% | 44.8% | | 35.2% | 40.0% | |
| **Undifferentiated** | 2.8% | 0% | | 0.0% | 0% | |
| **Mean tumor size in mm** | 27 | 27 | 0.933 | 26 | 34 | <0.001 |

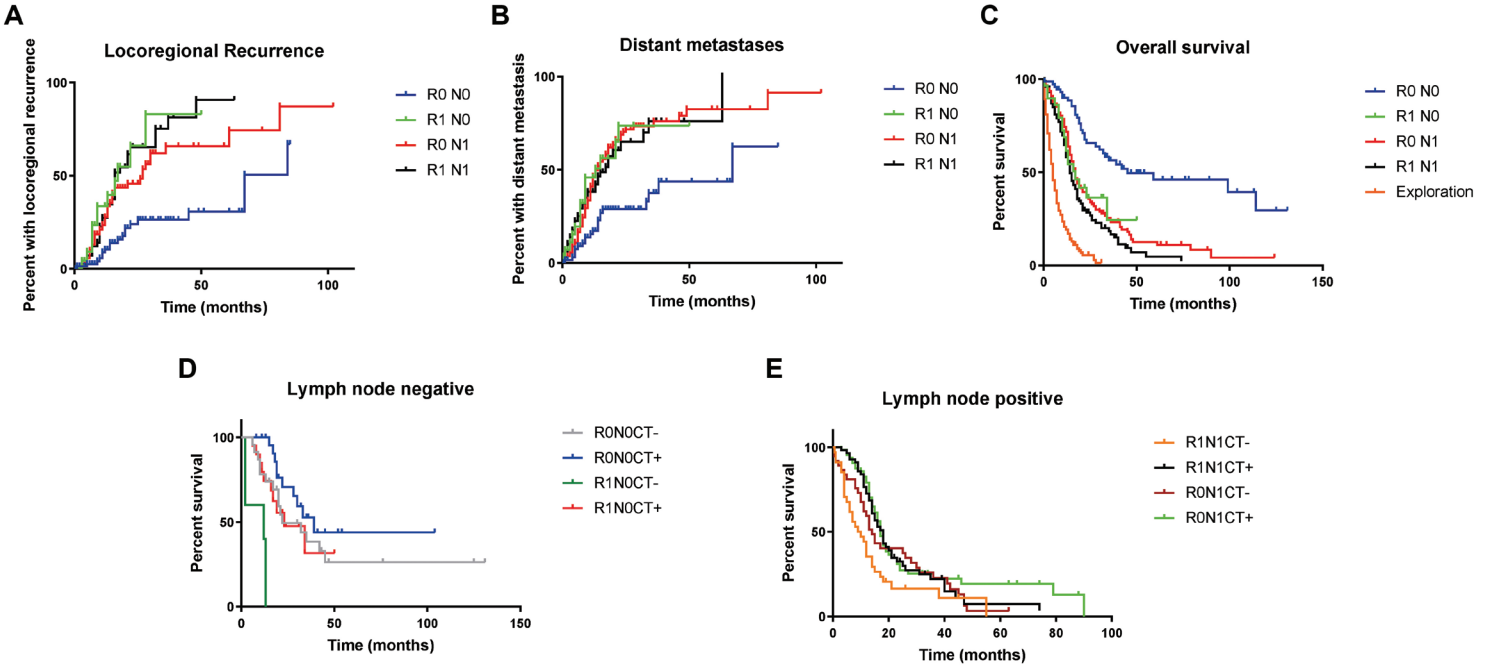



**Figure 4.** Subset analysis of the effect of margin status (R0 or R1) and lymph node status (N0 or N1) on (A) local recurrence, (B) distant metastases, (C) overall survival, and effect of adjuvant therapy on overall survival grouped by lymph node negative (D), and lymph node positive (E) patients. For comparison purposes, the overall survival of patients who underwent exploratory surgery only (without resection) is plotted in panel C.

## DISCUSSION

Patient stratification in order to determine the optimal primary treatment modality with respect to pancreatic cancer surgery is challenging. Our results show a clear difference between R0 and R1 resection with respect to the clinically relevant outcomes OS and DFS. Several studies have gone one step further when defining clear margins, using a resection margin of ≥2 mm rather than >1 mm.[23-25] Potentially, the benefits associated with achieving an R0 resection in our study could have been even more robust if we had used a margin of ≥2 mm for R0 resections.



The posterior margin is often reported as the clinically relevant margin;[22, 23] however, this margin is the most challenging to clear.[4] In their recent study, Osipov et al., included the posterior surface, vascular groove, and uncinate margins in the posterior margin,[23] in accordance with criteria established by the American Joint Committee on Cancer. Their results are consistent with this study, in which the vascular margin was found to be the margin that has clinical consequences with respect to local recurrence. When we sorted the margins in a similar manner to that by Osipov et al., we found that 64.4% of R1 margins were posterior margins. In their recent study including 1151 patients, Ghaneh et al. found that an R1 direct posterior resection margin was associated with reduced overall survival and recurrence-free survival, whereas an R1 direct positive superior mesenteric margin was associated with local recurrence; for both of the margins, however, an R1 <1 mm did not affect clinically relevant outcomes.[6] On the other hand, other groups found that the transection margin of the pancreatic neck and the SMA-facing margin were the only significant R1 sites of R1 with respect to prognosis.[31] Although it is currently unclear why involvement of one margin would have higher prognostic value than another margin, the answer may lie in differences in the density of bloodvessels, nerves, and/or lymphatic vessels surrounding the pancreas. Another important factor to consider is that the resection commonly performed for pancreatic cancer is already quite an extensive procedure. Oftentimes, in order to resect more tumor the only option available to the surgeon is to perform a vascular resection. Therefore, a highly sensitive detection method for detecting the tumor's boundaries is essential, as the surgeon can still make a difference in the extent of the resection at the vascular margin and, according to this study, patient outcome.

A striking finding from our study is the relatively high recurrence rate within 6 months after surgery in both the R0 and R1 groups. This finding indicates that several lesions were not detected by preoperative imaging, possibly due to the use of conventional imaging modalities (i.e., computed tomography and MRI), which are currently not sufficiently sensitive for identifying small lesions. This issue is clinically relevant as mean OS of these patients was only 8 months compared to 11 months of OS in patients who receive palliative chemotherapy due to non-resectable or metastatic disease with FOLFIRINOX (leucovorin and fluorouracil combined with irinotecan and oxaliplatin). Thus, the patients with early recurrence often have a poorer prognosis following surgery.

We believe that focus should shift toward improving the detection of distant disease and determining the feasibility of local resection prior to performing pancreatic cancer surgery. For example, the development of detection methods with improved sensitivity will allow clinicians to select patients for the optimal primary treatment approach—i.e., direct surgery or neoadjuvant therapy—thereby resulting in improved outcome following resection. New molecular imaging modalities, such as fluorescence or photoacoustic imaging, could be used to improve the detection of tumor-positive lymph nodes and the resection at difficult margins such as the posterior margin.[32-34] These modalities provide both anatomical and molecular information. These imaging techniques, use an exogenous imaging agent directed against the tumor allowing the surgeon to image the tumor using a tumor-specific approach, providing important additional information during the resection. In addition, molecular imaging may be beneficial in terms of staging the disease. On the other hand contrast-enhanced ultrasound and/or tumor-specific PET imaging could be useful for preoperative detection of distant metastases and local staging. These methods can be used to detect disseminated disease in a specific manner, thereby increasing sensitivity and potentially improving early detection; alternatively, the surgeon may choose to stop a resection that is likely to have little or no oncological benefit.

Previous reports noted that R1 status can not only be a reflection of surgical quality, but can also be a reflection of the tumor's biological behavior.[26, 27] In our study, we found a significant difference in perineural invasion, tumor-positive lymph nodes, and tumor stage in our R1 patient group. These results are similar

to those reported by Kimbrough et al., who found a significantly higher lymph node ratio and more microvascular invasion in their R1 group.[35] This difference may also explain the difference in OS between our R1 and R0 patient groups.

Since the introduction of FOLFIRINOX for treating pancreatic cancer, chemotherapy has become an additional treatment modality that appears to improve resection rates and the outcome of patients with pancreatic cancer. In support of this notion, a recent study found that patients who undergo R1 resection followed by adjuvant therapy have similar OS compared to patients who undergo R0 resection.[23] Thus, if R0 and R1 are determined primarily by tumor biological behavior—e.g., lymphangioinvasion and lymph node status—then patients with tumors with aggressive biological behavior might reach the same improved prognosis as patients with tumors with less aggressive biological behavior after receiving (neo)adjuvant therapy.



Based on a subset analysis in our study, tumor biological behavior appears to have only a limited effect in N0 patients. Our results support the notion that the outcome of these patients is influenced primarily by margin status. Therefore, we suggest that in cases of suspected N0 disease based on preoperative—and possibly intraoperative—imaging, the surgeon should make every reasonable effort to achieve radical resection. Based on our results, involvement of the large vessels should be examined thoroughly during surgery, as the vascular margin is the margin at risk in nearly half of all R1 resections. Novel techniques such as fluorescence-guided surgery could aid the surgeon in these situations. In addition, these patients should receive adjuvant chemotherapy and/or local radiotherapy in order to improve an aggressive biological behaviour associated with potential R1 resection.

## CONCLUSIONS

Here, we report the results of a large, single-hospital retrospective analysis of pancreatic cancer patients treated at a specialized pancreatic cancer center, in which we used a consistent R1 definition to examine the prognostic effect of specific positive margins. We found that patients with R0 resection have significantly longer survival, and a R1 vascular margin appears to be the most

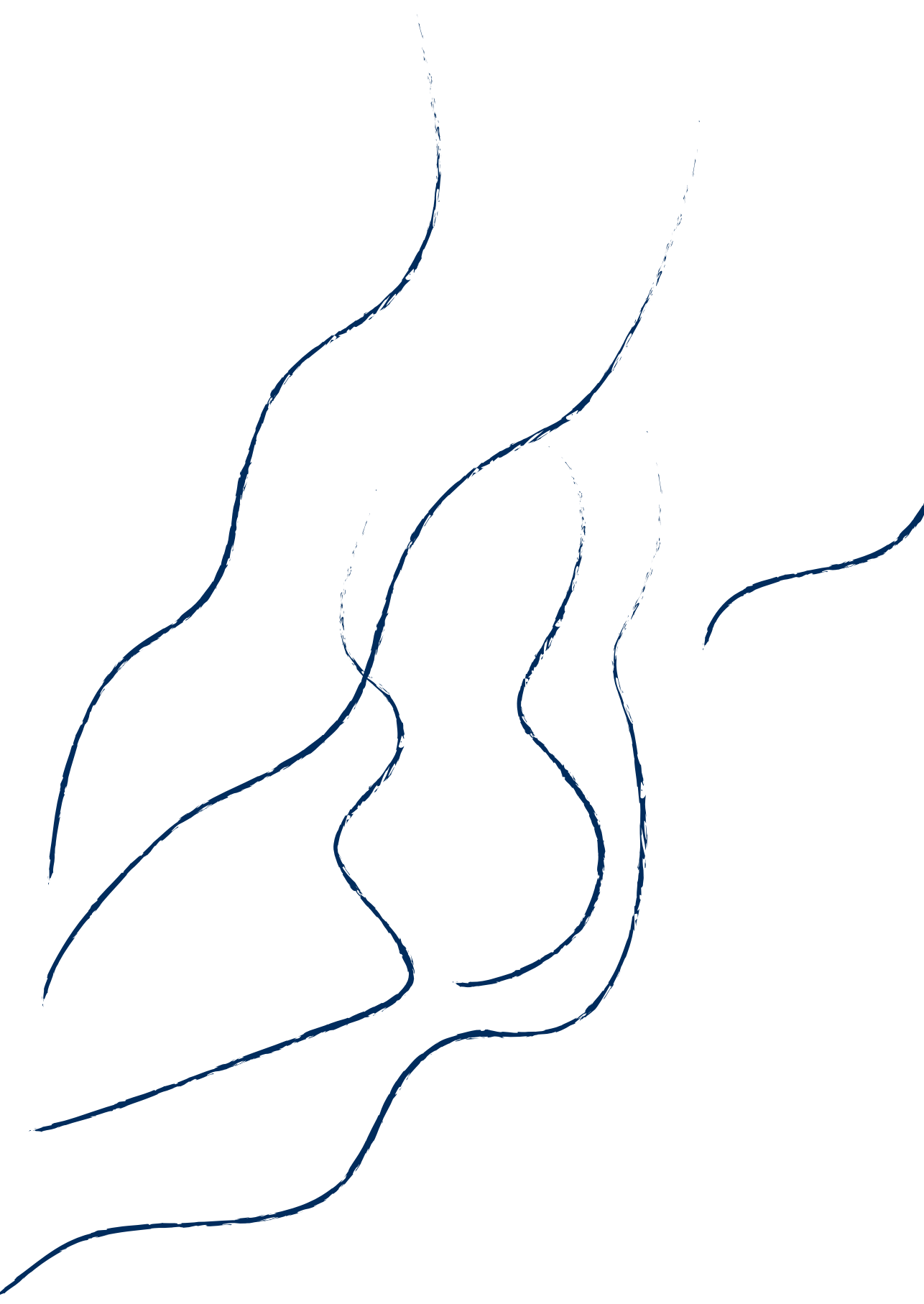
clinically relevant margin. Furthermore, our data support the notion that R1 status is likely associated with more aggressive tumor biological behavior, thus identifying patients with a high risk of recurrence and who may benefit the most from adjuvant or neoadjuvant chemotherapy. Moreover, we found that achieving radical resection can change the outcome in lymph node-negative patients; therefore, involvement of the large vessels should be thoroughly examined intraoperative in patients with suspected N0 disease in order to achieve maximum local control.

# REFERENCES


1. Vincent, A., et al., Pancreatic cancer. Lancet, 2011. 378(9791): p. 607-20.
2. Jemal, A., et al., Cancer statistics, 2010. CA Cancer J Clin, 2010. 60(5): p. 277-300.
3. Alexakis, N., et al., Current standards of surgery for pancreatic cancer. Br J Surg, 2004. 91(11): p. 1410-27.
4. Ethun, C.G. and D.A. Kooby, The importance of surgical margins in pancreatic cancer. J Surg Oncol, 2016. 113(3): p. 283-8.
5. Yeo, C.J., et al., Pancreaticoduodenectomy for cancer of the head of the pancreas. 201 patients. Ann Surg, 1995. 221(6): p. 721-31; discussion 731-3.
6. Ghaneh, P., et al., The Impact of Positive Resection Margins on Survival and Recurrence Following Resection and Adjuvant Chemotherapy for Pancreatic Ductal Adenocarcinoma. Ann Surg, 2017.
7. Raut, C.P., et al., Impact of resection status on pattern of failure and survival after pancreaticoduodenectomy for pancreatic adenocarcinoma. Ann Surg, 2007. 246(1): p. 52-60.
8. Neoptolemos, J.P., et al., Adjuvant chemotherapy with fluorouracil plus folinic acid vs gemcitabine following pancreatic cancer resection: a randomized controlled trial. Jama, 2010. 304(10): p. 1073-81.
9. Neoptolemos, J.P., et al., A randomized trial of chemoradiotherapy and chemotherapy after resection of pancreatic cancer. N Engl J Med, 2004. 350(12): p. 1200-10.
10. Kato, K., et al., Prognostic factors for survival after extended pancreatectomy for pancreatic head cancer: influence of resection margin status on survival. Pancreas, 2009. 38(6): p. 605-12.
11. Verbeke, C.S., Resection margins and R1 rates in pancreatic cancer--are we there yet? Histopathology, 2008. 52(7): p. 787-96.
12. Khalifa, M.A., V. Maksymov, and C. Rowsell, Retroperitoneal margin of the pancreaticoduodenectomy specimen: anatomic mapping for the surgical pathologist. Virchows Arch, 2009. 454(2): p. 125-31.
13. Khalifa, M.A., Intraoperative assessment of the Whipple resection specimen. J Clin Pathol, 2007. 60(9): p. 975-80.
14. Verbeke, C.S., et al., Redefining the R1 resection in pancreatic cancer. Br J Surg, 2006. 93(10): p. 1232-7.
15. Esposito, I., et al., Most pancreatic cancer resections are R1 resections. Ann Surg Oncol, 2008. 15(6): p. 1651-60.
16. Willett, C.G., et al., Resection margins in carcinoma of the head of the pancreas. Implications for radiation therapy. Ann Surg, 1993. 217(2): p. 144-8.
17. Nitecki, S.S., et al., Long-term survival after resection for ductal adenocarcinoma of the pancreas. Is it really improving? Ann Surg, 1995. 221(1): p. 59-66.
18. Sperti, C., et al., Survival after resection for ductal adenocarcinoma of the pancreas. Br J Surg, 1996. 83(5): p. 625-31.
19. Millikan, K.W., et al., Prognostic factors associated with resectable adenocarcinoma of the head of the pancreas. Am Surg, 1999. 65(7): p. 618-23; discussion 623-4.
20. Sohn, T.A., et al., Resected adenocarcinoma of the pancreas-616 patients: results, outcomes, and prognostic indicators. J Gastrointest Surg, 2000. 4(6): p. 567-79.
21. Verbeke, C.S., Resection margins in pancreatic cancer. Surg Clin North Am, 2013. 93(3): p. 647-62.
22. Gnerlich, J.L., et al., Microscopic margins and patterns of treatment failure in resected pancreatic adenocarcinoma. Arch Surg, 2012. 147(8): p. 753-60.
23. Osipov, A., et al., Redefining the Positive Margin in Pancreatic Cancer: Impact on Patterns of Failure, Long-Term Survival and Adjuvant Therapy. Ann Surg Oncol, 2017.
24. Chang, D.K., et al., Margin clearance and outcome in resected pancreatic cancer. J Clin Oncol, 2009. 27(17): p. 2855-62.
25. Gebauer, F., et al., Resection margin clearance in pancreatic cancer after implementation of the Leeds Pathology Protocol (LEEPP): clinically relevant or just academic? World J Surg, 2015. 39(2): p. 493-9.
26. Hernandez, J., et al., Survival after pancreaticoduodenectomy is not improved by extending resections to achieve negative margins. Ann Surg, 2009. 250(1): p. 76-80.

27. Vogel, I., et al., Detection and prognostic impact of disseminated tumor cells in pancreatic carcinoma. Pancreatology, 2002. 2(2): p. 79-88.
28. Van den Broeck, A., et al., Patterns of recurrence after curative resection of pancreatic ductal adenocarcinoma. Eur J Surg Oncol, 2009. 35(6): p. 600-4.
29. Pahk E, J.R., Kluger Y, Epelbaum R, Lachter J, Predictors of Early Recurrence of Adenocarcinoma of the Head of the Pancreas after Curative Resection. JOP. J Pancreas (Online), 2015. Nov 09; 16(6):597-600.
30. Fischer, R., et al., Early recurrence of pancreatic cancer after resection and during adjuvant chemotherapy. Saudi J Gastroenterol, 2012. 18(2): p. 118-21.
31. Jamieson, N.B., et al., Positive mobilization margins alone do not influence survival following pancreatico-duodenectomy for pancreatic ductal adenocarcinoma. Ann Surg, 2010. 251(6): p. 1003-10.
32. Vahrmeijer, A.L., et al., Image-guided cancer surgery using near-infrared fluorescence. Nat Rev Clin Oncol, 2013. 10(9): p. 507-18.
33. Zackrisson, S., S.M. van de Ven, and S.S. Gambhir, Light in and sound out: emerging translational strategies for photoacoustic imaging. Cancer Res, 2014. 74(4): p. 979-1004.
34. Handgraaf, H.J., et al., Current and future intraoperative imaging strategies to increase radical resection rates in pancreatic cancer surgery. Biomed Res Int, 2014. 2014: p. 890230.
35. Kimbrough, C.W., et al., Tumor-positive resection margins reflect an aggressive tumor biology in pancreatic cancer. J Surg Oncol, 2013. 107(6): p. 602-7.

03



Chapter | 4

# Selection of optimal molecular targets for tumor-specific imaging in pancreatic ductal adenocarcinoma

Tummers WS[1], Farina Sarasqueta A[2], Boonstra MC[1], Prevoo HA[1], Sier CF[1], Mieog JS[1], Morreau H[2], Van Eijck CH[3], Kuppen PJ[1], Van de Velde CJ[1], Bonsing BA[1], Vahrmeijer AL[1], Swijnenburg RJ[1].

[1] Department of Surgery, Leiden University Medical Center, Albinusdreef 2, 2300 RC, Leiden, The Netherlands. [2] Department of Pathology, Leiden University Medical Center, Albinusdreef 2, 2300 RC, Leiden, The Netherlands. [3] Department of Surgery, Erasmus Medical Center, Rotterdam, The Netherlands.

*Oncotarget. 2017 May 26;8(34):56816-56828.*

## ABSTRACT

Discrimination of pancreatic ductal adenocarcinoma (PDAC) from chronic pancreatitis (CP) or peritumoral inflammation is challenging, both at preoperative imaging and during surgery, but it is crucial for proper therapy selection. Tumor-specific molecular imaging aims to enhance this discrimination and to help select and stratify patients for resection. We evaluated various biomarkers for the specific identification of PDAC and associated lymph node metastases. Using immunohistochemistry (IHC), expression levels and patterns were investigated of integrin αvβ6, carcinoembryonic antigen-related cell adhesion molecule 5 (CEACAM5), Cathepsin E (Cath E), epithelial growth factor receptor (EGFR), hepatocyte growth factor receptor (c-MET), thymocyte differentiation antigen 1 (Thy1), and urokinase-type plasminogen activator receptor (uPAR). In a first cohort, multiple types of pancreatic tissue were evaluated (n=62); normal pancreatic tissue (n=8), CP (n=7), PDAC (n=9), tumor associated lymph nodes (n=32), and PDAC after neoadjuvant radiochemotherapy (n=6). In a second cohort, tissues were investigated (n=55) with IHC and immunofluorescence (IF) for concordance of biomarker expression in all tissue types, obtained from an individual patient. Integrin αvβ6 and CEACAM5 showed significantly higher expression levels in PDAC versus normal pancreatic tissue ($P=0.001$ and $P<0.001$, respectively) and CP ($P=0.003$ and $P<0.001$, respectively). Avβ6 and CEACAM5 expression identified tumor-positive lymph nodes correctly in 84% and 68%, respectively, and in 100% of tumor-negative nodes for both biomarkers. In conclusion, αvβ6 and CEACAM5 are excellent biomarkers to differentiate PDAC from surrounding tissue and to identify lymph node metastases. Individually or combined, these biomarkers are promising targets for tumor-specific molecular imaging of PDAC.

# INTRODUCTION

Pancreatic ductal adenocarcinoma (PDAC) is predicted to become the second cause of cancer-related death in 2030.[1] Patients with PDAC have a dismal prognosis, with a five-year survival rate of less than 5%.[2] At this point, complete surgical resection is the only potential curative treatment. However, at the time of primary diagnosis, 75% to 85% of patients has advanced unresectable disease due to locoregional spread and metastasis.[3, 4] Therefore, accurate identification of potential candidates for resection is crucial to prevent unnecessary surgical risks and delay in systemic therapy.[5] Another challenge during surgery, is that despite careful selection of resectable patients using CT, MRI and/or PET imaging, incomplete (R1) resection occurs in up to 70% of cases.[6] Failure to identify tumor-positive margins during surgery is not surprising, and is due to the tumor's characteristic to quickly spread beyond the pancreas via perineural and perivascular pathways[7] and the inability of the surgeon to differentiate between tumor and (peritumoral) inflammatory pancreatic tissue.[8, 9] This is also challenging in pre-operative imaging with conventional technique since both PDAC and chronic pancreatitis (CP) may present similar due to abundant stroma.



To improve surgical outcomes, novel neoadjuvant treatment protocols, such as FOLFIRINOX, are being successfully implied in the treatment of PDAC. Unfortunately, a drawback of these neoadjuvant therapies is that current imaging modalities are unable to differentiate between vital tumor and radiochemotherapy-induced tumor necrosis and fibrosis.[10-12] In addition, neoadjuvant treatment effects worsen the ability of the surgeon to differentiate (vital) tumor form fibrotic pancreatic tissue and often times, serial frozen section analysis is required to assess whether to continue a resection.

Tumor imaging using molecularly targeted probes has the potential to play an important role in improving patient management and treatment in these situations. This technique can be used for tumor detection, characterization, staging, and response assessment to neoadjuvant treatment. Moreover, it can facilitate image-guided therapy, and provide surgical guidance during tumor resection.[13] Recently, a first-in-human study was conducted using intra-operative tumor-specific imaging. A targeting ligand combined with a fluorophore was

used for the detection of tumor-specific biomarkers for diagnostic imaging and surgical decision-making in ovarium cancer [14].

For tumor-specific imaging, a biomarker is required to function as a target. In PDAC, a large number of biomarkers are known to be overexpressed. However, a limited number of these markers are eligible candidates for targeted imaging. Potential biomarkers for tumor-specific targeting must possess certain characteristics, such as homogeneous expression, upregulation of more than ten times compared to normal and surrounding tissue, and localization on the cellular membrane.[15-17] A preliminary study from our own research group identified several potential targets which are overexpressed in pancreatic tumor compared to normal pancreatic tissues; integrin αvβ6, carcinoembryonic antigen (CEA), epidermal growth factor receptor (EGFR), and urokinase plasminogen activator receptor (uPAR).[18] These biomarkers have also shown their potential for tumor-targeted imaging in pre-clinical studies.[15, 19-31] However, a potential target for clinically relevant differentiation between PDAC and peritumoral inflammation or CP has yet to be identified. Next to the ability to discriminate PDAC from CP, the target also needs to be able to identify lymph node metastases and differentiate between vital tumor cells versus necrosis and fibrosis in patients that have received neoadjuvant therapy.

The primary aim of this study was to evaluate the ability of integrin αvβ6, carcinoembryonic antigen-related cell adhesion molecule 5 (CEACAM5), Cathepsin E (Cath E), epithelial growth factor receptor (EGFR), hepatocyte growth factor receptor (c-MET), thymocyte differentiation antigen 1 (Thy1), and urokinase-type plasminogen activator receptor (uPAR) as targets to differentiate between PDAC, CP and normal pancreatic tissue for tumor-specific imaging and for the potential to develop clinically translatable imaging agents targeting these markers. The biomarkers were selected based on a literature search and our previous study using tissue microarrays (TMA) of 137 patients.[18, 19, 32, 33]

# MATERIALS AND METHODS

## Patient and tissue selection

Medical records and tissue specimens were retrospectively reviewed from patients who underwent pancreatic resection at the Leiden University Medical Center (LUMC) and Erasmus Medical Center (EMC) in Rotterdam between January 2011 and September 2015. Patients were selected with the histological diagnosis PDAC (n=8) or CP (n=7). In addition, normal pancreatic tissue lying adjacent to a PDAC was obtained from nine patients (n=9). Locoregional lymph nodes (n=32; n=17 tumor-negative, n=15 tumor-positive) were included from the PDAC patients to identify biomarker expression in lymph node metastasis. For our second cohort, all tissues (n=55; normal pancreatic parenchyma, inflamed pancreatic tissue, and PDAC tissue) were obtained from individual patients (n=12). All tissue samples were reviewed by a specialized pathologist before inclusion in the study. Tumor differentiation grades according to guidelines established by the World Health Organization were included. Colonic (n=3) and duodenal tissues (n=3) (from Department of Pathology, LUMC) were included as controls to assess biomarker expression in the peripancreatic organs. Patterns of expression of tumor biomarkers on pancreatic surgical specimens following neoadjuvant therapy were assessed in a small cohort (n=6) of patients who received radiochemotherapy; three cycles of gemcitabine and 15 fractions of 36 Gy radiotherapy during two cycles (PREOPANC trial).



## Antibodies and reagents

The antibodies used for immunohistochemical (IHC) staining are shown in supplementary table 2.

## Immunohistochemistry on tissue sections

Formalin-fixed, paraffin-embedded (FFPE) tissue blocks were collected from the Pathology Department of the LUMC and EMC. Tissue sections of 5 µm thickness were obtained from two different types of tissue blocks, one type with standard measurement of 40 x 26 mm, and the other type of 75 x 50 mm. The second type was used to determine the expression pattern across the entire specimen. All tissue slides used in the study were immunohistochemically assessed. For the second cohort of slides, additional immunofluorescence was performed. For preparation of IHC staining, the slides were deparaffinized with xylene

**Table 1.** Suitability of biomarkers. Overview of the characteristics of the analyzed biomarkers for determination of the suitability of the biomarker as tumor-target for molecular-imaging during pancreatic cancer surgery; Integrin Avβ6, carcinoembryonic antigen (CEACAM5), epithelial growth factor receptor (EGFR), hepatocyte growth factor receptor (or c-MET), urokinase-type plasminogen activator receptor (uPAR), and Cathepsin E (Cath E). No upregulation (-). Heterogeneous upregulation in tumor (+). Diffuse expression of target (++).

| Target | Localization | Upregulation in PDAC compared to normal | Upregulation in PDAC compared to CP | Sensitivity of target for lymph node metastases | Diffuse upregulation throughout the tumor | Main advantage | Main disadvantage |
|---|---|---|---|---|---|---|---|
| αvβ6 | Cell membrane | p<0.001 | p<0.001 | 84% | ++ | Diffuse, strong expression. | Expression on normal ductal structures. |
| CEACAM5 | Cell membrane | p<0.001 | p<0.001 | 68% | + | No expression in normal pancreatic tissue and CP. | Heterogeneous expression and loss of expression after neoadjuvant treatment. |
| EGFR | Cell membrane | p=0.031 | p=1.000 | 93% | ++ | EGFR-mediated cellular internalization of targeted particles. | Relatively high expression on normal duodenal tissue, thereby changing surgical field. |
| uPAR | Cell membrane | p<0.001 | p<0.001 | 69% | ++ | Expression both on tumor and tumor surrounding stromal cells. | High uPAR expression in negative lymph nodes. |
| CathE | Intracellular | p<0.001 | p<0.001 | 54% | + | Ideal for imaging purposes due to possible use of activatable probes, and therefore increasing signal-to-background ratio. | Intracellular location of target requires a probe capable of internalization. |

and rehydrated in serially diluted ethanol solutions (100%-50%), followed by demineralized water according to standard protocols. Endogenous peroxidase activity was blocked by incubation in 0.3% hydrogen peroxidase in phosphate buffered saline (PBS) for 20 min. Antigen retrieval for CEACAM5, Thy1, and uPAR was performed by heat induction at 95°C using PT Link (Dako) with low-pH Envision FLEX target retrieval solution (pH 6.0, citrate buffer, Dako). For c-MET and Cath E, the high-pH Envision FLEX target retrieval solution was used (pH 9.0, citrate buffer, Dako). For αvβ6 and EGFR staining, antigen retrieval was performed with 0.4% pepsin incubation (Dako) at 37°C for 10 min.

Following antigen retrieval, the tissue sections were incubated overnight with the primary antibodies in 100 µl for standard tissue sections and 500 µl for the large tissue sections at room temperature. A pre-determined optimal dilution was used for all antibodies; anti-αvβ6 antibodies 1:800, anti-CEACAM5 antibodies 1:1000, anti-EGFR antibodies 1:100, anti-CD90/Thy1 antibodies 1:800, anti-MET antibodies 1:8000, anti-Cath E antibodies 1:1000, and anti-uPAR antibodies 1:800. The slides were washed with PBS, followed by incubation with secondary antibody for 30 minutes at room temperature. After additional washing, the staining was visualized with 3,3-diaminobenzidine tetrahydrochloride solution (DAKO, Glustrup, Denmark) at room temperature for 5 minutes and counterstained with hematoxylin for 20 seconds. Finally, the tissue sections were dehydrated and mounted in Pertex (Histolab, Rockville, MD, USA).



### IHC analysis

All stained sections with standard measurements (40 x 26 mm) were scanned and viewed at 40x magnification using the Philips Ultra-Fast Scanner 1.6 RA (Philips, Eindhoven, Netherlands). The large tissue sections were viewed under the microscope. Evaluation of the immunohistochemical staining was performed blinded independently by two observers (W.S.F.J.T. and A.F.S.). The following scoring method was used; percentage specific staining (normal/PDAC/CP) was scored as percentage of total tissue 0=<10%, 1=10-25%, 2=26-50%, 3=51-75%, 4=>75%. Staining intensity was scored as 0=none, 1=weak, 2=moderate, 3=strong (Figure S6). Undesired staining of structures other than investigated tissues (i.e., normal/tumor/inflammation/stroma) was scored as 0=none, 1=moderate, 2=strong. In tumor tissue, a comparison was made between staining at invasive

border compared to core of the tumor. This was scored as tumor core vs invasive border: 0=lower, 1=similar, 2=stronger.

### Interim analysis to assess biomarker suitability

Primary analysis of all biomarker characteristics included expression pattern, expression in normal pancreatic parenchyma, pancreatitis, PDAC and expression in tumor-positive and tumor-negative lymph nodes. Next an interim analysis of the different biomarkers was performed to assess the suitability of these markers as targets for tumor-specific molecular imaging of PDAC. After this analysis the most suitable biomarkers (αvβ6 and CEACAM5) were chosen for further assessment to specifically identify their potential in clinically relevant situations, tailored to tumor-specific molecular imaging."

### Immunofluorescence

Double immunofluorescent staining of αvβ6 and CEACAM5 was performed on FFPE tissue sections of normal pancreatic tissue, PDAC, and CP. The slides were treated similar as described above. Antigen retrieval for both targets was performed by heat induction at 95°C using PT Link with a low-pH Envision FLEX target retrieval solution. Sections were incubated with 5% Fetal Bovine Serum in PBS for 10 minutes at room temperature prior to incubation with primary antibodies. Both primary antibodies against αvβ6 and CEACAM5 were applied overnight at room temperature. These were detected using secondary antibodies mentioned before; anti-IgG1-AF488 for αvβ6 and anti-IgG2a-AF647 for CEACAM5. After washing three times in PBS, nuclei were stained with 4',6-diamidino-2-phenylindole (DAPI, Prolong Gold, Life Technologies) and stored at 4°C. The slides were examined using a Leica DM5500B digital fluorescence microscope (Leica Microsystems B.V., Son, the Netherlands) equipped with a Leica DFC365FX camera using LAS X software for image acquisition and processing.

### Statistical analysis

The statistical analysis was performed using SPSS version 20.0 software for Windows (SPSS, IBM Corporation, Somer NY, USA) and GraphPad Prism 6 (GraphPad, Software, Inc, La Jolla CA, USA). Mean percentage staining and difference in staining between tissues was calculated with One-way ANOVA with post-hoc Bonferroni correction. In all tests, results were considered statistically significant at the level of $P<0.05$.

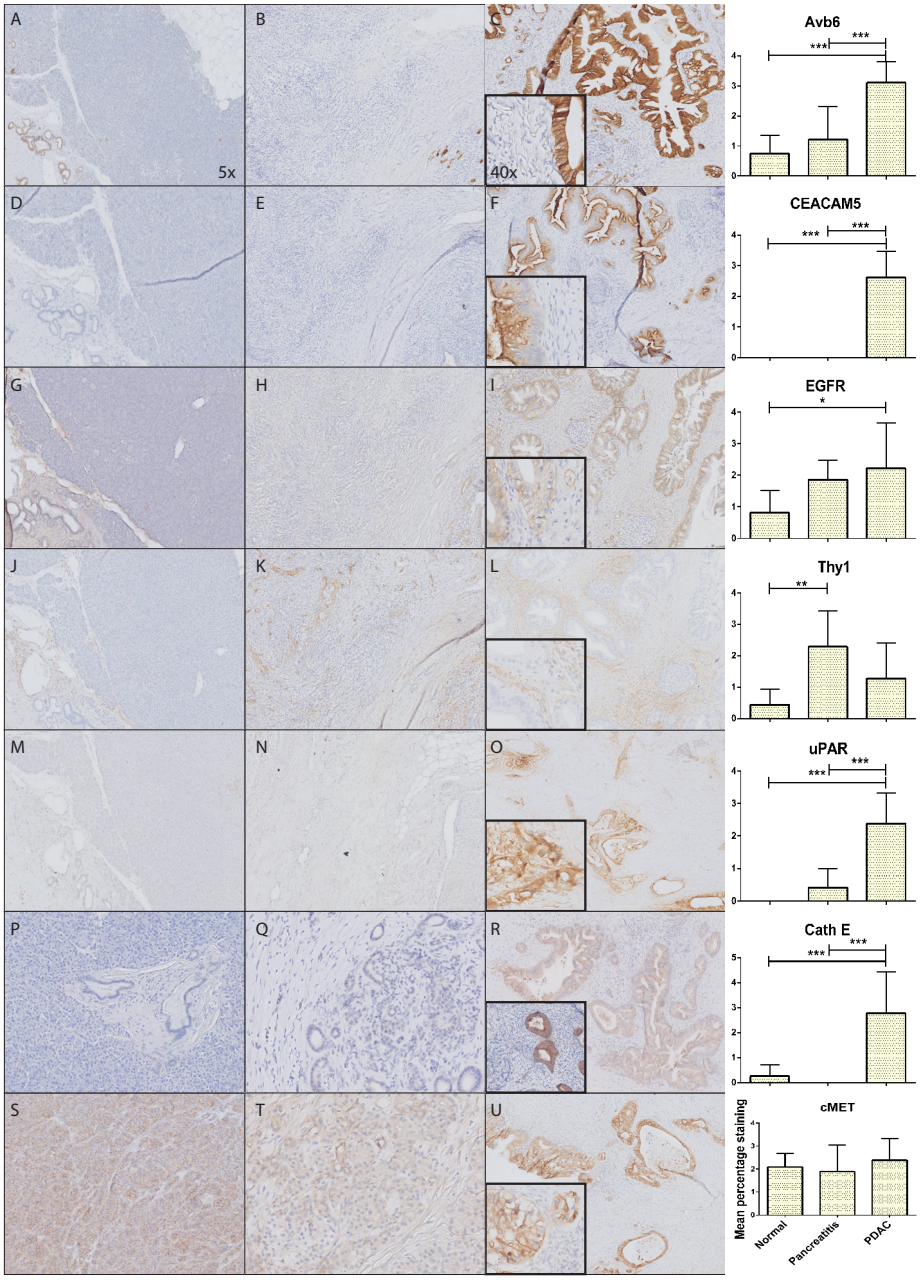



**Figure 1. Expression patterns of investigated markers.** Representative images of immunohistochemically staining patterns in PDAC of all molecular markers; αvβ6 (A-C), CEACAM5 (D-F), EGFR (G-I), Thy1 (J-L), uPAR (M-O), CathE (P-R), cMET (S-U) showing respectively from left to right normal pancreatic tissue, CP, PDAC and graphical representation of mean percentage staining on all the tissue slides (*: p<0.05, **: p<0.01, ***: p<0.001).

## RESULTS

In the first cohort, a total of 62 tissues (n=8 PDAC, n=7 CP, n=9 normal pancreatic tissue, n=32 lymph nodes, n=6 PDAC after neoadjuvant radiochemotherapy) were stained for all biomarkers to assess expression patterns. In the second cohort, a total of 55 tissue slides were stained with the two most suitable biomarkers (n=12 PDAC, n=12 CP, n=12 normal pancreatic tissue, n=19 lymph nodes). Patient and tumor characteristics are summarized in Supplementary table 1.

### *Avβ6, CEACAM5, CathE and uPAR are significantly higher expressed in PDAC versus CP.*

All biomarkers were overexpressed in PDAC, except for c-MET (Fig 1S-U) and Thy 1 (Fig 1J-L), which showed equal or even higher staining in normal pancreatic tissue or CP compared to PDAC. Although there was abundant Thy1 stromal staining in PDAC, it was also present in stroma of adjacent normal and inflamed pancreatic tissue. Therefore, both targets were excluded from further analysis. All other targets showed significant higher expression in PDAC compared to normal pancreatic tissue; αvβ6 (Fig 1A-C) ($p < 0.001$), CEACAM5 (Fig 1D-F) ($p < 0.001$), EGFR (Fig 1G-I) ($p < 0.05$), Cath E (Fig 1P-R) ($p < 0.001$), and uPAR (Fig 1M-O) ($p < 0.001$). Avβ6 was homogeneously expressed, uPAR, and Cath E were slightly heterogeneously expressed, and all other biomarkers showed a markedly heterogeneous expression pattern in PDAC tissue (Figure S1). Furthermore, only CEACAM5 expression in PDAC was slightly more intense in the invasive border compared to the tumor core. The following biomarkers were significantly overexpressed in PDAC versus CP; αvβ6 (Fig 1B-C) ($p<0.001$), CEACAM5 (Fig 1E-F) ($p < 0.001$), Cath E (Fig 1Q-R) ($p < 0.001$), and uPAR (Fig 1N-O) ($p < 0.001$). All targets, except for CEACAM5, showed expression in the duodenum especially at the luminal side (not shown). This was also the case in colonic tissue where there was luminal staining for most targets except for uPAR (not shown).

Interestingly, immunohistochemical staining for CEACAM5 (Figure S2) and uPAR showed complete absence of staining in normal pancreatic parenchyma. Avβ6 showed moderate staining in normal ductal structures, but there was a significantly higher expression in malignant ducti. The substantially higher ratio of ductal structures in malignant pancreas compared to normal pancreatic

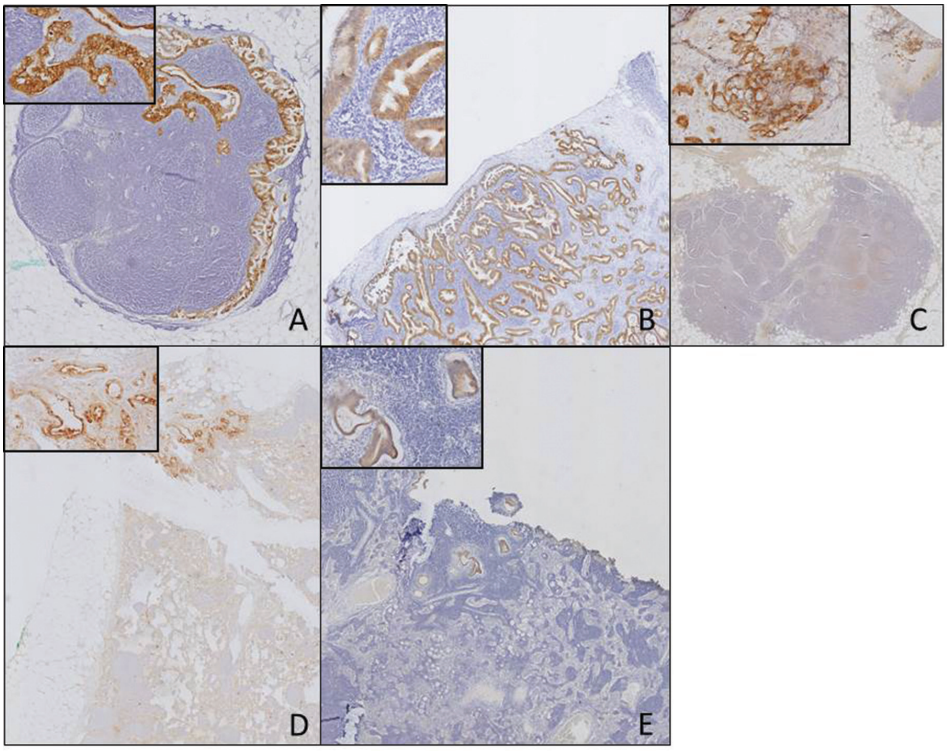



**Figure 2**. **Biomarker expression in tumor-positive lymph nodes.** Biomarker expression in tumor-positive lymph nodes for the different biomarkers αvβ6 (A), CEACAM5 (B), EGFR (C), uPAR (D), CathE (E) (Objective 1x, insert 20x).



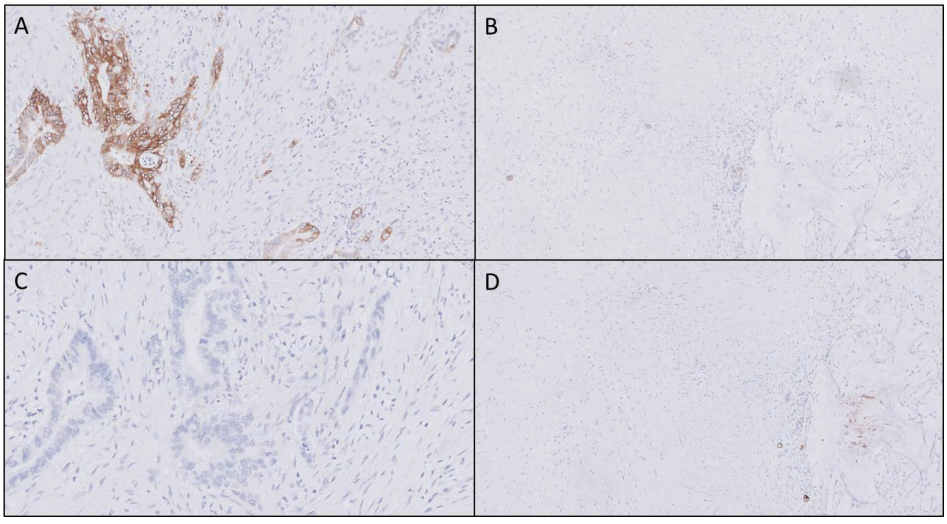



**Figure 3. Biomarker expression after neoadjuvant therapy.** In all neoadjuvant treated tissue a markedly higher αvβ6 expression was identified in vital tumor tissue (A) compared to surrounding fibrosis or necrosis (B) after neoadjuvant therapy. CEACAM5 biomarker expression showed increased heterogeneity after neoadjuvant therapy in the tumor (C), therefore clear distinction between vital tumor and fibrosis and necrosis is not possible (C and D) (Objective 10x).

parenchyma adds to the significant increase total of marker expression per high power field. (Figure S3).

### *Avβ6 specifically differentiates tumor-positive and tumor-negative lymph nodes.*

Next, we investigated biomarker expression in tumor-positive and –negative lymph node. A total of 17 tumor-positive and 15 tumor-negative nodes were stained. The described biomarkers identified the investigated positive and negative lymph nodes correctly with, respectively, a sensitivity and specificity of; αvβ6 (84%; 100%), CEACAM5 (68%; 100%), EGFR (93%; 67%), Cath E (54%; 83%), and uPAR (69%; 67%). Figure 2A shows CEACAM5 expression in both tumor-positive and tumor-negative lymph node, figure 2B shows αvβ6 in identical lymph nodes for comparison.

An interim analysis to assess the suitability of the biomarker panel as targets for tumor-specific molecular imaging of PDAC was performed, shown in table 1. Biomarkers αvβ6 and CEACAM5 met most of the criteria of an optimal tumor-specific biomarker and were selected for further evaluation.

### *Biomarker patterns change after neoadjuvant radiochemotherapy.*

Molecular targeted imaging could be useful tool for neoadjuvant therapy response monitoring. The consequence of neoadjuvant therapy on αvβ6 and CEACAM5 expression was assessed by staining tissues from patients who received radiochemotherapy. In all investigated neoadjuvantly treated tumors, there was a markedly higher αvβ6 expression seen in the remaining vital tumor cells compared to the surrounding fibrosis and necrosis, as shown in Figure 3A and 3B. This level of expression was comparable to the expression in PDAC without neoadjuvant therapy, as previously shown. CEACAM5 expression in vital tumor cells after neoadjuvant therapy was reduced, as shown in Figure 3C, compared to PDAC not treated neoadjuvantly. As a result, no difference in expression of CEACAM5 between vital tumor cells and surrounding fibrosis and necrosis was seen (Figure 3C and 3D). In the samples of two out of six patients there was no expression of CEACAM5 in the remaining vital PDAC cells. Due to small sample size, we were not able to determine significance of results.

*Avβ6 and CEACAM5 expression is markedly different between normal pancreatic parenchyma, peritumoral inflammation, and PDAC of individual patients.*

In a second cohort, normal pancreatic parenchyma, peritumoral inflammation and PDAC of individual patients (n=12) were included in order to mimic the actual clinical situation. In 11 out of 12 patients, αvβ6 staining in PDAC was clearly higher compared to inflammation and to normal pancreatic parenchyma (4 and 2 times higher, respectively). CEACAM5 expression was only present in PDAC, and therefore, the staining pattern was markedly different between normal pancreatic parenchyma, peritumoral inflammation and PDAC in all patients except for two who did not express CEACAM5 in any of their tissue samples (Figure S4). In concordance with the first patient cohort, CEACAM5 staining of PDAC was weaker and more heterogeneous compared to αvβ6. In Figure 4, expression of CEACAM5 (Figure 4B) and αvβ6 (Figure 4C) in PDAC, peritumoral inflammation, and normal pancreatic parenchym of one individual patient are presented next to the corresponding H&E stain (A), showing the difference in expression even in such close proximity.



*Multiplexing for optimal discrimination between malignant and benign tissue.*

Double staining of CEACAM5 and αvβ6 using immunofluorescence showed that multiplexing by targeting both biomarkers leads to an improved discrimination between malignant and benign pancreatic tissue and identification of all PDAC tissue. Examples of using multiplexing to achieve improved detection are shown in figure 5, and figure S5. This improved detection is obtained by the different expression patterns of both targets, as also shown in figure 1, which are complementary to each other. Targeting αvβ6 will identify all PDAC as shown above, and CEACAM5 reduce the false positive staining by αvβ6 in normal pancreatic parenchyma and CP.

## DISCUSSION

Imaging using tumor-specific molecular probes has the potential to solve some of the challenges regarding PDAC diagnosis, treatment response monitoring and surgery. For tumor-specific molecular imaging to be successful, it is essential to have suitable biomarkers that can be targeted by molecular probes and that are

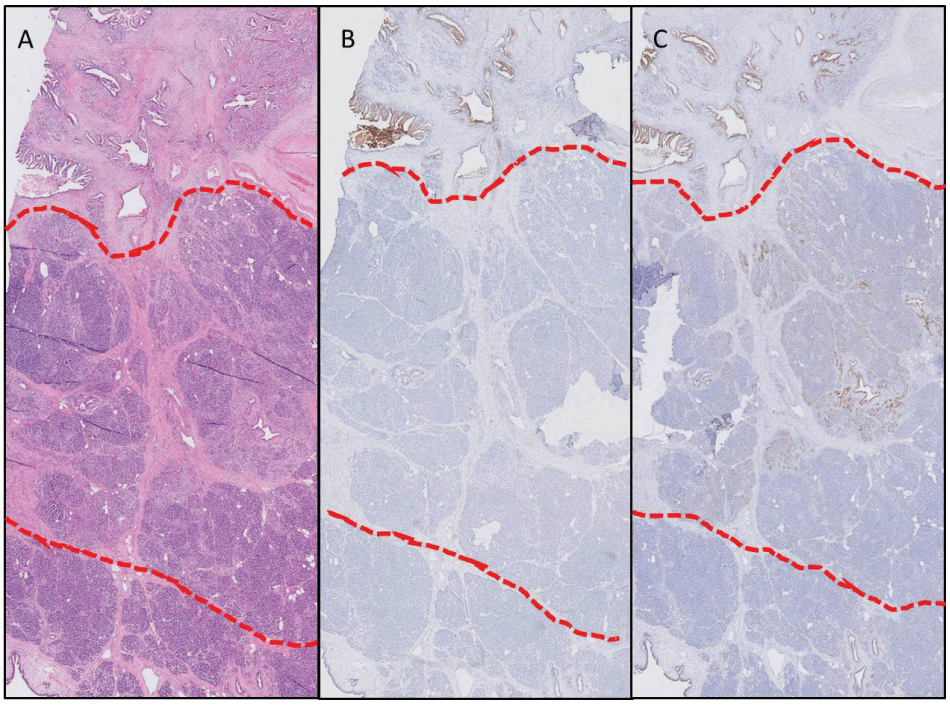



**Figure 4. Biomarker expression in different tissue types within one patient**. Expression of CEACAM5 (B) and αvβ6 (C) of one individual patient with the corresponding H&E slide (A) in PDAC (above red line), peritumoral inflammation (between red lines), and normal pancreatic parenchyma (below red lines), showing the difference in expression even in such a close proximity (Objective 2x)."

able to distinguish primary PDAC and metastases from normal pancreatic tissue, CP or acute (peritumoral) inflammation. With the current imaging modalities, the differentiation between PDAC and CP remains a challenge as still 7-13% of pancreatectomies are performed for benign pathology.[34] Molecular imaging can potentially also improve the outcome of PDAC patients by providing the ability to identify small tumor nodules in an early stage and therefore increasing the chance of cure and improving survival rates.[35, 36] Another major problem for PDAC surgery is the high recurrence rate within 6-12 months, which suggests that local or distant micrometastases were already present at the time of surgery.[37, 38] This underscores that conventional imaging modalities (i.e., MRI, CT and PET) lack the sensitivity to detect small amounts of tumor leading to highly morbid surgical procedures for patients that do provide the desired oncologic benefit. A technique that improves the stratification of patients to ensure they receive the proper therapy could serve as a helpful tool for personalized treatment in

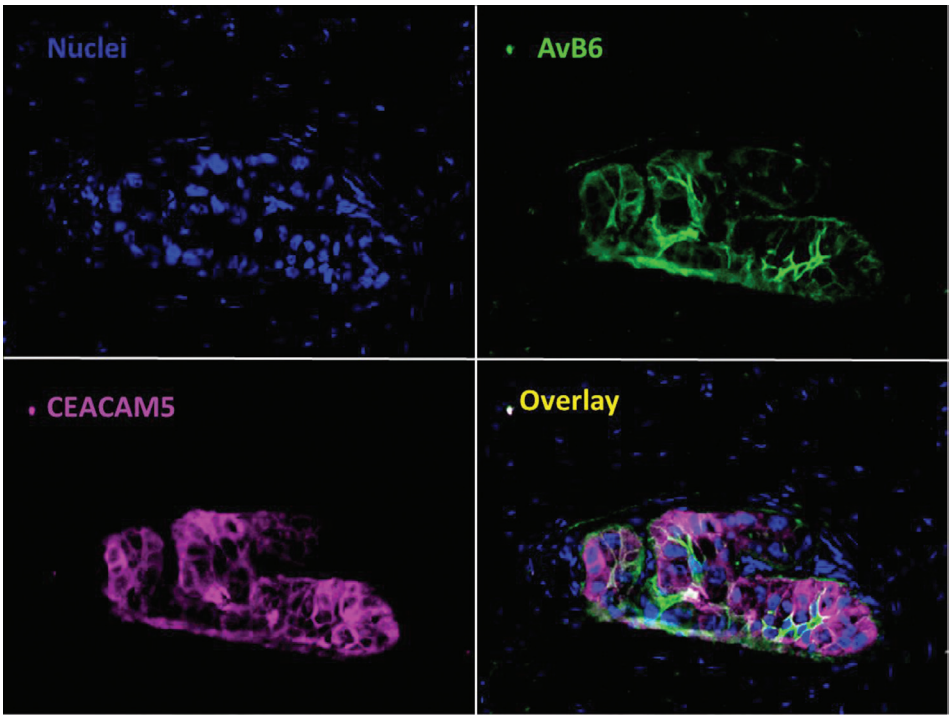



**Figure 5. Value of multiplexing in PDAC.** Immunofluorescent staining of αvβ6 and CEACAM5 simultaneously in PDAC. Showing the additional value of using two biomarkers to target all tumor tissue compared to one biomarker (Objective 40x).



PDAC. Examples of tumor-specific imaging modalities include: ultrasound, CT, PET, and fluorescent optical imaging. Fluorescent optical imaging has shown the ability to detect lesions <2mm as described by Warram, et al..[39] Of course, this modality can only be used during surgery but will lead to better stratification intraoperatively.

For PDAC, the greatest improvements in patient outcome would likely be the result of better selection of patients surgery, preoperative visualization of all tumor-positive lymph nodes and distant metastases, or the decision to abort surgery in a noncurative procedure. This study implies that molecular imaging using tumor-specific targets, such as αvβ6 and CEACAM5, can help to guide this process. The main advantage of the present study is the use of tissue sections that represent a cross section of the entire pancreas which is preferred above tissue microarray (TMA) cores, as we could assess exact staining patterns

more thoroughly in a larger surface and can recognize heterogeneity more reliably. This change in technique potentially explains why substantially higher expression rates are found in normal ductal pancreatic tissue compared to the literature.[18, 32, 40] To assess clinical relevance of the technique and represent the clinical situation during imaging and surgery of PDAC, lymph nodes, CP and peritumoral inflammation as well as unremarkable pancreatic parenchyma were included from the same unique patients. To our knowledge, this is the first report comparing the expression of biomarkers not only in different tissue types but also in benign and malignant lesions within the same organ from a single patient leading to the identification of ideal biomarkers for preoperative and intraoperative imaging.[27, 28, 30, 41] The results of CEACAM5 and αvβ6 in PDAC tissues are in line with most previous reports.[21, 27, 30, 31] However in contrast, Allum et al. and Jewkes et al. both reported CEA staining in CP.[28, 42] For their study, they used the monoclonal anti-CEA antibodies, 11-285-14 and 11-359-6, but it is unknown if their antibodies were directed against CEACAM5 or another subtype of CEA.

The fact that CEACAM5 could be a potential biomarker for the tumor-specific identification of PDAC would lead to other advantages. CEA is known to be present in soluble form in the serum for multiple cancer types. Recent studies have reported a positive relation between CEA levels in cancer tissue and serum CEA levels,[43, 44] while other studies did not show this relation.[45-48] For now, this phenomena is mainly studied in colorectal cancer and the correlation between serum CEA and tissue CEA in PDAC is unclear, but is subject of investigation in our group.

As shown in this study as well as in literature, no individual biomarker is perfect. For most tumor types, one unique biomarker is not sufficient for exact tumor-specific identification, as shown, and therefore the potential to perform multiplexing is crucial. In this study, we showed the advantage of using probes with different fluorescent labels for multiplexing purposes, An example of a technique which is optimal for multiplexing is Raman imaging. Several different nanoparticles can be produced by modifying the Raman surface and therefore generating unique spectral signatures.[49] Unfortunately, this technique is still far from wide clinical use. To target multiple biomarkers with fluorescence imaging, diabodies are the ligand of choice now. However, if a diabody was used with

one fluorescent label to target CEACAM5 and αvβ6, exact differentiation would not have been possible between normal pancreatic tissue, CP and inflammation, and PDAC since both targets have their own strengths in this differentiation. Targeting both biomarkers with different fluorescently-labeled ligands might thus be beneficial for imaging purposes.

Since the successful introduction of novel neoadjuvant regimens for PDAC, like FOLFIRINOX, resectability rates have increased up to 51%.[50] However, a major drawback of this success is that after neoadjuvant treatment conventional imaging modalities are not able to differentiate between vital tumor cells and radiochemotherapy-induced tumor necrosis and fibrosis, and are therefore no longer able to predict resectability.[10] A potential role for targeted imaging, would require that the parts of the tumor that have remained vital unless neoadjuvant therapy would have to retain their expression levels. Avβ6 was shown to possess that capacity. CEACAM5 expression, on the other hand, was reduced compared to in PDAC tissue without neoadjuvant treatment. Two potential explanations for this effect could be: (i) there is tumor heterogeneity where the subtype with CEACAM5 expression is selectively killed by the (radio)chemotherapy,[51-53] or (ii) the neoadjuvant therapy has a selective effect on the cell genome.[54] However, before final conclusions can be drawn in neoadjuvant treated tissues, these results need to be validated in a larger series of patients. Another limitation of our approach in this series is that the biomarker expression before (radio) chemotherapy is unknown. However, based on the available literature and our presented results, we feel confident that biomarker expression of these tumors prior to therapy is comparable to expression in tumors that are not treated with neoadjuvant therapy.



A potential hurdle for the clinical translation of tumor-targeted imaging could be need for agents directed against different targets in the various cancer types, which is costly and a regulatory burden. For example, the role of c-MET as a biomarker in fluorescence imaging seems to be cancer type-specific. Burggraaf et al. showed the potential of c-MET as biomarker in colon cancer,[55] whereas in PDAC, its role is less clear. In this study, as with others, c-MET shows relevant overexpression in normal pancreatic tissue, excluding it as target for tumor-specific molecular imaging applications.[56] Also biomarkers targeting stromal components and microenvironment such as uPAR and Thy1 are suggested for

molecular imaging of cancer.[19, 57] However, as shown, biomarkers targeting the microenvironment of PDAC, are less useful when extravasation occurs because abundant stroma exists not only in PDAC, but also in normal pancreatic tissue and especially in chronic and acute pancreatitis. Another main disadvantage of uPAR was the expression in negative lymph nodes, potentially due to its natural expression on macrophages. This is in line with a recently published review paper from Petrushnko et al..[58] Since lymph node identification was one of our main criteria, uPAR was not included in the second cohort for evaluation although it performed similar to CEACAM5 on several other characteristics.

In conclusion, both CEACAM5 and αvβ6 are promising candidates for tumor-specific molecular imaging for PDAC. Especially when used in combination, these biomarkers can discriminate between normal pancreatic tissue, CP and peritumoral inflammation, and PDAC. Also, αvβ6 can help identify vital tumor after neoadjuvant radiochemotherapy and identify lymph nodes metastases. Therefore, agents recognizing both biomarkers, combined with a different label or two separate agents, would have the potential to create a huge impact in PDAC diagnostics, therapy and patient outcome.

# REFERENCES


1. Rahib L, Smith BD, Aizenberg R, Rosenzweig AB, Fleshman JM, Matrisian LM. Projecting cancer incidence and deaths to 2030: the unexpected burden of thyroid, liver, and pancreas cancers in the United States. Cancer Res. 2014; 74: 2913-21. doi: 10.1158/0008-5472.can-14-0155.
2. Vincent A, Herman J, Schulick R, Hruban RH, Goggins M. Pancreatic cancer. Lancet. 2011; 378: 607-20. doi: 10.1016/s0140-6736(10)62307-0.
3. Stathis A, Moore MJ. Advanced pancreatic carcinoma: current treatment and future challenges. Nat Rev Clin Oncol. 2010; 7: 163-72. doi: 10.1038/nrclinonc.2009.236.
4. Barugola G, Partelli S, Marcucci S, Sartori N, Capelli P, Bassi C, Pederzoli P, Falconi M. Resectable pancreatic cancer: who really benefits from resection? Ann Surg Oncol. 2009; 16: 3316-22. doi: 10.1245/s10434-009-0670-7.
5. Parsons CM, Sutcliffe JL, Bold RJ. Preoperative evaluation of pancreatic adenocarcinoma. J Hepatobiliary PancreatSurg. 2008; 15: 429-35. doi: 10.1007/s00534-007-1240-7 [doi].
6. Verbeke CS. Resection margins in pancreatic cancer. Surg Clin North Am. 2013; 93: 647-62. doi: 10.1016/j.suc.2013.02.008.
7. Zhang JF, Hua R, Sun YW, Liu W, Huo YM, Liu DJ, Li J. Influence of perineural invasion on survival and recurrence in patients with resected pancreatic cancer. Asian Pac J Cancer Prev. 2013; 14: 5133-9. doi:
8. Vahrmeijer AL, Hutteman M, van der Vorst JR, van de Velde CJ, Frangioni JV. Image-guided cancer surgery using near-infrared fluorescence. Nat Rev Clin Oncol. 2013; 10: 507-18. doi: 10.1038/nrclinonc.2013.123.
9. Rosenthal EL, Warram JM, de Boer E, Chung TK, Korb ML, Brandwein-Gensler M, Strong TV, Schmalbach C, Morlandt A, Agarwal G, Hartman YE, Carroll W, Richman JS, et al. Safety and Tumor-specificity of Cetuximab-IRDye800 for Surgical Navigation in Head and Neck Cancer. Clin Cancer Res. 2015. doi: 10.1158/1078-0432.ccr-14-3284.
10. Ferrone CR, Marchegiani G, Hong TS, Ryan DP, Deshpande V, McDonnell EI, Sabbatino F, Santos DD, Allen JN, Blaszkowsky LS, Clark JW, Faris JE, Goyal L, et al. Radiological and surgical implications of neoadjuvant treatment with FOLFIRINOX for locally advanced and borderline resectable pancreatic cancer. Ann Surg. 2015; 261: 12-7. doi: 10.1097/SLA.0000000000000867.
11. Hartwig W, Werner J, Jager D, Debus J, Buchler MW. Improvement of surgical results for pancreatic cancer. Lancet Oncol. 2013; 14: e476-85. doi: 10.1016/s1470-2045(13)70172-4.
12. Sahani DV, Bonaffini PA, Catalano OA, Guimaraes AR, Blake MA. State-of-the-art PET/CT of the pancreas: current role and emerging indications. Radiographics. 2012; 32: 1133-58; discussion 58-60. doi: 10.1148/rg.324115143.
13. Streeter JE, Herrera-Loeza SG, Neel NF, Yeh JJ, Dayton PA. A Comparative Evaluation of Ultrasound Molecular Imaging, Perfusion Imaging, and Volume Measurements in Evaluating Response to Therapy in Patient-Derived Xenografts. Technology in Cancer Research & Treatment. 2013; 12: 311-21. doi:
14. van Dam GM, Themelis G, Crane LM, Harlaar NJ, Pleijhuis RG, Kelder W, Sarantopoulos A, de Jong JS, Arts HJ, van der Zee AG, Bart J, Low PS, Ntziachristos V. Intraoperative tumor-specific fluorescence imaging in ovarian cancer by folate receptor-alpha targeting: first in-human results. Nat Med. 2011; 17: 1315-9. doi: 10.1038/nm.2472.
15. Harsha HC, Kandasamy K, Ranganathan P, Rani S, Ramabadran S, Gollapudi S, Balakrishnan L, Dwivedi SB, Telikicherla D, Selvan LD, Goel R, Mathivanan S, Marimuthu A, et al. A compendium of potential biomarkers of pancreatic cancer. PLoS Med. 2009; 6: e1000046. doi: 10.1371/journal.pmed.1000046.
16. Sega EI, Low PS. Tumor detection using folate receptor-targeted imaging agents. Cancer Metastasis Rev. 2008; 27: 655-64. doi: 10.1007/s10555-008-9155-6.

17. van Oosten M, Crane LM, Bart J, van Leeuwen FW, van Dam GM. Selecting Potential Targetable Biomarkers for Imaging Purposes in Colorectal Cancer Using TArget Selection Criteria (TASC): A Novel Target Identification Tool. Transl Oncol. 2011; 4: 71-82. doi:
18. de Geus SW, Boogerd LS, Swijnenburg RJ, Mieog JS, Tummers WS, Prevoo HA, Sier CF, Morreau H, Bonsing BA, van de Velde CJ, Vahrmeijer AL, Kuppen PJ. Selecting Tumor-Specific Molecular Targets in Pancreatic Adenocarcinoma: Paving the Way for Image-Guided Pancreatic Surgery. Mol Imaging Biol. 2016. doi: 10.1007/s11307-016-0959-4.
19. Foygel K, Wang H, Machtaler S, Lutz AM, Chen R, Pysz M, Lowe AW, Tian L, Carrigan T, Brentnall TA, Willmann JK. Detection of pancreatic ductal adenocarcinoma in mice by ultrasound imaging of thymocyte differentiation antigen 1. Gastroenterology. 2013; 145: 885-94. doi: S0016-5085(13)00913-X [pii];10.1053/j.gastro.2013.06.011 [doi].
20. Boonstra MC, van Driel PB, van Willigen DM, Stammes MA, Prevoo HA, Tummers QR, Mazar AP, Beekman FJ, Kuppen PJ, van de Velde CJ, Lowik CW, Frangioni JV, van Leeuwen FW, et al. uPAR-targeted multimodal tracer for pre- and intraoperative imaging in cancer surgery. Oncotarget. 2015. doi:
21. Boonstra MC, Tolner B, Schaafsma BE, Boogerd LS, Prevoo HA, Bhavsar G, Kuppen PJ, Sier CF, Bonsing BA, Frangioni JV, van de Velde CJ, Chester KA, Vahrmeijer AL. Pre-clinical evaluation of a novel CEA-targeting near-infrared fluorescent tracer delineating colorectal and pancreatic tumors. Int J Cancer. 2015. doi: 10.1002/ijc.29571.
22. Kimura RH, Teed R, Hackel BJ, Pysz MA, Chuang CZ, Sathirachinda A, Willmann JK, Gambhir SS. Pharmacokinetically stabilized cystine knot peptides that bind alpha-v-beta-6 integrin with single-digit nanomolar affinities for detection of pancreatic cancer. Clin Cancer Res. 2012; 18: 839-49. doi: 1078-0432.CCR-11-1116 [pii];10.1158/1078-0432.CCR-11-1116 [doi].
23. Hildenbrand R, Niedergethmann M, Marx A, Belharazem D, Allgayer H, Schleger C, Strobel P. Amplification of the urokinase-type plasminogen activator receptor (uPAR) gene in ductal pancreatic carcinomas identifies a clinically high-risk group. Am J Pathol. 2009; 174: 2246-53. doi: 10.2353/ajpath.2009.080785.
24. Hackel BJ, Kimura RH, Miao Z, Liu H, Sathirachinda A, Cheng Z, Chin FT, Gambhir SS. 18F-fluorobenzoate-labeled cystine knot peptides for PET imaging of integrin alphavbeta6. J NuclMed. 2013; 54: 1101-5. doi: jnumed.112.110759 [pii];10.2967/jnumed.112.110759 [doi].
25. Metildi CA, Kaushal S, Luiken GA, Hoffman RM, Bouvet M. Advantages of fluorescence-guided laparoscopic surgery of pancreatic cancer labeled with fluorescent anti-carcinoembryonic antigen antibodies in an orthotopic mouse model. J Am Coll Surg. 2014; 219: 132-41. doi: 10.1016/j.jamcollsurg.2014.02.021.
26. Paudyal B, Paudyal P, Shah D, Tominaga H, Tsushima Y, Endo K. Detection of vascular endothelial growth factor in colon cancer xenografts using bevacizumab based near infrared fluorophore conjugate. J Biomed Sci. 2014; 21: 35. doi: 10.1186/1423-0127-21-35.
27. Sipos B, Hahn D, Carceller A, Piulats J, Hedderich J, Kalthoff H, Goodman SL, Kosmahl M, Kloppel G. Immunohistochemical screening for beta6-integrin subunit expression in adenocarcinomas using a novel monoclonal antibody reveals strong up-regulation in pancreatic ductal adenocarcinomas in vivo and in vitro. Histopathology. 2004; 45: 226-36. doi: 10.1111/j.1365-2559.2004.01919.x.
28. Allum WH, Stokes HJ, Macdonald F, Fielding JW. Demonstration of carcinoembryonic antigen (CEA) expression in normal, chronically inflamed, and malignant pancreatic tissue by immunohistochemistry. J Clin Pathol. 1986; 39: 610-4. doi:
29. Handra-Luca A, Hammel P, Sauvanet A, Lesty C, Ruszniewski P, Couvelard A. EGFR expression in pancreatic adenocarcinoma. Relationship to tumour morphology and cell adhesion proteins. J Clin Pathol. 2014; 67: 295-300. doi: 10.1136/jclinpath-2013-201662.

30. Gebauer F, Wicklein D, Horst J, Sundermann P, Maar H, Streichert T, Tachezy M, Izbicki JR, Bockhorn M, Schumacher U. Carcinoembryonic antigen-related cell adhesion molecules (CEACAM) 1, 5 and 6 as biomarkers in pancreatic cancer. PLoS One. 2014; 9: e113023. doi: 10.1371/journal.pone.0113023.
31. Hammarstrom S. The carcinoembryonic antigen (CEA) family: structures, suggested functions and expression in normal and malignant tissues. Semin Cancer Biol. 1999; 9: 67-81. doi: 10.1006/scbi.1998.0119.
32. Zhu J, Thakolwiboon S, Liu X, Zhang M, Lubman DM. Overexpression of CD90 (Thy-1) in pancreatic adenocarcinoma present in the tumor microenvironment. PLoS One. 2014; 9: e115507. doi: 10.1371/journal.pone.0115507.
33. Cruz-Monserrate Z, Abd-Elgaliel WR, Grote T, Deng D, Ji B, Arumugam T, Wang H, Tung CH, Logsdon CD. Detection of pancreatic cancer tumours and precursor lesions by cathepsin E activity in mouse models. Gut. 2012; 61: 1315-22. doi: 10.1136/gutjnl-2011-300544.
34. Gerritsen A, Molenaar IQ, Bollen TL, Nio CY, Dijkgraaf MG, van Santvoort HC, Offerhaus GJ, Brosens LA, Biermann K, Sieders E, de Jong KP, van Dam RM, van der Harst E, et al. Preoperative characteristics of patients with presumed pancreatic cancer but ultimately benign disease: a multicenter series of 344 pancreatoduodenectomies. Ann Surg Oncol. 2014; 21: 3999-4006. doi: 10.1245/s10434-014-3810-7.
35. Tummala P, Junaidi O, Agarwal B. Imaging of pancreatic cancer: An overview. J Gastrointest Oncol. 2011; 2: 168-74. doi: 10.3978/j.issn.2078-6891.2011.036.
36. Agarwal B, Correa AM, Ho L. Survival in pancreatic carcinoma based on tumor size. Pancreas. 2008; 36: e15-20. doi: 10.1097/mpa.0b013e31814de421.
37. Fischer R, Breidert M, Keck T, Makowiec F, Lohrmann C, Harder J. Early recurrence of pancreatic cancer after resection and during adjuvant chemotherapy. Saudi J Gastroenterol. 2012; 18: 118-21. doi: 10.4103/1319-3767.93815.
38. Shimada K, Sakamoto Y, Sano T, Kosuge T. The role of paraaortic lymph node involvement on early recurrence and survival after macroscopic curative resection with extended lymphadenectomy for pancreatic carcinoma. J Am Coll Surg. 2006; 203: 345-52. doi: 10.1016/j.jamcollsurg.2006.05.289.
39. Warram JM, de Boer E, Moore LS, Schmalbach CE, Withrow KP, Carroll WR, Richman JS, Morlandt AB, Brandwein-Gensler M, Rosenthal EL. A ratiometric threshold for determining presence of cancer during fluorescence-guided surgery. J Surg Oncol. 2015; 112: 2-8. doi: 10.1002/jso.23946.
40. Hausner SH, Abbey CK, Bold RJ, Gagnon MK, Marik J, Marshall JF, Stanecki CE, Sutcliffe JL. Targeted in vivo imaging of integrin alphavbeta6 with an improved radiotracer and its relevance in a pancreatic tumor model. Cancer Research. 2009; 69: 5843-50. doi:
41. Park SJ, Gu MJ, Lee DS, Yun SS, Kim HJ, Choi JH. EGFR expression in pancreatic intraepithelial neoplasia and ductal adenocarcinoma. Int J Clin Exp Pathol. 2015; 8: 8298-304. doi:
42. Jewkes AJ, Macdonald F, Downing R, Drolc Z, Allum WH. Labelled antibody imaging in pancreatic cancer, cholangiocarcinoma, chronic pancreatitis and sclerosing cholangitis. Eur J Surg Oncol. 1991; 17: 354-7. doi:
43. Park JW, Chang HJ, Kim BC, Yeo HY, Kim DY. Clinical validity of tissue carcinoembryonic antigen expression as ancillary to serum carcinoembryonic antigen concentration in patients curatively resected for colorectal cancer. Colorectal Dis. 2013; 15: e503-11. doi: 10.1111/codi.12304.
44. Saito G, Sadahiro S, Okada K, Tanaka A, Suzuki T, Kamijo A. Relation between Carcinoembryonic Antigen Levels in Colon Cancer Tissue and Serum Carcinoembryonic Antigen Levels at Initial Surgery and Recurrence. Oncology. 2016. doi: 10.1159/000447062.
45. Khoo SK, Warner NL, Lie JT, Mackay IR. Carcinoembryonic antigenic activity of tissue extracts: a quantitative study of malignant and benign neoplasms, cirrhotic liver, normal adult and fetal organs. Int J Cancer. 1973; 11: 681-7. doi:

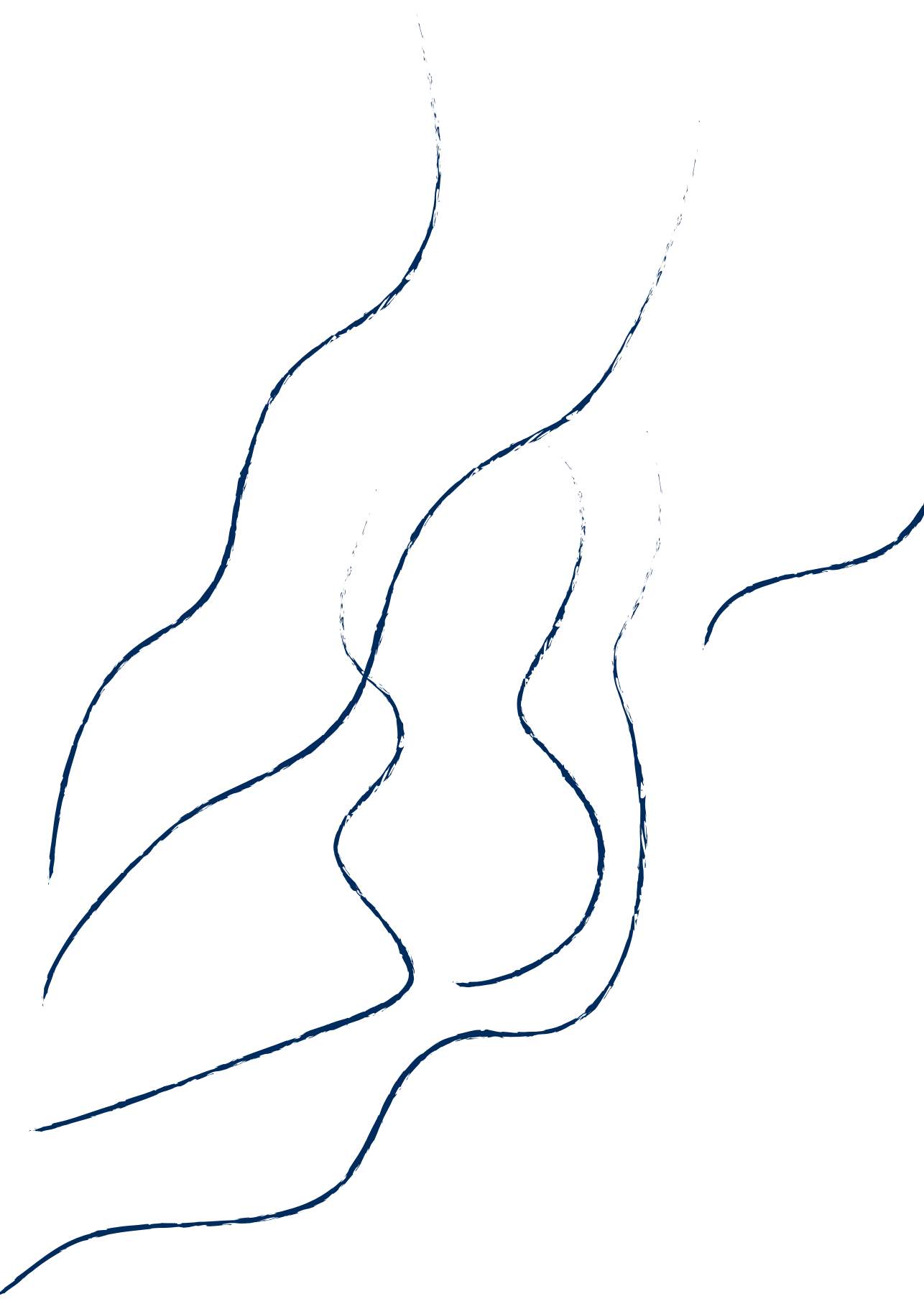
46. Cosimelli M, De Peppo F, Castelli M, Giannarelli D, Schinaia G, Castaldo P, Buttini GL, Sciarretta F, Bigotti G, Di Filippo F, et al. Multivariate analysis of a tissue CEA, TPA, and CA 19.9 quantitative study in colorectal cancer patients. A preliminary finding. Dis Colon Rectum. 1989; 32: 389-97. doi:
47. Nakagoe T, Sawai T, Ayabe H, Nakazaki T, Ishikaw H, Hatano K, Kajiwara K, Miyashita K, Matsuo T, Nogawa T, Arisawa K. Prognostic value of carcinoembryonic antigen (CEA) in tumor tissue of patients with colorectal cancer. Anticancer Res. 2001; 21: 3031-6. doi:
48. Nazato DM, Matos LL, Waisberg DR, Souza JR, Martins LC, Waisberg J. Prognostic value of carcinoembryonic antigen distribution in tumor tissue of colorectal carcinoma. Arq Gastroenterol. 2009; 46: 26-31. doi:
49. Zavaleta CL, Kircher MF, Gambhir SS. Raman's "effect" on molecular imaging. J Nucl Med. 2011; 52: 1839-44. doi: 10.2967/jnumed.111.087775.
50. Blazer M, Wu C, Goldberg RM, Phillips G, Schmidt C, Muscarella P, Wuthrick E, Williams TM, Reardon J, Ellison EC, Bloomston M, Bekaii-Saab T. Neoadjuvant modified (m) FOLFIRINOX for locally advanced unresectable (LAPC) and borderline resectable (BRPC) adenocarcinoma of the pancreas. Ann Surg Oncol. 2015; 22: 1153-9. doi: 10.1245/s10434-014-4225-1.
51. Sahoo S, Lester SC. Pathology of breast carcinomas after neoadjuvant chemotherapy: an overview with recommendations on specimen processing and reporting. Arch Pathol Lab Med. 2009; 133: 633-42. doi: 10.1043/1543-2165-133.4.633.
52. Bracci L, Schiavoni G, Sistigu A, Belardelli F. Immune-based mechanisms of cytotoxic chemotherapy: implications for the design of novel and rationale-based combined treatments against cancer. Cell Death Differ. 2014; 21: 15-25. doi: 10.1038/cdd.2013.67.
53. Letai A. Cell Death and Cancer Therapy: Don't Forget to Kill the Cancer Cell! Clin Cancer Res. 2015; 21: 5015-20. doi: 10.1158/1078-0432.ccr-15-1204.
54. Merlo LM, Pepper JW, Reid BJ, Maley CC. Cancer as an evolutionary and ecological process. Nat Rev Cancer. 2006; 6: 924-35. doi: 10.1038/nrc2013.
55. Burggraaf J, Kamerling IM, Gordon PB, Schrier L, de Kam ML, Kales AJ, Bendiksen R, Indrevoll B, Bjerke RM, Moestue SA, Yazdanfar S, Langers AM, Swaerd-Nordmo M, et al. Detection of colorectal polyps in humans using an intravenously administered fluorescent peptide targeted against c-Met. Nat Med. 2015. doi: 10.1038/nm.3641.
56. Kiehne K, Herzig KH, Folsch UR. c-met expression in pancreatic cancer and effects of hepatocyte growth factor on pancreatic cancer cell growth. Pancreas. 1997; 15: 35-40. doi:
57. Boonstra MC, Prakash J, Van De Velde CJ, Mesker WE, Kuppen PJ, Vahrmeijer AL, Sier CF. Stromal Targets for Fluorescent-Guided Oncologic Surgery. Front Oncol. 2015; 5: 254. doi: 10.3389/fonc.2015.00254.
58. Petrushnko W, Gundara JS, De Reuver PR, O'Grady G, Samra JS, Mittal A. Systematic review of peri-operative prognostic biomarkers in pancreatic ductal adenocarcinoma. HPB (Oxford). 2016; 18: 652-63. doi: 10.1016/j.hpb.2016.05.004.

04



Part | II

# Validation of Targeted Molecular Imaging for Pancreatic Cancer



Chapter | 5

# Preclinical development and validation of multimodal probe for the tumor-specific imaging of pancreatic cancer

Tummers WS [1 2], Kimura RH [1], Abou-Elkacem L [1], Beinat C [1], Vahrmeijer AL [2], Swijnenburg RJ [2], Willmann JK [1], Gambhir SS [3]

[1] Department of Radiology, Molecular Imaging Program at Stanford (MIPS), Stanford University, Stanford, CA, 94305, USA. [2] Department of Surgery, Leiden University Medical Center, Albinusdreef 2, 2300 RC, Leiden, The Netherlands. [3] Departments of Radiology, Bioengineering, and Materials Science & Engineering, Molecular Imaging Program at Stanford. Canary Center at Stanford for Early Cancer Detection. Stanford University, Stanford, CA, 94305, USA.

*Clin Cancer Res. 2018 Apr 1;24(7):1667-1676.*

## ABSTRACT

**Purpose:** Intraoperative near-infrared fluorescence (NIRF) imaging could help stratification for the proper primary treatment for patients with pancreatic ductal adenocarcinoma (PDAC), and achieve complete resection since it allows visualization of cancer in real time. Integrin αvβ6, a target specific for PDAC, is present in >90% of patients, and is able to differentiate between pancreatitis and PDAC. A clinically translatable αvβ6-targeting NIRF agent was developed, based on a previously developed cysteine knottin peptide for PET imaging, R01-MG, and validated in preclinical mouse models.

**Experimental Design:** The applicability of the agent was tested for cell and tissue binding characteristics using cell-based plate assays, subcutaneous and orthotopic pancreatic models, and a transgenic mouse model of PDAC development (Pdx1-Cre$^{tg/+}$;KRas $^{LSL\ G12D/+}$;Ink4a/Arf$^{-/-}$). IRDye800CW was conjugated to R01-MG in a 1:1 ratio. R01-MG-IRDye800, was compared to a control peptide and IRDye800 alone.

**Results:** In subcutaneous tumor models a significantly higher tumor-to-background ratio (TBR) was seen in BxPC-3 tumors (2.5±0.1) compared to MiaPaCa-2 (1.2±0.1) ($p<0.001$), and to the control peptide (1.6±0.4) ($p<0.005$). In an orthotopic tumor model tumor-specific uptake of R01-MG-IRDye800 was shown compared to IRDye800 alone (TBR 2.7 versus 0.86). The fluorescent signal in tumors of transgenic mice was significantly higher, TBR of 3.6±0.94, compared to the normal pancreas of wild type controls, TBR of 1.0±0.17 ($p<0.001$).

**Conclusion**: R01-MG-IRDye800 shows specific targeting to αvβ6, and holds promise as a diagnostic and therapeutic tool to recognize PDAC for fluorescence-guided surgery. This agent can help improve the stratification of patients for a potentially curative, margin-negative resection.

# INTRODUCTION

Pancreatic ductal adenocarcinoma (PDAC) has a dismal prognosis.[1, 2] In fact, it is the fourth leading cause of cancer-related deaths in the western world; 43,090 patients are estimated to die of PDAC in 2017 in the Unites States. The median size of a PDAC at the time of diagnosis is ~3.1cm, and this has not changed in the past three decades despite major advances in both anatomical and molecular imaging technologies as well as in vitro diagnostics.[3, 4] Early detection of pancreatic cancer is difficult because patients are often asymptomatic or present with non-specific symptoms until late stage disease.[4, 5] After diagnosis the patient selection for surgical resection is challenging. A potential curative resection can only be achieved in a minority of patients, and is dependent on tumor stage and grade. Two major predictors of long-term survival after resection are the achievement of tumor free resection margins and the absence of systemic metastases. Unfortunately, margin-positive resections (R1) are a frequent phenomenon (up to 70%) as is the emergence of distant metastases soon after surgery, which were likely present at the time of surgery in the form of visually occult micrometastases.[6-8] Failure to identify tumor-positive margins during surgery is not surprising, due to the tumor characteristics to quickly spread beyond the pancreas via perineural and perivascular pathways[9] and the inability of the surgeon to differentiate between tumor and (peritumoral) inflammatory tissue, such as associated chronic pancreatitis.[10, 11]



The integration of innovative molecular imaging techniques into the operating room can lead to the transformation of current gold standard intraoperative imaging modalities, such as intra-operative ultrasound and the surgeon's eyes, into pancreatic cancer-specific molecular imaging tools. Optical imaging in real-time, using a novel near-infrared fluorescent pancreatic cancer-targeting imaging agent, could add relevant information to the surgeon, by enhancing tumor margins and improving the detection of visually occult lesions. This would improve the selection of patients for the most suitable primary treatment.

In previous studies, out of a panel of different biomarkers, we selected integrin avβ6 as the most promising target for pancreatic cancer detection, based on its potential to discriminate tumor and inflammation, to identify lymph node

metastases, to differentiate between viable tumor cells and necrosis in patients who received neoadjuvant therapy.[12, 13]

We previously developed a cysteine knottin that binds to integrin αvβ6 with subnanomolar affinity (Kd~1nM).[14] At this point, this peptide is tested in a Phase I trial in humans as a targeted PET tracer, [18F]FP-R01-MG-F2, without any safety concerns (eIND #126379). Zhang et al. recently published data showing the development and preclinical validation of R01 conjugated to the photoacoustic dye Atto-740.[15] Zhang showed selective binding of the imaging agent to αvβ6-positive tumors. However, this agent exhibited hepatobiliary clearance marked by high uptake in the liver, spleen, and intestine. For a pancreatic cancer imaging agent, a renal clearance pathway is preferred for a due to the close proximity of the liver, and therefore potential interference of signal. Since the PET tracer show renal clearance the fluorescent dye was changed to achieve

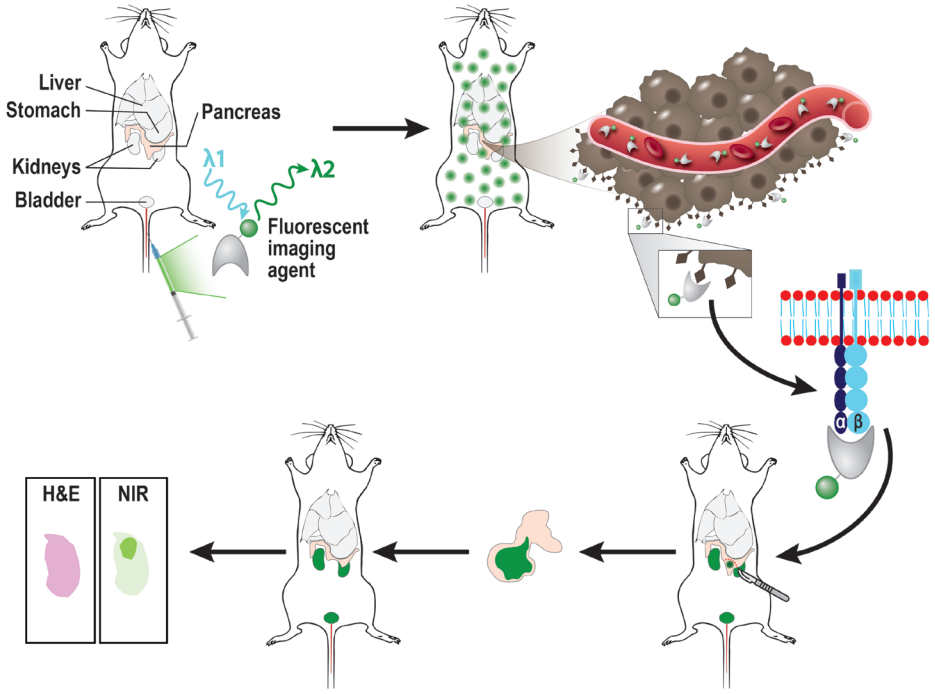



**Figure 1.** Schematic overview of imaging agent concept. Agent is injected intravenously, and migrates via the vessel to the target of interest (αvβ6). Resection of the pancreatic cancer can be performed guided by fluorescent signal, and fluorescent signal at microscopic level is conformed with tumor status on histopathology. The agent preferably has renal clearance, since fluorescent signal from the liver in case of a hepatic route could interfere with signal from the tumor.

these favorable pharmacokinetics. The NIR fluorescent dye IRDye800 is known to clear via the kidneys, and has a high extinction coefficient.[16] In addition, IRDye800 is already tested extensively in humans and shown safe in clinical studies.[11, 17] Therefore, IRDye800 was the NIR fluorescent dye of choice in the current study. The preferred imaging concept is shown in figure 1, highlighting the preference of an intravenously injected agent. This agent needs to bind selectively to the tumor receptors, facilitating fluorescence-guided resection, and excretion by the kidney's is favorable in pancreatic cancer surgery. Lastly, the fluorescent signal needs to be correlated to tumor status on H&E to ensure specific binding.

Here, we show the development and validation of a novel αvβ6-targeting probe for intraoperative tumor-specific fluorescent imaging of PDAC, with high potential for clinical translation.



## MATERIALS AND METHODS

### Materials and reagents

All Fmoc amino acids and Rink Amide resin were purchased from CS Bio Co. (Menlo Park, CA). Peptide synthesis were carried out following the standard solid phase Fmoc synthesis. Analysis and purification of the peptides was performed using the Dionex Summit high-performance liquid chromatography (HPLC) system (Dionex Corporation, Sunnyvale, CA) and reverse phase HPLC column Higins Analytical (Higins Analytical, Mountain View, CA) (C18, 4.6 mm × 250 mm). The mobile phase was 0.1% trifluoroacetic acid (TFA; Thermo Fisher Scientific, Pittsburgh, PA)) in water (solvent A) and 0.1% TFA in 90 % acetonitrile (CH3CN; Thermo Fisher Scientific, Pittsburgh, PA) in water (solvent B). Matrix assisted laser desorption/ionization time-of-flight mass spectrometry (MALDI-TOF MS) was performed by the Canary Center proteomics facility on AB Sciex 5800 TOF/TOF System (Foster City, CA).

### Development of tumor-specific fluorescent probe

Knottin peptide R01-MG targeted integrin αvβ6 were synthesized using the described standard solid phase Fmoc synthesis, and folded and purified as previously described.[18] For labeling of the knottin peptide R01-MG, IRDye800

N-hydroxysuccinimide (NHS) ester (LI-COR Biosciences, Lincoln, Nebraska) was dissolved in anhydrous, amine-free dimethylformamide (DMF; Sigma Aldrich, St Louis, MO) to a 0.5 mg/ml solution. Knottin peptide R01-MG was dissolved in Dulbecco's Phosphate-Buffered Saline (DPBS; Life technologies, Foster City, CA) to a 1.5 mg/ml solution. IRDye800 NHS solution was mixed with knottin peptide R01 solution in 1:1 molar ratio. The reaction mixture was incubated and protected from light for up to 1 hour at room temperature. The reaction mixture was injected directly onto the HPLC column, and the separation of the product mixture followed using absorbance at 780 nm. The imaging agent had a retention time of 16.89 minutes and m/z of 4817. The lyophilized IRDye800-peptide was dissolved in 100uL dimethyl sulfoxide (DMSO; Thermo Fisher Scientific, Pittsburgh, PA) and 100uL DPBS. Maximum absorption wavelength of R01-MG-IRDye800 agent was performed using Cary50 (Varian).

### Development of control cysteine knottin

The tumor-specific probe is based on the trypsin inhibitor, momordica cochinchinensis trypsin inhibitor (MCoTI-II). For the control cysteine knottin the binding sequence of R01-MG to αvβ6 was replaced with the MCoTI-II sequence at these positions, to develop a control knottin most similar to the original R01-MG. This resulted in the following sequence; N'-GCPRILMRCRRDSDCPGACICRGNGYCG. Synthesis, folding and purification was performed as described. The control cysteine knottin had a retention time of 20.60 minutes and m/z of 3033. The control peptide was labeled with IRDye800 N-hydroxysuccinimide (NHS) ester (LI-COR Biosciences, Lincoln, Nebraska, USA) in a similar fashion as R01-MG-IRDye800. The reaction mixture was injected directly onto the HPLC column, and the separation of the product mixture followed using absorbance at 780 nm. The imaging agent had a retention time of 16.53 minutes.

### Photostability

100 µL of R01-MG-IRDye800 (0.5x10-6 M) was placed in a 96-well plate in the SpectraMax Gemini EM microplate reader (Molecular Devices, Ramsey, MN, USA) in triplicate and scanned with laser light using maximum absorption wavelength (750 nm) and emission wavelength (800nm) for 30 min. Photobleaching was determined by the change in fluorescent intensity over time.

### Human cancer cell lines

A total of six cancer cell lines were used for the cell-based experiments, including four pancreatic cancer cell lines (BxPC-3, BxPC-3-luc2, MiaPaCa-2, and AsPC-1), one colorectal cancer cell line (HCT-116), and one epidermoid carcinoma (A431). All cell lines, except for BxPC-3-luc2, were purchased from American Type Culture Collection (ATCC, Manassas, VA) and expression was authenticated within 6 months before the in vitro experiments. The BxPC-3-luc2 cell line was purchased from PerkinElmer (MA). BxPC-3 (CRL-1687TM), provided by ATCC, was used as source for the parental cell line. BxPC-3 and BxPC-3-luc2 cells were cultured in RPMI-1640 medium containing 10% fetal bovine serum, 1 % penicillin and streptomycin. MiaPaCa-2, HCT-116 and A431 cells were cultured in DMEM containing 10% fetal bovine serum, 1 % penicillin and streptomycin. For MiaPaCa-2 cells, also 2.5% horse serum was added according to ATCC guidelines.



### Mouse cancer cell lines

The binding of R01-MG-IRDye800 to mouse αvβ6 was assessed to determine the *in vivo* specific binding to mouse αvβ6. The following two cell lines were used; a mouse breast cancer cell line (4T1), and mouse colon carcinoma cell line (CT-26). All cell lines were purchased from American Type Culture Collection (ATCC, Manassas, VA) and expression was authenticated within 6 months before the in vitro experiments. A maximum of ten passages was performed for all cells, between thawing and use in the described experiments. CT-26 cells were cultured in DMEM medium containing 10% fetal bovine serum, 1 % penicillin and streptomycin. 4T1 cells were cultured in RPMI-1640 medium containing 10% fetal bovine serum, 1 % penicillin and streptomycin.

### Flow cytometry

All cells were tested for αvβ6 expression using flow cytometry. The cells were grown to 90% confluence and detached with trypsin/EDTA. After evaluation of cell viability using trypan blue, cells were adjusted to 1 x $10^6$ per tube in ice-cold PBS with 4% formaldehyde for fixation and incubated in a binding buffer containing DMEM, 0.1% BDA and 0.1% NaN3 with 100ul of anti-αvβ6 mouse monoclonal antibody (10D5, ab77906, Abcam, Cambridge, United Kingdom) for 1h at room temperature. After incubation, cells were washed thrice and incubated with the secondary antibody anti-mouse IgG $F(ab)_2$ fragment

conjugated to Alexa Fluor® 647 (#4410, Cell Signaling Technology, Danvers, MA, United States, 1/800) for 30 min. After three washing steps with the washing buffer, cells were resuspended in 500ul PBS. Samples were measured on the Scanford flow cytometer (Custom Stanford and Cytek upgraded FACScan Analyzer) and $1x10^5$ cells were counted.

## Cell binding study

Human cancer cell lines BxPC-3 (αvβ6 positive) and MiaPaCa-2 (αvβ6-negative), and murine cancer cell lines 4T1 (αvβ6 positive) and CT-26 (αvβ6-negative) were placed in a 8 well chamberslide (0.7 $cm^2$, Nunc™ Lab-Tek™ II Chamber Slide™ System; ThermoFisher Scientific, Waltham, MA, USA) and grown to ~85% confluence. Cells were fixed for 20 min at 4 °C with 1% formaldehyde. R01-MG-IRDye800 was diluted in integrin-binding buffer (IBB). The IBB was similar as previously described [19], and added to the chamberslide with concentration of 0.1 μM, 0.2 μM or 0.5 μM and incubated at room temperature for 2 h. After being washed with DPBS three times, the chamber was removed and the nuclei were counter stained with ProLong® Gold Antifade Mountant with DAPI (ThermoFisher Scientific, MA, Waltham, USA). The cellular binding of R01-MG-IRDye800 was assessed by co-staining of cells with DAPI and fluorescence with the EVOS Cell Imaging Systems (EVOS FL Cell Imaging System, ThermoFisher Scientific, MA, USA) with EVOS light cube Cy7, excitation 710-740 and emission: 775-746, and EVOS light cube DAPI, excitation: 357-344 and emission: 447-460. For quantitative analysis, mean fluorescent intensity (MFI), defined as total counts/region of interest (ROI) pixel area, was calculated using custom ROI generated for each specimen using the imaging software ImageJ version 1.50i and bundled with 64-bit Java for Windows (National Institutes of Health, Bethesda, MD; http://rsb.info.nih.gov/nih-image). Specificity of the binding was determined by a blocking experiment with incubation of BxPC-3-luc2 cells with 0.5 μM of R01-MG-IRDye800 and varying amounts of R01-MG (50x (25 μM) – 150x (75 μM) – 200x (100 μM) excess), and by incubation of BxPC-3-luc2 cells with IRDye800 0.5 μM alone. All samples were done in triplicates. For IRDye800 alone, IRDye800-NHS ester was used which is equal to the dye used in the agent. The NHS ester was reacted with water before injection, to ensure no reaction with amine groups could take place. A linear regression analysis was performed to determine if there was a linear correlation between concentration

and fluorescent signal; for BxPC-3 (Y = 118171*X + 11944) and for MiaPaCa-2 (Y = 23296*X + 9738).

To identify fluorescence intensity with increasing amount of αvβ6 receptors, an experiment was designed with both BxPC-3 and MiaPaCa-2 cells, in varying percentages; with the lowest amount of receptors in 100% MiaPaCa-2, and increasing amounts onwards; 20% BxPC-3 - 80% MiaPaCa-2, 40% BxPC-3 - 60% MiaPaCa-2, 60% BxPC-3 - 40% MiaPaCa-2, 80% BxPC-3 - 20% MiaPaCa-2, and 100% BxPC-3. The cells were incubated with 0.5 μM of R01-MG-IRDye800 for 2 h. Additional cell experiments were performed comparing R01-MG-IRDye800 to the newly synthesized control peptide. BxPC-3 cells were placed on a 8-well chamberslide, and after fixation incubated with both agents separately at concentration of 0.1 μM, 0.2 μM or 0.5 μM.



## Fluorescent imaging of αvβ6 in Small Animal Models

### *Subcutaneous mouse model of human pancreatic cancer*

The Administrative Panel on Laboratory Animal Care of Stanford University approved all procedures using laboratory animals. Eight week old nude female mice (n=20) (Charles River) were injected with 1 million BxPC-3-luc2, A431, or MiaPaCa-2-luc cells into the right shoulder. Mice bearing 0.4-0.8 cm tumors (n=8 BxPC-3-luc2, n=3 A431, n=4 MiaPaCa-2) for R01-MG-IRDye800, and n=5 for control cysteine knottin) were fluorescently imaged at 800 nm using a commercially fluorescent imaging system (The Pearl Impulse imaging platform (LI–COR Biosciences, Lincoln, NE). For each animal we first obtained pre-injection images at 800 nm. R01-MG-IRDye800 (30 μM), the control cysteine knottin (30 μM), or IRDye800 alone (30uM) was dissolved in 200 μL PBS (pH 7.4) and administered to mice via tail-vein injection. The data was acquired from 30 min up to 24h after the injection of the imaging agent.

### *Xenograft mouse model of human pancreatic cancer*

Human AsPC1 pancreatic ductal adenocarcinoma cells (αvβ6 positive) (ATCC, Manassas, VA) were cultured to 70%–80% confluency. AsPC-1 cells were cultured in DMEM medium containing 10% fetal bovine serum, 1% penicillin and streptomycin. AsPC1 cells were suspended in culture medium and mixed 1:1 with Matrigel® (BD Biosciences, San Jose, CA) for orthotopic implantation. Sterile insulin syringes were loaded with the mixture and kept on ice until

orthotopic implantation. After midline laparotomy, the pancreas of nu/nu mice was exposed, and AsPC1 cells (total of $6 \times 10^6$ cells, dissolved in 25 µL Matrigel containing epidermal growth factor [0.7 ng/mL], insulin-like growth factor [16 ng/mL], and transforming growth factor–β [2.3 ng/mL]; BD Biosciences, San Jose, CA) were co-injected into the body or tail of the pancreas in 8 female nude mice (6–8 weeks old; Charles River, Wilmington, MA). The abdomen was then closed by layers. Orthotopic xenografts were allowed to grow for 21 days. R01-MG-IRDye800 (30 µM) or IRDye800 (30 µM) was dissolved in 200 µL PBS (pH 7.4) and administered to mice via tail-vein injection. The data was acquired from 30 min up to 24h after the injection of the imaging agent.

### *Transgenic Mouse Model of PDAC*

The transgenic pancreatic cancer mouse model (Pdx1-Cretg/+; KRasLSL G12D/+; Ink4a/Arf–/–) was used (n = 10), which spontaneously develops foci of pancreatic cancer within 4–7 weeks of age.[20] Tumor diameters ranged between 3.0 and 4.8 mm. Age-matched littermates without $KRas^{G12D}$ mutation were used as normal wildtype control (n = 10). R01-MG-IRDye800 (30 µM) was dissolved in 200 µL PBS (pH 7.4) and administered to mice via tail-vein injection, in both the wildtype controls and tumor-bearing mice.

## Toxicity of R01-MG-IRDye800 in mice

The toxicity of R01-MG-IRDye800 in living mice was determined in Nu/Nu mice (n=3). After injection of R01-MG-IRDye800 (30 µM) the mice were followed for three weeks and weight and overall appearance was assessed. In addition, blood draws were done to assess effect on red and white blood cells, aspartate transaminase (ASAT), alanine transaminase (ALAT) and creatinine.

## *Ex vivo* imaging and biodistribution

All the mice were sacrificed between 6 or 24 h postinjection of the imaging agent as described above. Optical imaging of the excised organs was carried out using The Pearl Impulse imaging platform at 800 nm for biodistribution studies.

## NIR-fluorescent animal imaging analysis

The Pearl Impulse small animal imaging system (LI-COR) was used for NIR-fluorescence measurements to measure NIR-fluorescent signals of the tumor, biodistribution analysis and to calculate TBR (tumor-to-background ratios).

The specific and control images were normalized and regions of interest were marked. The background signals were extracted from the surrounding tissue that was defined as the (normal) tissue/organ that lies around the tumor. After measuring the signal intensity from the macroscopic images they were divided by each other using the following formula: TBR = mean signal tumor/ mean signal surrounding tissue.

## Histology

Formalin-fixed paraffin-embedded tumor tissues were sectioned at 5 μm thickness and fluorescence imaging was performed using the Odyssey NIR scanner (LI-COR Biosciences). All histologic sections were stained with standard hematoxylin-eosin immunohistochemical staining (H&E). To confirm the presence of αvβ6, additional sections were stained with immunohistochemistry (IHC) for anti-human αvβ6 (1/80, 6.2A1, Biogen Idec, Cambridge, MA). For preparation of IHC staining, the slides were deparaffinized with xylene and rehydrated in serially diluted ethanol solutions (100%-50%), followed by demineralized water according to standard protocols. Endogenous peroxidase activity was blocked by incubation in 0.3% hydrogen peroxidase in phosphate buffered saline (PBS) for 20 min. Antigen retrieval for αvβ6 was performed with 0.4% pepsin incubation (Dako) at 37°C for 10 min. Following antigen retrieval, the tissue sections were incubated overnight with the primary antibodies in 100 μl for standard tissue sections at room temperature. The slides were washed with PBS, followed by incubation with secondary antibody at room temperature according to the Vectastain ABC HRP kit (Peroxidase, Mouse IgG, Vector Laboratories Inc., Burlingame, CA). After additional washing, the staining was visualized with 3,3-diaminobenzidine tetrahydrochloride solution (DAKO, Glustrup, Denmark) at room temperature for 5 minutes and counterstained with hematoxylin for 20 seconds. Finally, the tissue sections were dehydrated and mounted in Pertex (Histolab, Rockville, MD, USA).

## Statistical Analysis

Analyses were performed in SPSS 22.0 (IBM technologies). All data were presented as the mean ± standard deviations. Means were compared using Independent-Samples T test, or with One-way ANOVA with post-hoc Bonferroni correction. A P-value of less than .05 was considered to indicate a significant

difference. Graphs and linear regression were performed in GraphPad Prism 7.0 (version 7.02, IBM Corp.)

## RESULTS

### IRDye800 (NIRF dye) conjugation of the cysteine knottins

R01-MG was synthesized, and labeled with IRDye800CW at 1:1 ratio (Figure S1A). In addition the control cysteine knottin was synthesized (Figure S1B), and conjugated following the same protocol. R01-MG-IRDye800 showed high stability without clear decrease in fluorescent signal after laser exposure at 750nm for 30 minutes (Figure S1C). This correlates to the stability of IRDye800 alone.[21]

### avβ6 expression on cancer cell lines

The expression of αvβ6 in the cancer cell lines (listed above) was evaluated by flow cytometry using the monoclonal antibody, 10D5, and shown in the supplementary figures (Figure S2). Four of the cancer cell lines showed high αvβ6 expression; BxPC-3-luc2, A431, AsPC-1 and 4T1. Three cancer cell lines showed none or low αvβ6 expression; MiaPaCa-2, HCT-116, CT-26. Based on these experiments, we selected BxPC-3 and A431 as positive and MiaPaCa-2 as negative controls respectively for further studies.

### R01-MG-IRDye800 specificity

The retained αvβ6-specificity of R01-MG-IRDye800 was confirmed using chamberslide assays. An increase in agent concentration resulted in an almost linear increase in signal intensity in the αvβ6 positive cell line (BxPC-3), while the αvβ6 negative cell line (MiaPaCa-2) showed limited signal intensity (Figure 2A). The difference between the cell lines was observed for all the different concentration tested, however staining at the lowest concentration [0.1uM] was also weak in BxPC-3 cells (Figure 2A). Competition of R01-MG-IRDye800 with unlabeled R01-MG resulted in a 77.2% reduction in NIR signal intensity, suggesting that the αvβ6-specific binding capacity of R01-MG after conjugation to IRDye800 remained. In addition, in a cell assay with different concentration of αvβ6 receptors, simulated by different percentages of BxPC-3 and MiaPaca-2

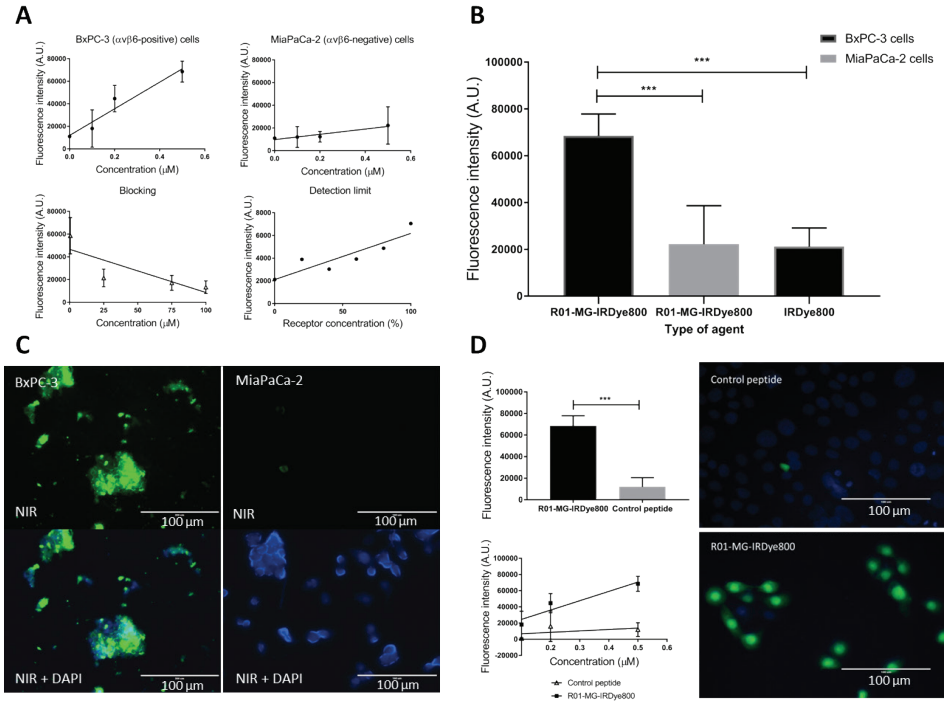



**Figure 2**. Cell binding study of R01-MG-IRDye800. (**A**) Graphic representation of fluorescent signal in BxPC-3 (αvβ6-positive), MiaPaCa-2 (αvβ6-negative) cells with regression line, after blocking with R01-MG, and with different concentrations of αvβ6-receptors. (**B**) Comparison of fluorescent signal in αvβ6-positive, and –negative cells after incubation with R01-MG-IRDye800, and after incubation with IRDye800 alone. (**C**) Representative fluorescence microscopy images of BxPC-3 cells with fluorescent signal at 800nm (green) and in overlay with DAPI signal (blue) to co-stain cell nuclei, and MiaPaCa-2 cells without any fluorescent signal at 800nm, but with DAPI-signal (blue). (**D**) Comparison between R01-MG-IRDye800 and newly synthesized fluorescent control knottin in BxPC-3 cells. ***; p<0.001, graphs are mean ± SD.

cells together, an increase in receptors led to a linear increase in fluorescent signal ($R^2$ = 0.80) (Figure 2A).

A significant difference in fluorescent (figure 2B, C) signal between BxPC-3 and MiaPaCa-2 cells was detected (p<0.001), and after 2h of incubation the fluorescent signal in BxPC-3 cells was 3.1 fold higher compared to the MiaPaca-2 cells. To control for non-specific staining of the fluorescent dye, incubation with the fluorescent dye alone, [0.5uM] IRDye800, was performed. The fluorescence intensity was 2.7 times lower compared to the incubation of [0.5uM] R01-MG-IRDye800 in BxPC-3 cells (p<0.001) and equal to the intensity in MiaPaCa-2 (p=1.000), indicating the specific binding of R01-MG-IRDye800 to αvβ6 (Figure

2B). A significant ($p<0.001$) lower fluorescent signal was observed after incubation with the control cysteine knottin, compared to R01-MG-IRDye800 as shown in Figure 2D. There was no fluorescent signal observed in both cell lines after incubation with PBS.

## Mouse models

### *Specificity of R01-MG-IRDye800 in subcutaneous mouse models*

To validate the performance of R01-MG-IRDye800 in living subjects, three different mouse models were used: (1) a subcutaneous model with different cell lines, (2)an orthotopic, intrapancreatic xenograftmodel using different cell lines, and (3) a spontaneous transgenic pancreatic cancer model. Subcutaneous tumor models were used to compare the binding of R01-MG-IRDye800 in αvβ6-positive and –negative tumors, and to determine the TBR over time (Figure 3A). The highest TBR for BxPC-3 mice was measured 20h post injection (4.08 ± 0.95) (Figure 3B). There was a difference in TBR between BxPC-3 tumors (2.5 ± 0.1), MiaPaCa-2 tumors (1.2 ± 0.1), and A431 tumors (1.8 ± 0.5), with a linear increase in TBR for both the BxPC-3 tumors and A431 tumors over time. The TBR of MiaPaCa-2 tumors remained stable at~1.0 during the investigated period of 5 hours (Figure 3C). BxPC-3 tumors had a significantly higher TBR compared to MiaPaCa-2 tumors ($p<0.001$) (Figure 3D). As controls R01-MG-IRDye800 was compared to a control peptide and fluorescent dye alone. The TBR of the mice injected with R01-MG-IRDye800 after 24h (3.5 ± 0.95) was significantly ($p<0.005$) higher compared to control peptide (1.6 ± 0.36), and dye alone (1.4 ± 0.2) ($p<0.005$) suggesting specific targeting of αvβ6 by R01-MG-IRDye800 (Figure 3E). In addition, compared to IRDye800 alone, a clear increase in mean TBR was seen over time for R01-MG-IRDye800, compared to an approximately constant mean TBR for IRDye800. This difference was significant from T=4h after injection (T=0h $p=0.95$, T=1h $p=0.16$, T=3h $p=0.05$, T=4h $p<0.001$, T=6h $p<0.001$, T=24h $p<0.005$) (Figure 3F).

### *αvβ6 binding and biodistribution in orthotopic mouse models*

The efficacy of R01-MG-IRDye800 to bind and detect αvβ6 *in vivo* was evaluated in pancreatic cancer orthotopic xenografts implanted in nude mice. A mean TBR of 2.7 ± 1.22 at 24 hours post-injection was measured, compared to a mean TBR of 0.86 ± 0.13 for IRDye800 alone (Figure 4A). *Ex vivo* NIR-fluorescence measurements showed tumor specificity of the tracer with a mean TBR of 6.96 ±

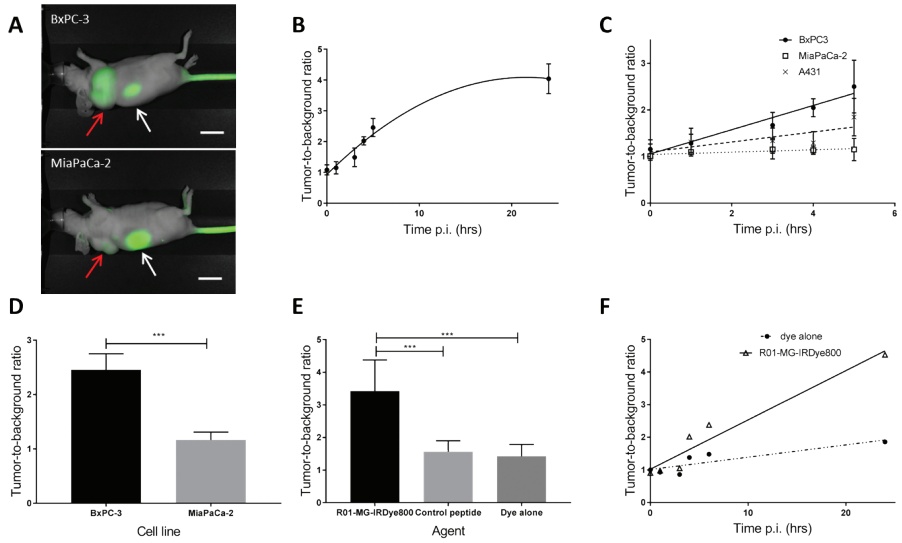



**Figure 3**. Preclinical validation R01-MG-IRDye800 in subcutaneous tumor models at 800nm. (**A**) Representative image of mouse with BxPC-3 and MiaPaCa-2 tumor 4h post-injection of R01-MG-IRDye800, and clear excretion via de kidneys. The tumor is indicated with a red arrow, the kidneys with white arrow. (**B**) Tumor-to-background ratio over time in BxPC-3 tumors with nonlinear fit curve, and (**C**) in tumors with different levels of αvβ6. (**D**) Comparison of maximum TBR in BxPC-3 and MiaPaCa-2 tumors, 5h post injection. (**E**) Validation of αvβ6-specific binding with R01-MG-IRDye800 compared to a control cysteine knottin and the fluorescent dye alone at maximum TBR, and (**F**) over time. Scale bar represent 1 cm. Graphs are mean ± SD.

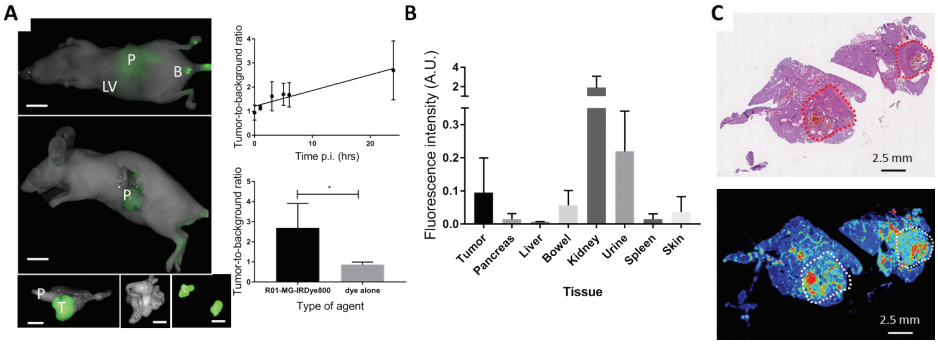



**Figure 4.** Validation in pancreatic cancer orthotopic xenografts at 800nm. (**A**) Representative images of tumor visualization using R01-MG-IRDye800, both in vivo and ex vivo. Ex vivo the pancreas with tumor is shown (left), the bowel (middle), and the kidney's (right). TBR in vivo over time, and comparison of maximum TBR between R01-MG-IRDye800 and IRDye800 alone. (**B**). Biodistribution of R01-MG-IRDye800, with highest uptake in the kidneys. (**C**) Correlation between tumor on H&E (outlined in red), and increased fluorescent signal. Scale bar represent 1 cm, unless indicated differently. P = pancreas, B = bladder, LV = liver. Graphs are mean ± SD.

2.2. Biodistribution assays showed high fluorescence in the kidneys (MFI 1.12 AU) and urine (MFI 0.22 AU) compared to the liver (MFI 0.007 AU) indicating a renal clearance route, and some fluorescence in the bowel (MFI 0.03 AU) and skin (MFI 0.02 AU) (Figure 4B). Fluorescence in the bowel can be explained by mild αvβ6 expression in gastro-intestinal tract mucosa.[22, 23] At the microscopic level, high fluorescence matched well with location of the tumor on H&E (Figure 4C).

### *Validation in transgenic mouse models*

In the spontaneous transgenic tumor mouse model, the tumor could be visualized, even with the skin intact, and fluorescence localized at tumor regions was clearly visible *ex vivo* (Figure 5A). Even a subcentimeter metastasic lesion on the bowel (0.7 x 0.5 cm) could be visualized with fluorescence, corresponding to tumor-positive H&E (Figure 5B). In mice with the tumor genotype, the TBR

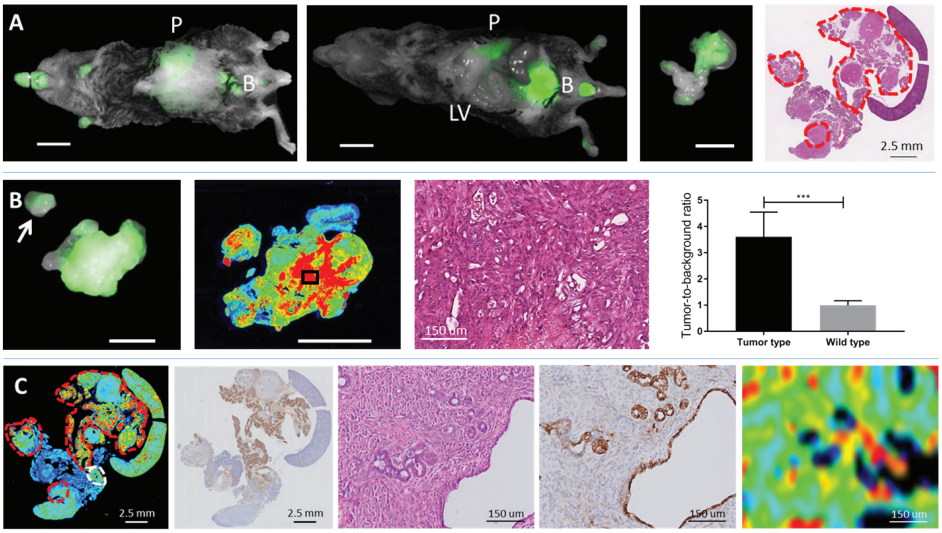



**Figure 5.** Fluorescent imaging and validation of R01-MG-IRDye800 in transgenic mice model at 800nm. (**A**) In vivo fluorescent imaging of mouse with pancreatic cancer, showing agent excretion via the kidneys in mouse with skin and without skin. In addition, ex vivo fluorescent imaging of resected pancreas with localized fluorescence and corresponding H&E section of entire pancreas with tumor localizations (outlined in red). (**B**) Ex vivo fluorescent imaging of primary tumor with subcentimeter metastasis on the bowel (white arrow), and corresponding fluorescence intensity scan with Odyssey Imaging System (LI-COR) showing high fluorescence in tumor areas, with corresponding H&E section of PDAC (black box). In addition, a graphic representation of mean TBR in transgenic mice of tumor versus normal pancreas ($p<0.001$). (**C**) Immunohistochemical correlation between fluorescent signal, tumor status and αvβ6 expression. Scale bar represent 1 cm, unless indicated differently. P = pancreas, B = bladder, LV = liver. Graphs are mean ± SD.

obtained with R01-MG-IRDye800 (3.6 ± 0.94) was significantly higher compared to the TBR in the normal pancreas of the WT controls after R01-MG-IRDye800 infusion (1.0 ± 0.17) ($p<0.001$) (Figure 5B). Fluorescent signal, and tumor status corresponded well to αvβ6 expression as assessed by immunohistochemistry (Figure 5C). To resemble the human situation, fluorescent signal provided by R01-MG-IRDye800 showed successful distinction between PDAC and peritumoral inflammation when in close proximity, even on microscopic level (Figure S3).

### Toxicity of R01-MG-IRDye800

Pilot toxicity of the agent was determined in nude mice (N=3) by measurement of weight and hematology and chemistry blood panels. There was no significant difference observed in weight of mice pre-injection of R01-MG-IRDye800, directly after injection ($p=0.054$) and after the observation period of 3 weeks ($p=0.732$). The liver panel slightly increased after agent injection, and red blood cells count decreased, but all returned to baseline levels after follow-up. A slight increase in white blood cell count and creatinine was also seen, but these levels remained within normal limits for the entire observation period (Figure S4).



## DISCUSSION

To improve the dismal prognosis of patients with PDAC, focus should be on early detection, improved patient selection for treatment and better surgical outcomes. A significant number of patients with PDAC present while the disease has already spread and will therefore not benefit from surgery as primary treatment. A limitation of conventional imaging techniques, such as CT and MRI, is the low sensitivity for detection of subcentimeter lesions and therefore metastatic spread is not always detected prior to surgery.[24] To overcome this limitation, optical imaging could be an additional tool to be applied during a diagnostic laparoscopy, prior to resection, to screen the abdomen for potential metastatic spread, such as liver or peritoneal metastases. For superficial lesions, fluorescent imaging is superior. Adjacent to that, for a more thorough screening of the liver, optoacoustic imaging could be added to provide sufficient depth penetration.[10, 25] If no spread is found in this initial stage, the surgery can proceed using the same optical imaging techniques to guide the resection. During resection, use of optical imaging can improve radical resection rates

by enhancing tumor margins and increase detection of tumor-positive lymph nodes.[26]

Previously, Hutteman et al. showed the use of the non-targeted optical imaging agent, Indocyanine Green (ICG), for the detection of PDAC. It was concluded that no useful tumor demarcation could be visualized after intravenous injection of ICG. However, the common bile duct and biliary anastomoses were clearly visualized.[27] Clinical trials performed in other malignancies, such as ovarian cancer, using tumor-specific imaging agents, showed successful use of this technique for the specific identification of cancer during surgery.[11, 28-30]

Integrin αvβ6 has been shown to be a promising target for identification of PDAC, and differentiation with pancreatitis and normal pancreatic tissue, with retained expression in vital tumor cells after neoadjuvant therapy.[12, 13, 15, 31, 32] Nowadays, the majority of patients will receive neoadjuvant therapy prior to surgery due to late onset of symptoms and therefore, presentation with locally advanced disease, or borderline resectable tumors. Currently, the distinction after neoadjuvant therapy between necrosis, fibrosis and vital tumor is impossible using conventional imaging techniques, and tumor-specific imaging could potentially fill this gap and be of added value in the diagnostic process.

Cysteine knottin peptides are relatively small (3-4 kDa), and have been extensively validated as alternative molecular imaging agents to antibodies.[31, 33, 34] We showed that the previously engineered cysteine knottin peptide R01-MG[18] demonstrated high and specific tumor uptake and high tumor-to-normal tissue ratios in mouse models of integrin αvβ6-positive PDAC, after conjugation to the near-infrared fluorescent dye, IRDye800. Moreover, the agent did not accumulate in integrin αvβ6-negative tumors. Due to the well-defined secondary structure, cysteine knottin peptides possess improved *in vivo* stability, and resist both chemical and physical insult compared to linear peptides, such as "A20".[18, 35-37] R01-MG-IRDye800 targets integrin αvβ6 with high affinity binding (Kd = 1.2 nM) and in a highly specific manner,[18] compared to for example cyclic-RGD, which mainly targets αvβ3, but also αvβ5, α5β1, α6β4, α4β1, and αvβ6.[38]

To prove that R01-MG-IRDye800 specifically targets αvβ6, and fluorescent signal in the tumor is not due to enhanced permeability and retention (EPR)

effect, especially seen in subcutaneous tumor models,[39] we have chosen to use a humanized transgenic mouse model. In addition, we performed several control studies using IRDye800 alone, and a newly synthesized control peptide with similar characteristics as the targeting peptide. Furthermore, to minimize non-specific leakage of the agent to the tumor, subcutaneous tumors with BxPC-3 cells were used which are known to be poorly leaky tumors, and therefore minimize EPR effect.[40] Our studies showed that the fluorescent signal of R01-MG-IRDye800 was significantly higher compared to both controls, indicating specific binding of R01-MG-IRDye800 to αvβ6.

A limitation of using optical imaging as described here, is the use of one target to image the tissue of interest compared to multiplexing, targeting of multiple markers, to increase the detection sensitivity and potentially assess aggressiveness of the tumor.[41] Ideally, you would be able to deliver a cocktail of imaging agents to patients, each targeting a specific biomarker that is known to be overexpressed in PDAC and supplement each other for improved detection.[13] However, at this point none of the newly developed NIR tumor-specific optical imaging agents is approved by the U.S. Food and Drug Administration (FDA), which is partly due to the comprehensive process and costs associated with getting regulatory approval for an optical imaging agent, and the current lack of proven patient benefit.[42] Therefore, the possibility to deliver multiple agents at once, can probably not be realized in the near future. A benefit of the investigated target is that αvβ6 is overexpressed in > 95% of PDAC patients, and significantly higher expressed in PDAC versus pancreatitis and normal pancreatic tissue.[13] Therefore, it is expected that multiplexing will not cause significant benefits over the use of R01-MG-IRDye800 as a single agent. As reported above, the differentiation between chronic pancreatitis and PDAC is one of the aspects where tumor-specific molecular imaging can be of additional benefit to the patient. A limitation of this study is that the agent is not tested in chronic pancreatitis mouse models. However, we know from previous performed research that αvβ6 expression is significantly lower in pancreatitis compared to PDAC.[12, 13] In addition, we did address the difference in fluorescent signal between PDAC and peritumoral inflammation, because if the technique is able to do this, it would fill a clinically relevant gap in conventional imaging techniques. Based on our results, and due to high specific binding of the agent,

no limitations are expected for the clinical use of this agent for tumor-specific detection.

Our developed agent has high potential for clinical translation into patients, since it consists of two parts that are already successfully translated into humans. The cysteine knot peptide, R01-MG, is currently used in the clinic as an αvβ6-targeting PET tracer for the detection of pancreatic cancer (eIND #126379, NCT02683824) and the NIR fluorescent dye, IRDye800CW, has already been used for fluorescence-guided surgery in multiple clinical trials.[11, 30] We performed a pilot toxicology study that showed that the newly developed agent was well tolerated. However, some changes in hematology and chemistry blood panels were seen immediately after injection, which could potentially be due to the agent. These levels returned within the normal range after observation, but before final conclusions can be drawn, larger toxicology studies need to be performed to determine the meaning of these changes.

In conclusion, the developed optical imaging agent R01-MG-IRDye800 binds selectively to αvβ6. In cell studies, R01-MG-IRDye800 outperformed all controls, and a clear correlation between levels of receptor expression and fluorescence signal was found. In multiple preclinical mouse models, tumor-specific targeting was achieved, with favorable renal clearance. The agent exhibited high tumor-to-background ratios, and clear correlation between fluorescence signal and histopathologic evidence of PDAC. Thanks to the fact that this agent contains two elements, R01-MG and IRDye800 that were already proven to be safe for use in humans, we do not expect major hurdles for the clinical translation of this optical imaging agent.

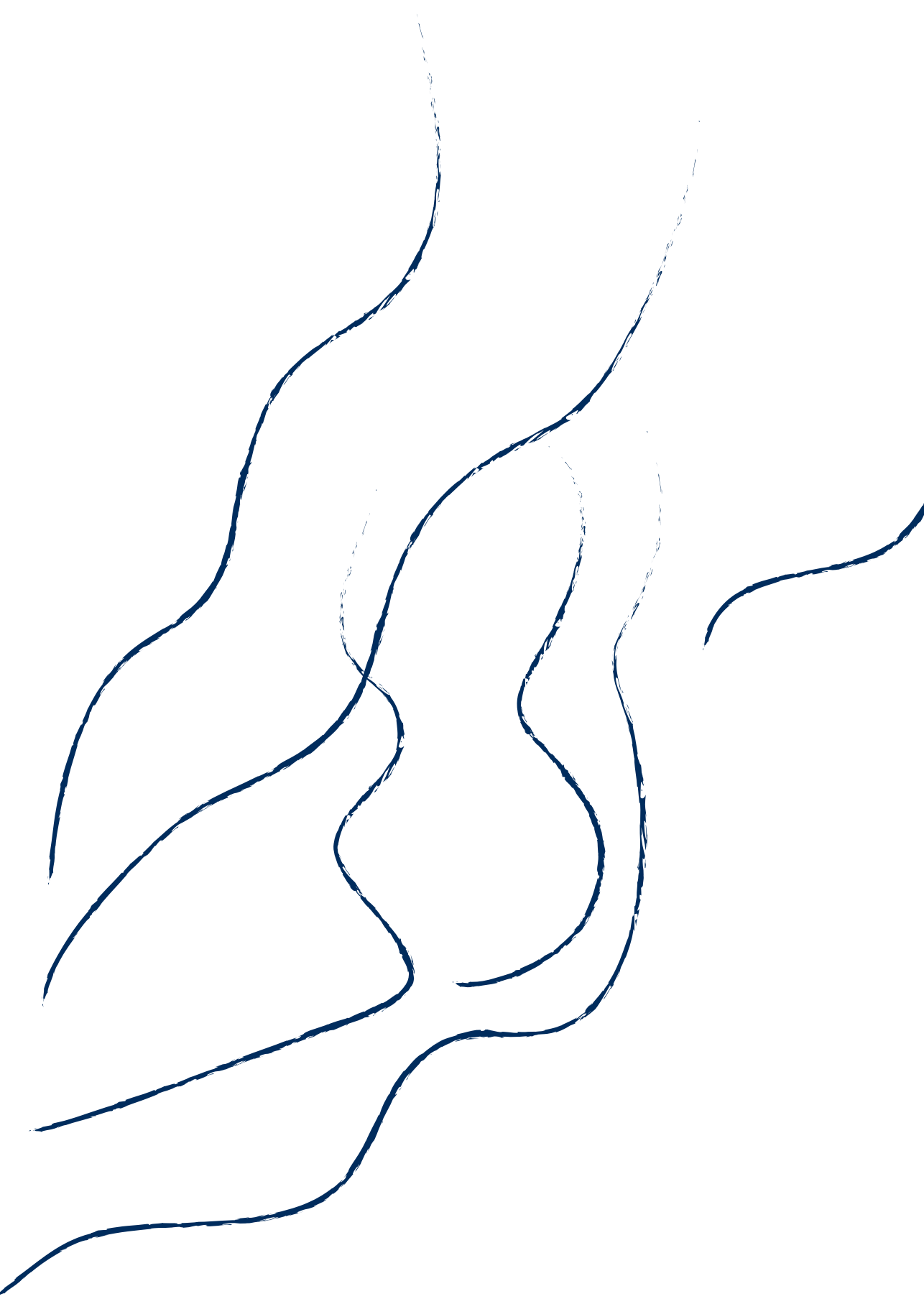
## ACKNOWLEDGMENTS.

We would like to thank James Strommer, Stanford University, for his contribution to the graphical design.

# REFERENCES


1. Jemal, A., et al., Cancer statistics, 2010. CA Cancer J Clin, 2010. 60(5): p. 277-300.
2. American Cancer Society, I. Key Statistics for Pancreatic Cancer. 2017 [cited 2017 July 31].
3. Laeseke, P.F., et al., Combining in Vitro Diagnostics with in Vivo Imaging for Earlier Detection of Pancreatic Ductal Adenocarcinoma: Challenges and Solutions. Radiology, 2015. 277(3): p. 644-61.
4. Tummala, P., O. Junaidi, and B. Agarwal, Imaging of pancreatic cancer: An overview. J Gastrointest Oncol, 2011. 2(3): p. 168-74.
5. Jang, J.Y., et al., A prospective randomized controlled study comparing outcomes of standard resection and extended resection, including dissection of the nerve plexus and various lymph nodes, in patients with pancreatic head cancer. Ann Surg, 2014. 259(4): p. 656-64.
6. Verbeke, C.S., Resection margins and R1 rates in pancreatic cancer--are we there yet? Histopathology, 2008. 52(7): p. 787-96.
7. Verbeke, C.S., et al., Redefining the R1 resection in pancreatic cancer. Br J Surg, 2006. 93(10): p. 1232-7.
8. Verbeek, F.P., et al., Image-guided hepatopancreatobiliary surgery using near-infrared fluorescent light. J Hepatobiliary Pancreat Sci, 2012. 19(6): p. 626-37.
9. Zhang, J.F., et al., Influence of perineural invasion on survival and recurrence in patients with resected pancreatic cancer. Asian Pac J Cancer Prev, 2013. 14(9): p. 5133-9.
10. Vahrmeijer, A.L., et al., Image-guided cancer surgery using near-infrared fluorescence. Nat Rev Clin Oncol, 2013. 10(9): p. 507-18.
11. Rosenthal, E.L., et al., Safety and Tumor-specificity of Cetuximab-IRDye800 for Surgical Navigation in Head and Neck Cancer. Clin Cancer Res, 2015.
12. de Geus, S.W., et al., Selecting Tumor-Specific Molecular Targets in Pancreatic Adenocarcinoma: Paving the Way for Image-Guided Pancreatic Surgery. Mol Imaging Biol, 2016.
13. Tummers WS, F.S.A., Boonstra MC, Prevoo HA, Sier CF, Mioeg JS, Morreau J, van Eijck C, Kuppen P, van de Velde CJ, Bonsing BA, Vahrmeijer AL, Swijnenburg RJ Selection of optimal molecular targets for tumor-specific imaging in pancreatic ductal adenocarcinoma. Oncotarget, 2017. May.
14. Kimura, R.H., et al., Pharmacokinetically stabilized cystine knot peptides that bind alpha-v-beta-6 integrin with single-digit nanomolar affinities for detection of pancreatic cancer. Clin Cancer Res, 2012. 18(3): p. 839-49.
15. Zhang, C., et al., A Cystine Knot Peptide Targeting Integrin alphavbeta6 for Photoacoustic and Fluorescence Imaging of Tumors in Living Subjects. J Nucl Med, 2016.
16. LI-COR Website. IRDye® 800CW NHS Ester Properties. 2016. Available from: https://www.licor.com/clinical_translation/irdye_800CW_NHS_ester_optical_properties_and_structure.html.
17. Lamberts, L.E., et al., Tumor-Specific Uptake of Fluorescent Bevacizumab-IRDye800CW Microdosing in Patients with Primary Breast Cancer: A Phase I Feasibility Study. Clin Cancer Res, 2017. 23(11): p. 2730-2741.
18. Kimura, R.H., et al., Pharmacokinetically stabilized cystine knot peptides that bind alpha-v-beta-6 integrin with single-digit nanomolar affinities for detection of pancreatic cancer. Clin Cancer Res, 2012. 18(3): p. 839-849.
19. Kimura, R.H., et al., Engineered cystine knot peptides that bind alphavbeta3, alphavbeta5, and alpha5beta1 integrins with low-nanomolar affinity. Proteins, 2009. 77(2): p. 359-69.
20. Aguirre, A.J., et al., Activated Kras and Ink4a/Arf deficiency cooperate to produce metastatic pancreatic ductal adenocarcinoma. Genes Dev, 2003. 17(24): p. 3112-26.
21. Peng X, D.D., Volcheck WM, Bashford GR, Lamb DT, Grone DL, Zhang Y, Johnson CM, Phthalocyanine dye as an extremely photostable and highly fluorescent near-infrared labeling reagent. Proc. SPIE 6097, Optical Molecular Probes for Biomedical Applications, 60970E 2006.

22. Knight, P.A., et al., Enteric expression of the integrin alpha(v)beta(6) is essential for nematode-induced mucosal mast cell hyperplasia and expression of the granule chymase, mouse mast cell protease-1. Am J Pathol, 2002. 161(3): p. 771-9.
23. Brown, J.K., et al., Integrin-alphavbeta6, a putative receptor for foot-and-mouth disease virus, is constitutively expressed in ruminant airways. J Histochem Cytochem, 2006. 54(7): p. 807-16.
24. Lee, Y.J., et al., Hepatocellular carcinoma: diagnostic performance of multidetector CT and MR imaging-a systematic review and meta-analysis. Radiology, 2015. 275(1): p. 97-109.
25. Zackrisson, S., S.M. van de Ven, and S.S. Gambhir, Light in and sound out: emerging translational strategies for photoacoustic imaging. Cancer Res, 2014. 74(4): p. 979-1004.
26. Hiroshima, Y., et al., Fluorescence-guided surgery, but not bright-light surgery, prevents local recurrence in a pancreatic cancer patient derived orthotopic xenograft (PDOX) model resistant to neoadjuvant chemotherapy (NAC). Pancreatology, 2015. 15(3): p. 295-301.
27. Hutteman, M., et al., Near-infrared fluorescence imaging in patients undergoing pancreaticoduodenectomy. Eur Surg Res, 2011. 47(2): p. 90-7.
28. Hoogstins, C.E., et al., A Novel Tumor-Specific Agent for Intraoperative Near-Infrared Fluorescence Imaging: A Translational Study in Healthy Volunteers and Patients with Ovarian Cancer. Clin Cancer Res, 2016. 22(12): p. 2929-38.
29. Burggraaf, J., et al., Detection of colorectal polyps in humans using an intravenously administered fluorescent peptide targeted against c-Met. Nat Med, 2015.
30. van Dam, G.M., et al., Intraoperative tumor-specific fluorescence imaging in ovarian cancer by folate receptor-alpha targeting: first in-human results. Nat Med, 2011. 17(10): p. 1315-9.
31. Kimura, R.H., et al., Pharmacokinetically stabilized cystine knot peptides that bind alpha-v-beta-6 integrin with single-digit nanomolar affinities for detection of pancreatic cancer. 2012(1078-0432 (Print)).
32. Hackel, B.J., et al., 18F-fluorobenzoate-labeled cystine knot peptides for PET imaging of integrin alphavbeta6. 2013(1535-5667 (Electronic)).
33. Moore, S.J. and J.R. Cochran, Engineering knottins as novel binding agents. Methods Enzymol, 2012. 503: p. 223-51.
34. Sarah J.Moore, C.L.L., Jennifer R.Cochran, Knottins: disulfide-bonded therapeutic and diagnostic peptides. Drug Discov Today Technol, 2012. 9(1): p. e1-e70.
35. Hausner, S.H., et al., Evaluation of an integrin alphavbeta6-specific peptide labeled with [18F]fluorine by copper-free, strain-promoted click chemistry. 2013(1872-9614 (Electronic)).
36. Hausner, S.H., et al., Use of a peptide derived from foot-and-mouth disease virus for the noninvasive imaging of human cancer: generation and evaluation of 4-[18F] fluorobenzoyl A20FMDV2 for in vivo imaging of integrin alphavbeta6 expression with positron emission tomography. 2007(0008-5472 (Print)).
37. Hausner, S.H., et al., Targeted in vivo imaging of integrin alphavbeta6 with an improved radiotracer and its relevance in a pancreatic tumor model. Cancer Research, 2009. 69(14): p. 5843-5850.
38. Shi, J., F. Wang, and S. Liu, Radiolabeled cyclic RGD peptides as radiotracers for tumor imaging. Biophys Rep, 2016. 2(1): p. 1-20.
39. Prabhakar, U., et al., Challenges and key considerations of the enhanced permeability and retention effect for nanomedicine drug delivery in oncology. Cancer Res, 2013. 73(8): p. 2412-7.
40. Kunjachan, S., et al., Passive versus active tumor targeting using RGD- and NGR-modified polymeric nanomedicines. Nano Lett, 2014. 14(2): p. 972-81.
41. Zheng, X., et al., Successively activatable ultrasensitive probe for imaging tumour acidity and hypoxia. 2017. 1: p. 0057.
42. Tummers, W.S., et al., Regulatory Aspects of Optical Methods and Exogenous Targets for Cancer Detection. Cancer Res, 2017. 77(9): p. 2197-2206.



Chapter | 6

# On-target probes for early detection

Sharon S. Hori*, Willemieke S. Tummers* and Sanjiv S. Gambhir

Sharon S. Hori[1*], Willemieke S. Tummers[1*] and Sanjiv S. Gambhir[1,2] are at the [1]Department of Radiology, Stanford University, 318 Campus Drive, Stanford, CA 94305, USA and [2]Department of Bioengineering, Materials Science and Engineering, Bio-X, Stanford University, 318 Campus Drive, Stanford, CA 94305, USA.

*Nature Biomedical Engineering 2017; Apr 12. News and Views.*

A cost-effective strategy for early-stage cancer detection would be based on a two-step paradigm1. First, a sensitive and specific blood test screens for individuals in the general or high-risk population who display cancer-specific biomarkers released from tumour cells. Patients with abnormal blood biomarkers then undergo follow-up tests, in which sensitive molecularimaging techniques targeting multiple cancer markers assess the location, size and aggressive state of the putative tumour. Yet such a screening paradigm is not a reality. For tumour detection, current blood biomarkers and imaging probes require high sensitivity to accurately identify small early-stage lesions, as well as high specificity to accurately distinguish benign tissues from malignant transformations [1–3]. However, blood biomarkers such as cancer antigen 125 (CA125) and prostate-specific antigen (PSA) have had limited success in clinical practice because they are also frequently shed by healthy cells in physiological conditions. Even in the pursuit of other types of tumour-specific biomarker, such as patient-specific circulating tumour DNA, more sensitive methodologies and validation are required to provide substantial evidence that these methods can be effective in early cancer screening. On the molecular-imaging front, in which probes are engineered to non-invasively target and visualize a molecular marker indicative of disease in real time, the level of marker expression in cancer cells is often low or heterogeneous, leading to difficulties in distinguishing signals from the tumour and its healthy surrounding tissue, which in turn results in low detection sensitivity. For early cancer detection to succeed using blood-based and imaging approaches, better tumour-to-normal tissue ratios (TNRs) are needed, either by increasing the tumour signal, decreasing the background signal, or both. Two complementary developments reported in Nature Biomedical Engineering now demonstrate how higher TNRs can be achieved with nanoscale probes that are only activated within the tumour microenvironment.

On the one hand, Sangeeta Bhatia and colleagues show that intravenously delivered activity-based nanosensors (ABNs) decorated with tumour-targeting ligands and with peptides cleavable by specific proteases (proteolytic enzymes) overexpressed in the tumour microenvironment can overcome the blood-based detection problems plaguing endogenous secreted biomarkers for early cancer detection [4]. On interaction with specific tumour proteases, the peptide substrates, which are fluorescence-quenched,

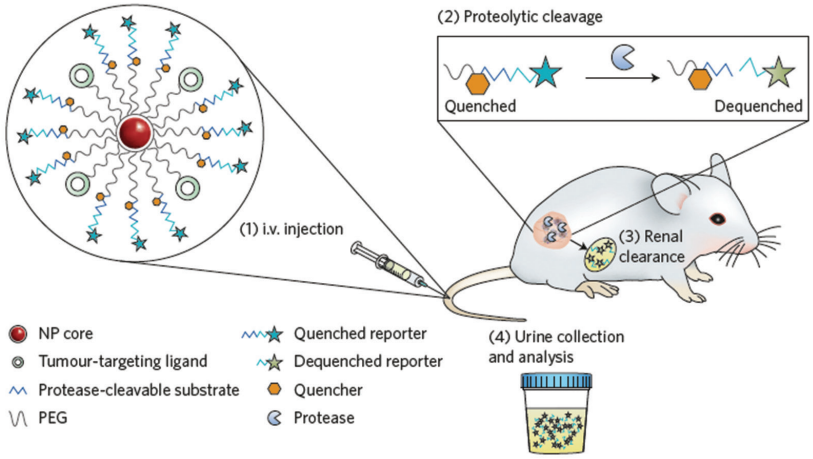



**Figure 1.** Optimized tumour-activated nanoparticle-based sensors, consisting of a nanoparticle (NP) core decorated with a protease-cleavable substrate and tumour-targeting ligands. Following intravenous (i.v.) injection of the nanoparticles (1), the quenched substrates are cleaved by highly expressed proteases in the tumour microenvironment, which subsequently emit a fluorescence signal (2). The dequenched urinary reporter enters the urine (3) and is detectable via a fluorescence assay (4). Figure adapted from ref. 4, Macmillan Publishers Ltd.



are cleaved and secreted in the urine, where they can be detected by a fluorescence assay (Fig. 1). On the other hand, Xiqun Jiang and colleagues describe the design of a molecular probe, a poly(ethylene glycol)-conjugated iridium (iii) complex (Ir-Im-PEG) that, when activated by two tumour-specific stimuli, results in imaging-signal amplification and thus improved detection sensitivity[5]. The probe responds progressively to subtle differences in extracellular pH and oxygen levels, and distinguishes healthy tissue (which is usually alkaline and normoxic) from tumour tissue (which is acidic and hypoxic).

Bhatia and co-authors, who have championed similar diagnostic nanosystems[6,7], have now optimized the presentation of the nanoparticle-coating substrates on the basis of mathematical modelling of the pharmacokinetics of the ABNs (ref. [6]) to increase the TNR. The authors focused on targeting matrix metalloproteinase 9 (MMP9), as MMP9 mRNA is shown to be upregulated in many human cancers at varying stages of disease[4]. Having previously predicted that a 100-fold improvement in tumour signal was needed to detect sub-5-mm sized tumours, the authors now report the detection of intraperitoneal ovarian tumours as small as 36 $mm^3$ in mice, outperforming by 2.4-fold the endogenous ovarian

cancer biomarker human epididymis secretory protein 4 (HE4). The authors also show with mouse xenograft models of epithelial cancer and colorectal liver metastasis that the optimized ABNs markedly increase the enzyme-generated diagnostic signal with respect to the signal expected on the basis of ABN accumulation in tumour alone. This suggests that exogenous biomarkers can be optimized to produce urine-based assays with increased sensitivity for the earlier detection of tumours.

Protease-based cancer-imaging probes are making their way from mouse xenograft models to human clinical trials[8]. One question to be answered is how accurately the preclinical results reported by Bhatia and collaborators will translate into early cancer screening in patients. MMP9 is highly expressed in the tumour microenvironment but is also expressed in normal tissue, so activation of ABNs at non-tumour sites may decrease the TNR. Assuming successful nanoparticle delivery and safety, Bhatia and colleagues predict that the ABNs could detect a human serous ovarian cancer 5 months earlier than the clinically relevant biomarker HE4. In reality, extrapolating the behaviour of the ABNs from mice to patients involves the consideration of allometric scaling between species, as well as taking into account biomarker pharmacokinetics, body weight or surface area, tumour vascularity, and possibly other cancerspecific properties. Ultimately, whether ABNs would be sufficiently sensitive and specific for early cancer detection in humans will have to be tested.

Nevertheless, there is a need for better tumour-specific blood-based biomarkers for cancer detection, be them endogenous factors or markers generated from exogenously administered nanoparticles or genetic constructs [9]. Beyond the binary distinction between presence and absence of disease, it is important to identify biomarkers that inform about the state of the malignant tumour. In this context, ABNs or other exogenous biomarkers could be designed to specifically target aggressive and lethal tumours (and to not be activated in benign tumours). Exogenously delivered ABNs, if multiplexed with appropriate enzyme-cleavable substrates and tumour-targeting ligands, may well be a valid strategy to increase the sensitivities and specificities of tumour diagnoses.

Following biomarker-based screening, imaging probes activated at the tumour site provide the possibility to image tissue at high TNRs and therefore validate

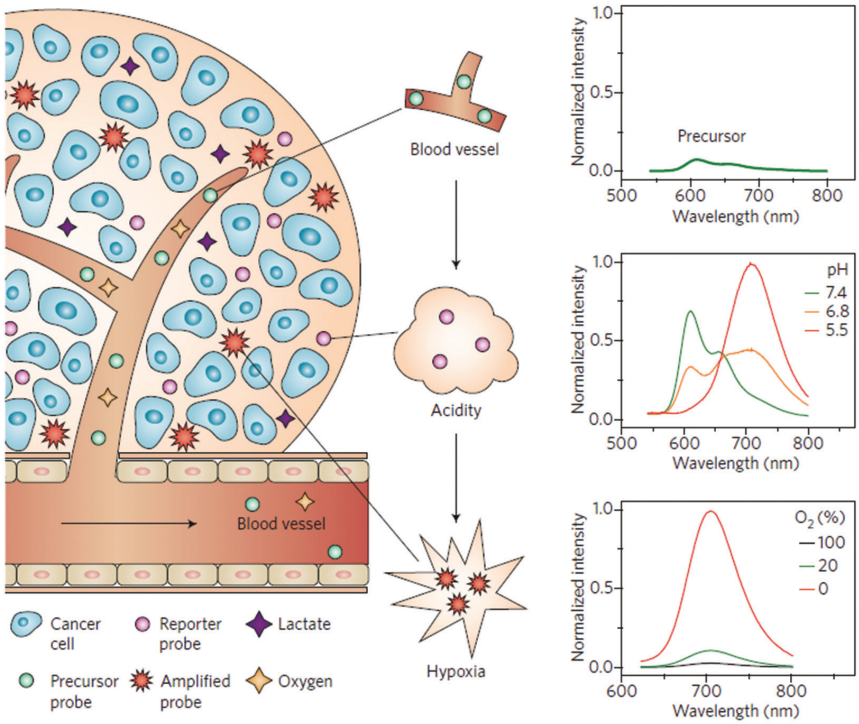



**Figure 2.** Tumour-activated imaging probe with signal amplification, driven by the conversion of theprobe's precursor form into the reporter form. The intravenously injected precursor probe emits at610 nm. In the acidic tumour microenvironment, the precursor form converts to the reporter form,which emits at 705 nm. At the hypoxic conditions of the tumour microenvironment, the optical signalis amplified. Emission spectra are shown at increasing-pH and decreasing-oxygen conditions. Figure adapted from ref. 5, Macmillan Publishers Ltd.

the potential presence and location of the disease. Jiang and colleagues exploited events occurring in the tumour microenvironment to trigger signal amplification, in contrast to conventional amplification techniques based on chemical or physical modifications of the probe itself. In the acidic tumour environment (pH 6.5–6.9), hydrolysis of the aciditysensitive imine bond in the Ir-Im-PEG complex leads to the conversion of the precursor form of the probe (which emits light at 610 nm) to its reporter form (with emission at 705 nm). If the second stimulus (hypoxia) is also present in the microenvironment, the 705-nm signal is amplified[5] (Fig. 2) The increased sensitivity of this dual-activation approach enabled the detection of tumour nodules as small as 1 mm in diameter. However, one disadvantage of this approach is that optical imaging assays, although useful for localized and intraoperative imaging, may not be ideal for whole-body screening.

In contrast to the behaviour of other microenvironment-responsive probes [10–12], the cleavable Ir-Im-PEG reports coupled events (acidity and hypoxia), and by doing so enhances the detection signal. Indeed, when compared with a previously reported hypoxia-activated iridium macromolecule [13], Ir-Im-PEG achieved roughly a fourfold enhancement in TNR, and improved the detection of small tumour lesions in the liver. The higher TNR of the improved probe was generated by reducing the background signal rather than by increasing the optical signal, so it is possible that the brightness of the probe might not be sufficient for clinical use, for example during real-time surgical resections.

Jiang and co-authors used patient-derived tumour xenograft models and histological analyses of the human tumour microenvironment to validate the Ir-Im-PEG probe. Yet before this imaging approach can be translated to patients, efficacy and dose studies need to be carried out. Nevertheless, the improved sensitivity of Ir-Im-PEG highlights the advantages of enabling signal amplification and of focusing on multiplexing strategies rather than targeting individual markers. The authors' imaging approach could become widely used for the detection of solid tumours, in which subtle changes in acidity and hypoxia are generally present [14,15]. They also showed that such context-sensitive probes might have other applications, for example in wound healing, and that they could pave the way for monitoring the metabolic activity of cells to determine treatment response.

Synthetic nanoparticle systems and optical imaging probes are rarely approved for human use by the US Food and Drug Administration, mainly owing to safety issues, a complex regulatory system, scalability and manufacturing challenges, and a lack of proven benefit in humans. To improve and expedite the clinical translation of new probes for eventual clinical diagnostics, their development should plan for rigorous proof-of-safety and proof-of-benefit studies. These are critical steps in making earlier cancer detection with biomarkers and imaging probes feasible. Although the safety of the probes reported by Bhatia, Jiang and their respective co-authors remains unclear because high dosages might be needed to establish desired effects, it is not too early to state that the detection sensitivity benefits of tumour-activatable probes are promising.

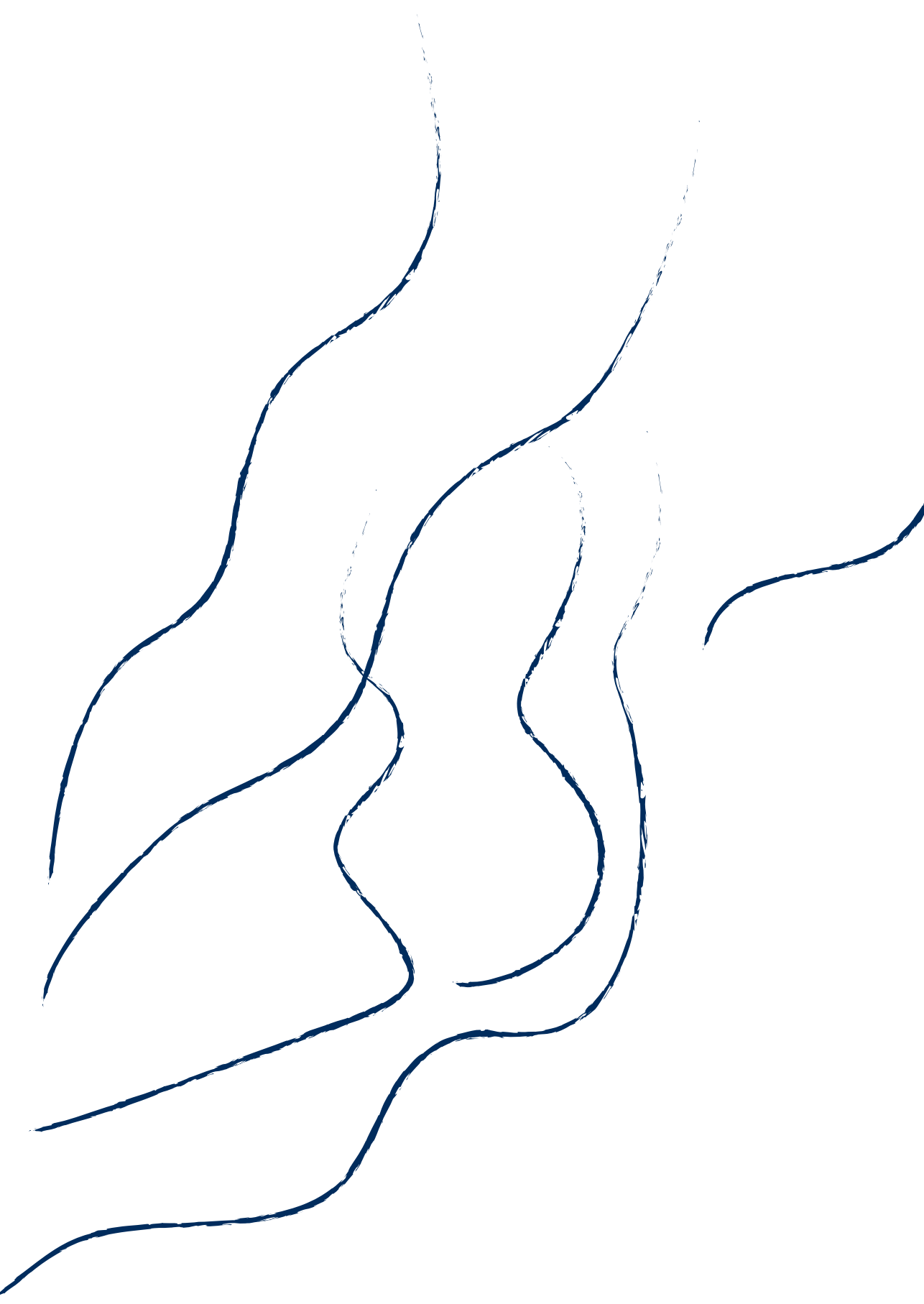
# REFERENCES


1. Lutz, A. M. et al. Early diagnosis of ovarian carcinoma: Is a solution in sight? Radiology 259, 329-345, (2011).
2. Lutz, A. M. Willmann, J. K. Cochran, F. V. Ray, P. & Gambhir, S. S. Cancer screening: A mathematical model relating secreted blood biomarker levels to tumor sizes. PLoS Med 5, e170, (2008).
3. Hori, S. S. & Gambhir, S. S. Mathematical model identifies blood biomarker-based early cancer detection strategies and limitations. Sci. Transl. Med. 3, 109ra116, (2011).
4. Kwon, E. J. Dudani, J. S. & Bhatia, S. N. Tumor-penetrating nanosensors of protease activity. Nat. Biomed. Eng. 1, XXXX, (2017).
5. Zheng, X. et al. Successively activatable probe for signal amplification and imaging of coupled biological events. Nat. Biomed. Eng. 1, XXXX, (2017).
6. Kwong, G. A. et al. Mathematical framework for activity-based cancer biomarkers. Proc. Natl Acad. Sci. USA 112, 12627-12632, (2015).
7. Kwong, G. A. et al. Mass-encoded synthetic biomarkers for multiplexed urinary monitoring of disease. Nat. Biotechnol. 31, 63-70, (2013).
8. Whitley, M. J. et al. A mouse-human phase 1 co-clinical trial of a protease-activated fluorescent probe for imaging cancer. Sci. Transl. Med. 8, 320ra324, (2016).
9. Ronald, J. A. Chuang, H. Y. Dragulescu-Andrasi, A. Hori, S. S. & Gambhir, S. S. Detecting cancers through tumor-activatable minicircles that lead to a detectable blood biomarker. Proc. Natl Acad. Sci. USA 112, 3068-3073, (2015).
10. Wang, Y. et al. A nanoparticle-based strategy for the imaging of a broad range of tumours by nonlinear amplification of microenvironment signals. Nat. Mater. 13, 204-212, (2014).
11. Jiang, T. et al. Tumor imaging by means of proteolytic activation of cell-penetrating peptides. Proc. Natl Acad. Sci. USA 101, 17867-17872, (2004).
12. Urano, Y. et al. Selective molecular imaging of viable cancer cells with ph-activatable fluorescence probes. Nat. Med. 15, 104-109, (2009).
13. Zheng, X. et al. Hypoxia-specific ultrasensitive detection of tumours and cancer cells in vivo. Nat. Commun. 6, 5834, (2015).
14. Webb, B. A. Chimenti, M. Jacobson, M. P. & Barber, D. L. Dysregulated ph: A perfect storm for cancer progression. Nat. Rev. Cancer 11, 671-677, (2011).
15. Gilkes, D. M. Semenza, G. L. & Wirtz, D. Hypoxia and the extracellular matrix: Drivers of tumour metastasis. Nat. Rev. Cancer 14, 430-439, (2014).



Part | III

# Clinical Translation of Targeted Molecular Imaging



Chapter | 7

# Regulatory Aspects of Optical Methods and Exogenous Targets for Cancer Detection

*Willemieke S Tummers[1], *Jason M Warram[2], Kiranya E Tipirneni[3], John Fengler[4], Paula Jacobs[5], Lalitha Shankar[5], Lori Henderson[5], ǂ Betsy Ballard[6], Brian W Pogue[7], Jamey P Weichert[8], Michael Bouvet[9], Jonathan Sorger[10], Christopher H Contag[11], John V Frangioni[12], Michael F Tweedle[13], James P Basilion[14], Sanjiv S Gambhir[15], Eben L Rosenthal[16]
*Authors contributed equally to this work

[1]Department of Radiology, Molecular Imaging Program, Stanford University, Stanford, CA. [2]Department of Otolaryngology, University of Alabama at Birmingham, Birmingham, AL. [3]Department of Surgery, University of Alabama at Birmingham, Birmingham, AL. [4]NOVADAQ, Burnaby, British Columbia, Canada. [5]National Cancer Institute, Bethesda, MD. [6]United States of America Food and Drug Administration, Silver Spring, MD. [7]Thayer School of Engineering, Dartmouth College, Hanover, NH. [8]Department of Radiology, University of Wisconsin, Madison, WI. [9]Department of Surgery, University of California San Diego, La Jolla, CA. [10] Intuitive Surgical Inc., Sunnyvale, CA. [11] Departments of Pediatrics, Radiology, Microbiology & Immunology, Stanford University, Stanford, CA. [12]Curadel, LLC, Marlborough, MA. [13]Department of Radiology, Ohio State University, Columbus, OH. [14]Department of Radiology, Case Western Reserve University, Cleveland, OH. [15]Departments of Radiology, Bioengineering, and Materials Science & Engineering, Molecular Imaging Program, Stanford University, Stanford, CA. [16]Department of Otolaryngology, Stanford University, Stanford, CA.

*Cancer Res. 2017 May 1;77(9):2197-2206.*

## ABSTRACT

Considerable advances in cancer-specific optical imaging have improved the precision of tumor resection. In comparison to traditional imaging modalities, this technology is unique in its ability to provide real-time feedback to the operating surgeon. Given the significant clinical implications of optical imaging, there is an urgent need to standardize surgical navigation tools and contrast agents to facilitate swift regulatory approval. Because fluorescence-enhanced surgery requires a combination of both device and drug, each may be developed in conjunction, or separately, which are important considerations in the approval process. This report is the result of a one-day meeting held on May 4, 2016 with officials from the National Cancer Institute (NCI), The Food and Drug Administration (FDA), members of ASIGS (American Society of Image-Guided Surgery) and members of the World Molecular Imaging Society (WMIS), which discussed consensus methods for FDA-directed human testing and approval of investigational optical imaging devices as well as contrast agents for surgical applications. The goal of this workshop was to discuss FDA approval requirements and the expectations for approval of these novel drugs and devices, packaged separately or in combination, within the context of optical surgical navigation. Additionally, the workshop acted to provide clarity to the research community on data collection and trial design. Reported here are the specific discussion items and recommendations from this critical and timely meeting.

## INTRODUCTION

Surgery with negative margins is the foundation for curative treatment in many solid cancers.[1] While conventional imaging modalities such as magnetic resonance imaging (MRI), computed tomography (CT), positron emission tomography (PET), and ultrasound (US) facilitate surgical planning, they are generally difficult to integrate into the surgical environment. Most importantly, however, these traditional modalities do not reliably communicate real-time feedback to the surgeon except for ultrasound. Therefore, surgeons must depend on subjective palpation and subtle visual changes for achieving complete tumor clearance. Although intraoperative frozen tissue sectioning, staining, and microscopic visualization are routinely used for achieving negative margins, this is time-consuming, costly, and samples only a small proportion of the wound bed, which may lead to sampling error with false-negative results. Positive or close margins directly correlate with poorer outcomes, often necessitating post-operative adjuvant therapy and, in some instances, a second operation.[2] Conversely, aggressive radical resections can remove normal tissue, leading to excessive morbidity and/or disfigurement. Thus, real-time surgical guidance for differentiating tumor and healthy tissue is crucial to both improved overall survival in addition to preservation of tissue function and appearance.



The recent advances in optical contrast imaging have brought forth a myriad of cancer-specific agents that have the ability to expand the information required for the surgeon to make informed clinical decisions. These optical imaging techniques are highly variable with a wide range of imaging wavelenghts and spatial scales.[3] Together, these developments offer tremendous advantages to the field of surgical guidance, with an unparalleled ability to transform surgical oncology. In fact, due to their potential for high signal to noise ratios (SNR) and sensitivity to a broad range of spatial resolution, optical fluorescence imaging has the potential to impact patient care in multiple arenas. For example, in comparison to shorter wavelengths, the penetrating deep tissue properties of near-infrared (NIR) fluorescence has led to a focus on similar long-emitting fluorophores for this and many other optical imaging applications (see NIH Research Portfolio Online Reporting Tools (RePORT) for details).[4] Nevertheless, there are a number of variables that impact the success of intraoperative optical imaging that are intrinsic to the imaging hardware or the molecular probe itself.

Perhaps the greatest variable, however, is inter- and intratumor heterogeneity. Despite three decades of research to identify tissue-specific targets and develop effective imaging agents, 5-aminolevulinic acid (5-ALA) is the only real-time, cancer-specific agent available in the clinic today. Administered orally or topically, 5-ALA is converted intratumorally to fluorescent protoporphyrin IX. Currently, 5-ALA is approved for oral administration in Europe, Canada, and Japan to highlight brain tumors during cytoreductive surgery. The 5-ALA ester derivative hexaminolevulinate (HAL) is approved for topical use for bladder cancer detection in both the United States and Europe.[5, 6] The use of 5-ALA was shown to be successful during intracranial tumor resection[5] by achieving more complete resection and improving progression-free survival in patients with malignant glioma, which suggests that it carries the potential for use in other cancer types with similar favorable outcomes.[7-9]

There are a number of additional tumor-specific molecular probes that are widely applicable to several cancer types that have been described,[10] and an increasing amount of clinical trials are being conducted to evaluate both their safety and efficacy. Favorable safety data from non-human primates allows antibody-based optical imaging to build on the advances in immunotherapy and immunoPET imaging.[11] For example, cetuximab conjugated to IRDye800 (cetuximab-IRDye800) has been studied in phase 1 clinical trials and has demonstrated the ability to identify subclinical tumor in patients with head and neck cancer.[12] However, successful regulatory approval for the widespread use of this technology requires additional clinical trials. These trials must be designed and performed according to the standards of the FDA Investigational New Drug Application (IND) recommendations to demonstrate safety and patient benefit as well as the Centers for Medicare & Medicaid Services (CMS) for cost-effectiveness. Over the past few years, the number of FDA submissions for IND or Investigational Device Exemptions (IDE) related to optical imaging has doubled annually, with 26 clinical trials currently planned or already underway.

A unique feature of fluorescent optical imaging is that it facilitates real-time decision-making by guiding surgeons to potential areas of microscopic disease in a macroscopic setting. From a regulatory standpoint this deserves special considerations since real-time feedback not only fosters dynamic decision

making but also permits adjustments to the treatment plan, which is not possible with current pre-operative imaging modalities.

In February 2015, the American Society of Image Guided Surgery (ASIGS) held a meeting with surgeons and scientists in the field of Image Guided Surgery to critically evaluate imaging platform technologies and optical imaging agents. The goal of this meeting was to provide recommendations regarding trial development and the regulatory approval process, and come to an agreement on how this technology could be used to meet the needs of cancer patients.[13] Since then, several new clinical trials have incorporated major elements from the resulting ASIGS consensus report. However, the appropriate clinical trial endpoints that meet FDA requirements for successful device and/or drug approval remain ill-defined due to a lack of precedence and diagnostic/therapeutic crossover inherent to this technology. As such, these potential setbacks formed the basis of the one-day workshop on May 4, 2016, which included representatives from the National Cancer Institute (NCI), the FDA, members of ASIGS and members of the World Molecular Imaging Society (WMIS). The primary aim was to define consensus methods and endpoints for FDA-regulated human testing and approval of investigational optical imaging devices and contrast agents (drugs) in surgery. The first step was to report FDA considerations for evaluation of any new device or drug, and obtain their guidance on how devices, drugs, or their combination, would most effectively obtain market approval. Recognizing that there is significant controversy regarding this topic, we have summarized to the best of our ability the findings and recommendations from this meeting. This report can critically assist in the development of optical imaging products, and the regulatory pathways for their approval. The meeting was recorded and can be viewed online at URL https://videocast.nih.gov/PastEvents.asp.



## PRECEDENCE

When approving imaging devices and agents for clinical use, the FDA relies on data supplied by marketing applications and regulatory bodies. Taking this into consideration, the field should identify clinically meaningful endpoints as well as surrogates of clinical benefit to aid the approval pathways of any new promising

technologies, including optical imaging. However, this task is confounded by the paucity of clinical data on contrast-enhanced oncologic imaging agents, which consequently results in limited or lack of regulatory precedents. Therefore, it is critical to identify clinical developmental pathways for optical imaging in oncological surgery using similar yet appropriate modalities and companion agents that can be used for FDA's consideration. For instance, the use of MRI-guided surgery in brain cancer is analogous to fluorescence-guided surgery, where enhancement is used to influence surgical decisions and has previously shown benefit in patient outcome.[14] However, MRI procedures do not use products that have been specifically approved by FDA for surgical intervention; hence, FDA does not consider MRI-guided surgery an established predicate for fluorescence-guided surgery. Until these approaches have been thoroughly evaluated by the FDA, we will not have any certain guidance documents to clearly define the principles of study design and appropriate outcome measures based on safety and benefit to the patient.

## IMAGING DEVICES

A wide range of intraoperative fluorescence imaging devices have been developed by academic and commercial institutions that use similar illumination strategies, light sources, detectors, device architectures and collection geometries. Systems for use in open surgery, laparoscopic, thoracoscopic, and robot-assisted procedures have all been described, and likely represent a broad range of sensitivities to a given set of fluorophores, and differences inherent to their background noise levels. Because they have been developed with a specific usage in mind, they differ significantly in their fields-of-view, resolution, and wavelengths. Although the concept of these devices is relatively straightforward in that they simply require a light source, filters, detector(s), and display, there are specific challenges intrinsic to the system design. These include having appropriate light sources with a variety of wavelengths but within the prescribed safety standards for illumination,[15] adequate filter design to eliminate excitation and ambient light for use with one or more fluorophores, detectors with the appropriate spectral range and sensitivity with good SNR, real-time readout superimposed on a reference image, and ultimately, a user-friendly and ergonomic design. The ideal optical imaging system for the OR

should have additional characteristics, such as seamless operation with room lights, quantitative pattern recognition, and favorable ergonomic characteristics for use in a demanding environment. For a more detailed overview of the different characteristics imaging systems should possess and the challenges for development we would to refer to the review paper by DSouza et al.[3] While many of the current systems include these features, there is considerable variation among these devices, and industry standards are only just emerging. Most of these instruments possess a broad range of wavelength imaging capabilities, which translates to a potential for imaging several distinct fluorophores. This imaging potential is further compounded by the fact that any fluorophore can be conjugated to a number of targeting moieties. For these reasons, many different molecular formulations could be used with the same instrument. The FDA will review an application for a new drug intended for use in combination with a specific instrument or intended for use with multiple instruments as designated by the applicant drug manufacturers who need to carefully consider instrument design and capabilities before undertaking clinical development of a new drug.

## FDA regulatory pathways for Device approval



For imaging devices, the FDA regulatory process is directed by the Center for Devices & Radiological Health (CDRH). This process begins with an optional pre-submission meeting with the FDA after a "Q-submission" request to the Agency has been requested. This meeting serves as a forum for individual sponsors and the FDA to discuss the planned Investigational Device Exemption (IDE) or marketing application/clearance submission. The subsequent route to regulatory clearance or approval for devices depends primarily upon the level of risk associated with the clinical application of the device. When the goal is simply anatomical, such as locating lymph nodes or blood vessels, the FDA typically views optical imaging systems as relatively low risk. Optical imaging systems used to visualize anatomy in clinical investigations could be considered "non-significant risk" (NSR) devices, and an IDE is not required. Upon establishing safety and efficacy through the completion of such a clinical investigation, a sponsor can subsequently submit a traditional 510(k) application for market clearance if "substantial equivalence" to a predicate device is claimed.[16]

Optical imaging systems used in the diagnosis, prognosis, and/or treatment of diseases, however, are by default designated significant risk devices (SR) by the FDA regardless of disease severity. If the study sponsor intends to use such devices during an investigational human study, the FDA requires the study sponsor to file an IDE application.[17] For combination drug and device products, an Investigational New Drug (IND) application for the associated molecular agent being used may be filed in place of an IDE, if the Center for Drug Evaluation Research (CDER) is assigned as the lead review center.

Depending on the intended use of the imaging system, the sponsor presents the appropriate NSR or SR designation to the local Institutional Review Board (IRB) for review. Once IRB *and* IDE (for significant risk devices) are granted, the sponsor is free to proceed with the investigation. The issue of NSR/SR designation has been discussed and documented in detail previously.[18] The required elements for an IDE application can be found on the FDA website and are summarized in Table 1.[19] Ultimately, a pre-market approval (PMA) application is filed for market approval of Class III medical devices. The information requested by the FDA for PMA approval depends upon its intended use and any specific claims about the device that have been made by the sponsor. Evidence must support the intended use claim. For device approval under a PMA, information on device labeling, performance specifications, valid scientific evidence, tissue effects of the product, mechanism-of-action, and clinical outcomes will be required.[20] Guidance documents for PMA submissions can also be found on the FDA website.

## Currently approved devices

Currently, there are several optical imaging devices that have been cleared by the FDA mainly for non-cancer indications. All 510(k) cleared devices can be found in the FDA database.[21] A recent review by dSouza et al. compares the existing fluorescent imaging devices and provides basic criteria for the comparison of different images for specific applications.[3] To summarize these devices, a tabular overview detailing currently cleared devices are shown in table 2 along with more detailed information included in supplemental materials. For the main advantages and disadvantages of these devices we refer to the following reviews.[3, 22, 23]

**Table 1.** Different types and characteristics of Investigational Device Exemption (IDE) studies

| | Early feasibility study | Feasibility study | Pivotal study |
|---|---|---|---|
| **Sample size** | • Small number of patients, < 15 (approximate). | • More patients than EFS. | • Number of patients determined by statistical needs. |
| **Criteria** | • Fundamental questions about device performance & safety exist<br>• Expected changes to design of prototype device.<br>• Limited nonclinical data available. | • Sufficient information is known about the design, procedure or indication to justify clinical studies with more patients than EFS. | • Device is the final design and there is significant information known about the design, procedure and indication. |
| **Purpose** | • To demonstrate a proof of concept.<br>• Early look at safety/efficacy.<br>• Examine human factors and work flow.<br>• Determine what design or procedure changes could optimize the therapy.<br>• Determine patient characteristics that may impact device performance. | • Capture preliminary safety and effectiveness.<br>• Plan an appropriate pivotal study. | • Demonstrate safety and effectiveness to support a marketing application. |



## Standardization of Devices and Device Performance

Best practices for evaluating safety and performance of medical imaging devices are regularly published in the form of standards documents. While performance standards are commonly used in established medical imaging fields, such as the FDA-recognized PET imaging standards published by NEMA,[24] only safety standards currently exist for optical imaging. Standards that address performance typically recommend phantom-based test methods. Specifically, these documents identify relevant characteristics (e.g., spatial resolution, uniformity, sensitivity, dynamic range), provide guidelines for testing (e.g., phantom material property range/geometry, methods for calculating metrics), and describe viable test methods for a performance characteristic. Standardization improves FDA's ability to understand device working mechanisms and overall effectiveness, for benefit-risk assessments and substantial equivalence determinations. They also help to facilitate device development, standardize clinical trials and ensure product quality.

**Table 2**. Tabular overview detailing the currently 510(k) cleared devices.

| Fluorescence imaging system | Company | Year approved/510(k) cleared | FDA 510(k) number | Predicate device(s) |
|---|---|---|---|---|
| **SPY™ Intra-operative Imaging System** | Novadaq Technologies Inc. | 2005 | K042961 | The Philips Integra Series 2 Systems (K984545)<br>Heidelberg Retinal Angiographic System (K944261) |
| **PDE Fluorescent Angiographic system** | Hamamatsu Photonics K.K. | 2012 | K110480 | Novadaq Technologies Inc.'s SPY Imaging System SP2000 (K063345)<br>SPY Fluorescent Imaging System SP2001 (K073130) |
| **Fluobeam 800 Clinic® Imaging Device** | Fluoptics | 2014 | K132475 | Hamamatsu Photonics K.K., PDE Fluorescent Angiographic System (K133719) |
| **da Vinci® Firefly™ Imaging System** | Intuitive Surgical | 2014 | K141077 | da Vinci Xi Surgical System device (K131861)<br>da Vinci Fluorescence Imaging Vision System (K101077) |
| **The Artemis Handheld Imaging System** | Quest Medical Imaging | 2015 | K143474 | PDE of Hamamatsu (K110480)<br>Fluobeam of Fluoptics (K132475) |
| **VS3-IR-MMS System** | VisionSense Ltd | 2015 | K150018 | Novadaq Technologies SPY Imaging System (K063345) |
| **PINPOINT Endoscopic Fluorescence Imaging System** | Novadaq Technologies Inc. | 2016 | K161792 | PINPOINT Endoscopic Fluorescence Imaging System (K150956) |

The use of a phantom or physical standard to ensure device performance is well accepted, yet the idea of requiring device developers or manufacturers to adhere to an equivalent standard remains somewhat controversial. This is largely due to the fact that optical imaging and fluorescent probes represent innovative, rapidly changing areas. Therefore, in addition to adhering to basic principles of image quality assessment, methods should be applicable to a wide range of devices and contrast agents. Furthermore, testing should be as "minimally burdensome" as possible, which includes factors such as complexity of preparation/execution and ability to assess multiple image quality characteristics simultaneously, or in relatively rapid succession.

Establishment of performance standards begins with research on phantom-based test methods. While much progress has been made in this area, more work is needed to optimize methods addressing key characteristics. Professional

societies can use this research as the basis for generating publications that outline scientific consensus on best practices. Finally, authorship of a standard is performed by a standards organization (e.g., IEC, NEMA) committee that can draw on published consensus documents. Therefore, members of academia and industry are strongly encouraged to participate in optical safety and performance testing research, scientific consensus building and standards development that will inform and impact the regulatory process.

Unlike PET, which relies upon annihilation events to produce photons at a specific energy (all emissions lead to 511 keV gamma rays), optical imaging must consider its interactive properties with regards to the wavelength or frequency of the tissue being imaged. In many respects, each of the 16 regions of the optical imaging spectrum falling between 500 and 1300nm is unique. However, the specific parameters to be used to define these tools and the community designated to regulate these optical instruments has yet to be determined. The onus may lie on both the FDA and device manufacturers to determine such characteristics and whether they are better suited for regulation at the industry or federal level. For other imaging modalities, there are established testing parameters like spatial resolution, uniformity, distortion, sensitivity, linearity, and field of view, all of which may be applicable to optical imaging but with additional considerations for optics.[24] These may include dynamic range, spatial resolution, background collection, and sensitivity. To date, no accepted standard phantom for optical imaging or minimum requirements for device performance exist.



## Preclinical Safety Testing

Light safety standards typically used to ensure optical device safety do not address the increased potential for injury when light interacts with an exogenous agent present in tissue.[15] Many fluorescence contrast agents (e.g., protoporphyrin IX, IR700DX, Cy5) are known to produce photochemical damage in DNA and other cellular components due to light-induced generation of reactive oxygen species. While beneficial for photodynamic therapy and photoimmunotherapy,[25] this behavior presents a potential safety risk for imaging products. Contrast agents exhibiting strong absorption may intensify local energy absorption, increasing the risk of photothermal or mechanical (cavitation) damage.[26] Furthermore, novel nanoparticles may introduce unique hazards – such as highly localized fluence

"hot spots" due to plasmon resonance effects. While no guidance documents have been developed to address testing of optical imaging contrast agents, a recent guidance published by FDA/CDER provides general recommendations for preclinical testing of medications' photochemical safety[27] through the use of chemical assays for evaluating production of reactive oxygen species as well as *in vitro* and *in vivo* assays for assessing damage to cells and tissues. In the absence of standards or even well-validated best practices to clarify potential issues with novel contrast-enhanced optical products, preclinical testing, which may include in vitro cellular, phantom or tissue testing, or *in vivo* animal studies, is often warranted on a case by case basis to ensure patient safety.

## IMAGING AGENTS

The challenge for cancer imaging agents is the detection of small lesions while maintaining a high tumor-to-background ratio (TBR). There are two major classes of optical agents: targeted and non-targeted probes. The targeted probes consist of a signaling moiety, a vehicle, and a targeting ligand. These can be further divided into "always-on" and "activatable" probes.[28] Probe diversity further adds to the complexity of the approval process. Pharmacokinetics plays an important role in regulatory issues; for example, the longer an agent stays in the body the more significant the safety issues. Properties like molecule size, composition, and relative mass of signaling and targeting moieties result in different biodistribution and clearance rates. Not only toxicity should be taken into account when developing targeted contrast agents, but also other design considerations such as stability in human serum, specificity and sensitivity for the target.[29] Additionally, the route of administration will influence safety issues, such that topical application may be more favorable from a safety standpoint due to low systemic absorption as compared to intravenous (IV) administration. However, there are practical considerations when using topical formulations not encountered with IV administration, such as an inability to wash off unbound probe, non-uniformity of delivery, local tissue toxicity and barrier effects of the tissue surface (e.g. the stratum corneum of the skin). These different elements affect data collection and interpretation, and must be considered in pursuit of regulatory approval and subsequent clinical studies. Therefore, a more standardized process for imaging agents could help improve

development and approval. This would improve the FDA's ability to understand safety, working mechanism and overall effectiveness. However, the field also points out concerns regarding standardization in agent development, since this can slow down the rapidly changing chemistry in this field. A full review of these issues for imaging agents can be found elsewhere.[30]

Currently only the non-specific NIR imaging agent indocyanine green (ICG) is approved by the FDA for imaging purposes. However, at this point novel NIR fluorophores are developed with a substantially higher fluorescent yield compared to ICG and in contrast to ICG, these molecules can be conjugated to a targeting ligand, leading to targeted imaging agents.[3] An example of such a fluorophore that is already tested extensively and shown safe in humans is IRDye 800CW (LI-COR Biosciences, Lincoln, NE). Additionally, ZW800 (Curadel, Marlborough, MA) is another advanced NIR fluorophore that is nearing clinical testing.[31]



Due to unique physiological and mechanical characteristics of these agents, all will require distinct safety and toxicity studies. The range of wavelengths combined with the range of agent types makes this area of imaging different than PET, MRI, or single-photon emission computed tomography (SPECT). Using an approved drug as an imaging vehicle that can be coupled to a fluorescent molecule, analogous to incorporating a radionuclide into a drug for PET imaging, might seem like a way to improve the efficiency of the clinical translation process due to known biodistribution, targeting and safety profiles. However, since fluorophores are often large in comparison to the approved pharmaceutical agent, the new entity may confer significant differences from the approved drug, and the FDA considers this a New Molecular Entity (NME), which limits many of the predicate drug advantages.[32] The NME will be reviewed as a novel compound and require NME-specific safety and efficacy data. In diagnostic imaging, there is an option to perform a traditional dose-ranging Phase I clinical trial, or if the agent is likely to be visualized at very low doses, an exploratory IND can be initiated when the intended dose is limited to a microdose level (⩽ 100 μg and 1/100 of the therapeutic dose or ⩽ 30 nanomoles of a protein). Using this pathway, the early safety testing should demonstrate that the safety profile of the NME is similar to the previously approved parent compound. This approach will provide early information on biodistribution and streamline the testing and

approval process. For radioactively labeled agents, the FDA has developed a specific mechanism to facilitate early data acquisition through the Radioactive Drugs Research Committee (RDRC) mechanism, whereby radioactively labeled agents can be used to perform certain clinical research without IND approval. Information regarding metabolism, pathophysiology, or biochemistry can thus be obtained through early phase studies. The most important difference between an eIND and the studies conducted via the RDRC mechanism is that the RDRC can only review basic science research proposals for the use of radioactive drugs in humans, but is not intended for therapeutic or diagnostic purposes, nor for determining safety and efficacy.[33]

### Nonclinical safety and toxicity studies

The potential toxicity for investigational agents needs to be balanced by potential benefits. For traditional diagnostic imaging agents undergoing early clinical testing serious or clinically important adverse reactions are generally not acceptable. Nonclinical safety and toxicity studies should be designed to establish a wide safety margin. However, because many new agents are being proposed for surgical resection of malignancies, which inherently involve major procedures for life-threatening diseases, higher levels of risk may be justified by the nature of the procedure's anticipated benefits. When diagnostic imaging agents are evaluated for use to guide therapeutic decisions, there may be some flexibility (see below in Early Phase Clinical Trials). At this point current studies, both in humans and in preclinical setting, have not raised any specific safety issues for human use of NIR fluorophores since they have shown low or completely absent toxicity.

Nonclinical drug studies require identification of drug-target organs, characterization of pharmacology and toxicology, starting dose determination with dose escalation scheme, and study-tailored drug usage information. For NME, there are specific studies typically required prior to the onset of a Phase I trial (Table 3).[34] However, it is important to note that with appropriate scientific justification, the FDA may allow trials to proceed without some of the required studies after thorough discussion in a pre-IND meeting. The criteria mentioned are for targeted contrast agent and focus specifically on the physiochemical properties of the agent, biodistribution, and clearance pathway. It is the opinion of the field that it is crucial to analyze these properties at this point of the

approval process. For modified existing agents, the requirements are variable and, in some instances, no new preclinical studies are required. Bridging toxicity studies may be required. When a change is made to the route of administration, dose, or population of an already approved agent, the FDA encourages early discussion since they will individually evaluate the need for any additional preclinical studies. Moreover, for certain nonclinical studies (e.g. reproductive toxicology), the sponsor may submit a waiver request to the FDA.[35] For certain agents like nanoparticles, which are known to accumulate in off-target organs, the FDA might request chronic toxicology studies.

**Table 3.** Non-clinical studies needed for New Molecular Entity (NME) before Phase I trial can be conducted for optical imaging agents

| Study | Explanation |
|---|---|
| **Proof-of-concept** | Studies showing proof-of-concept of the NME. |
| **Safety Pharmacology** | To measure functional indices of potential toxicity. The aim of the safety pharmacology studies should be to reveal any functional effects on major physiological systems. |
| **Pharmacokinetics and Toxicokinetics** | Single and multiple dose pharmacokinetics, toxicokinetics, and tissue distribution studies. Information on absorption, disposition, and clearance in relevant animal models should be collected. |
| **Expanded single dose toxicity study (can be combined with repeat dose toxicity study)** | Single dose studies should generate useful data to describe the relationship of dose to systemic and/or local toxicity.<br>Repeated dose toxicity must be done when there is a chance for a secondary dose. |
| **Special toxicology** | e.g. phototoxicity, route irritancy, blood compatibility. |
| **In vitro genotoxicity study** | The use of standard genotoxicity studies for assessing the genotoxic potential of biotechnology-derived pharmaceuticals is not considered appropriate. |

*Note that FDA may permit delaying or omitting some of these studies during a pre-IND meeting

## FDA regulatory pathways for drug approval

When a sponsor considers development of a broad-range optical imaging agent with use for multiple cancer types and subsequent FDA approval, a study can be conducted to demonstrate generalization of efficacy across a number of cancers, by extrapolating data when similar methods are applicable for the proposed cancer types. In this setting, the trial design typically does not address a therapeutic indication and instead seeks approval as a contrast agent. Lymphoseek,[36] which is widely used for sentinel lymph node biopsy, followed a similar process for approval. These studies additionally serve to establish differences in pharmacokinetics and biodistribution among a range of tumor types and disease states. However, early phase trials should continue to focus on safety followed by efficacy. As such, it may be preferential to begin studies in a well-defined population, as this better facilitates successful completion of desired trial endpoints and further minimizes variability in results. Conversely, one benefit of feasibility testing in a variety of tumor types is the ability to confirm the proposed mechanism of visualization. For example, if the feasibility of an imaging agent has been demonstrated in the imaging of diseased blood-brain-barrier (BBB), which is typical of brain cancer, there is no additional need to show efficacy in subsequent brain cancer histologies. Another example is 2-deoxy-2-($^{18}$F)fluoro-D-glucose (FDG), an agent approved for imaging glucose metabolism upregulation, which is known to occur in multiple cancers; therefore, FDG is amendable to imaging multiple types of cancer. To be successful in drug development, the FDA encourages early interaction to optimize the efficiency of clinical data development and, therefore, optimize data usefulness, enhance communications with regulators, and expedite the drug development process. The intended indication of the product must be clear in the strategic plan and well-known at the onset of development. Therefore, this “target” indication should be a leading consideration in the trial design.

## Case-by-case evaluation by the FDA

The FDA believes that open discussion of the scientific and clinical considerations regarding optical imaging agents and devices will successfully advance this field. The agency further recognizes that each case requires individual assessment and that strict regulatory guidelines do not uniformly fit all products due to the complex nature of optical imaging. Additionally, the FDA has regulatory flexibility to meet the needs of any specific product when necessary. If the

science and rationale of an investigational optical product are sound, the FDA will perform an individual analysis of the studies that should be conducted to collect safety and efficacy data for approval.[34]

## COMBINATION DRUG AND DEVICE PRODUCTS

Optical imaging technologies for intraoperative imaging tend to be device and drug combinations,[37] which may be beneficial for commercialization. The decision of whether or not to submit a combined application is entirely dependent upon the sponsor, not the FDA. Nevertheless, the FDA will examine each device and/or drug submission to determine the appropriate product designation (combination or individual) based on desired labeling.

When a specific medical device is to be used with certain drug products, labeling for either product may be accomplished in a number of ways. For example, it may fall under general labeling, whereby the medical device (or drug) has a broad indication and without restrictions for use with a specific drug (or device). Additionally, one-way labeling may be applicable when a drug (or device) is for use with a specific device (or drug), but the device (or drug) can be used with multiple drugs (or devices). Lastly, two-way labeling or cross-labeling where the drug and device are tied together and seen as a combination product.



By definition, a combination product refers to 2 or more different regulated components (such as a drug with device).[38] Optical imaging usually includes two products that are sold separately but labeled for use together.[38] An e(3) product is one that is developed for use with another already approved product, which according to the investigational plan, are both necessary for its intended use. If used with a device, labeling of a previously approved product will be seen as a combination product. An e(4) product has both an investigational drug and an investigational device component and specifies that both are required for their intended use. The assignment of the combination product to a lead FDA center (e.g. CDER, CBER, or CDRH) is based on the primary mode of action (PMOA) of the product. The PMOA is defined as the single mode of action of a combination product that provides the most important therapeutic action.[38] The assignment algorithm considers precedence (i.e. where has similar technology

been assigned) in assigning a lead center. The lead center will become the point of contact for the sponsor and will communicate with other centers for the purposes of regulatory review. Consequently, there is a need for only one marketing application for most combination products, either an NDA or PMA. However, a sponsor can choose to submit two marketing applications.

If the sponsor wishes for a drug to be indicated for use with multiple devices, it does not automatically imply that it will be a combination product. This is especially true when said devices are already approved. Regardless, there must be technical and clinical data available to support the use of multiple devices in addition to one-way or general labeling.

The best examples of this approach are PET agents, which can be used on a range of PET imaging devices. When a PET scanner is cleared for human use, it is not indicated for a specific PET agent but rather for positron-emitting radionuclides, which is a broad label. The reason for this is that the FDA has evidence that PET devices operate with sufficient similarity. For optical imaging, however, this is not yet the case. As such, the FDA must continue to develop a similar level of experience when using an optical imaging agent with multiple devices. When comparing optical imaging devices to PET or MRI, there are several aspects to consider. First, there are orders of magnitude variations in signal levels, which makes it difficult to draw a parallel with the other techniques. Secondly, there is a wide variety of devices, large dynamic range differences (causing as much as 6 orders of magnitude variation in sensitivity), wavelength variation, and varying performance with room lights that will change background sensitivity, and intensity variation due to distance.

## CLINICAL TRIAL TYPES AND IMPORTANCE OF DESIGN

### Early feasibility studies - Devices

For the development of medical devices, it can be valuable to use the Early Feasibility Study (EFS) program as a regulatory tool, which is similar to a phase I study for drug development.[39] The goal of the EFS program is to enhance patient access to beneficial technology and supporting innovation in the clinical sector.

A sponsor can conduct an EFS IDE trial when there are significant unknowns regarding device performance, because the device is early in development or is intended for a new use. Therefore, a small number of subjects are permitted for clinical investigation. The differences between the different types of IDE trials are shown in Table 1. Also part of the EFS guidance are recommendations on the optimal path for filing a pre-submission for an IDE.[40] Early discussion with the FDA can be very helpful to agree on a test plan that will support the IDE and can help avoid unnecessary testing, which can be time consuming and expensive.[19] Additionally, it may be possible, in some instances, to use novel devices for certain preliminary clinical studies without formal FDA approval, which would only require local Institutional Review Board (IRB) approval.

### Pharmacology in clinical trials - Drugs

The pharmacology requirements during the clinical drug development process are primarily divided into safety and efficacy considerations (Table 4). Safety issues are based on what is being delivered to the patient (manufacturing), dosing, and appropriate monitoring during the trial. Recommendations on trial design, which are made by the FDA, can aid in making the process successful. The primary goal for efficacy trials is to determine a "near-optimal" dose, a process that is often finalized in Phase II. For the FDA, the definition of near-optimal is a dose regimen and imaging condition that are superior to alternatives, which have been studied for safety and pilot efficacy. This will require the investigation of a dose escalation scheme with 3 imaging windows, and the ability to conclude whether or not more will be better or fewer will be just as good. Early on, pharmacokinetic assessment can assist in the selection of optimal imaging window, timing of repeat dosing, and amount of repeat dosing. The goal should be to correlate concentrations to clinical outcome, which is typically performed in Phase III studies.



### Phase I and II trials for Imaging Agents and Combination Products

As stated previously, potential risk vs. potential benefit considerations for investigational diagnostic tests require that the test products (drug and associated cameras/devices) have relatively low safety risks. However, when agents are developed to have an effect on therapeutic decisions, are supported by proof of concept data, and trials are designed to show improvement in clinically important outcomes it may be justifiable to adjust the safety threshold

**Table 4.** Safety and Efficacy requirements at all different phases of drug development

| Study | Requirements |
|---|---|
| **First-in-human** | Minimum requirements for conducting study to establish safety data.<br>Safety:<br>• Collect early dosing information.<br>• Determine entry criteria; e.g. renal impairment.<br>• Monitoring cardiac safety; at baseline and after imaging.<br>• Adverse event collection during imaging and follow-up.<br>Important data set to obtain<br>• Sufficient PK sampling.<br>• Drug interactions on concentration.<br>• Imaging characteristics at various doses and time points |
| **Phase-II trial** | Controlled clinical study to collect early effectiveness data and generate hypotheses.<br>Safety:<br>• Same as Phase I, but supported by evidence obtained previously.<br>• Gain early understanding of the expected adverse event profile.<br>Efficacy:<br>• Refine dosing to determine "near optimal" dose.<br>• PK sampling for assessment of PK linearity.<br>• Develop imaging interpretation standards. |
| **End-of-Phase II meeting** | Generally considered the most important meeting between sponsor and FDA.<br>• Near optimal dose is determined, both in safety and efficacy manner.<br>• Determine what needs to be measured in future studies.<br>• Acquire input from FDA on how specific populations will be addressed in the label. |
| **Phase III trial** | Safety:<br>• Same as Phase II, but supported by evidence obtained previously.<br>• Sufficiently powered for statistical determinants.<br>Efficacy:<br>• Clinically meaningful primary endpoint success.<br>• Sufficient PK sampling to inform dose adjustment during or at end of trial for a typical patient and specific populations. |
| **Pre-NDA/BLA meeting** | • Review data to fulfill recommendations made at end-of phase 2.<br>• Review organization of future application: study reports and datasets. |

in order to match potential benefits. For those agents or product combinations that claim improvement on patient survival, the safety requirements may be less

stringent than those agents that claim a lesser benefit. The main focus of trial design for phase I and II trials should be to collect sufficient safety data and information to define achievable endpoints for clinical benefit and also collect data that supports the intended clinical use and indication statement (Table 4). When conducting Phase I and early Phase II studies, it is important that the standard of care be maintained to protect patients from imaging products that have not yet been provided preliminary evidence of effectiveness.

## Efficacy endpoints in clinical trials

During design of clinical trials, endpoints need to align with the proposed drug/device labeling indication and, therefore, high standard clinical claims will require more clinically meaningful evidence. The FDA works with a risk-benefit approach such that any risks must be outweighed by increased benefits. The variety of potential efficacy endpoints is demonstrated in Table 5 and includes clinical therapeutic outcomes as well as measures of diagnostic performance.

**Table 5.** Types of efficacy endpoints

| Endpoint | Explanation |
|---|---|
| **Exploratory** | Used for development of hypotheses, pharmacodynamics measurements. |
| **Primary** | Used to demonstrate efficacy. |
| **Secondary** | Support efficacy, provide information on safety and efficacy in specific subpopulations. |



To gain FDA approval for new drug applications (NDA),[41] the study needs to show benefit to the patient. Endpoints that simply correlate fluorescence with the location of a known tumor are not considered sufficient for approval; rather evidence must be shown that imaging will have a positive benefit for the patient. An example discussed was the identification of positive tumor margins in a defined clinical setting. For example, if after standard surgical resection additional malignant lesions are identified, then this would indicate the potential benefit of the imaging, assuming that a more complete removal of malignant tissue for this type of cancer is directly correlated with survival or other clinical benefit such as reduced need for reoperation. This means the FDA does not specifically require direct measurement of survival endpoints for this

indication. It can be sufficient to show improved detection of positive margins when the new technology is used, since the correlation between clear margins and survival is already well established for many types of cancer. The same may be true for debulking surgeries. For example, if prior evidence indicates that debulking correlates to better outcomes, it may be sufficient to show that the optical technique improves the surgical safety and effectiveness of debulking procedures.

One of the important considerations for the conduct of imaging studies what procedures will be used to minimize bias. There was little consensus to better understand which clinical trial methodologies would be most efficient, cost effective and scientifically reproducible. Trial randomization increases the number of patients required for studies in several cancer types. Additionally, it is impossible to effectively blind the operating surgeon, who would most certainly realize when optical imaging was being utilized. An intra-patient controlled study can be adequately designed to test the hypothesis that the optical technique provides additional information that contributes to the tactile or visual information provided by standard of care. To tackle these problems the FDA established a recommendation panel. An example of a clinical setting where an intra-patient control study can be used successfully is a study of primary breast cancer resection. A pre-specification of optical agent diagnostic performance and definition of the meaningful improvement to be achieved by the investigational product in the clinical trials need to be defined in the clinical protocol before study initiation.

## FUNDING AND RESOURCES AT NCI FOR MOLECULAR IMAGING AGENTS

The NIH and NCI have resources available to support molecular imaging research. Only funding specifically for imaging will be discussed here. Some grant opportunities for early phase clinical trials are available for image-guided drug delivery, for combination of pre-clinical and clinical studies, and for collaborations between academia and industry to translate imaging systems for cancer imaging. Additionally, there are the SBIRs and STTRs for industry support. More extensive information can be found at the NIH website[42] and special imaging grant opportunities are listed at: http://imaging.cancer.gov/

researchfunding/fundingopportunities/currentcip. The NCI also has the NExT program for alleviating the substantial resource strain required to translate experimental therapeutics into the clinic. This program provides access to NCI recourses and expertise.[43]

For late Phase II and Phase III trials, the NCI has the NCI National Clinical Trial Network (NTCN) to conduct large-scale clinical trials. The ECOG-ACRIN group is specialized in imaging.[44] Lastly the NCI can provide help in regulatory issues and provide resources during pre-submission phases. It is also important to note that the nanocharacterization lab (NCL) can be a useful resource for nanoparticle based agents and is an important resource within the NIH.[45]

## CONSIDERATIONS

Reimbursement by the CMS for optical imaging is an important consideration for industry investment. Traditionally, this is initiated after FDA approval has been granted. The goal of CMS is to assess whether new technologies are reasonable and necessary. Therefore, they may require patient and cost-effectiveness outcome data. In contrast, the FDA has a different responsibility when evaluating new technologies, namely assessing safety and effectiveness. However, the FDA can assist in designing trials in collaboration with CMS to additionally assess those outcomes.



There was consensus that target-specific imaging agents are the most likely to have a long-term benefit when compared to non-specific agents like indocyanine green. However, the general opinion was that the field should first focus on more generalizable agents so as to expand the technique using fluorescent guidance beyond purely surgical applications. Clinical translation must be efficient, but it is rather unlikely that multiple agents will be approved in a timely manner. It is important to note that continued education of the CMS is likely necessary in considering molecular imaging agents, which has been the case for many years with the FDA regarding such agents. Lack of CMS reimbursement will be a key factor in hindering the widespread use of molecular imaging agents for intraoperative imaging. Thus, a consortium that includes professional societies, industry, NIH, and private foundations will be important to better educate

the CMS and ultimately obtain reimbursement for specific molecular imaging agents.

When considering improvement of the approval process for devices and agents, regulatory and commercial incentives must be taken into account. While decoupling agents and devices would certainly aid in the advancement of optical imaging, this may not be in the economic interests of the manufacturers. The reason for this may not be solely financial, but also safety driven. When devices and drugs are coupled, a rigorous safety profile must be established, which is further associated with a higher regulatory burden.

## CONCLUSION

The ultimate goal of NIR-fluorescent contrast-enhanced oncologic surgery is to provide information to the surgeon that lies beyond that of the visible light spectrum and amplify contrast enhancement in different tissue types. By improving visual detection of tumors, the surgeon gains critical information that can translate to improved overall outcomes for the patient. Since optical imaging techniques lead to real-time feedback, there is a direct and instantaneous effect on patient care and decision-making. While this is one of the main advantages of contrast-enhanced oncologic resection, it nonetheless requires proof of benefit to the patient. Thus, the field must clearly demonstrate the benefit in clinical trials and thoroughly assess relevant outcomes. The investigational imaging agent/device's proposed "indication for use" will direct all future studies needed for approval and, therefore, should be chosen carefully. Lastly, the use of predicate devices and agents, when available, should help accelerate the eventual approval of new optical imaging technology.

| Summary statements |
| --- |
| 1. Contrast-enhanced surgery should be considered a complementary technique for the surgeon rather than a diagnostic tool. This technique is used to provide additional information to assist the surgeon in making clinical decisions to improve procedural outcomes. |
| 2. Proving performance equality in different imaging devices (as in PET imaging) is critical to demonstrate so that imaging agents may be used on multiple devices. |
| 3. Identifying a predicate device can help guide the approval pathway for a new or equivalent device. |
| 4. If an optical imaging system is intended for the diagnosis, prognosis, or treatment of cancer during an investigational human study, such use is determined to be "significant risk" and FDA requires the study sponsor to file an Investigational Device Exemption (IDE) application. |
| 5. Optical imaging products are traditionally viewed as combination products by the FDA. |
| 6. Additional toxicity of imaging agents should be well justified by the benefit since the invasiveness of procedure does not factor into the FDA classification considerations. |
| 7. Clinical trials must be designed to obtain safety and efficacy data for the intended indication of use. |
| 8. If the sponsor wants a drug to be indicated for use with multiple devices, there must be technical and clinical data available to support the use of multiple devices. |
| 9. Clinical trials must prove patient benefit before FDA approval can be obtained since optical imaging inevitably influences patient care and decision making in real-time. |
| 10. The FDA does not specifically require direct measurement of survival endpoints to show benefit for the contrast-enhanced surgery indication. It can be sufficient to show improved detection of positive margins when the new technology is used, since the correlation between clear margins and survival is already well established for many types of cancer. |

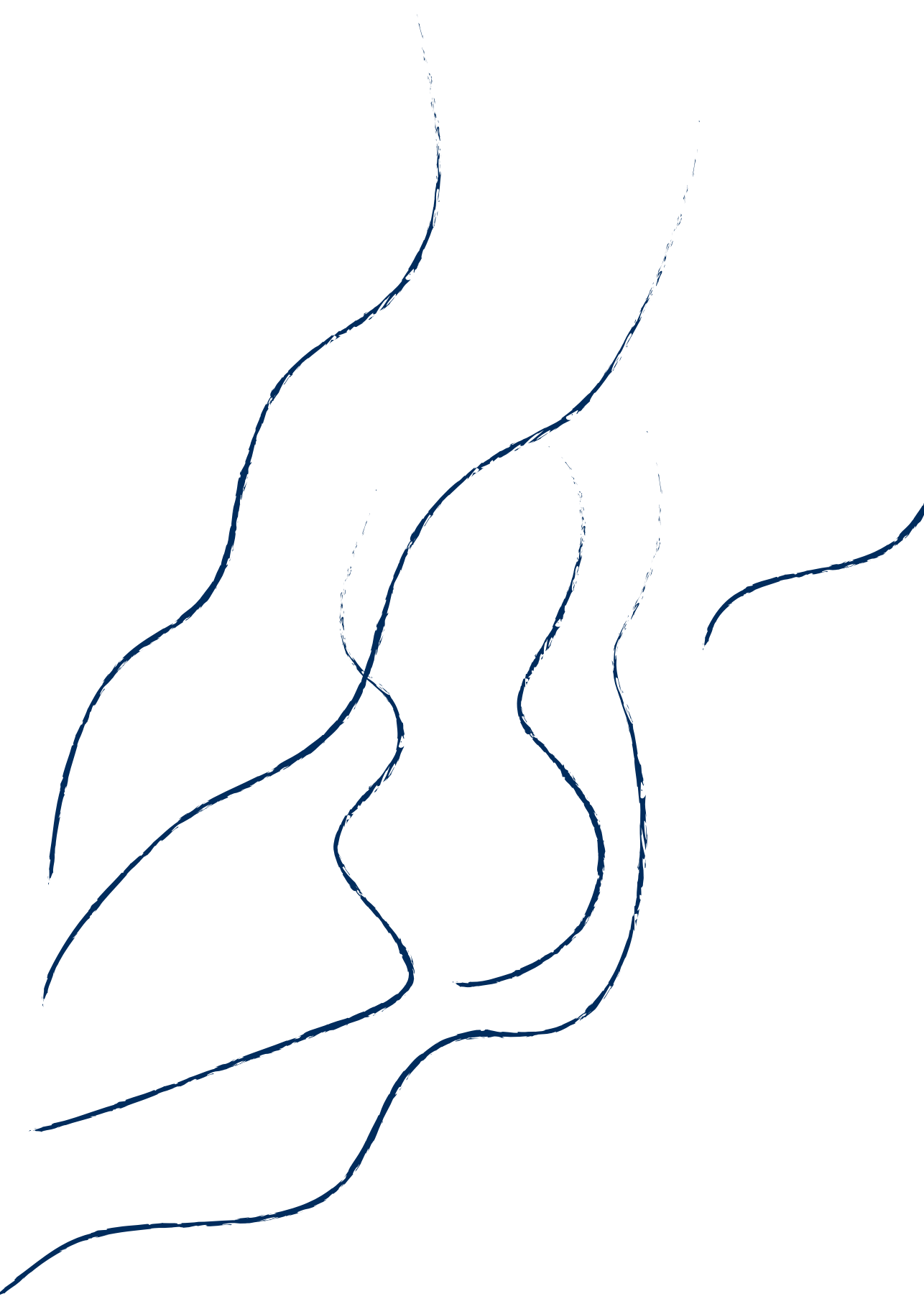
# REFERENCES


1. American Cancer Society Website. Cancer Facts and Statistics. www.cancer.org (2016).
2. Eldeeb, H., Macmillan, C., Elwell, C., Hammod. A. The Effect of the Surgical Margins on the Outcome of Patients with Head and Neck Squamous Cell Carcinoma: Single Institution Experience. Cancer Biol Med. 9(1), 29–33 (2012)
3. DSouza A.V., Lin H., Henderson E.R., Samkoe K.S., Pogue B.W. Review of fluorescence guided surgery systems: identification of key performance capabilities beyond indocyanine green imaging. J. Biomed. Opt. 21(8), 080901 (2016).
4. Research Portfolio Online Reporting Tools (RePORT) National Institutes of Health Website. https://report.nih.gov/ (2016).
5. Daniltchenko, D.I., Riedl C.R., Sachs M.D., Koenig F., Daha K.L., Pflueger H., et al. Long-term benefit of 5-aminolevulinic acid fluorescence assisted transurethral resection of superficial bladder cancer: 5-year results of a prospective randomized study. J Urol. 174(6), 2129-33, discussion 2133 (2005)
6. Sievert, K.D. & Kruck, S. Hexyl aminolevulinate fluorescence cystoscopy in bladder cancer. Expert Rev Anticancer Ther. 9(8), 1055-63 (2009)
7. Colditz, M.J. & Jeffree, R.L. Aminolevulinic acid (ALA)-protoporphyrin IX fluorescence guided tumour resection. Part 1: Clinical, radiological and pathological studies. J Clin Neurosci. 19(11), 1471-4 (2012)
8. Stummer, W., Pichlmeier, U., Meinel, T., Wiestler, O.D., Zanella, F., Reulen, H.J. ALA-Glioma Study Group. Fluorescence-guided surgery with 5-aminolevulinic acid for resection of malignant glioma: a randomised controlled multicentre phase III trial. Lancet Oncol. 7(5), 392-401 (2006)
9. Roberts, D.W., Valdés P.A., Harris B.T., Hartov A., Fan X., Ji S., et al. Glioblastoma multiforme treatment with clinical trials for surgical resection (aminolevulinic acid). Neurosurg Clin N Am. 23(3), 371-7 (2012)
10. Garland, M., Yim, J.J., Bogyo, M. A Bright Future for Precision Medicine: Advances in Fluorescent Chemical Probe Design and Their Clinical Application. Cell Chem Biol. 23(1), 122-36 (2016)
11. Zinn, K.R., Korb M, Samuel S, Warram J.M., Dion D., Killingsworth C., et al. IND-directed safety and biodistribution study of intravenously injected cetuximab-IRDye800 in cynomolgus macaques. Mol Imaging Biol. 17(1), 49-57 (2015)
12. Rosenthal, E.L., Warram J.M., de Boer E., Chung T.K., Korb M.L., Brandwein-Gensler M., et al. Safety and Tumor Specificity of Cetuximab-IRDye800 for Surgical Navigation in Head and Neck Cancer. Clin Cancer Res. 21(16), 3658-66 (2015)
13. Rosenthal, E.L., Warram J.M., de Boer E., Basilion J.P., Biel M.A., Bogyo M., et al. Successful Translation of Fluorescence Navigation During Oncologic Surgery: A Consensus Report. J Nucl Med. 57(1), 144-50 (2016).
14. Eyüpoglu, I.Y., Hore N., Merkel A., Buslei R., Buchfelder M., Savaskan N. Supra-complete surgery via dual intraoperative visualization approach (DiVA) prolongs patient survival in glioblastoma. Oncotarget. 7(18), 25755-68 (2016).
15. American National Standard for Safe Use of Lasers, ANSI Z136 1–2000, Laser Institute of America, Orlando, FL, 2000.
16. Guidance for Industry and Food and Drug Administration Staff: The 510(k) Program: Evaluating Substantial Equivalence in Premarket Notifications [510(k)]. U.S. Food and Drug Administration Web site. http://www.fda.gov/downloads/MedicalDevices/.../UCM284443.pdf. (2014)
17. Code of Federal Regulations, title 21, chapter I, 21 CFR §812.3(m). U.S. Food and Drug Administration Web site. http://www.ecfr.gov/cgi-bin/text-idx?SID=27caafb08e9bede44619aedad9231082&mc=true&tpl=/ecfrbrowse/Title21/21cfr812_main_02.tpl (2016).
18. Gibbs-Strauss, S.L., Rosenberg, M., Clough, B.L., Troyan, S.L., Frangioni, J.V. First-in-human clinical trials of imaging devices: an example from optical imaging. Conf Proc IEEE Eng Med Biol Soc. 2009, 2001-4 (2009).

19. Device Regulation and Guidance. U.S. Food and Drug Administration Web site. http://www.fda.gov/MedicalDevices/DeviceRegulationandGuidance/HowtoMarketYourDevice/InvestigationalDeviceExemptionIDE/ucm046706.htm (2016).
20. Code of Federal Regulations, title 21, chapter I, 21 CFR §860.7. U.S. Food and Drug Administration Web site. http://www.ecfr.gov/cgi-bin/text-idx?SID=b9a04cd8ddd62484ee6abd663b8115e2&mc=true&tpl=/ecfrbrowse/Title21/21cfrv8_02.tpl#0 (2016).
21. 510(k) Premarket Notification Database. U.S. Food and Drug Administration Web site. http://www.accessdata.fda.gov/scripts/cdrh/cfdocs/cfPMN/pmn.cfm (2016).
22. Chi C., Du Y., Ye J., Kou D., Qiu J., Wang J., et al., Intraoperative imaging-guided cancer surgery: from current fluorescence molecular imaging methods to future multi-modality imaging technology. Theranostics 4(11), 1072–1084 (2014)
23. Gioux S., Choi H.S., Frangioni J.V., Image-guided surgery using invisible near-infrared light: fundamentals of clinical translation. Mol. Imaging 9(5), 237–255 (2010)
24. Guidance for Industry: Guidance for the Submission of Premarket Notifications for Emission Computed Tomography Devices and Accessories (SPECT and PET) and Nuclear Tomography Systems. U.S. Food and Drug Administration Web site. http://www.fda.gov/MedicalDevices/DeviceRegulationandGuidance/GuidanceDocuments/ucm073794.htm#6a (2015).
25. Mitsunaga, M., Ogawa M., Kosaka N., Rosenblum L.T., Choyke P.L., Kobayashi H. Cancer cell–selective in vivo near infrared photoimmunotherapy targeting specificmembrane molecules. Nat. Med. 17(12), 1685-92 (2011).
26. Qin, Z., Bischof, J.C. Thermophysical and biological responses of gold nanoparticle laser heating. Chem. Soc. Rev. 41, 1191-1217 (2012).
27. "S10 Photosafety Evaluation of Pharmaceuticals, Guidance for Industry" U.S. Department of Health and Human Services, Food and Drug Administration, Center for Drug Evaluation and Research (CDER), Center for Biologics Evaluation and Research (CBER), 2015
28. Kobayashi, H., Choyke, P.L. Target-cancer-cell-specific activatable fluorescence imaging probes: rational design and in vivo applications. Acc. Chem. Res. 44(2), 83-90 (2011).
29. Nguyen Q.T., Tsien R.Y., Fluorescence-guided surgery with live molecular navigation—a new cutting edge. Nat. Rev. Cancer 13(9), 653–662 (2013).
30. James, M.L., Gambhir, S.S. A Molecular Imaging Primer: Modalities, Imaging Agents, and Applications. Physiol Rev. 92(2), 897-965 (2012).
31. Choi H.S. Gibbs S.L., Lee J.H., Kim S.H., Ashitate Y., Liu F., et al., Targeted zwitterionic near-infrared fluorophores for improved optical imaging. Nat. Biotechnol. 31(2), 148–153 (2013)
32. Scheuer, W., van Dam, G.M., Dobosz, M., Schwaiger, M., Ntziachristos, V. Drug-based optical agents: infiltrating clinics at lower risk. Sci Transl Med. 4(134), 134ps11 (2012).
33. Guidance for Industry and Researchers: The Radioactive Drug Research Committee: Human Research Without An Investigational New Drug Application. U.S. Food and Drug Administration Web site. http://www.fda.gov/downloads/Drugs/.../Guidances/UCM163892.pdf (2010).
34. Guidance for Industry: M3(R2) Nonclinical Safety Studies for the Conduct of Human Clinical Trials and Marketing Authorization for Pharmaceuticals. U.S. Food and Drug Administration Web site. http://www.fda.gov/downloads/Drugs/GuidanceCompliance RegulatoryInformation/Guidances/UCM073246.pdf (2010).
35. Code of Federal Regulations, title 21, chapter I, 21 CFR §312.10. U.S. Food and Drug Administration Web site. http://www.ecfr.gov/cgi-bin/text-idx?SID=78e15ff63e94ba03ba54cecc5e277b12&mc=true&tpl=/ecfrbrowse/Title21/21cfrv5_02.tpl#0 (2016).

36. Drugs.com [Internet]. Lymphoseek Approval History; c2000-16 [Cited: 2016 July 10]. Available from: https://www.drugs.com/history/lymphoseek.html.
37. Combination Products. U.S. Food and Drug Administration Web site. www.fda.gov/CombinationProducts/default.htm.
38. Code of Federal Regulations, title 21, chapter I, 21 CFR §3.2. U.S. Food and Drug Administration Web site. http://www.ecfr.gov/cgi-bin/text-idx?SID=dec14a8c39e51510260360b91a916921&mc=true&tpl=/ecfrbrowse/Title21/21cfr3_main_02.tpl (2016).
39. Guidance for Industry and Food and Drug Administration Staff: Investigational Device Exemptions (IDEs) for Early Feasibility Medical Device Clinical Studies, Including Certain First in Human (FIH) Studies. U.S. Food and Drug Administration Web site. http://www.fda.gov/downloads/MedicalDevices/DeviceRegulationandGuidance/GuidanceDocuments/UCM279103.pdf2 (2013).
40. Guidance for Industry and Food and Drug Administration Staff: Requests for Feedback on Medical Device Submissions: The Pre-Submission Program and Meetings with Food and Drug Administration Staff. http://www.fda.gov/downloads/MedicalDevices/DeviceRegulationandGuidance/GuidanceDocuments/UCM311176.pdf (2014).
41. Code of Federal Regulations, title 21, chapter I, 21 CFR §314.126. U.S. Food and Drug Administration Web site. http://www.ecfr.gov/cgi-bin/text-idx?SID=a9064882d83357f36ab1b199d832c6e1&mc=true&tpl=/ecfrbrowse/Title21/21cfrv5_02.tpl#0 (2016).
42. NIH's Central Resource for Grant and Funding Information. National Institutes of Health, Office of Extramural Research Web site. http://grants.nih.gov/funding/index.htm (2016).
43. NeXT NCI Experimental Therapeutics Program. Consultation on Development of Small Molecules, Biologics, and Imaging Products Intended for Cancer Patients. National Cancer Institute Web site. http://next.cancer.gov/experimentalTherapeutics/form.htm (2016).
44. ECOG-ACRIN Cancer Research Group Website. National Cancer Institute. http://ecog-acrin.org/. Last updated 2015. Accessed July 27, 2016.
45. Nanotechnology Characterization Lab. National Cancer Institute. http://ncl.cancer.gov/ (2016).

07



Chapter | 8

# Guide for Successful Clinical Translation of Optical Imaging Agents for Molecular Imaging

Willemieke S. Tummers[1], Eben L. Rosenthal[2], Sanjiv S. Gambhir[3]

[1]Department of Radiology, Molecular Imaging Program, Stanford University, Stanford, CA. [2]Department of Otolaryngology, Stanford University, Stanford, CA. [3]Departments of Radiology, Bioengineering, and Materials Science & Engineering, Molecular Imaging Program at Stanford, Canary Center at Stanford for Cancer Early Detection. Stanford University, Stanford, CA.

## ABSTRACT

Optical molecular imaging with the use of tumor-specific molecular imaging agents (MI agent) has the potential to provide a personalized approach to both medical therapy and surgical procedures. This technique can improve patient stratification, increase margin-negative resections, detect metastatic spread, monitor therapy, and potentially improve overall patient care. To reach these goals, U.S. Food and Drug Administration (FDA)-approval is the first and very crucial step for successful and widespread clinical translation, which is often followed by acquisition of value data to receive insurance reimbursement. Data requirements for FDA approval vary considerably, but there are some constants: there is a need to demonstrate safety and efficacy of the novel MI agent and technique, and for the sponsor it is necessary to achieve this with the lowest cost and in shortest amount of time. Success or failure of optical MI agents will critically depend on the design of clinical trials and the chosen endpoints. Here we will provide some insights into the process of engaging the FDA in the evaluation of tumor-specific MI agents, and guide the way for designing optimal optical imaging clinical trials.

## INTRODUCTION

Molecular imaging allows non-invasive visualization of biological processes at cellular and subcellular levels in a living subject by integrating both disease- and patient-specific information and it is often fused with traditional anatomical images.[1] Molecular imaging serves as a tool to acquire sequential and consistent information on the subject of interest enabling a precise understanding of the biological process and design studies with better statistical power and even reduce the number of subjects involved, following the Replacement, Reduction, Refinement (3 R's) principle.[2] There are high expectations of this personalized approach to therapy, since it could result in improved stratification of patients and will ensure that patients receive the most appropriate treatment. Ultimately, this approach can improve patient care. Molecular imaging can be applied to a wide range of indications, such as treatment, diagnostics, drug development, and monitoring of drug action.[3,4] Molecular imaging could identify early failures in development of therapeutic agents (in phase I or II trials), which would result in reduction in time and cost for getting an agent to market. An example of an MI agent used for multiple indications is FDG-PET, which has proved useful not only in diagnostics but also in obtaining information on drug efficacy far earlier compared to the availability of survival data, thereby, identifying if a clinical trial is worth continuing.[5-8]



Recent maturation in optical imaging technology with targeted MI agents to visualize cancer is of high interest in the field, and since 2007 the number of publications increased with eightfold and 38 clinical trials have been done in this field.[9-10] When using tumor-specific molecular imaging to image a tissue of interest, certain criteria need to be met: a tissue-specific target, a way to reach the target of interest, and highly sensitive, efficient imaging techniques.[11] To leverage the potential of molecular imaging in cancer treatment, U.S. Food and Drug Administration (FDA)-approved MI agents are needed. Countless preclinical studies have been published in recent years on identifying tissue-specific targets and developing optical MI agents suggesting its great potential. However, until now only the non-specific (not targeted to a specific biomarker) optical MI agents indocyanine green (ICG) and methylene blue (MB), and the specific MI agent 5-ALA are approved for clinical use. Reasons for the failure of clinical translation of novel optical MI agents include high costs, both for GMP

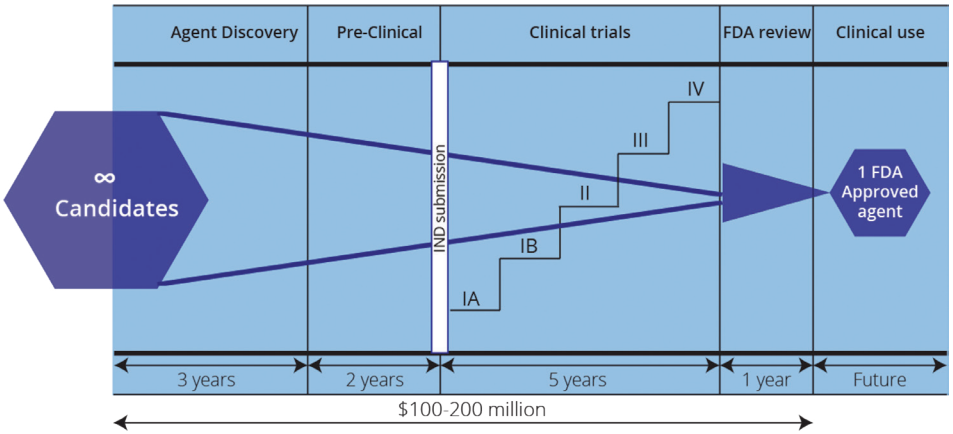



**Figure 1.** Schematic overview of the clinical translation of optical imaging agents, from MI agent discovery till the approval of one MI agent. This figure provides an overview of the expensive and time-consuming process of the development of a novel MI agent. The timeline gives an indication of the required time per phase but is dependent on the chosen agent. In case of an existing compound, both the costs and the time will decrease. Adapted for optical imaging agents. Original source: PhRMA

manufacturing and toxicology studies, lack of reimbursement, and the high bar for demonstrating clinical value established by the FDA. Obtaining FDA approval not only allows use in the clinic but also the right to commercially market the application, and the ability to apply for reimbursement from the Centers for Medicare & Medicaid Services (CMS).

The translation of therapeutic drugs from bench to bedside is around $0.8-1.7 billion with an estimated timeline of about 10-17 years.[12-14] Of all initiated new therapeutics only 10% will reach it past the FDA's Investigational New Drug (IND) stage, with up to 45% agents are found to lack clinical efficacy in phase III trials.[13-17] Failure in phase III studies is often considered to be a result of inappropriate data collection in Phase I or II and poor Phase III study design. In 2006, Nunn reported that the costs of bringing a new MI agent to the market are reduced compared to therapeutic drugs, around $100-150 million,[18] however a hurdle of these MI agents is that they serve a smaller market, are used less frequently, and therefore generate less per patient revenue. A long investment cycle, the narrow patient population, the single use per patient, and 90% chance of failure make MI agents a complex investment (Figure 1).

United States health spending continues to shift from traditional to specialty medicines (accounting for $384 of the $895 per person per year spent on medicines) and new brands accounted for 13 billion dollars of growth in 2016.[19, 20] To address the overwhelming number and complexity of medical product development, the FDA launched the "Critical Path Initiative". Since 2004, the number of approved new molecular entities (NME) or new biologics license applications (BLA) has increased, and the median total time to approval has decreased indicating the effectiveness of the new FDA regulations. To address these same issues for the optical imaging world, there has been several collaborative meetings between the optical imaging field, the FDA and National Cancer Institute (NCI).[21, 22]

The aim of this review is to provide a detailed overview of the required steps for successful clinical translation of optical MI agents for intra-operative use in oncologic surgery and suggestions for trial design to show clinical benefit and successful targeting for this specific class of MI agents.

## POSITRON EMISSION TOMOGRAPHY (PET) TRACERS AS PRECEDENCE FOR OPTICAL IMAGING AGENTS



New technologic developments have resulted in a growing interest in optical imaging over the last 10-20 years, as a result there is corresponding development in the regulatory strategies by the FDA. Although the first optical agent was approved in the early 1950's, PET radiopharmaceuticals have been consistently developed for clinical application and evaluated for new indications. In 2012, the FDA released the guidelines titled "Investigational New Drug Applications for Positron Emission Tomography (PET) Drugs" to improve understanding of the development path for novel PET tracers.[23] Specific mechanisms were developed to facilitate early data acquisition, the Radioactive Drugs Research Committee (RDRC) mechanism, where radioactive labeled agents can be used to perform early-stage research without FDA IND approval through a local committee. Information regarding metabolism, pathophysiology, or biochemistry can therefore be obtained in early development of the agent. The RDRC is created by the FDA to review research proposals for the use of radioactive drugs in humans but not for therapeutic, diagnostic purposes, or for safety and efficacy.

The RDRC is designed to review first-in-human studies (such as an exploratory IND (eIND)) which are designed to identify the safety and/or efficacy of an MI agent for a potential clinical application.

From a regulatory standpoint, there is a significant difference between PET and optical MI agents. When a PET agent is approved, it will be approved with a general label, and therefore can be used in conjunction with a range of PET devices. Moreover, when a PET scanner is approved for human use, it is not linked as a combination product to a specific PET agent, but for any positron-emitting radionuclide. This broad approval is granted because the FDA has a high level of confidence that PET devices operate sufficiently similar. This is not yet the case for optical MI agents and imaging systems since the similarity of performance is yet unproven. An important consideration to take into account when comparing optical imaging to PET agents that optical MI agents have key differences: 1) tissue penetration is less than or equal to 5-8 mm, 2) it has orders of magnitude lower signal intensity, 3) there is broad device variation (large dynamic range differences, wavelength variation, and performance can depend on ambient light).[24, 25]

## REGULATORY VIEW ON OPTICAL MOLECULAR IMAGING AGENTS

The regulatory process for MI agents is handled by the Center for Drug Evaluation Research (CDER) within the US FDA. There are certain milestones and requirements that need to be met during the development process. The process will start with an Investigational New Drug application (IND), for which a pre-submission (Pre-IND) meeting with the FDA is encouraged. Successful demonstration of safety and efficacy in early phase trials can lead to Phase III trials which are necessary for demonstration of clinical utility and safety for a New Drug Application (NDA) or Biologics License Application (BLA). During the pre-IND meeting the FDA will comment on the proposed methods both for GMP manufacturing and clinical testing. Optical MI agents tend not to be treated as a drug for regulatory purposes, but instead as a combination products since MI agents require a complementary imaging instrument to facilitate visualization. It is unclear if the optical MI agent will require a marriage to an individual

imaging instrument[26] or if two products can be sold separately but labeled for use together.[27] This remains an evolving regulatory area and a more extensive elaboration on combination products in optical imaging is reviewed elsewhere.[22]

For regulatory bodies such as the FDA and European Medicines Agency (EMA), optical MI agents add another complexity into field, because they are used in real-time during procedures to expand the visual information of the clinician, thereby enabling them to make informed decisions based on unique data provided by the device and MI agent combination. From a regulatory point of view, the fact that intra-operative optical imaging occurs during the procedure gives the clinician the opportunity to alter their treatment plan based on real-time imaging information. As a result, these MI agents deserve unique consideration relative to other imaging modalities that are most frequently used exclusively in the diagnostics arena or the surgical planning process.

## DIFFERENCES BETWEEN REGULATORY PATHWAYS IN UNITED STATES AND EUROPE



In the United States, the FDA is responsible for protecting the public health by assuring the safety, efficacy and security drugs, and medical devices.[28] In Europe, the European Medicines Agency (EMA) has the mandate to centrally approve new drugs for the European Union (EU). The mission of the EMA is to make science-based decisions and to regulate medicines. One of the main differences between the FDA and EMA is that the EMA itself is a collaborative effort, opposed to a government organization. The agency has members from all EU countries, and with expansion of the EU, the structure gets increasingly complex compared to the review group of the FDA.[29] An important similarity is that both agencies are participants in The International Council for Harmonisation of Technical Requirements for Pharmaceuticals for Human Use (ICH) guidance. This project started in 1990 involving the regulators and research-based industries from the US, EU and Japan.[30] Details regarding the review process by the different agencies world-wide is reviewed elsewhere.[31]

When an MI agent is approved by the EMA in Europe, it doesn't mean that the same MI agent is also approved in the United States. Despite submission of

identical requests for drugs, with the same supporting data, both regulatory bodies can end up with a different decision regarding approval. Trotta, et al. looked at 100 indications for 42 cancer drugs evaluated by both the EMA and FDA between 1995 and 2008 and found that 19 indications were not approved by one of the two agencies.[32] Important to note is that most of the differences in authorization are not in drugs where there is a clear risk-benefit profile. An example of different approval decisions in the field of optical MI agents is 5-aminolevulinic acid (5-ALA). This MI agent is administered orally or topically, and converted intratumorally to fluorescent protoporphyrin IX. 5-ALA is approved for oral administration to highlight brain tumors for a long time in Europe, Canada, and Japan, but not till recently in the United States.[33]

Another difference between the FDA and EMA is that the EMA is not responsible for clinical testing. The FDA on the other hand stringently regulates clinical trials. An IND needs to be submitted to the FDA along with all the preclinical data to seek permission for clinical testing, where the EMA most often only becomes involved when a company seeks authorization for a new drug after the development process. Another important difference is that the FDA carries out its own analysis of patient data to assess the reproducibility of the results, where the EMA requests more detailed information from the sponsor if something needs to be explored further. Lastly, a crucial difference is found when looking at marketing approval. The EMA does not grant marketing approval and will only give scientific opinions. In the US, one of the main reasons for a sponsor to get an NDA or BLA is to be able to market the application. This also gives the FDA the power to cancel a marketing approval if the product no longer meets the FDA specifications of safety and efficacy.[38, 34]

Despite the discussed differences, there is significant collaboration between the two regulatory agencies. There are collaborations on specific topics, called clusters, which focus on topic areas that have been identified as requiring intensified exchange of information and collaboration; for example, pharmacovigilance, medicines for cancer, and orphan medicines.




**Figure 2.** Translational path for a novel MI agent from bench-to-bedside. The development of a novel MI agent consists of several essential steps to ensure successful clinical translation and FDA approval. Here, an overview is given of these steps, from the clinical need, to development of a novel agent all the way to routine intra-operative use and the order in which these steps need to be taken.

## CLINICAL TRANSLATION PATHWAY

The path from an idea for an novel MI agent all the way to an approved agent the is routinely use in patient care is a time consuming and costly path. In this paper we aim to provide insight in this comprehensive process. Figure 2 provides a schematic representation.

## Target and agent discovery

The discovery process of a new MI agent often begins with the identification of a certain biological process unique to the tumor (such as a receptor or enzyme) that can function as a tumor-specific target. One of the main pitfalls prior to clinical translation is a non-functioning target or agent; thereby making this step one of the most important steps in developing a MI agent.[35] Biomarkers suitable for tumor-specific targeting must possess certain characteristics such as diffuse expression throughout tumor tissue (intra-tumor homogeneity), consistent expression within a given tumor type (inter-tumor homogeneity), and significant up-regulation compared to normal or surrounding tissues.[36] There are several potential approaches for a probe to interact with the target of interest. In 2008, Willmann et al.[3] discussed the direct approach where the probe directly binds to the target for assessing target expression. This is a sensitive and specific method, but if the target is not consistently expressed in multiple tumor types it would require development and regulatory approval for probes directed at each different target, which is a costly and time-consuming method. Alternatively, an enzyme could be targeted that is overexpressed in multiple cancer types by administration of an activatable MI agent.[3] From a regulatory point of view, MI agents applicable to a broad range of cancer types are likely to have a higher success rate in this phase of development since clinical translation needs to be as efficient as possible, and it is unlikely that tens-hundreds of different MI agents will be approved in a timely manner.

For tumor-specific optical imaging, the MI agent needs to consist of at least two entities; the targeting ligand and an optical signaling component.[1] There are numerous categories of available ligands that can be designed to target the marker of interest including small molecules, peptides, aptamers, antibodies, engineered protein fragments, and nanoparticles. All these MI agents have different toxicities, biodistribution, tumor interactions, and pharmacokinetic properties, but it is beyond the scope of this review to describe all of these molecules. Details are reviewed elsewhere.[1, 37] The signaling component consists of a fluorescent dye in case of optical imaging. Mostly used dyes are near-infrared (NIR) dyes due to increased depth penetration and the inability of the human eye to detect this signal. A good MI agent must possess high binding affinity, high selectivity for the target, excellent stability, lack of toxicity, emission in NIR window, and when possible, multiplexing capabilities. In the

ideal situation, you would have a MI agent that has rapid binding to the target and uptake by the tumor, urinary excretion compared to hepatic clearance, and persistent accumulation at the target site. Besides that, relatively simple and cost effective synthesis would enhance the clinical translation capacity. The use of approved drugs as MI agents, when combined to a signaling moiety, reduces the cost and risk of the early phase translation process due to known biodistribution, toxicity and targeting profile. However, when an existing approved agent is bioconjugated, (e.g., to a fluorescent dye), the FDA considers this agent to be a new entity, but may require less extensive non-clinical safety and toxicity studies compared to an entirely new compound.[38]

Currently, most clinical trials are performed using a MI agent that is injected intravenously into the patient. These agents reach all organs and therefore, toxicity and excretion are crucial elements. Now, topical agents become more of interest since both toxicity and clearance are negligible and reduced amounts are needed. However, these agents have not been introduced into clinical trials and therefore, focus of this paper will mainly be on intravenous MI agents.

## Non-clinical phase of development



Although imaging research remains dependent on preclinical animal models for initial testing, promising results in those models do not always translate well to human studies. However, until there is a more suitable model, preclinical imaging, and safety and toxicity data from animal studies are crucial to facilitate human testing. The goal of the nonclinical safety and toxicity testing is to assess toxicity in target organs, characterization of pharmacology, determination of a start dose and dose escalation scheme, and toxicity in relation to dose. Using body surface area or PK/PD modeling, the dose administered to animals can be used to calculate the starting dose in clinical trials.[39] Since MI agents are seen by the FDA as diagnostic tools toxicity should be mild, not to exceed a grade 1 reaction. Thus, nonclinical safety and toxicity studies should be designed to establish a wide safety margin. However, in this case were the clinical intended use is to guide invasive procedures, e.g. intra-operative oncologic resections, it is possible that the FDA would consider higher levels of allowable toxicity, if appropriately justified.

In this review paper we will describe the clinical translation pathway of a novel MI agent, targeting αvβ6, to clarify the entire process. This MI agent, R01-MG-IRDye800, will be used to detect pancreatic cancer and consists of a peptide and a fluorescent agent.[40, 41] R01-MG-IRDye800 counts as a New Molecular Entities (NME), and for these agents there are certain studies required before a Phase I trial can be started. Nonclinical studies help to facilitate the timely conduct of clinical trials and therefore timing of those studies is crucial (Table 1).[42] In this phase the ICH guidance requires analysis of systemic exposure achieved in animals and its relationship to dose level and the time course. The route of administration, extent of exposure, and metabolites must be taken into account.[43] For modification of an existing MI agent, such as fluorescently-labeled antibodies, the requirements for non-clinical safety and toxicity studies are variable, and in certain circumstances, very limited additional studies are required. When a change is made in the route of administration, dose or population of an already approved agent, the FDA will also do a case by case evaluation for the required nonclinical studies that are needed, therefore researches should search for early consultation with the FDA, to avoid performing unnecessary tests wasting time and resources.[44]

### *Product development plan*

When initiating a new product, the FDA encourages researchers and sponsors to provide a Target Product Profile (TPP) which outlines a comprehensive approval process and defines the clinical indication, to ensure focus during the approval process. A TPP is a development tool with a statement of the overall intended use of the MI agent, and provides information at a particular time in development while documenting the specific studies intended to support development. Ideally it can minimize late-stage drug development failure, increase the probability that safety and efficacy data are adequate, improve labeling content, and possibly decrease the total time to approval. Therefore, a TPP enables the sponsor to pursue the desired outcome in the most efficient manner.[45]

## eIND and IND submission

After obtaining the required non-clinical data, the next step is to apply for an IND. There are four types of INDs: exploratory IND (eIND), investigator IND, emergency use IND, and treatment IND. The IND application must contain

information regarding (i) animal pharmacology and toxicology, (ii) manufacturing information, and (iii) clinical protocol and investigator information. On the FDA website detailed information can be found on the complete IND application and the information required for submission. It goes beyond the scope of this article to describe all the specific information needed for an IND submission.[46] An overview of the FDA process after IND submission is provided in Figure 2. Once the IND is submitted, the investigator must wait 30 days before initiating the proposed clinical trial. The FDA will typically request additional information before the close of 30 days or issue a 'Study May Proceed Letter' to indicate their approval of the study. Subsequent changes or additions to the protocol (using the same agent) must be submitted to the FDA, but a 30-day waiting period is not necessary.

For most imaging studies early human data is desirable due to expected discrepancies between preclinical and clinical results. For that reason the FDA has developed the exploratory IND (eIND). This process makes it possible to test agents in clinical trials that involves a very limited human exposure (microdose administration), and has no diagnostic or therapeutic intent. This approach uses the concept that "the best model for man is man." An eIND study is intended to provide information on pharmacokinetics, -dynamics, and metabolism in humans and these studies are conducted before the dose escalation, safety and tolerance studies. Because eIND studies present fewer potential risks compared to traditional phase I studies, an eIND study in humans can be initiated with less preclinical support.[47, 48] After consultation of the FDA, a microdose study can even be conducted when the later intended dose is higher than a microdose, as is the case for optical imaging agents. It has been estimated that the time for drug development can be reduced by 12-18 months when using the microdosing technique compared to the traditional first-in-human studies.[49, 50] This can lead to a significant cost reduction, taking into account that a reduction of development time by 25% would lead to 16% cost savings.[51, 52] Time savings are not always realized without proper planning since after the eIND trial closes, the investigator will still need to submit a conventional IND for dose escalation studies. In case of our agent, an eIND was submitted for use of the peptide, R01-MG, as a radiolabeled PET-tracer. For the MI agent, R01-MG-IRDye800, an IND will be submitted with support of the data obtained from the eIND.

**Table 1.** Recommended nonclinical data needed for New Molecular Entities (NME) before the sponsor can proceed to the various phases of clinical translation.

| Study type | Before Phase 1 | Before Phase 2 | Before Phase 3 | Before NDA |
|---|---|---|---|---|
| **Safety pharmacology** | Major organs, and organ systems the drug is intended to visualize | | | |
| **Toxicokinetic pharmacokinetic** | Based on ICH guidance. The exposure in the animals should ideally equal or just exceed the maximum expected exposure (or known to be attained) in patients. | | | |
| **Expanded single-dose toxicity** | Expanded acute single dose (can potentially be combined with repeat dose toxicity) | | | |
| **Short-term (2 to 4 weeks) multiple toxicity** | | Short term repeat-dose toxicity | | |
| **Special toxicity** | Conduct as necessary; e.g. phototoxicity, route irritancy, blood compatibility | | | |
| **Genotoxicity** | In vitro, not required for microdose | Complete battery, not required for microdose | | |
| **Immunotoxicity** | | | May be needed based on molecular structure, biodistribution pattern, class concern, or clinical or nonclinical signal | |
| **Reproductive and developmental toxicity** | | | Limited studies are needed or waiver can be obtained | |
| **Drug interaction** | | | | As needed |

Compared to clinical studies using higher doses, non-clinical toxicity studies for microdose applications can be done with a single mammalian species to showcase safety instead of one rodent and one non-rodent species (Table 2). Obviating the need to test the agent in large animals or higher dosages significantly reduces costs and required time. There are also some potential weaknesses associated with the approach of microdosing, since there is still limited experience with this type of study, and it has not yet shown its real advantage with a sufficiently large number of MI agents. Secondly, a microdose may not predict the actual behavior of the dose that will be used in later clinical trials, giving a false sense of bioavailability and safety.

**Table 2.** Comparison of required preclinical studies for micro-dose initiated studies compared to traditional single dose preclinical studies.

| **Clinical** | | **Non-clinical** | | |
|---|---|---|---|---|
| **Dose to be administered** | **Start and maximum dose** | **Pharmacology** | **General toxicity study** | **Genotoxicity** |
| Micro-dose | Can be the same, but not allowed to exceed 100 µg | In vitro; target/receptor profiling.<br><br>Mode of action and/or effects characterization in PD model, to support human dose selection | Extended single dose toxicity study (in one species, by intended route of administration) and max of 1000-fold the clinical dose on mg/kg basis) | Not recommended |
| Single dose studies at subtherapeutic doses or into anticipated therapeutic range | Starting dose based on toxicity observed in most sensitive species. Maximum dose: can be up to ½ NOAEL, when relevant toxicity is anticipated to monitorable and reversible in human | In vitro; target/receptor profiling.<br><br>Mode of action and/or effects characterization in PD model, to support human dose selection.<br><br>Core battery of safety pharmacology (cardiovascular, CVS, respiratory system) | Extended single dose toxicity study in two species by intended route of administration with: toxicokinetics, hematology, clinical chemistry, necropsy, and histopathology data. | Ames assay |

(NOAEL = no observed adverse effect level) (PD = pharmacodynamics) (CVS = central nervous system)

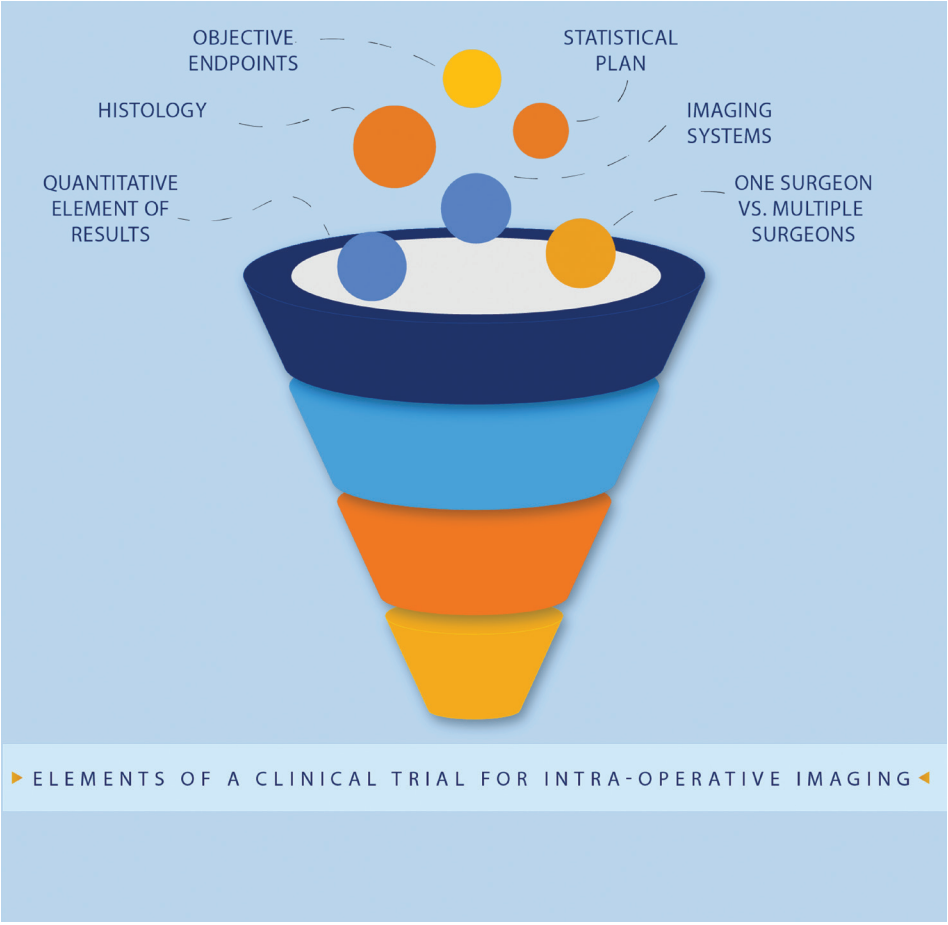



**Figure 3**. To conduct a well-designed clinical trial for intra-operative imaging, several elements need to be addressed. Here a graphic representation is given of the most important aspects that should be addressed, and need to be taken into account when designing a clinical trial for optical intra-operative imaging.

## Clinical translation

In contrast to clinical studies with the non-specific fluorescent dyes ICG and MB there are a limited number of clinical studies done with tumor-specific optical imaging agents.[53-59] Looking at these current clinical trials done for MI agents, most of these do not follow appropriate methodology for the different phases of clinical trials. Only five of 53 listed clinical trials for optical imaging in cancer done in the US and Europe, are done with the proper controls in a randomized controlled fashion (see overview Table S1).[9, 10] Optical imaging agents are mostly tested using open label single group assignment, which introduces

investigator bias since the investigational method is applied to all investigated subjects, without randomization, blinding or controls. Because the clinical utility in surgical optical imaging studies is often vague (surgeon's judgment) and has substantial variability between surgeons and by the same surgeon, it is difficult to objectively prove the benefit of optical imaging in clinical trials for regulatory approval. This emphasizes the need for creative study designs that will show patient benefit necessary to attain regulatory approval without being cost-prohibitive. Ultimately, the studies need to address that the imaging information will affect clinical care immediately since the information is available in real time.

The use of 5-aminolevulinic acid (5-ALA) in the surgery of malignant glioma was one of the first "proof-of-principle" explorations to confirm that intra-operative optical imaging could be used to improve surgical resections.[60] Stummer et al. showed in a randomized clinical trial from 17 centers in Germany with 322 patients that the use of 5-ALA enables more complete resections of contrast-enhancing tumors, leading to improved progression-free survival in patients with malignant glioma compared to the standard of care white light resections.[33] The primary endpoints of this study were the number of patients without contrast-enhancing tumor on early MRI (i.e., that obtained within 72 h after surgery) and 6-month progression-free survival as assessed by MRI. Secondary endpoints were volume of residual tumor on postoperative MRI, overall survival, neurological deficit, and toxic effects.[33] Clinically relevant endpoints that show benefit are necessary for FDA approval, and subsequently to payers who will want to see added value.



### *Elements of an optical imaging trial*

Clinical trials for intra-operative imaging are unique is a sense that certain elements are only applicable for these kind of trials. Below, several crucial elements of a clinical trial for intra-operative imaging are discussed (see figure 3). In addition, it is important to recognize that surgeons typically operate using pattern recognition and experience. Therefore, MI agents should be considered as adjunct to clinical judgement as an additional source of information – just as abnormalities on an anatomical image are placed into the context of the disease and the patient.

### *Endpoints*

During the design of clinical trials, endpoints need to align with the proposed labeling indication which is the desired marketing application. The FDA works with a risk-benefit approach so when the MI agent contains more risk, more benefit needs to be shown. To gain FDA approval for a NDA, the study needs to show direct benefit to the patient or intermediate clinical endpoints that have been shown to predict clinical benefit. For example, if the use of R01-MG-IRDye800 can reduce positive surgical margins, and since positive margins are known to correlate with poor clinical outcome, that would likely be sufficient to demonstrate clinical benefit.[22] The same is true for decreased re-operation rate to re-excise breast cancer, or reduced local recurrence in pancreatic cancer. Clinical endpoints in phase II trials should be chosen to mirror the anticipated phase III study so that appropriate power calculations can be established. Furthermore, showing clinical patient benefit at an early stage helps to fund more expensive phase III trials, where the more comprehensive and clinically relevant endpoints are needed.[61]

### *Statistical design*

For early phase trials sample size justification could range from a formal powered sample size based on clinical outcomes to a sample size with the main justification that the sample size is based on feasibility. The sample size will increase with smaller α and increase for a larger power.[60] When the main aim of the study is to determine feasibility, determining the actual sample size is difficult. However, for situations where the intention is that later, more definitive, studies may be carried out, the proper sample size to start with is 12 per group.[62] The ICH states that the number of subjects in a clinical trial should always be large enough to provide a reliable answer to the questions addressed. This number is usually determined by the primary objective of the trial. If the sample size is determined on some other basis, as in this case for feasibility studies, this should be made clear and justified.[63] For an extensive elaboration on statistical principles for clinical trials, please also see the FDA guidelines.[63]

### *Role of histology*

In studies in which MI agents are used to identify cancer, histology is crucial to determine the successful targeting of the cancer by the MI agent. Pathohistological assessment is the gold standard to determine whether

resected tissue is indeed tumor tissue and these results are correlated to the fluorescent signal. The optimal method for doing this correlation is to compare histologically confirmed tumor and fluorescence on the same microscopy slide.[64] Unfortunately, in this case the gold standard is not perfect, since pathologic examination is prone to sampling error. If the tissue sectioning process does not successfully capture the tumor (in a 5 um slice) on a glass slide, the tumor can be missed. In a study by Rosenthal et al, using cetuximab-IRDye800 in head and neck cancer, it was seen that 8% of lymph nodes were called negative by histology but positive by fluorescence. These were investigated further and found to contain cancer.[65] Furthermore, it also needs to be confirmed that the MI agent targets the appropriate biomarker by performing immunohistochemical analysis. Therefore, in all of these clinical trials, the *ex vivo* investigation of the tissue should play an important role.

### *Imaging systems*

Imaging systems are essential in optical imaging trials, and especially the difference between systems is important. The currently available imaging systems all have their own sensitivity, dynamic range, and wavelength variation. For now, in multicenter studies the same camera should be used until it is proven that the systems operate sufficiently similar, as is the case with PET devices. Imaging systems used in clinical trials need to be chosen based upon performance standards needed for that indication. In addition, issues around calibration, validation, and interpretation need to be established before a specific imaging system is picked to be used in a trial.[66]



### *Quantitative element*

Currently, a major problem in optical imaging trials is the lack of a quantitative element compared to PET imaging trials. Quantitative results are needed to generate objective results and convince the regulatory agencies. For now, the field has mostly focused on generating images, showing fluorescent signal at the position of the tumor. With the described differences in imaging systems, those images are not comparable between different trials and it is challenging to place these results in the appropriate context. Currently, more groups are investigating the more quantitative element of optical imaging.[67]

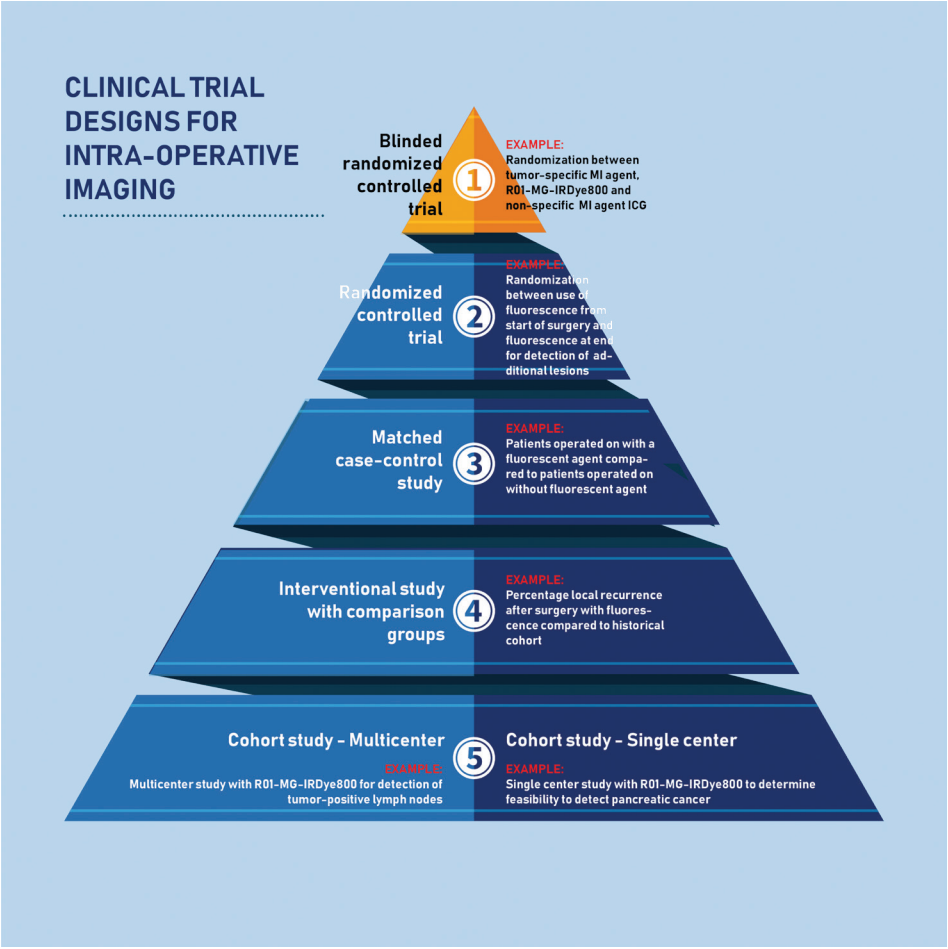



**Figure 4.** The design of a clinical trial determines the validity of the generated data. Here, a schematic representation is provided of the different trial designs that can be used for intra-operative imaging trials. On top of the pyramid the trial that generates the most rigorous data and can be used to show patient benefit: the blinded randomized controlled trial. At the bottom the trial that generates less rigorous data but can be used to show efficacy: the cohort study, either in multi- or single center fashion. All trial designs are accompanied by an example based on the pancreatic cancer MI agent.

### *Single surgeon study to multicenter study*

Another elements that needs to be taken into account in surgical clinical trials is the difference in surgical technique and experience between the different surgeons participating in the trial. In phase I trials, the decision to use only one surgeon could improve the reliability of feasibility data. However, multicenter studies with numerous amounts of surgeons are needed to show that the

promising results from early phase trials persist and that eventually wide-spread use is justified.

## CLINICAL TRIAL DESIGNS

Clinical trials can be broadly divided into prospective and retrospective studies. In case of optical imaging studies the majority of studies will be prospective since the use of optical imaging with exogenous MI agents is a new phenomenon for which the patient needs to be injected with an investigational product. Only in case of clinical trials with the non-specific ICG, retrospective cohorts are described.[68] The use of an exogenous MI agent also means that optical imaging studies are always interventional studies. Different clinical trial designs can be placed in an hierarchy based on the generated scientific rigor (figure 4). Rigor is research is mostly defined using the criteria of validity, reliability, and objectivity.[69] Trials with high scientific rigor are mostly also challenging to perform. Here, we discuss the different trial designs applied to optical imaging trials, with an MI agent for the detection of pancreatic cancer to serve as an example.



### *Blinded randomized controlled trial*

Blind assessment ensures that treatment and analysis of outcomes are not biased. Also, the FDA requires that when studies are conducted with subjective endpoints to show efficacy, the evaluator of the results needs to be blinded. At this point, most optical imaging studies have relative subjective endpoints such as tumor-to-background ratio (TBR) to determine efficacy. TBR values are highly affected by the chosen background by the investigator and currently, no strict rules are set to determine what should be chosen as background. Therefore, blinding in optical imaging studies is important, yet difficult to achieve. In intra-operative cases as discussed here, the surgeon cannot be blinded for the imaging results. However, multiple blinded studies are performed in the field of surgery showing the possibility of this design, even in surgical trials. The most rigorous trial design would be a blinded RCT with two different agents of which one is the tumor-specific agent, R01-MG-IRDye800, and one the non-specific agent, ICG. Here, the surgeon, pathologist and investigator can be blinded. In addition, even without an second agent double blinding can be achieved in

optical imaging trials if the pathologist and evaluator are blinded for where in the tissue fluorescence was seen in the operating room.

According to the literature, double-blind randomized controlled trials (RCT) are assumed to be insusceptible to bias, and are therefore accepted as the gold standard for clinical trial designs.[70] However, there is also criticism regarding RCTs and its place above all other study designs in the hierarchy of trial designs.[71, 72] Despite these criticisms, for now the main consensus is that studies looking at therapeutic and/or diagnostic agents should be done in a randomized fashion. As is known, control groups and randomization ensure that the control and test group are identical on average and that only the test conditions differ, which improves validity of the results.[33, 73] One could argue that the limited sample size of most early stage optical clinical trials are not amendable to randomization. For these cases, non-random allocation methods have been proposed as an alternative to achieve statistical significance and distribute individuals better between groups in cases with a small sample size.[72]

### *Randomized controlled trial*

Even in cases where blinding is challenging there are several strategies to perform trials a randomized fashion – including comparing judgment of the surgeon prior to imaging and after exposure to the fluorescent imaging data. Patients could be randomized between starting the surgery with inspection using fluorescence and without. A difference in detected tumor-positive lymph nodes could for example be used as outcome measure in pancreatic cancer patients. These and other methods to mimic blinding are recognized by the FDA. For example, the use of placebo which is infused in some patients (not necessarily half) could serve as an excellent control for randomization.

Randomization in optical imaging trials for surgical procedures are complicated by the variation of the surgical procedure based on stage, regional disease, tumor size/location, and variable anatomy. Furthermore, surgical technique and skill sets differ between surgeons and there is often limited agreement between surgeons on how to send margins (from the patient or from the specimen). Finally, there is to be some expected difference in tumor biology heterogeneity and patient variability. One strategy to accommodate this variability is to have each patient, tumor and surgeon serve as their own control. In this case,

one compares the added value of the fluorescent imaging compared to a conventional image on the screen in the same procedure. This can especially well be performed in cases of minimally invasive surgery.

*Matched case-control study*

To achieve rigor results, all optical imaging studies should at least be done by using a control group even in early phases. Third in rank, behind the randomized design, matched case-control study could lead to important data. In this case one could choose to compare patients operated on with the fluorescent agent and patient without an fluorescent agent matched based on demographics and tumor characteristics. This cannot be performed in a blinded fashion, and randomization could potentially lead to unethical situations, but a matched case-control study can be performed. In pancreatic cancer studies overall survival or disease-free survival of both patient groups could be used as an endpoint, even as the amount of tumor-positive resection margins.

*Interventional study with comparison group*

As mentioned above, optical imaging studies are always investigational studies because an MI agent is injected into or applied onto the patient. Going down the pyramid, the next form for a clinical trial is a study where a comparison group is used without matching. In these cases, historical cohorts could be used to compare the new data. For example, the amount of detected tumor-positive lymph nodes or percentages local recurrence could be compared to results acquired over the past years in a hospital or a nation. The disadvantage of using historical cohorts is the mismatch between the compared groups, and potentially the influence of under or over reporting of the intended outcome.

*Multicenter cohort study*

The first multicenter clinical trials are conducted in the field of optical imaging, and currently even an international study is initiated. All these trials are cohort studies were all patients receive the agent, and no comparison is made. These studies are not fit to show benefit of this technique over the standard-of-care, and are mainly performed to proof feasibility. One could question if a large international multicenter study is needed just to show feasibility and if a comparison group would not dramatically improve the rigor of the scientific data coming from those kind of trials.

### *Single center cohort study*

On the bottom of the pyramid is the single center cohort study, were a novel agent is tested in one hospital. A significant amount of this type of studies are performed in the field of optical imaging to show safety and feasibility. For this purpose, this trial design is well-suited since a limited amount of patients are needed. However, one should question the external validity of this data, especially when the surgeries are performed by one surgeon only. The clinical relevance of the data generated in single center cohort studies could be improved when multiple surgeons are involved.

### *Other clinical trial approaches*

Specific to optical imaging, there are also certain clinical trial approaches only applicable to this type of trials, which do not fit the above mentioned standard classification. For example, an approach that could be used to mimic a controlled trial comparing intra-operative use of optical imaging to a standard-of-care surgery, is a trial where the surgery is performed only using white light and after the surgeon is finished, the NIR light is turned on and the fluorescence will show what is left behind. These lesions will be analyzed by pathology to determine the amount of additional lesions found.

## PHASES OF CLINICAL TRIALS

All the discussed trial designs can be applied to the different phases of clinical trials.

### *Phase IA: First-in-human studies, assessing safety and tolerability*

In contrast to microdose studies that are conducted to get information on pharmacokinetics, -dynamics, and metabolism in humans, phase IA studies of MI agents should start with testing the optical imaging agent in healthy volunteers or highly selected patients to determine safety and pharmacokinetic properties. For R01-MG-IRDye800 this first step will be taken in healthy volunteers. Healthy volunteers have several advantages over patients: first pharmacokinetics can be assessed in more detail, and second all observed effects can be contributed to the MI agent compared to patients who mostly have comorbidities and potential drug interactions. In phase IB, the safety and feasibility of a MI agent

is tested typically through a dose-escalation study. Pharmacodynamic studies and studies relating drug blood levels to imaging signal (PK/PD studies) may be conducted in healthy volunteer subjects or in patients with the target disease. The pharmacodynamic data are important to guide the dosing schedule and timing in later studies.[74] The pharmacologic requirements during clinical trials for MI agent development are divided into safety and efficacy goals. The safety thresholds for imaging agents are high since these agents are diagnostic tools and do no offer therapeutic advantage. The efficacy goal of early phase clinical trials should be to determine a "near optimal" dose - a process that is mostly completed in Phase II but should start at the first-in-human trial. For FDA, the definition of near-optimal is a dose regimen and imaging condition that are superior to alternatives. This will require the investigation of a dose escalation scheme with at least 3 cohorts, and the ability to answer if a higher dose will be better or if a lower dose will be sufficient. Furthermore, the optimal imaging time point of the MI agent (optimal time after injection of agent) should be considered.

### *Phase IB trials*

#### Dose-escalation studies

Most optical imaging Phase IB studies start with a dose-escalation and timing study. The goal of a dose-escalation study for optical imaging should be to establish the recommended dose and timing in phase II trials. The guiding principle is to avoid exposing too many patients to suboptimal doses while preserving safety and maintaining rapid accrual. A dose-escalation study has many components, including starting dose, dose increment, dose-escalation method, number of patients per dose level, specification of dose-limiting toxicity (DLT), and recommended dose for phase II trials. As for MI agents, it is unusual to include language regarding the maximum tolerated dose (MTD). There are broadly two designs that can be used for dose-escalation studies: the rule-based designs, which include the traditional 3+3 design and its variations, and the model-based designs.[75] For optical imaging, the rule-based design is the most applicable since the used dose is relatively low and therefore, DLT is not expected to be reached and there is no therapeutic effect to determine the optimal dose. In imaging studies, the 3+3 design focuses on identifying the lowest dose that will generate the optimal signal to noise ratio. In this design, the first cohort is treated at a starting dose that is considered to be safe based

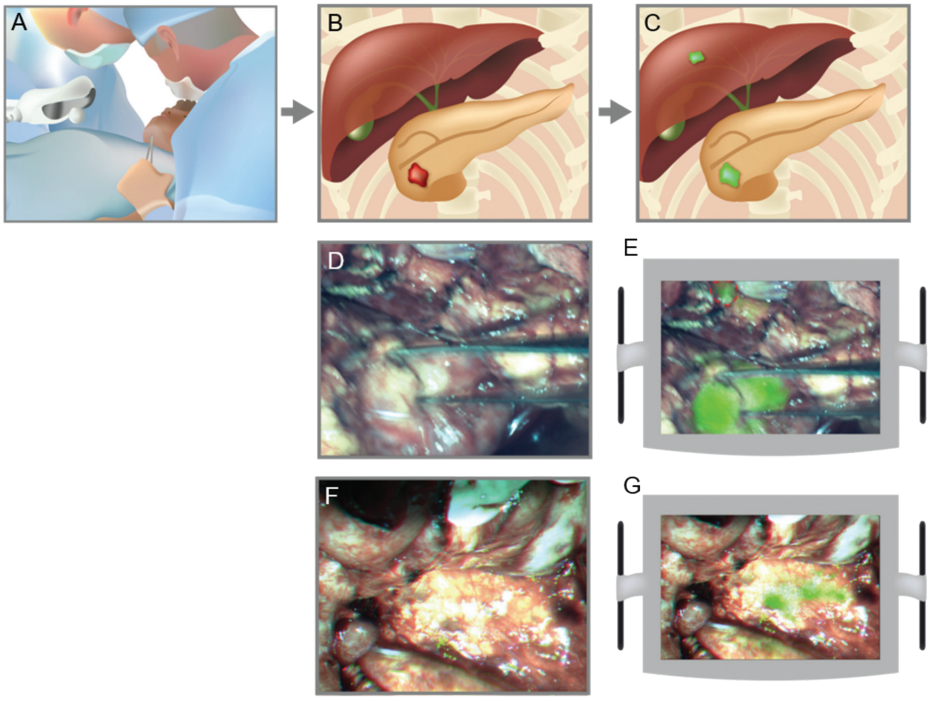



**Figure 5.** Detection of additional lesions in pancreatic cancer surgery. The detection of additional lesions with the use of NIR fluorescence is an endpoint that can be used to show efficacy of NIR fluorescent imaging during surgery. The MI agent is injected into the patient prior to surgery Here a schematic representation of this trial design is provided, with the assessment by surgeon (A) using white light (B), and afterwards identification of potential additional lesions on the screen when using NIR fluorescence (C). Clinical examples are provided of pancreatic cancer surgery, of both the primary tumor (D, white light, and E, NIR fluorescence) and lymph nodes (F, white light, and G, NIR fluorescence) using Cetuximab-IRDye800 targeting EGFR.

on extrapolation from animal toxicological data, and the subsequent cohorts are treated at increasing dose levels that have been fixed in advance.[76] The dose-escalation normally stops in imaging studies when either two patients in a cohort of three to six patients experience a DLT or when the higher dose level generates a signal to noise ratio equivalent to the lower cohort. For R01-MG-IRDye800 a 3+3 design is chosen with a fixed starting dose of 2 mg and increments up to 16 mg per patient. The most optimal cohort will be expanded by 3 patients.

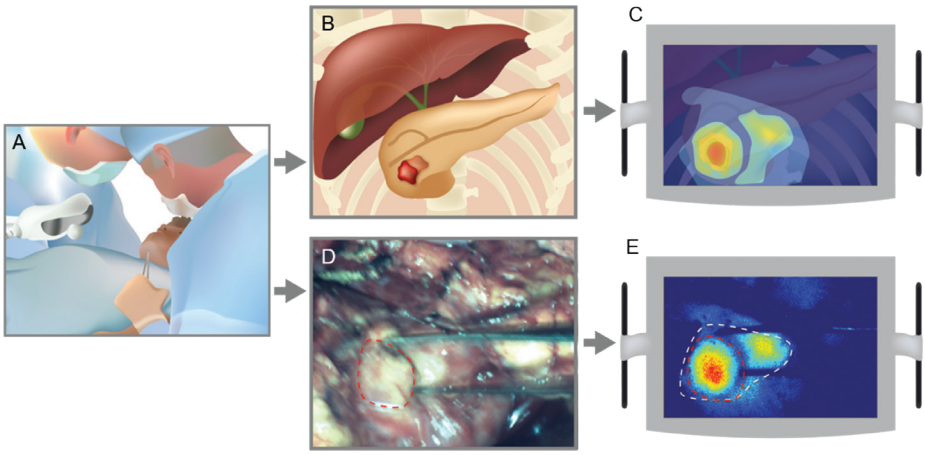



**Figure 6**. Assessment of resection margins. The assessment of resection margins with fluorescence is another method to show efficacy of fluorescence imaging during surgery. The MI agent is injected into the patient prior to surgery. Here a schematic representation of resection margin determination by the surgeon (A) is shown, using white light (B), and after the use of NIR fluorescence (C). Clinical examples are provided were the red dotted line is the resection margin determine using only white light (D), and the margin after assessment with NIR fluorescence (E, white dotted line). Here, additional resection will be performed based on the NIR fluorescence.



## Efficacy studies

Determining efficacy in optical imaging studies can be done in several ways. The most important assessment that needs to be done at this phase is to determine if fluorescence signals correlates with histological evidence of tumor. This is best accomplished during *ex vivo* imaging of the specimen and histopathologic analysis in combination with H&E stain. However, since this is an intra-operative technique, the primary clinical endpoints and efficacy assessments should be done in the operating room as well. In intra-operative setting there are two main methods to assess efficacy. In case of our R01-MG-IRDye800 agent, the primary endpoint to show efficacy is based on additional lesions found. This first method is explained in figure 5; one could let the surgeon assess the surgical field with standard white light for suspicious lesions and afterwards turn on the NIR fluorescent light to identify additional lesions. The second methods is shown in figure 6; here the surgeon needs to outline the intended resection margin based on white light assessment, and afterwards compare this outline to the outline determined when applying NIR fluorescence. This last method is beneficial in tumor types where the resection of too much healthy tissue

increased morbidity, such a head and neck and brain cancer. A disadvantage of both these methods are the missed potential lesions that are both not seen with white light and also not seen by the additional NIR fluorescence, since these lesions will not be assessed by pathology. However, until now there is not a method developed to assess these double false negative lesions.

### *Phase II trials*

The goal of phase II trials should be to acquire more proof for the benefit of the investigated imaging technique and MI agent in a larger, but homogeneous, patient population, and determine the dose and regimen for phase III trials. When conducting a phase II trial, it is important to note that at this point the agent still offers no real advantage to study subjects, and therefore, investigators need to ensure that standard of care procedures are maintained.[59] At the end of the phase II trials, the end-of-phase-II meeting is held with the FDA, which is considered the most important meeting for a sponsor. This meeting will determine whether or not the sponsor can initiate a phase III trial.

### *Phase III and Phase IV*

Phase III trials are conducted in a larger population to determine efficacy, benefit, and compare it to commonly used procedures. In this phase the added value of the optical imaging agent should be determined with clinically relevant endpoints. A great example of a properly conducted phase III trial for the use of optical imaging during surgery is the previously mentioned RCT conducted by Stummer et al. regarding the use of 5-ALA in glioma surgery.[33] Studies in phase III need to be blinded randomized controlled trials. However, as mentioned before, also the ICH guidelines and FDA encourage investigators to perform randomized, controlled trials to improve the validation of observations in earlier phases of investigation. After finishing the phase III study, the sponsor will submit a NDA application and have the pre-NDA meeting with the FDA to determine if the MI agent meets the criteria for a NDA or BLA. Phase IV trials are not necessary for approval of the MI agent, but are important for optimizing the agent in a large population. These trials look at the different effect of the imaging agent in various populations. Normally in this phase the side effects of long term use will also be determined, however that is not applicable for optical imaging agents since they mostly be one-time use.

## INDUSTRY AND ACADEMIC PARTNERSHIPS

It is generally accepted that academia can generate highly innovative products, but successful delivery to the market where it will benefit patients almost always requires working with an industry partner with the appropriate expertise. Working with public-private partnerships (PPPs) accelerates the clinical translation by combining the expertise and resources of universities and industry. For example, industry partners would provide the facilities for cGMP production of the imaging agents, imaging systems, and data handling, while the university and hospital network regulate the clinical trials. With this strategy all parties bring their own field of expertise, making the process more efficient and providing greater quality of the achieved product.[62] These kind of collaborations can also be achieved by international partnerships between different academic centers with several advantages. In the case of R01-MG-IRDye800, a collaboration between Stanford University and Leiden University Medical Center ensured timely and efficient clinical translation of this novel MI agent due to the unique expertise of both centers. In addition, collaboration between industry and universities can also result in new hypothesis generating research, such as converting failed therapeutic drugs into MI agents. Chemical libraries underlying a developed drug can also provide a wealth of information for potential imaging agents.[3] Additionally, many components of drug and imaging agent development are similar, and therefore the exchange of knowledge and experience are crucial for an efficient clinical translation process.



## CONCLUSION

In summary, the use of optical molecular imaging for tumor-specific identification of cancer is an emerging field with the potential to change the way medicine is practiced. it is not surprising then that the clinical development and approval process of these agents has recently received considerable attention. However, this technique will only be approved by the FDA in patient care if the field can identify clinical settings that will provide clear clinical utility and patient benefit in well-designed clinical trials. Although the potential of tumor-specific optical imaging is yet to be realized, several early-phase clinical trials have already shown safety and efficacy in specific cancer types and tumor-specific intraoperative optical imaging is likely to play an important role in the identification and treatment of cancer in the near future.

# REFERENCES


1. James, M.L. and S.S. Gambhir, A molecular imaging primer: modalities, imaging agents, and applications. Physiol Rev, 2012. 92(2): p. 897-965.
2. Russell, WMS, and Burch, RL. The principles of humane experimental technique. 1e edition. Methuen & Co. Ltd, London (1959)
3. Willmann, J.K., et al., Molecular imaging in drug development. Nat Rev Drug Discov, 2008. 7(7): p. 591-607.
4. Iagaru A, Chen X, Gambhir SS. Molecular imaging can accelerate anti-angiogenic drug development and testing. Nat Clin Pract Oncol. 2007 Oct;4(10):556-7. Epub 2007 Aug 28.
5. Eschmann, S.M., et al., 18F-FDG PET for assessment of therapy response and preoperative re-evaluation after neoadjuvant radio-chemotherapy in stage III non-small cell lung cancer. Eur J Nucl Med Mol Imaging, 2007. 34(4): p. 463-71.
6. Levine, E.A., et al., Predictive value of 18-fluoro-deoxy-glucose-positron emission tomography (18F-FDG-PET) in the identification of responders to chemoradiation therapy for the treatment of locally advanced esophageal cancer. Ann Surg, 2006. 243(4): p. 472-8.
7. Ware, R.E., et al., Usefulness of fluorine-18 fluorodeoxyglucose positron emission tomography in patients with a residual structural abnormality after definitive treatment for squamous cell carcinoma of the head and neck. Head Neck, 2004. 26(12): p. 1008-17.
8. Rudin, M. and R. Weissleder, Molecular imaging in drug discovery and development. Nat Rev Drug Discov, 2003. 2(2): p. 123-31.
9. NIH US National Library of Medicine ClinicalTrials.gov. Website. www.clinicaltrials.gov
10. EU Clinical Trials Register. Website. www.clinicaltrialsregister.eu
11. Jaffer, F.A. and R. Weissleder, Molecular imaging in the clinical arena. Jama, 2005. 293(7): p. 855-62.
12. Reichert, J.M., Trends in development and approval times for new therapeutics in the United States. Nat Rev Drug Discov, 2003. 2(9): p. 695-702.
13. DiMasi, J.A., Innovating by developing new uses of already-approved drugs: trends in the marketing approval of supplemental indications. Clin Ther, 2013. 35(6): p. 808-18.
14. Gassman O, Reepmeyer G, Zedtwitz M. Leading Pharmaceutical Innovation: Trends and Drivers for Growth in the Pharmaceutical Industry. 2nd. New York: Springer-Verlag Berlin Heidelberg; 2008. DOI: 10.1007/978-3-540-77636-9
15. Kola, I. and J. Landis, Can the pharmaceutical industry reduce attrition rates? Nat Rev Drug Discov, 2004. 3(8): p. 711-5.
16. Moreno, L. and A.D. Pearson, How can attrition rates be reduced in cancer drug discovery? Expert Opin Drug Discov, 2013. 8(4): p. 363-8.
17. Seddon, B.M. and P. Workman, The role of functional and molecular imaging in cancer drug discovery and development. Br J Radiol, 2003. 76 Spec No 2: p. S128-38.
18. Nunn, A.D., The cost of developing imaging agents for routine clinical use. Invest Radiol, 2006. 41(3): p. 206-12.
19. Quintiles IMS Instutite. Medicines Use and Spending in the U.S. A Review of 2016 and Outlook to 2021.
20. Innovation or Stagnation: Challenge and Opportunity on the Critical Path to New Medical Products. 2004. Food and Drug Administration Web site. http://www.fda.gov/oc/initiatives/criticalpath/whitepaper.html
21. Rosenthal EL, Warram JM, de Boer E, Basilion JP, Biel MA, Bogyo M, Bouvet M, Brigman BE, Colson YL, DeMeester SR, Gurtner GC, Ishizawa T, Jacobs PM, Keereweer S, Liao JC, Nguyen QT, Olson JM, Paulsen KD, Rieves D, Sumer BD, Tweedle MF, Vahrmeijer AL, Weichert JP, Wilson BC, Zenn MR, Zinn KR, van Dam GM. Successful Translation of Fluorescence Navigation During Oncologic Surgery: A Consensus Report. J Nucl Med. 2016 Jan;57(1):144-50. PMID: 26449839
22. Tummers WS, Warram JM, Tipirneni KE, Fengler J, Jacobs P, Shankar L, Henderson L, Ballard B, Pogue BW, Weichert JP, Bouvet M, Sorger J, Contag CH, Frangioni JV, Tweedle MF, Basilion JP, Gambhir SS, Rosenthal EL. Regulatory Aspects of Optical Methods and Exogenous Targets for Cancer Detection. Cancer Research 2017. (in press)

23. Guidance: Investigational New Drug Applications for Positron Emission Tomography (PET) Drugs. U.S. Department of Health and Human Services Food and Drug Administration, Center for Drug Evaluation and Research (CDER). U.S. Food and Drug Administration Web site. http://www.fda.gov/downloads/drugs/.../guidances/ucm291573.pdf (2012)
24. Pogue BW, Paulsen KD, Samkoe KS, Elliott JT, Hasan T, Strong TV, Draney DR, Feldwisch J. Vision 20/20: Molecular-guided surgical oncology based upon tumor metabolism or immunologic phenotype: Technological pathways for point of care imaging and intervention. Med Phys. 2016 Jun;43(6):3143
25. Chi C, Du Y, Ye J, Kou D, Qiu J, Wang J, Tian J, Chen X. Intraoperative imaging-guided cancer surgery: from current fluorescence molecular imaging methods to future multi-modality imaging technology. Theranostics. 2014 Aug 15;4(11):1072-84.
26. Combination Products. U.S. Food and Drug Administration Web site. www.fda.gov/CombinationProducts/default.htm.
27. Code of Federal Regulations, title 21, chapter I, 21 CFR §3.2. U.S. Food and Drug Administration Web site. http://www.ecfr.gov/cgi-bin/text-idx?SID=dec14a8c39e51510260360b91a916921&mc=true&tpl=/ecfrbrowse/Title21/21cfr3_main_02.tpl (2016).
28. U.S. Food and Drug Administration Web site. www.fda.gov
29. Beishon M. Approval rating: how do the EMA and FDA compare? Cancerworld. January-February 2014, 12-17.
30. The International Council for Harmonisation of Technical Requirements for Pharmaceuticals for Human Use (ICH) Web site. www.ich.org
31. Hirako M, McAuslane N, Salek S, et al. A Comparison of the Drug Review Process at Five International Regulatory Agencies. Drug Information Journal, Vol. 41, pp. 291–308, 2007
32. Trotta F, Leufkens HG, Schellens JH, Laing R, Tafuri G. Evaluation of oncology drugs at the European Medicines Agency and US Food and Drug Administration: when differences have an impact on clinical practice. J Clin Oncol. 2011 Jun 1;29(16):2266-72.
33. Stummer W, Pichlmeier U, Meinel T, Wiestler OD, Zanella F, Reulen HJ; ALA-Glioma Study Group. Fluorescence-guided surgery with 5-aminolevulinic acid for resection of malignant glioma: a randomised controlled multicentre phase III trial. Lancet Oncol. 2006 May;7(5):392-401
34. European Medicines Agency Web site. www.ema.europa.eu
35. Hughes, J.P., et al., Principles of early drug discovery. Br J Pharmacol, 2011. 162(6): p. 1239-49.
36. van Oosten, M., et al., Selecting Potential Targetable Biomarkers for Imaging Purposes in Colorectal Cancer Using TArget Selection Criteria (TASC): A Novel Target Identification Tool. Transl Oncol, 2011. 4(2): p. 71-82.
37. Warram JM, de Boer E, Sorace AG, Chung TK, Kim H, Pleijhuis RG, van Dam GM, Rosenthal EL. Antibody based imaging strategies for cancer. Cancer Metastasis Rev. 2014 Sep;33(2-3):809-22.
38. Scheuer, W., et al., Drug-based optical agents: infiltrating clinics at lower risk. Sci Transl Med, 2012. 4(134): p. 134ps11.
39. Reagan-Shaw S, Nihal M, Ahmad N. Dose translation from animal to human studies revisited. FASEB J. 2008 Mar;22(3):659-61. Epub 2007 Oct 17.
40. Kimura RH, Teed R, Hackel BJ, et al. Pharmacokinetically stabilized cystine knot peptides that bind alpha-v-beta-6 integrin with single-digit nanomolar affinities for detection of pancreatic cancer. Clin Cancer Res. 2012 Feb 1;18(3):839-49
41. Tummers WS, Kimura RH, Abou-Elkacem L, et al. Development and Preclinical Validation of a Cysteine Knottin Peptide Targeting Integrin αvβ6 for Near-infrared Fluorescent-guided Surgery in Pancreatic Cancer. Clin Cancer Res. 2018 Apr 1;24(7):1667-1676
42. Guidance for Industry: M3(R2) Nonclinical Safety Studies for the Conduct of Human Clinical Trials and Marketing Authorization for Pharmaceuticals. U.S. Food and Drug Administration Web site. http://www.fda.gov/downloads/Drugs/GuidanceComplianceRegulatoryInformation/Guidances/UCM073246.pdf (2010).

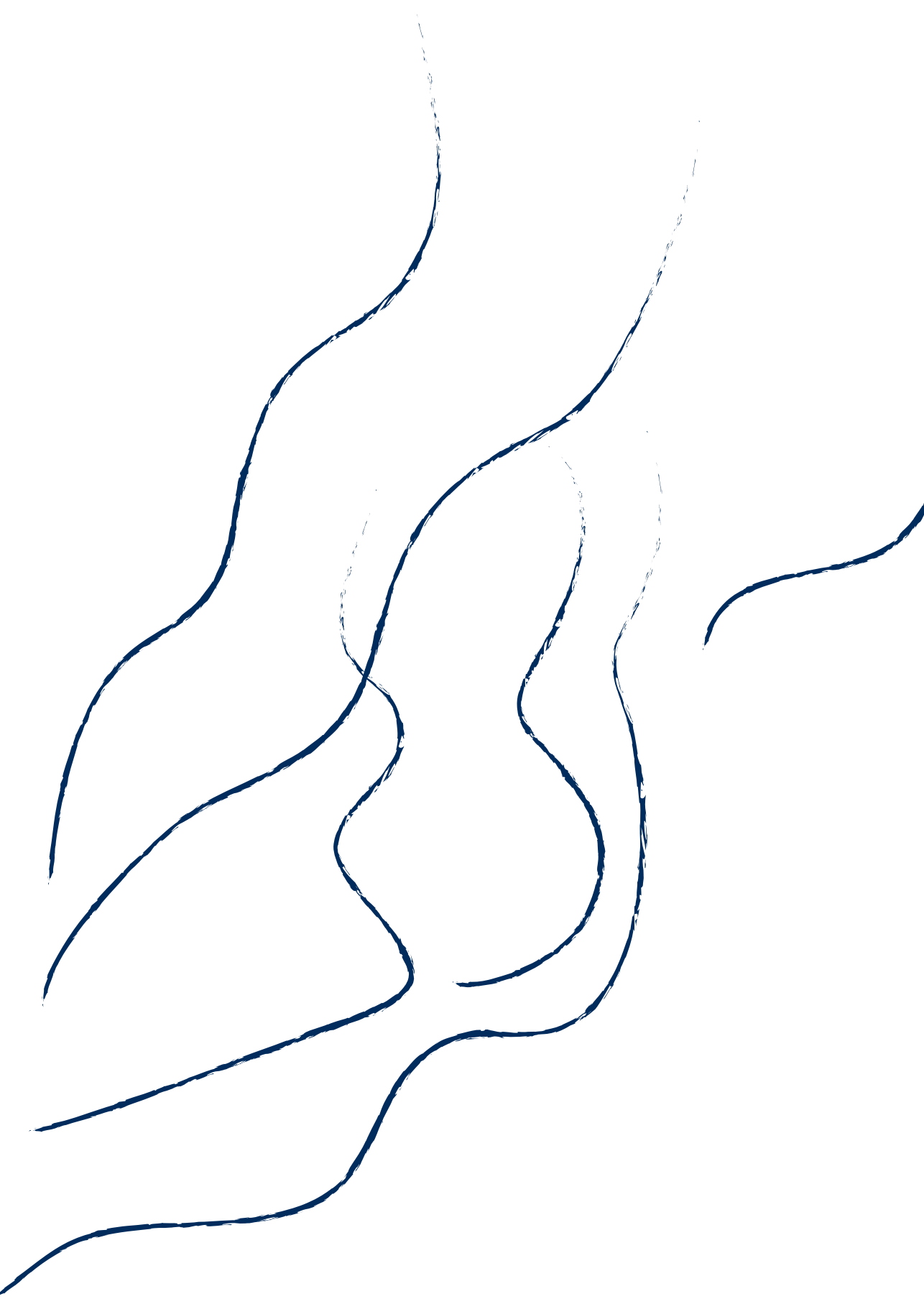
43. ICH harmonised tripartite guideline. Note for guidance on toxicokinetics: The assessment of systemic exposure in toxicity studies, S3A. ICH web site. http://www.ich.org/fileadmin/Public_Web_Site/ICH_Products/Guidelines/Safety/S3A/Step4/S3A_Guideline.pdf (1994)
44. Guidance for Industry: Developing Medical Imaging Drug and Biological Products. Part 1: Conducting Safety Assessments. U.S. Food and Drug Administration Web site. http://www.fda.gov/downloads/Drugs/.../Guidances/ucm071600.pdf (2004)
45. Guidance for industry: and Review Staff Target Product Profile — A Strategic Development Process Tool. U.S. Food and Drug Administration Web site. http://www.fda.gov/downloads/drugs/guidancecomplianceregulatory information/guidances/ucm080593.pdf (2007)
46. U.S. Food and Drug Administration Web site. http://www.fda.gov/Drugs/DevelopmentApprovalProcess/HowDrugsareDevelopedand Approved/ApprovalApplications/InvestigationalNew DrugINDApplication/default.htm
47. Guidance for Industry, Investigators, and Reviewers. Exploratory IND Studies. U.S. Food and Drug Administration Web site. https://www.fda.gov/downloads/drugs/.../guidances/ucm078933.pdf (2006)
48. Position paper on non-clinical safety studies to support clinical trials with a single microdose: CPMP/SWP/2599/02/Rev1. Committee for Medical Products for Human Use, EMA. (2004)
49. Garner, R.C., Less is more: the human microdosing concept. Drug Discov Today, 2005. 10(7): p. 449-51.
50. Wilding, I.R. and J.A. Bell, Improved early clinical development through human microdosing studies. Drug Discov Today, 2005. 10(13): p. 890-4.
51. DiMasi, J.A., The value of improving the productivity of the drug development process: faster times and better decisions. Pharmacoeconomics, 2002. 20 Suppl 3: p. 1-10.
52. VanBrocklin HF. Radiopharmaceuticals for Drug Development: United States Regulatory Perspective. Current Radiopharmaceuticals (2008) 1: 2-6
53. Rosenthal EL, Warram JM, de Boer E, Chung TK, Korb ML, Brandwein-Gensler M, Strong TV, Schmalbach CE, Morlandt AB, Agarwal G, Hartman YE, Carroll WR, Richman JS, Clemons LK, Nabell LM, Zinn KR. Safety and Tumor Specificity of Cetuximab-IRDye800 for Surgical Navigation in Head and Neck Cancer. Clin Cancer Res. 2015 Aug 15;21(16):3658-66.
54. van Dam GM, Themelis G, Crane LM, Harlaar NJ, Pleijhuis RG, Kelder W, Sarantopoulos A, de Jong JS, Arts HJ, van der Zee AG, Bart J, Low PS, Ntziachristos V. Intraoperative tumor-specific fluorescence imaging in ovarian cancer by folate receptor-α targeting: first in-human results. Nat Med. 2011 Sep 18;17(10):1315-9.
55. Tummers QR, Hoogstins CE, Gaarenstroom KN, et al. Intraoperative imaging of folate receptor alpha positive ovarian and breast cancer using the tumor specific agent EC17. Oncotarget. 2016;7(22):32144-32155
56. Hoogstins CE, Tummers QR, Gaarenstroom KN, de Kroon CD, Trimbos JB, Bosse T, Smit VT, Vuyk J, van de Velde CJ, Cohen AF, Low PS, Burggraaf J, Vahrmeijer AL. A Novel Tumor-Specific Agent for Intraoperative Near-Infrared Fluorescence Imaging: A Translational Study in Healthy Volunteers and Patients with Ovarian Cancer. Clin Cancer Res. 2016 Jun 15;22(12):2929-38. doi: 10.1158/1078-0432.CCR-15-2640.
57. Burggraaf J, Kamerling IM, Gordon PB, Schrier L, de Kam ML, Kales AJ1, Bendiksen R, Indrevoll B, Bjerke RM, Moestue SA, Yazdanfar S, Langers AM, Swaerd-Nordmo M, Torheim G, Warren MV, Morreau H, Voorneveld PW, Buckle T, van Leeuwen FW, Ødegårdstuen LI, Dalsgaard GT, Healey A, Hardwick JC. Detection of colorectal polyps in humans using an intravenously administered fluorescent peptide targeted against c-Met. Nat Med. 2015 Aug;21(8):955-61. doi: 10.1038/nm.3641
58. Boogerd LSF, Hoogstins CES, Schaap DP, et al. Safety and effectiveness of SGM-101, a fluorescent antibody targeting carcinoembryonic antigen, for intraoperative detection of colorectal cancer: a dose-escalation pilot study. Lancet Gastroenterol Hepatol. 2018 Jan 17.

59. Tummers WS, Miller SE, Teraphongphom NT, et al. Intraoperative Pancreatic Cancer Detection using Tumor-Specific Multimodality Molecular Imaging. Ann Surg Oncol. 2018 Apr 17.
60. Rosenthal EL, Warram JM, Bland KI, Zinn KR. The status of contemporary image-guided modalities in oncologic surgery. Ann Surg. 2015 Jan;261(1):46-55.
61. Tipirneni KE, Warram JM, Moore LS, et al. Oncologic Procedures Amenable to Fluorescence-guided Surgery. Ann Surg. 2017 Jul;266(1):36-47.
62. Julious SA, Tan SB, and Machin D. An Introduction to Statistics in Early Phase Trials, edited by Steven Julious, et al., John Wiley & Sons, Incorporated, 2010. ProQuest Ebook Central
63. Guidance for Industry: E9 Statistical Principles for Clinical Trials. U.S. Food and Drug Administration Web site. https://www.fda.gov/downloads/drugs/guidancecompliance regulatoryinformation/guidances/ucm073137.pdf (1998)
64. de Boer E, Warram JM, Tucker MD, Hartman YE, Moore LS, de Jong JS, Chung TK, Korb ML, Zinn KR, van Dam GM, Rosenthal EL, Brandwein-Gensler MS. In Vivo Fluorescence Immunohistochemistry: Localization of Fluorescently Labeled Cetuximab in Squamous Cell Carcinomas. Sci Rep. 2015 Jun 29;5:10169.
65. Rosenthal EL, Moore LS, Tipirneni K, et al. Sensitivity and Specificity of Cetuximab-IRDye800CW to Identify Regional Metastatic Disease in Head and Neck Cancer. Clin Cancer Res. 2017 Aug 15;23(16):4744-4752
66. Pogue BW, Paulsen KD, Samkoe KS, et al. Vision 20/20: Molecular-guided surgical oncology based upon tumor metabolism or immunologic phenotype: Technological pathways for point of care imaging and intervention. Med Phys. 2016 Jun;43(6):3143-3156.
67. Koch M, de Jong JS, Glatz J, et al. Threshold Analysis and Biodistribution of Fluorescently Labeled Bevacizumab in Human Breast Cancer. Cancer Res. 2017 Feb 1;77(3):623-631.
68. Handgraaf HJ, Boogerd LS, Höppener DJ, et al. Long-term follow-up after near-infrared fluorescence-guided resection of colorectal liver metastases: A retrospective multicenter analysis. Eur J Surg Oncol. 2017 Aug;43(8):1463-1471.
69. Tobin GA, Begley CM. Methodological rigour within a qualitative framework. J Adv Nurs. 2004 Nov;48(4):388-96.
70. Rorty, R. Philosophy and the mirror of Nature. Princeton: Princeton University Press, 1979
71. Grossman J, Mackenzie FJ. The randomized controlled trial: gold standard, or merely standard? Perspect Biol Med. 2005 Autumn;48(4):516-34
72. Kaptchuk TJ. The double-blind, randomized, placebo-controlled trial: gold standard or golden calf? J Clin Epidemiol. 2001 Jun;54(6):541-9
73. Kunz R, Oxman AD. The unpredictability paradox: review of empirical comparisons of randomised and non-randomised clinical trials. BMJ. 1998 Oct 31;317(7167):1185-90
74. ICH Guidelines: Topic E 8 General Considerations for Clinical Trials. European Medicines Agency Web site. http://www.ema.europa.eu/docs/en_GB/document_library/Scientific_guideline/2009/09/WC500002877.pdf (1998)
75. Le Tourneau C, Lee JJ, Siu LL. Dose escalation methods in phase I cancer clinical trials. J Natl Cancer Inst. 2009 May 20;101(10):708-20.
76. Storer BE. Design and analysis of Phase I clinical trials. Biometrics, Vol. 45, No. 3 (Sep., 1989), 925-937.
77. Agdeppa, E.D. and M.E. Spilker, A review of imaging agent development. AAPS J. 2009 Jun;11(2):286-99.



Part | IV

# Clinical Application of Targeted Molecular Imaging for Pancreatic Cancer



Chapter | 9

# Clinical Translation of Integrin αvβ6 Cystine Knot Positron Emission Tomography (PET) Tracers

[1]Richard H. Kimura, [1†]Willemieke Tummers, [2†]Ling Wang, [1†]Bin Shen, [2†]Li Huo, [3†]Fabian V. Filipp, [1]Lotfi Abou-Elkacem, [1]Lucia Baratto, [1]Frezghi Habte, [1]Rammohan Devulapally, [1]Timothy H. Witney, [1]Yan Cheng, [1]Thomas Haywood, [3]Suhas Tikole, [1]Subhendu Chakraborti, [4]Jay Nix, [5]Christopher A. Bonagura, [1]Negin Hatami, [4]Brendan C. Visser, [4]George A. Poultsides, [4]Jeffrey Norton, [1]Arutselvan Natarajan, [1]Ohad Ilovich, [1]Shyam Srinivas, [1]Ananth Srinivasan, [1]Ramasamy Paulmurugan, [1]Juergen Willmann, [1]Frederick T. Chin, [1]Zhen Cheng, [1]Andrei Iagaru, [2]Fang Li, [6§1]Sanjiv S. Gambhir

[1]Department of Radiology, Molecular Imaging Program at Stanford (MIPS), Stanford University, Stanford CA 94305, USA. [2]Department of Nuclear Medicine, Peking Union Medical College, Beijing 100730, China. [3]Department of Quantitative Systems Biology, University of California Merced, Merced CA 95343, USA. [4]Department of Surgery, Stanford University, Stanford CA 94305, [5]Advanced Light Source, Lawrence Berkeley National Laboratory, Berkeley CA 94720 USA. [6]Art Robbins Instruments, Sunnyvale CA 94089, USA.

[†]Equal Contribution. [§]Corresponding Author.

* *Data presented at World Molecular Imaging Conference 2017, Philadelphia*

## ABSTRACT

**Background**: This study describes the bench-to-bedside process of developing, validating and translating a novel PET tracer for detection of cancer through molecular recognition of integrin αvβ6 receptors. Integrin αvβ6 is an extracellular matrix (ECM) protein that is dysregulated and overexpressed in pancreatic cancer.

**Methods:** A cystine knot peptide was engineered to selectively bind integrin αvβ6. Preclinical mouse models guided PET tracer development providing feedback for the optimization of tracer pharmacokinetics, maximization of tumor uptake and minimization of background uptake in normal tissues. Toxicity of the non-radioactive reference standard, [$^{19}$F]FP-R$_0$1-MG, was evaluated in a rat model.

**Results:** The lead PET tracer, [$^{18}$F]FP-R$_0$1-MG, was produced under cGMP guidelines and evaluated in 5 healthy human volunteers. Upon verification of its safety, [$^{18}$F]FP-R$_0$1-MG was administered to pancreatic cancer patients and compared to [$^{18}$F]FDG PET in the same patient. [$^{18}$F]FP-R$_0$1-MG was produced in high specific activity (~5000 mCi/μmol) and purity (99%). In mouse models, tumor, liver, muscle and kidney uptake was ~5%ID/g, ~1%ID/g, ~0.5%ID/g and ~30%ID/g, respectively, 1 hr p.i.. Tumor-to-muscle ratio was ~ 5:1 at 1 hr p.i. The reference standard [$^{19}$F]FP-R$_0$1-MG did not produce any toxic effects in a rat model at 250x the imaging dose needed for human studies normalized to mass of subject. Upon clinical translation, [$^{18}$F]FP-R$_0$1-MG was well tolerated in 5 healthy human volunteers. The tracer cleared via the kidneys, which were determined to be the dose limiting organ. Next, [$^{18}$F]FP-R$_0$1-MG was evaluated for detection of pancreatic cancer. Tumor uptake was rapid and homogeneous. In contrast, a small focal point of uptake ($SUV_{mean}$ = 4, 1hr p.i.), which mapped precisely to an implanted stent, was observed for [$^{18}$F]FDG PET.

**Conclusion:** [$^{18}$F]FP-R$_0$1-MG demonstrated promise in detecting pancreatic cancers in human subjects. Although notable uptake of the tracer resulted in the stomach and small intestines, pancreatic tumors were easily identifiable because of high uptake in tumor tissue compared to normal pancreas.

## INTRODUCTION

Positron emission tomography (PET) imaging, using targeted agents, is an effective way to detect cancer. Accumulation of targeted PET tracers in tumor tissues provides a way to image cancer cells *in vivo* through proteins overexpressed on their cell surface. In contrast, [$^{18}$F]FDG (deoxyglucose analog) is based on the accumulation of sugar by metabolically hyperactive cancer cells.[1] However, [$^{18}$F]FDG accumulation in non-malignant tissues, such as inflammation, decreases diagnostic specificity.[2-6] Additionally, some small or low grade tumors do not accumulate sufficient levels of [$^{18}$F]FDG.[7, 8] In cases where [$^{18}$F]FDG PET falls short, such as the lack of accumulation by metastatic lymph nodes, or with confounding uptake by benign biological processes, or when background accumulation occurs by surrounding normal tissues, a targeted approach may provide more precise information that may be useful in cancer diagnosis, staging, treatment monitoring or disease management.[9-13]

Integrin receptors are extensively studied for the development of novel PET tracers.[14-18] Integrins are a family of proteins that mediate cellular adhesion to extracellular matrix (ECM) proteins.[19] In normal cells, integrins mediate contact events at their surface, and transduce signals to support gene expression of various ECM proteins that regulate differentiation, migration, proliferation, and apoptosis.[20] In certain disease states such as cancer, the expression of some integrins become dysregulated.[21, 22] A member of the integrin family, αvβ6, is overexpressed on the surface of many types of cancer cells.[23, 24] In a recent studies, IHC analysis revealed expression of integrin αvβ6 in PDAC compared to cancers of other systems.[23, 25] Expression of integrin αvβ6 was reported to be significantly higher in PDAC compared to chronic pancreatitis, and its expression was observed in tumor positive lymph nodes.[26] In well differentiated pancreatic tumors, elevated levels of integrin αvβ6 were reported in 100% of the samples (n=34) by immunological methods.[23, 25] Currently, a number of research groups, including ours, are developing peptide-based PET tracers to image integrin αvβ6 for cancer detection.[27-29]

The cystine knot secondary structure motif stabilizes knottin peptides so that it is protected against many forms of biological, chemical, and physical insult. The topological knot is formed by 3 disulfide bonds that thread the center of the

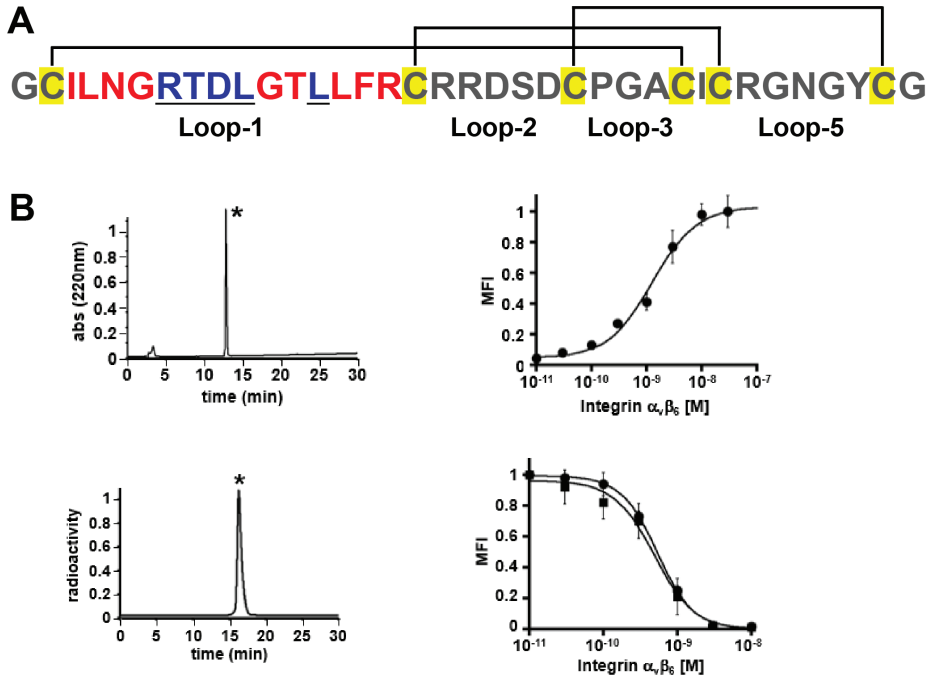



**Figure 1. Characteristics of Knottin.** (A) Primary structure of lead candidate $R_0$1-MG. The engineered active loop-1 is shown in red. The integrin αvβ6 core binding motif, RTDLxxL, is shown in blue. The framework residues are shown in gray. Cysteine residues are shown in yellow and the pattern of disulfide bonds are indicated by the connecting lines above the sequence. (B) The insert on top left shows the RP-HPLC trace of $R_0$1-MG, and the top right shows the equilibrium binding curve of between $R_0$1-MG expressed on yeast surface and soluble human integrin αvβ6 ($K_D$ = 1.24±0.21 nM). The insert on the bottom left shows the radio-RP-HPLC trace of the purified clinical-grade PET tracer [$^{18}$F]FP-$R_0$1-MG-F2, and on the bottom right the competition binding between unlabeled $R_0$1-MG ($IC_{50}$ = 0.61±0.31 nM, circles) or the N-terminus labeled version [$^{19}$F]FP-$R_0$1-MG-F2 ($IC_{50}$ = 0.56 ± 0.46 nM, squares) vs. yeast surface expressed $R_0$1-MG, respectively.

molecule. Knottins are found throughout nature in plants and animals serving in hist defense. Here, we engineered a trypsin inhibitor knotting into a cancer targeting ligand that recognizes integrin αvβ6 with single digit nanomolar binding affinity. In this study, we developed a stabilized integrin αvβ6 knottin and evaluated their ability to image cancer in living systems [$^{18}$F]FP PET tracers. In this pilot first-in-human study, we translated the lead cystine knot PET tracer, [$^{18}$F]FP-$R_0$1-MG-F2, and determined the ability to image pancreatic cancer.

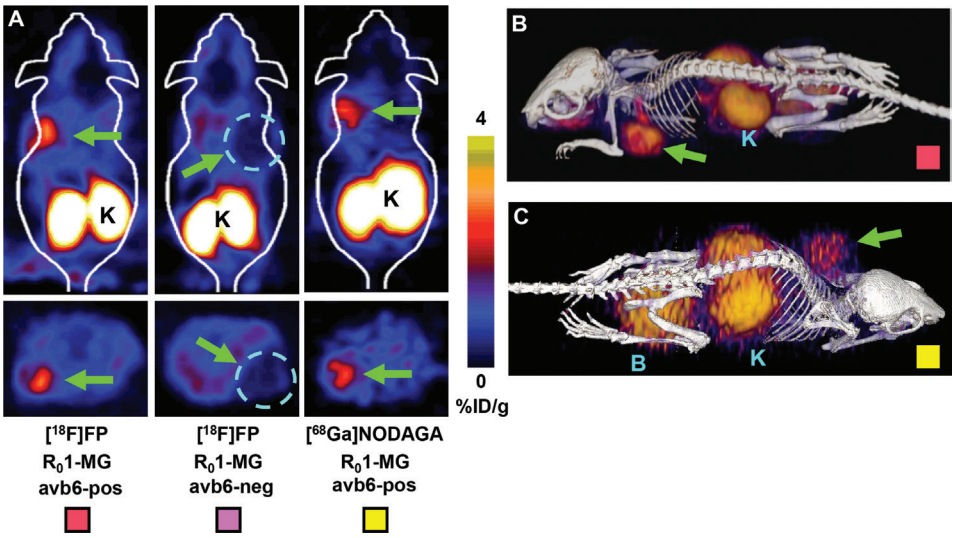



**Figure 2. Preclinical studies with $R_0$1-MG. (**A) Comparison at 1 hr post injection of the [$^{18}$F]FP labeled lead candidate $R_0$1-MG in integrin αvβ6 positive (red) vs αvβ6 negative tumor models (magenta, dashed circle in the figure). In vivo validation of the [$^{68}$Ga]NODAGA-$R_0$1-MG at 1 hr post injection (yellow). (B) Volume rendered PET/CT images of [$^{18}$F]FP-$R_0$1-MG (cyan) and (C) [$^{68}$Ga]NODAGA-$R_0$1-MG (yellow) in integrin αvβ6 positive models at 1 hr post injection. The green arrows point to the tumor. The letters K and B represent the kidneys and bladder, respectively. (A-C) Bar colors correspond to discrete box legend colors that identify the images.

# RESULTS



## Pre-clinical Development and Validation of $R_0$1-MG.

$R_0$1-MG emerged as the lead translational candidate (Figure 1A). It was produced by cGMP solid phase peptide synthesis, and its mass was verified by MALDI-TOF-MS. The precursor, reference standard and PET tracer were purified to > 95% chemical purity by reverse phase high pressure liquid chromatography (RP-HPLC, Figures 1B, left side). Equilibrium binding assays indicated that $R_0$1-MG ($K_D$ = 1.24±0.21 nM, Figure 1B) bind integrin $a_vb_6$ with high affinity that is comparable to the original peptide $R_0$1 ($K_D$ = 1.07±0.14 nM). Competition binding assays demonstrated that the FP group did not adversely affect high affinity binding to integrin αvβ6. The half maximal inhibitory concentration ($IC_{50}$) values for the unlabeled precursor and FP labeled standard were 0.61±0.31 nM and 0.56±0.46 nM, respectively (Figure 1B, right).

$R_0$1-MG was evaluated as a radiofluorinated PET ligand, [$^{18}$F]FP-$R_0$1-MG-F2, in pre-clinical models with either human integrin αvβ6 positive (~ 3.5%ID/g) or integrin αvβ6 negative (~0.5%ID/g) tumors (Figure 2A). Volume rendered PET/CT images of [$^{18}$F]FP-$R_0$1-MG (red) (Figure 2B) and [$^{68}$Ga]NODAGA-$R_0$1-MG (yellow) in integrin αvβ6 positive models at 1 hr post injection were generated (Figure 2C). Selective uptake was demonstrated in the integrin αvβ6 overexpressing tumors. At 1 hr p.i., tumor uptake was 2.8±0.3 %ID/g. Liver, muscle and kidney uptake was 1.2±0.4 %ID/g, 0.6±0.1 %ID/g and 30.4±5.5 %ID/g.

## Pharmacokinetic Evaluation of [$^{18}$F]FP-$R_0$1-MG-F2.

Dynamic PET/CT imaging in mice indicated that uptake of [$^{18}$F]FP-$R_0$1-MG-F2 in integrin αvβ6 expressing tumors was rapid and high. At 5 minutes p.i., the average tumor uptake value reached 5.4 ± 2.7 %ID/g, and plateaued at 5.7 ± 2.8 %ID/g at 60 minutes p.i.. Immediately upon tail vein injection, the PET tracer quickly entered and cleared both the heart and the liver. [$^{18}$F]FP-$R_0$1-MG-F2 cleared primarily via the kidneys where maximum uptake values of ~54 %ID/g were recorded at 4.5 minutes p.i.. Kidney uptake steadily decreased for the duration of the dynamic scan to ~16% ID/g at 60 min p.i., while the radiotracer accumulated in the bladder to ~110 %ID/g. Tumor-to-muscle ratio was approximately 8:1 and 5:1 at 30 and 60 minutes p.i, respectively. [$^{18}$F]FP-$R_0$1-MG-F2 did not accumulate to a great extent in liver, which gave rise to contrast ratios of ~7:1 to ~10:1 at time points beyond 30 minutes.

## cGMP Radiosynthesis and Toxicology Studies

In order to produce the reference standard and the PET tracer, the knottin precursor's sole amine, was used to couple the radioactive analog, [$^{18}$F]FP, through the electrophilic carbonyl carbon of the active nitrophenyl ester. Radiochemical purity of [$^{18}$F]FP-$R_0$1-MG-F2 ranged from 96.1% to 98.3%, and the chemical purify of the probe, for each synthesis, was greater than 99%. In addition, the probe remained stable in injection buffer for two radio half-lives after completion of the radiosynthesis. The specific activity of [$^{18}$F]FP-$R_0$1-MG-F2 was used to calculate the mass of tracer that would be administered to human from a PET study involving a dose of 15mCi.

For toxicological evaluation, the reference standard [$^{19}$F]FP-$R_0$1-MG-F2 was administered to 20 male and 20 female 7-week-old Sprague-Dawley rats at

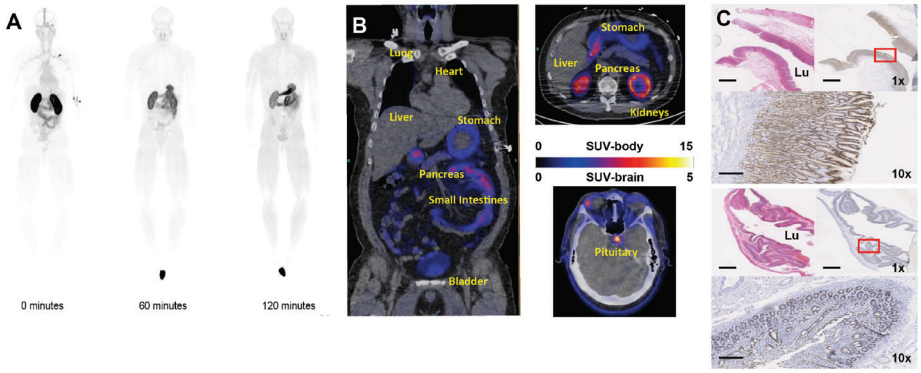



**Figure 3. [$^{18}$F]FP-R$_0$1-MG-F2 PET Imaging of Healthy Human Volunteer.** (A) Representative whole-body [$^{18}$F]FP-R$_0$1-MG-F2 maximum intensity projection (MIP) PET images of a healthy volunteer (50 year-old male) show the biodistribution of PET tracer at 3, 60 and 120 minutes post injection (p.i.). Focal uptake near the elbow and between the legs are the site of intravenous injection, and a tube containing the reference calibration standard, respectively. (B) Axial and coronal PET/CT images of the same healthy volunteer at 1 hr p.i. Close-ups of the chest and abdominal regions show the heart ($SUV_{mean}$ ~ 0.9), liver ($SUV_{mean}$ ~ 0.8), lung ($SUV_{mean}$ ~ 1.3), pancreas ($SUV_{mean}$ ~ 1.9), stomach ($SUV_{mean}$ ~ 12.6), small intestines ($SUV_{mean}$ ~ 7.8), kidneys ($SUV_{mean}$ ~ 14.3), and bladder (5.9). Accumulation of the tracer is evident in the pituitary gland ($SUV_{mean}$ ~ 5). (C) H&E staining and integrin αvβ6 immunohistochemical analysis of healthy stomach and small bowel tissue, where uptake was relatively high, shows expression of integrin αvβ6 on the luminal (Lu) side of these organs. Scale bars on the 1x and 10x images represent 2.5 cm and 250 μm, respectively.

250 times the anticipated clinical dose. Toxicity was evaluated on days three and fifteen following intravenous injection of the reference standard. All rats survived to the scheduled termination date and remained bright, alert and responsive during the course of the study. Under the conditions of this study, there were no treatment related findings in Sprague Dawley rats three or fifteen days after a single 1.1mg/kg intravenous dose of [$^{19}$F]FP-R$_0$1-MG-F2.[30]



## Evaluation of [$^{18}$F]FP-R$_0$1-MG-F2 in Healthy Human Volunteers

The following study was conducted in the Division of Nuclear Medicine and Molecular Imaging at Stanford University Nuclear Medicine Clinic under US-FDA eIND 126374 (S.S. Gambhir). A bolus of [$^{18}$F]FP-R$_0$1-MG-F2 was administered intravenously to five healthy male and female adult human volunteers; the mean ± SD injected dose of [$^{18}$F]FP-R$_0$1-MG-F2 was 7.5 ± 1.3 mCi and the mean injected mass was 12.5 ± 4.0 μg or 0.18 ± 0.06 μg/kg. No adverse effects were reported by volunteers or noticed by physicians and staff for up to 7 days after injection of [$^{18}$F]FP-R$_0$1-MG-F2.

The pharmacokinetics and biodistribution of [$^{18}$F]FP-$R_0$1-MG-F2 in a healthy volunteer (immediately, 1hr and 2hr after administration) are shown in Figure 3A. Transaxial PET/CT images show tracer distribution in the abdomen and brain (Figure 3B). [$^{18}$F]FP-$R_0$1-MG-F2 was renally cleared ($SUV_{mean}$ ~ 15) with notable uptake in the stomach ($SUV_{mean}$ ~10) and small intestines ($SUV_{mean}$ ~10) throughout the study. IHC confirmed the expression of integrin αvβ6 in normal stomach and small intestine tissues (Figure 3C). Uptake in most normal organs were relatively low (< $SUV_{mean}$ ~1) and decreased throughout study as the tracer steadily cleared these organs. Pancreatic uptake was slightly higher at 1 hr p.i. ($SUV_{mean}$ ~ 2). Throughout the study, tracer accumulation was also comparably higher for the pituitary gland ($SUV_{mean}$ ~ 4, 1 hr p.i.) and the large intestines ($SUV_{mean}$ ~ 3, 1 hr p.i.). The muscle $SUV_{mean}$ ~ 1.5 for the duration of the study. In agreement with pre-clinical models, the dose-limiting organ was determined to be kidney.

For an adult male, the kidneys received 0.1650 rem/mCi. Secondary uptake in the stomach and small intestines resulted in exposures of 0.0650 and 0.1100 rem/mCi, respectively. Dose calculations were low for the majority of organs including brain, muscle, liver, skin, thymus, lung and breast. The effective dose of [$^{18}$F]FP-$R_0$1-MG-F2 was 0.0335 rem/mCi for an adult male. Using the value for the kidney as dose-limiting, the maximum allowable exposure to [$^{18}$F]FP-$R_0$1-MG-F2 may be 30.30 mCi/dose or 1121.21 MBq/dose based on the 5 rem limit described in the US-FDA Code of Federal Regulations Title 21 Section 361.[31]

## Comparison Between [$^{18}$F]FP-$R_0$1-MG-F2 and [$^{18}$F]FDG in a Pancreatic Cancer Patient

Dosages of 10.2 mCi [$^{18}$F]FDG and 5.1 mCi [$^{18}$F]FP-$R_0$1-MG-F2 were separately administered on different days to a 70-year-old woman with pancreatic cancer scheduled for surgical resection. Imaging was conducted at the Division of Nuclear Medicine and Molecular Imaging at Stanford University Nuclear Medicine Clinic under US-FDA eIND 126374. Maximum intensity projection (MIP) PET, PET/CT and volume rendered PET/CT images show the biodistribution of [$^{18}$F]FP-$R_0$1-MG-F2 (Figure 4A) and [$^{18}$F]FDG (Figure 4B) approximately 1 hour after tracer administration.

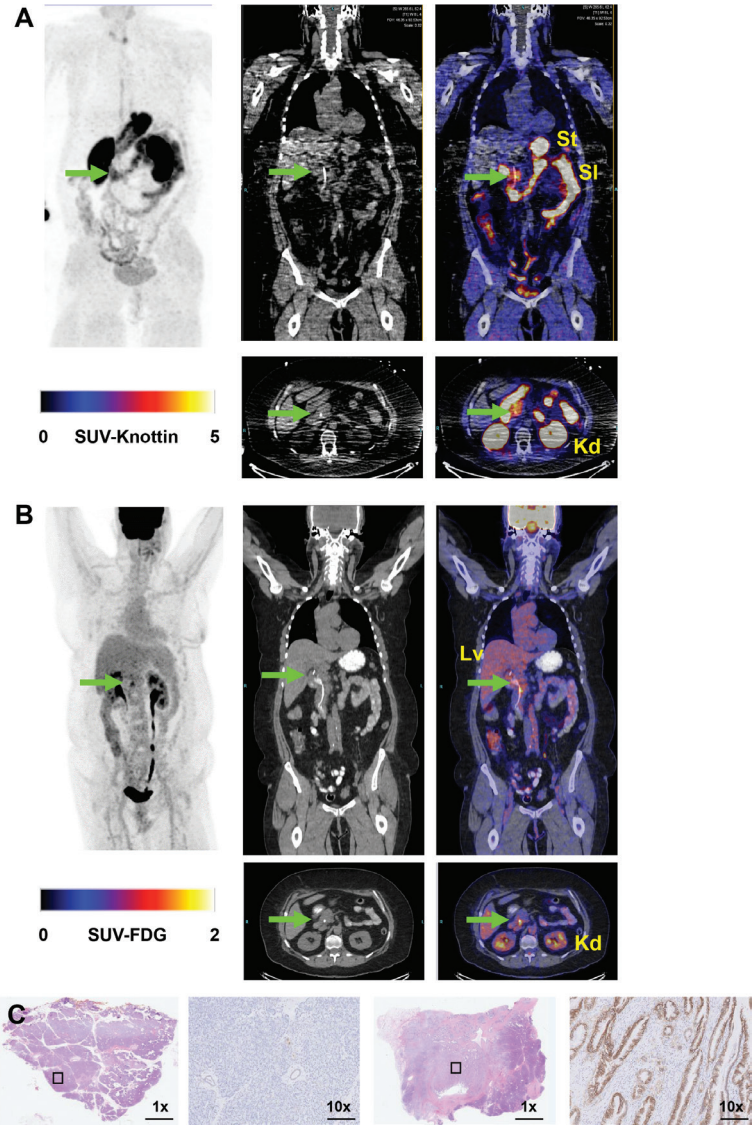



**Figure 4. [$^{18}$F]FP- $R_0$1-MG-F2 PET Imaging of Pancreatic Cancer.** (A) [$^{18}$F]FP- $R_0$1-MG-F2 and (B) [$^{18}$F]FDG images, from left to right, show MIP, CT, PET/CT (axial and coronal) images of a 71 year-old female pancreatic cancer patient at ~60 minutes post injection. The liver, kidneys, small intestines, stomach and spleen are denoted by Lv, Kd, SI, St, and Sp, respectively. The green arrow points to the tumor. (A) Accumulation of [$^{18}$F]FP- $R_0$1-MG-F2 at the head of the tumor is shown by the green arrow. PET/CT images demonstrate several regions of relatively high accumulation including the kidneys, the main clearance route, and the stomach (St), small intestines (SI) where integrin αvβ6 is expressed. (B) An area of focal [$^{18}$F]FDG uptake which is located within the tumor coincides with a biliary stent (white tube) that is apparent in the CT image. The tracer is seen draining out of the kidney (Kd) through the ureter and collecting in the bladder in the MIP, and volume rendered PET/CT images. (C) From left to right, H&E staining and IHC analysis of the resected pancreatic mass, which included some healthy pancreatic tissue. A section of normal pancreas (left) and a section of malignant tissue (right) are shown. Scale bars on the 1x and 10x images represent 2.5 cm and 250 μm, respectively.

[$^{18}$F]FP-$R_0$1-MG-F2 was distributed broadly through the tumor region (ROI ~ 8000 mm$^3$) and resulted in a $SUV_{mean}$ of 6.2 at 1 hr after tracer injection (Figure 4A). Comparatively, a region of focal uptake (ROI ~ 3000 mm$^3$, $SUV_{mean}$ = 4.1) of [$^{18}$F]FDG mapped precisely to a biliary stent that was implanted to circumvent the obstruction caused by the tumor (Figure 4B). Uptake of [$^{18}$F]FP-$R_0$1-MG-F2 and [$^{18}$F]FDG in the liver had $SUV_{means}$ of 0.9 and 2.9, respectively, at 1 hr p.i. $SUV_{means}$ of [$^{18}$F]FP-$R_0$1-MG-F2 the stomach and small intestines were 22.9 and 10.7, respectively, at 1 hr p.i. In comparison, $SUV_{means}$ of [$^{18}$F]FDG in the stomach and small intestine at 1 hr p.i. were 0.16 and 2.5, respectively. H&E staining and IHC analysis confirmed that the abnormal cells contained in the resected tissue expressed high levels of integrin αvβ6 as shown in Figure 4C.

## DISCUSSION

This manuscript describes the bench-to-bedside process of developing and translating a cystine knot PET tracer for detection of pancreatic cancer. In both pre-clinical small animal models and humans, accumulation of the knottin PET tracers within integrin αvβ6-positive tumors was rapid and sustained compared to either the healthy portion of the diseased organ or to surrounding normal tissue. The tracers cleared rapidly from circulation via renal filtration with a half-life of under 5 minutes. In contrast to the way FDG accumulated in the tumor of a pancreatic cancer patient, the uptake of the knottin PET tracer was more homogeneously distributed throughout the enlarged pancreatic mass, which highlights the different activities targeted by the two different types of PET tracers (glucose transporter vs ECM protein). Accumulation of the knottin PET tracers in normal human tissues was generally low with notable exceptions in the upper gut and pituitary gland.

Cystine knot peptides are a relatively new class of PET tracer that were first engineered for molecular recognition of integrins overexpressed in cancer. They have recently shown promise in pre-clinical models, not only as PET tracers, but in near infrared fluorescence imaging, molecularly-targeted ultrasound imaging, and in photoacoustic imaging.[15, 32, 33] Though initial studies $R_0$1-MG demonstrated high tumor uptake with acceptable off-target accumulation in healthy tissues,

and emerged as the lead candidate. Toxicological testing indicated that the lead was not harmful to rats even at 250x the imaging dose.

The pilot clinical trial began in healthy male and female human volunteers (n=5) where the knottin PET tracer demonstrated rapid renal clearance. Dosimetry studies confirmed our pre-clinical dose-estimations, and indicated the kidneys to be the dose-limiting organ. Notably, a substantial amount of tracer accumulation occurred in the stomach and small intestines. Tissue samples of healthy stomach and small intestines derived from another clinical study/procedure were made available to us for IHC analysis. These studies indicated relatively high levels of integrin αvβ6 expression in these tissues. Generally, the tracer demonstrated low levels of accumulation in most healthy tissues.

Afterwards, we evaluated cystine knot PET tracers ($R_0$1-MG) in pancreatic cancer where the initial results demonstrated promise in cancer detection. Accumulation of the PET tracer, [$^{18}$F]FP-$R_0$1-MG-F2, was rapid and remained high throughout the study. Here we were fortunate to have [$^{18}$F]FDG data from a previous study for comparative purposes. In this case, accumulation of [$^{18}$F]FDG by the tumor was concentrated at a biliary stent which was implanted to mitigate the pressure to the ducts caused by the tumor. Contrastingly in this same patient, the uptake of [$^{18}$F]FP-$R_0$1-MG was more uniformly distributed over a greater tumor volume. The difference in uptake profiles between the two classes of PET tracers probably reflects the different activities that are targeted (glucose transporter vs ECM protein). Although, we observed high tracer accumulation in neighboring stomach and small intestinal tissues, pancreatic tumors in three patients were easily discernable in their PET/CT images.



This pilot clinical study is limited mainly by the small sample size of pancreatic cancer patients that were evaluated with the knottin PET tracers. In addition, we found it informative to be able to directly compare the performance of the knottin PET tracers to the “gold standard” in PET imaging, [$^{18}$F]FDG, in pancreatic cancer. For pancreatic cancer, the challenge has been that patients usually do not undergo FDG PET scans as part of their care.

In conclusion, we have developed cystine knot PET tracers that effectively detect pancreatic cancer. We also begin to address an unmet clinical need

by providing new molecular imaging tools that can likely be coupled with strategies devised for earlier detection of pancreatic cancer. The knottin PET tracers demonstrated rapid and sustained accumulation in the tumor throughout the 2-hour clinical study. Low background uptake in organs or regions of the body prone to different cancers, together with several studies documenting the extent of integrin αvβ6 expression across many cancers, suggests that the $R_0$1-MG based PET tracers will have broad application in oncological molecular imaging. Taken together, the results from these pilot clinical studies encourages comprehensive evaluation of these new integrin αvβ6 cystine knot PET tracer across a broad range of indications and applications.

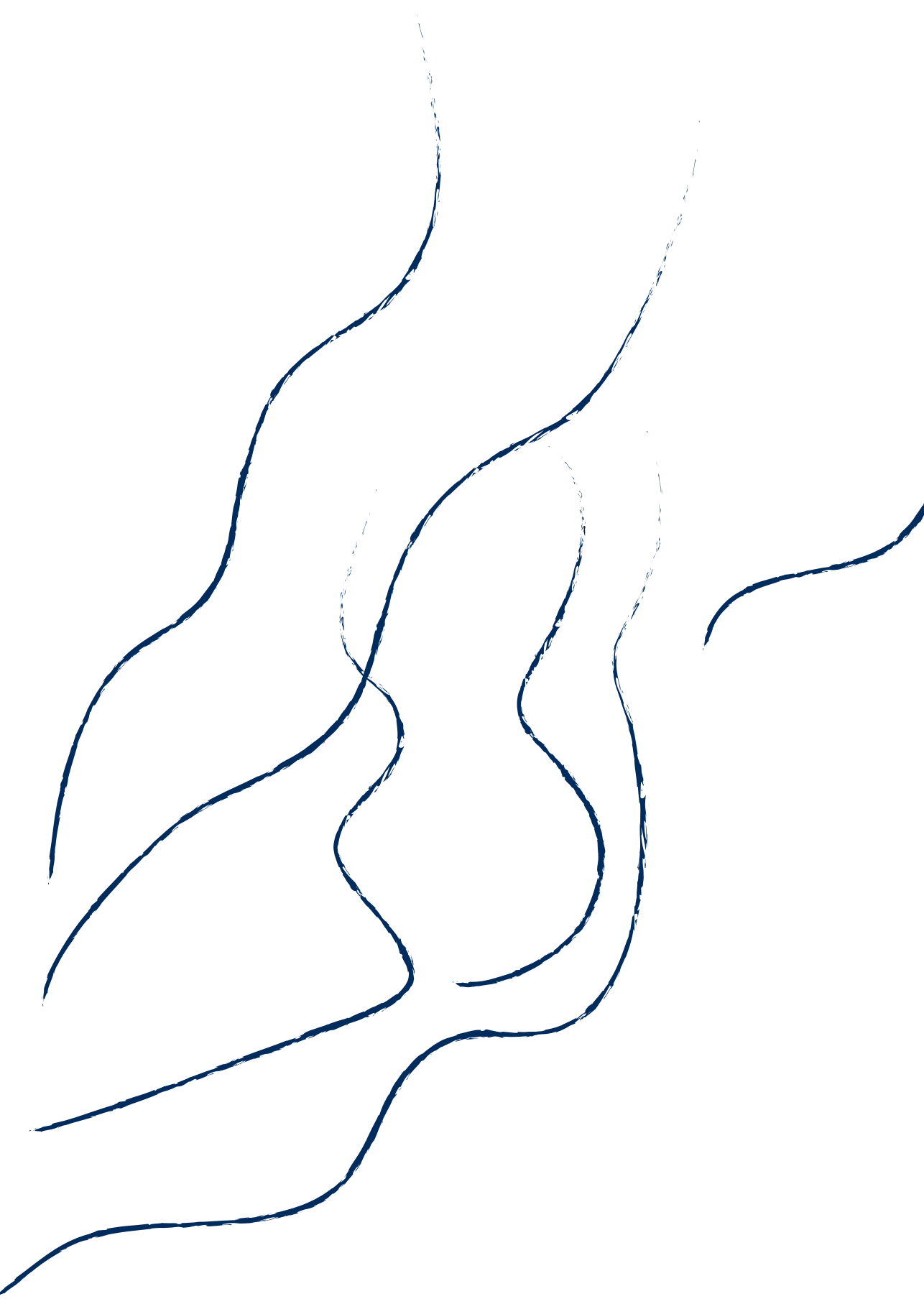
## ACKNOWLEDGEMENTS

This work was funded in part by DoE DE-SC0008397 (SSG, ZC, FTC), the NCI U01 CA210020 (SSG, JKW), and the Canary Foundation (SSG, RHK). F.V.F. is grateful for the support of grant CA154887 from the National Institutes of Health, National Cancer Institute, CRN-17-427258 by University of California, Cancer Research Coordinating Committee, and GRFP NSF National Science Foundation.

# REFERENCES


1. Som, P., H.L. Atkins, D. Bandoypadhyay, et al., A fluorinated glucose analog, 2-fluoro-2-deoxy-D-glucose (F-18): nontoxic tracer for rapid tumor detection. J Nucl Med., 1980. 21(7): p. 670-5.2.
2. Love, C., M.B. Tomas, G.G. Tronco, et al., FDG PET of infection and inflammation. Radiographics, 2005. 25(5): p. 1357-68.3.
3. Zhuang, H. and A. Alavi, 18-fluorodeoxyglucose positron emission tomographic imaging in the detection and monitoring of infection and inflammation. Semin Nucl Med, 2002. 32(1): p. 47-59.4.
4. Mochizuki, T., E. Tsukamoto, Y. Kuge, et al., FDG uptake and glucose transporter subtype expressions in experimental tumor and inflammation models. J Nucl Med, 2001. 42(10): p. 1551-5.5.
5. Corrigan, A.J., P.J. Schleyer, and G.J. Cook, Pitfalls and Artifacts in the Use of PET/CT in Oncology Imaging. Semin Nucl Med, 2015. 45(6): p. 481-99.6.
6. Sawada, S., H. Suehisa, T. Ueno, et al., Monitoring and management of lung cancer patients following curative-intent treatment: clinical utility of 2-deoxy-2-[fluorine-18] fluoro-d-glucose positron emission tomography/computed tomography. Lung Cancer (Auckl), 2016. 7: p. 45-51.7.
7. Khiewvan, B., D.A. Torigian, S. Emamzadehfard, et al., An update on the role of PET/CT and PET/MRI in ovarian cancer. Eur J Nucl Med Mol Imaging, 2017. 44(6): p. 1079-1091.8.
8. Griffeth, L.K., Use of PET/CT scanning in cancer patients: technical and practical considerations. Proceedings (Baylor University. Medical Center), 2005. 18(4): p. 321-330.9.
9. Lytras, D., S. Connor, L. Bosonnet, et al., Positron emission tomography does not add to computed tomography for the diagnosis and staging of pancreatic cancer. Dig Surg, 2005. 22(1-2): p. 55-61; discussion 62.10.
10. Nishiyama, Y., Y. Yamamoto, T. Monden, et al., Evaluation of delayed additional FDG PET imaging in patients with pancreatic tumour. Nucl Med Commun, 2005. 26(10): p. 895-901.11.
11. Sendler, A., N. Avril, H. Helmberger, et al., Preoperative evaluation of pancreatic masses with positron emission tomography using 18F-fluorodeoxyglucose: diagnostic limitations. World J Surg, 2000. 24(9): p. 1121-9.12.
12. Kauhanen, S.P., G. Komar, M.P. Seppanen, et al., A prospective diagnostic accuracy study of 18F-fluorodeoxyglucose positron emission tomography/computed tomography, multidetector row computed tomography, and magnetic resonance imaging in primary diagnosis and staging of pancreatic cancer. Ann Surg, 2009. 250(6): p. 957-63.13.
13. Sahani, D.V., P.A. Bonaffini, O.A. Catalano, et al., State-of-the-art PET/CT of the pancreas: current role and emerging indications. Radiographics, 2012. 32(4): p. 1133-58; discussion 1158-60.14.
14. Ruoslahti, E., RGD and other recognition sequences for integrins. Annu Rev Cell Dev Biol. , 1996. 12: p. 297-715.15.
15. Kimura, R.H., S.S. Cheng Z Fau - Gambhir, J.R. Gambhir Ss Fau - Cochran, et al., Engineered knottin peptides: a new class of agents for imaging integrin expression in living subjects. Cancer Res, 2009. 69(6): p. 2435-42.16.
16. Haubner, R., H. Beer Aj Fau - Wang, X. Wang H Fau - Chen, et al., Positron emission tomography tracers for imaging angiogenesis. Eur J Nucl Med Mol Imaging, 2010. 37(S1): p. 86-103.17.
17. Haubner, R., S. Maschauer, and O. Prante, PET radiopharmaceuticals for imaging integrin expression: tracers in clinical studies and recent developments. Biomed Res Int, 2014. 2014(2314-6141 (Electronic)).18.
18. Gaertner, F.C., H.J. Kessler H Fau - Wester, M. Wester Hj Fau - Schwaiger, et al., Radiolabelled RGD peptides for imaging and therapy. Eur J Nucl Med Mol Imaging, 2012. 39(S1): p. 126-138.19.

19. Hynes, R.O., Integrins: versatility, modulation, and signaling in cell adhesion. Cell, 1992. 3(69): p. 11-25.20.
20. Hynes, R.O., Integrins: bidirectional, allosteric signaling machines. Cell, 2002. 110(6): p. 673-87.21.
21. Desgrosellier, J.S. and D.A. Cheresh, Integrins in cancer: biological implications and therapeutic opportunities. Nat Rev Cancer, 2010. 10(1): p. 9-22.22.
22. Cox, D., N. Brennan M Fau - Moran, and N. Moran, Integrins as therapeutic targets: lessons and opportunities. Nat Rev Drug Discovery, 2010. 9(10): p. 804-20.23.
23. Bandyopadhyay, A. and S. Raghavan, Defining the role of integrin alphavbeta6 in cancer. Curr Drug Targets, 2009. 10(7): p. 645-52.24.
24. Liu, H., Y. Wu, F. Wang, et al., Molecular imaging of integrin alphavbeta6 expression in living subjects. Am J Nucl Med Mol Imaging, 2014. 4(4): p. 333-45.25.
25. Sipos, B., A. Hahn D Fau - Carceller, J. Carceller A Fau - Piulats, et al., Immunohistochemical screening for beta6-integrin subunit expression in adenocarcinomas using a novel monoclonal antibody reveals strong up-regulation in pancreatic ductal adenocarcinomas in vivo and in vitro. Histopathology, 2004. 45(3): p. 226-36.26.
26. Tummers, W.S., A. Farina-Sarasqueta, M.C. Boonstra, et al., Selection of optimal molecular targets for tumor-specific imaging in pancreatic ductal adenocarcinoma. Oncotarget, 2017.27.
27. Hausner, S.H., J. DiCara D Fau - Marik, J.F. Marik J Fau - Marshall, et al., Use of a peptide derived from foot-and-mouth disease virus for the noninvasive imaging of human cancer: generation and evaluation of 4-[18F] fluorobenzoyl A20FMDV2 for in vivo imaging of integrin alphavbeta6 expression with positron emission tomography. Cancer Res., 2007. 67(16): p. 7833-40.28.
28. Kimura, R.H., B.J. Teed R Fau - Hackel, M.A. Hackel Bj Fau - Pysz, et al., Pharmacokinetically stabilized cystine knot peptides that bind alpha-v-beta-6 integrin with single-digit nanomolar affinities for detection of pancreatic cancer. 2012. 18(3): p. 839-49.29.
29. Altmann, A., M. Sauter, S. Roesch, et al., Identification of a Novel ITGalphavbeta6-Binding Peptide Using Protein Separation and Phage Display. Clin Cancer Res, 2017. 23(15): p. 4170-4180.30.
30. Edgell, A., G. Kelly, and G. McMonagle, Final Study Report. 14-Day Single Intravenous Dose Toxicity Study of [19F]FP-R01-MG-F2 in Sprague Dawley Rats. 2015.31.
31. Code of Federal Regulations Title 21. United States Food and Drug Administration, 2017. Section 361.1.32.
32. Willmann, J.K., R.H. Kimura, N. Deshpande, et al., Targeted contrast-enhanced ultrasound imaging of tumor angiogenesis with contrast microbubbles conjugated to integrin-binding knottin peptides. J Nucl Med, 2010. 51(3): p. 433-40.33.
33. Zhang, C., R. Kimura, L. Abou-Elkacem, et al., A Cystine Knot Peptide Targeting Integrin alphavbeta6 for Photoacoustic and Fluorescence Imaging of Tumors in Living Subjects. J Nucl Med, 2016. 57(10): p. 1629-1634.



Chapter | 10

# Intraoperative Pancreatic Cancer Detection Using Tumor-Specific Multimodality Molecular Imaging

Willemieke S Tummers, MD [1 2], Sarah E Miller, B.S. [3], Nutte T Teraphongphom, Ph.D. [3], Adam Gomez, MD [4], Idan Steinberg, Ph.D. [1], David M Huland, Ph.D. [1], Steve Hong, MD [3], Sri-Rajasekhar Kothapalli, Ph.D. [1], Alifia Hasan, M.B.A. [3], Robert Ertsey, M.Sc. [3], Bert A Bonsing, MD, Ph.D. [2], Alexander L Vahrmeijer, MD, Ph.D. [2], Rutger-Jan Swijnenburg MD, Ph.D. [2], Teri A Longacre, MD [4], George A Fisher, MD [5], Sanjiv S Gambhir, MD, Ph.D. [6], George A Poultsides, MD [7], Eben L Rosenthal, M.D., F.A.C.S. [3].

[1] Department of Radiology, Molecular Imaging Program at Stanford (MIPS), Stanford University, Stanford, CA, 94305, USA. [2] Department of Surgery, Leiden University Medical Center, Albinusdreef 2, 2300 RC, Leiden, the Netherlands. [3] Department of Otolaryngology, Stanford University, Stanford, CA. [4] Department of Pathology, Stanford University, Stanford, CA. [5] Department of Medical Oncology, Stanford University, Stanford, CA. [6] Departments of Radiology, Bioengineering, and Materials Science & Engineering, Molecular Imaging Program at Stanford. Canary Center at Stanford for Early Cancer Detection. Stanford University, Stanford, CA, 94305, USA. [7] Department of Surgery, Stanford University, Stanford, CA.

*Ann Surg Oncol. 2018 Jul;25(7):1880-1888.*

## ABSTRACT

**Background:** Operative management of pancreatic ductal adenocarcinoma (PDAC) is complicated by several key decisions during the procedure. Identification of metastatic disease at the outset and when none is found, complete (R0) resection of primary tumor are key to optimizing clinical outcomes. The use of tumor-targeted molecular imaging, based upon photoacoustic and fluorescence optical imaging, can provide crucial information to the surgeon. Here, the first-in-human use of multimodality molecular imaging for intraoperative detection of pancreatic cancer is reported using cetuximab-IRDye800, a near-infrared fluorescent (NIRF) agent that binds to epidermal growth factor receptor (EGFR).

**Methods:** A dose-escalation study was performed to assess safety and feasibility of targeting and identifying PDAC in a tumor-specific manner using cetuximab-IRDye800 in patients undergoing surgical resection for pancreatic cancer. Patients received a loading dose of 100 mg unlabeled cetuximab prior to infusion of cetuximab-IRDye800 (50 mg or 100 mg). Multi-instrument fluorescence imaging was performed throughout the surgery in addition to fluorescence and photoacoustic imaging *ex vivo*.

**Results:** Seven patients with resectable pancreatic masses suspected to be PDAC were enrolled in this study. Fluorescence imaging successfully identified tumor with a significantly higher mean fluorescence intensity (MFI) in the tumor (0.09±0.06) versus surrounding normal pancreatic tissue (0.02±0.01), and pancreatitis (0.04±0.01) ($p<0.001$), with a sensitivity of 96.1% and specificity of 67.0%. The mean photoacoustic signal in the tumor site was 3.7-fold higher than surrounding tissue.

**Conclusion:** The safety and feasibilty of intra-operative tumor-specific detection of PDAC using cetuximab-IRDye800 with multimodal molecular imaging of the primary tumor and metastases was demonstrated.

## INTRODUCTION

Pancreatic ductal adenocarcinoma (PDAC) remains a highly lethal malignancy, with an expected median survival of around 25 months for patients undergoing surgery with adjuvant chemotherapy.[1, 2] After diagnosis of PDAC, patient selection for surgical resection is challenging at multiple stages during the procedure; detection of occult distant metastases, assessment of the extent of the primary tumor, peritumoral lymph nodes (LN), and the resection margins. There are two critical decisions that surgeons address during the procedure that will determine long-term survival of pancreatic cancer: the absence of metastatic and regional disease and cancer-free margins.[3-5] However, margin-positive resections are a frequent phenomenon (which occurs up to 70% of cases),[6] as is the emergence of distant metastases soon after surgery.[7] Failure to identify small tumor extensions during surgery is not surprising, due to the growth pattern of the tumor and the inability of the surgeon to differentiate between tumor and (peritumoral) inflammation.

The use of tumor-targeted imaging probes for photoacoustic and optical imaging modalities has the potential to provide real-time information to the surgeon to aid decision making. Photoacoustic imaging can provide intraoperative or transcutaneous images with functional information at clinically relevant depths (up to 5 cm) with submillimeter spatial resolution.[8] Fluorescent optical imaging, on the other hand, is superior for imaging of superficial lesions with a very high resolution.[9]



Despite significant investment in systemic therapy for small incremental gains in survival, there has been minimal investment in improving surgical outcomes. And although the value of intraoperative guidance in pancreatic cancer resection would seem obvious, previous studies have not demonstrated benefit when using the non-specific imaging agent indocyanine green (ICG).[10] Rosenthal et al. showed the successful use of cetuximab-IRDye800 to image sub-clinical fragments of squamous cell carcinoma arising in the head and neck cancer patients.[11] EGFR is also highly expressed in PDAC and is a good target for fluorescence imaging, due to its transmembrane position.[12-15] This study is the first example of tumor-specific multimodality molecular imaging for the accurate detection of primary PDAC, tumor-bearing LN, and distant metastases. The workflow of infusion, surgery and imaging is shown in Figure 1.

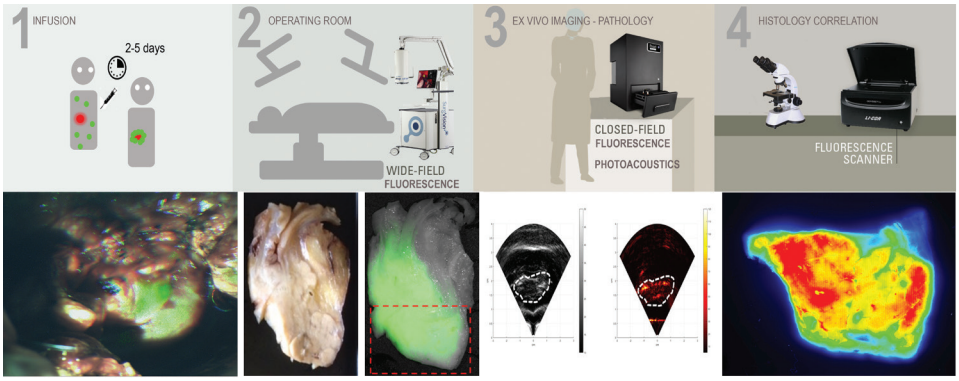



**Figure 1.** Schematic overview of workflow of clinical trial with imaging examples. **1. Infusion.** Infusion of a loading dose cetuximab (100 mg), and cetuximab-IRDye800 (50 or 100 mg) 2-5 days before surgical resection. **2. Operating room**. Intra-operative fluorescence imaging. **3. Ex vivo imaging - pathology.** Ex vivo fluorescence and photoacoustic imaging of surgical specimens. **4. Histology correlation.** Histologic correlation between histologically proven tumor or normal tissue with H&E and fluorescent signal.

## MATERIALS AND METHODS

### *Experimental design*

This study is a single-arm, open-label dose-escalation study, with the main objectives to determine safety and feasibility of tumor-specific multimodal molecular imaging for intraoperative detection of PDAC. Patients with suspected or biopsy-proven PDAC scheduled to undergo surgical resection at Stanford University Hospital were identified. A pretreatment dose of 100 mg unlabeled cetuximab was administered before the study drug to differentiate between a cetuximab reaction and a cetuximab-IRDye800 reaction, and to saturate the EGFR receptors in normal tissues with high expression (antigen sinks).[16] Two to five days after cetuximab-IRDye800 infusion patients underwent surgery.

### *Investigational agent: Cetuximab-IRDye800*

The cetuximab-IRDye800 was produced under cGMP conditions at the University of Alabama (UAB) Vector Production Facility as previously described,[17] before shipment to Stanford University Hospital Pharmacy (see also supplementary methods).

## Imaging

### *Intra-operative near-infrared (NIR) imaging*

Imaging during surgery was performed using the laparoscopic optical imaging system PINPOINT 9000 modified for IRDye800 fluorescent dye imaging (Novadaq, Burnaby, Canada), and the wide-field SurgVision Explorer (SurgVision BV, 't Harde, The Netherlands). During surgery, imaging was performed during inspection of the abdomen, before resection for the primary tumor, and after resection for the wound bed. This procedure is described in detail in the supplementary materials. Subsequently, all excised tissues were imaged *ex vivo* at a separate table in the OR directly after removal. Next, the surgical specimen was processed by the pathologist according to standard clinical practice to determine tumor status.

### *Ex vivo close-field NIR imaging*

The Pearl Impulse imaging platform (LI–COR Biosciences, Lincoln, NE) was used to image fresh tissues obtained in the operating room prior to paraffin embedding. The procedure is described in the supplementary methods.

### *Ex vivo photoacoustic imaging*

After excision of the specimen, *ex vivo* photoacoustic imaging was performed on the primary specimen and breadloaf sections of the tumor using a Stanford-build clinical hand-held photoacoustic imaging (PAI) and ultrasound transducer as previously described[18] [Kothapalli SR, et al. Nature Communications, under review], see also supplementary methods.



For detailed description of the imaging analysis for both fluorescent and photoacoustic imaging, see supplementary methods.

## Ethics approval

This study is performed in accordance with the tenets established by the Helsinki Declaration of 1975, ICH-GCP guidelines, and the laws and regulations of the United States. The Stanford University Institutional Review Board and the FDA approved the study protocol. All patients provided written informed consent prior to the start of any study-related procedures. The study was registered in the Clinical Trials Database of the U.S. National Institutes of Health, under number NCT02736578.

## Pathologic assessment

All resected lesions were examined for tumor status by a gastrointestinal pathologist with expertise in pancreatobiliary disease. A positive tumor that was fluorescent was considered a true positive, a negative lesion that was fluorescent was considered a false positive; and a positive tumor that was nonfluorescent was considered a false negative. Fluorescence positivity was determined based on the MFI of the raw data.

### *Histologic correlation*

Formalin-fixed paraffin-embedded tumor tissues were sectioned at 4 μm thickness and fluorescence imaging was performed using the Odyssey NIR scanner (Li-COR Biosciences). All histologic sections were stained with standard hematoxylin-eosin (H&E). To confirm the presence of EGFR, additional sections underwent immunohistochemical (IHC) analysis for EGFR expression utilizing anti-human EGFR. In addition, Ki-67 proliferation index was determined by IHC. See supplementary methods for further details. Appropriate positive and negative controls were included and evaluated with the specimens tested.

### *Fluorescence microscopy*

FFPE slides were prepared for fluorescence microscopy using the methods described in supplementary materials.

## Adverse events

Adverse events were classified according to the National Cancer Institute Common Terminology Criteria (Version 4.0), see supplementary methods.

## Statistical analysis

SPSS statistical software package (version 23.0, IBM Corp.) was used for statistical analyses. Differences in fluorescent signal per tissue type (tumor, pancreatitis, normal pancreatic tissue) were tested separately and between different dose groups, with One-way ANOVA with posthoc Bonferroni correction.

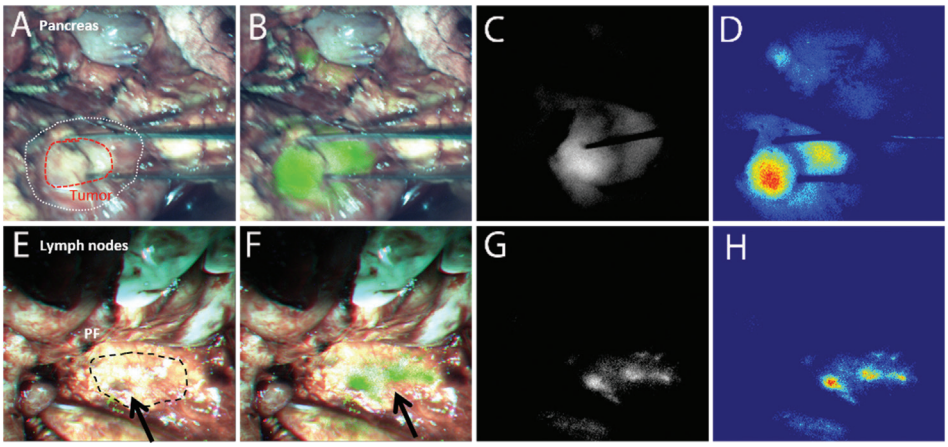



**Figure 2.** Intra-operative fluorescent imaging. Lesions could be clearly identified as shown in this figure; bright-field (2A and E), overlay (2B and F), grayscale (2C and G), and heat-map (2D and H) fluorescence imaging provided clear contrast between tumor and surrounding tissues during a Whipple procedure for both the primary tumor (A-D) and lymph nodes (E-H). PF = peripancreatic fat.

# RESULTS

## Patient and safety data

Between July 2016 and April 2017, ten patients were screened for trial eligibility. Eight patients with suspected PDAC received a loading dose Cetuximab, and 7 were enrolled. One patient was not enrolled since he had an infusion reaction on the loading dose Cetuximab. The other 7 patients went on to receive cetuximab-IRDye800. Patient and tumor characteristics are summarized in Table 1; 5 received 50 mg cetuximab-IRDye800 (cohort 1) and 2 received 100 mg cetuximab-IRDye800. There was one CTCAE grade-2 adverse event in cohort 1, fever, possibly related to cetuximab or cetuximab-IRDye800. No other possibly related adverse events occurred (Table 1). Two patients turned out to have neuroendocrine tumors at pathologic assessment, and one patient did not undergo resection due to liver metastases. Consistent with the literature regarding cetuximab administration for therapeutic purposes,[19, 20] a small increase of QTc interval was seen after infusion of the loading dose cetuximab with no further increase after cetuximab-IRDye800. QTc interval gradually decreased to baseline and none of the patients had persistent increased QTc after the observation period.

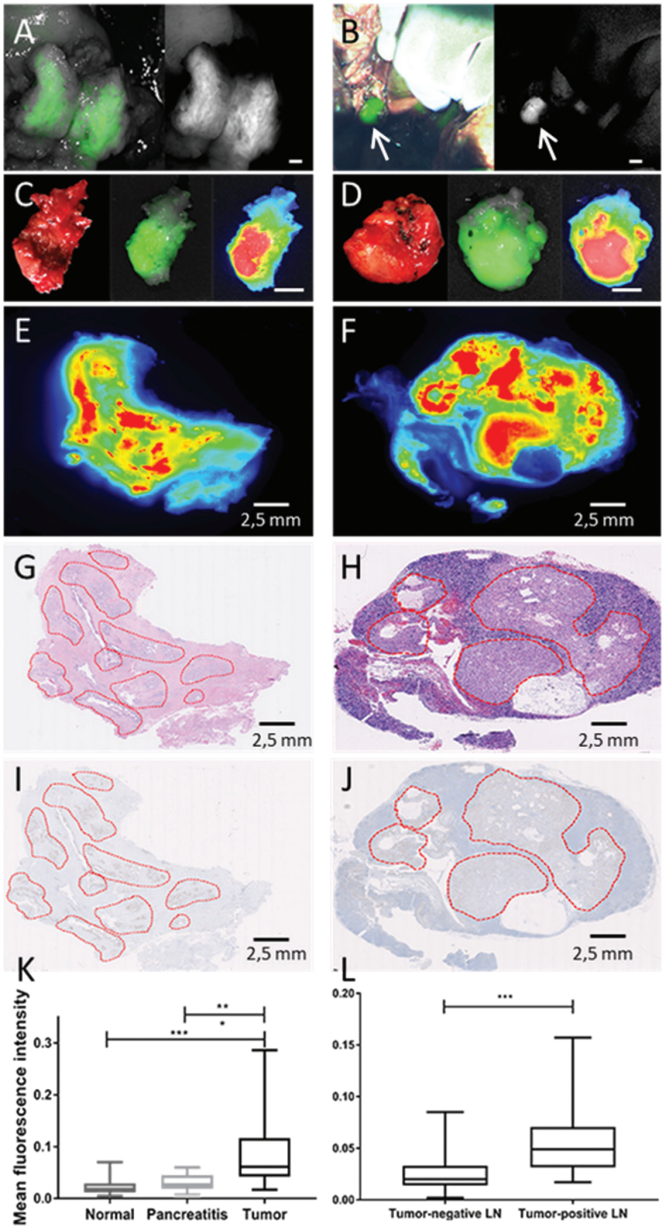



**Figure 3.** Correlation between intra-operative fluorescence and tumor-status. Identification of primary tumor (A) and tumor-bearing lymph node using fluorescence (B), with corresponding ex vivo fluorescence (C and D). Fluorescence of the primary tumor (E) is shown, and bisected lymph node on mesoscopic scale (F), with enhancements corresponding to the tumor on H&E, outlined in red (G + H)), and increased EGFR expression, also outlined (I + J). A graphic representation is shown of the mean fluorescence intensity (MFI) in normal pancreatic tissue, pancreatitis and tumor (K), and tumor-bearing and tumor-negative nodes (L). Scale bar represents 1 cm, unless indicated differently. ***; p<0.001

### Intra-operative NIR fluorescent imaging

Laparoscopic NIR-imaging was performed at the diagnostic laparoscopy prior to resection. All surgeries, except one, were converted to an open procedure and wide-field NIR imaging was performed during the subsequent procedure. The primary pancreatic tumor and/or LN could be clearly identified in every patient, as shown in Figure 2, bright-field (Fig. 2A and E), overlay (Fig. 2B and F), grayscale (Fig 2C and G), and heat-map (Fig 2D and H). Fluorescence imaging provided a clear contrast between tumor and surrounding tissues for both the primary tumor and LN dissection. The primary tumor could be identified in four of the six patients during surgical resection, with mean TBR of 2.3±0.72. In the other two patients, the tumor was situated below the peripancreatic fat (> 5mm depth) and was therefore intraoperatively not visible using NIR fluorescence. During surgery, tumor-bearing LN could be identified with mean TBR of 6.3±0.82. Back table imaging of the primary tumor in all patients demonstrated a mean TBR of 3.4±0.4.

### Correlation of fluorescence with histological disease

Correlation between fluorescent signal and histologic evidence of disease was established using close-field fluorescence imaging (Figure 3). The average fluorescent signal was significantly different in normal pancreatic tissue (MFI 0.02±0.01), pancreatitis (MFI 0.04±0.02), and tumor (MFI 0.09±0.06) ($p<0.001$) (Figure 3K). This allows tumor detection with a sensitivity of 96.1% (C.I. 92.19–98.43%) and specificity of 67.0% (C.I. 59.69–73.81%). There was no significant difference in MFI between normal pancreatic tissue (MFI 0.02±0.01; 0.03±0.02), pancreatitis (MFI 0.03±0.02; 0.06±0.03) and PDAC (MFI 0.09±0.06; 0.1±0.05) between the low and high dose cohort, respectively. Tumor-bearing LN (n=29) could be detected with significantly higher MFI (0.06±0.01) compared to tumor-negative (n=78) LN (0.02±0.002) ($p<0.001$) (Figure 3L). Interestingly, liver metastases could be detected as well by negative contrast (Figure S1).



### *Ex vivo* photoacoustic imaging

*Ex vivo* photoacoustic imaging of primary tumor and LN was performed using a custom built photoacoustic imaging system[21] in order to determine the potential utility of this strategy for eventual in vivo use. In this study, photoacoustic imaging could successfully be performed in all patients (n=4). (The device was not available for two patients). There was a clear increase in photoacoustic

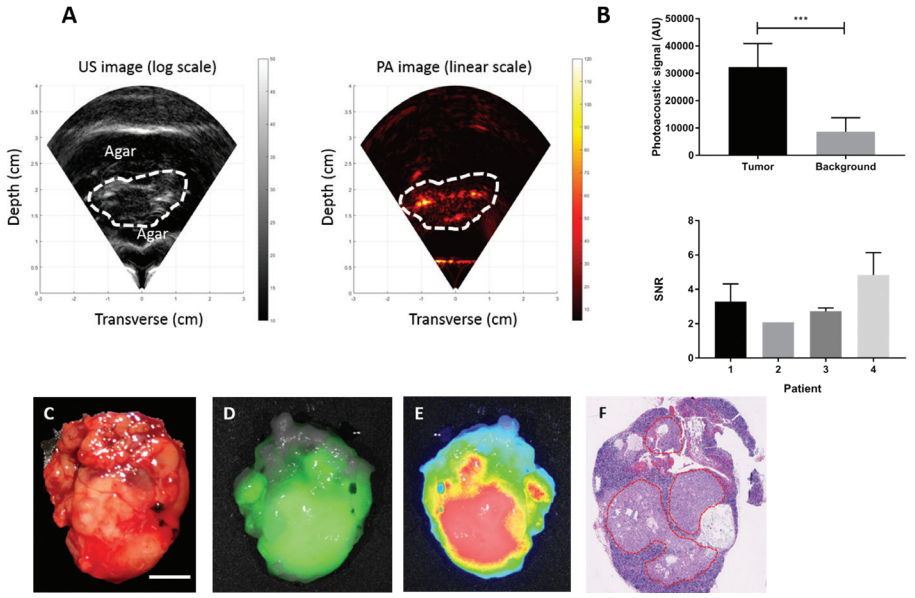



**Figure 4.** Photoacoustic and fluorescence imaging of tumor-bearing lymph node. Conventional ultrasound image of lymph node, surrounded by white dotted line and corresponding photoacoustic image (A). Mean photoacoustic signal in normal pancreatic tissue and tumor, and the signal-to-noise ratio (SNR) in photoacoustic signal per patient (B). Corresponding bright field (C), fluorescence overlay (D), heat-map fluorescent (E) images, and H&E section with outlined tumor (F) of tumor-bearing lymph node. ***; p<0.001. Scale bar represents 1 cm, unless indicated differently.

imaging signal in the primary tumor compared to surrounding pancreatic tissue (Figure S2), and in the tumor-bearing LN (Figure 4), which was consistent with the optical fluorescence imaging results. The mean photoacoustic signal in the tumor (32,286±1,660 AU) was significantly higher compared to background (8,651±902 AU) ($p<0.001$), which indicates a mean 3.7-fold increase in signal in the tumor compared to surrounding tissue (Figure 4B). A difference in signal-to-noise ratio (SNR) was observed between patients, as shown in Figure 4B. This trend was comparable to the difference in fluorescence imaging results in the same patients (Figure S2, Figure 5D).

## Molecular correlation

The correlation of fluorescence on microscopic level (Figure 5, panel I) was performed to correlate the uptake of the antibody-dye bioconjugate in the tumor, but not surrounding stromal elements. To perform this analysis a grid was overlaid on the fluorescently scanned slides to determine the MFI per specific area and then mapped to the histological grid as shown in (Figure 5,

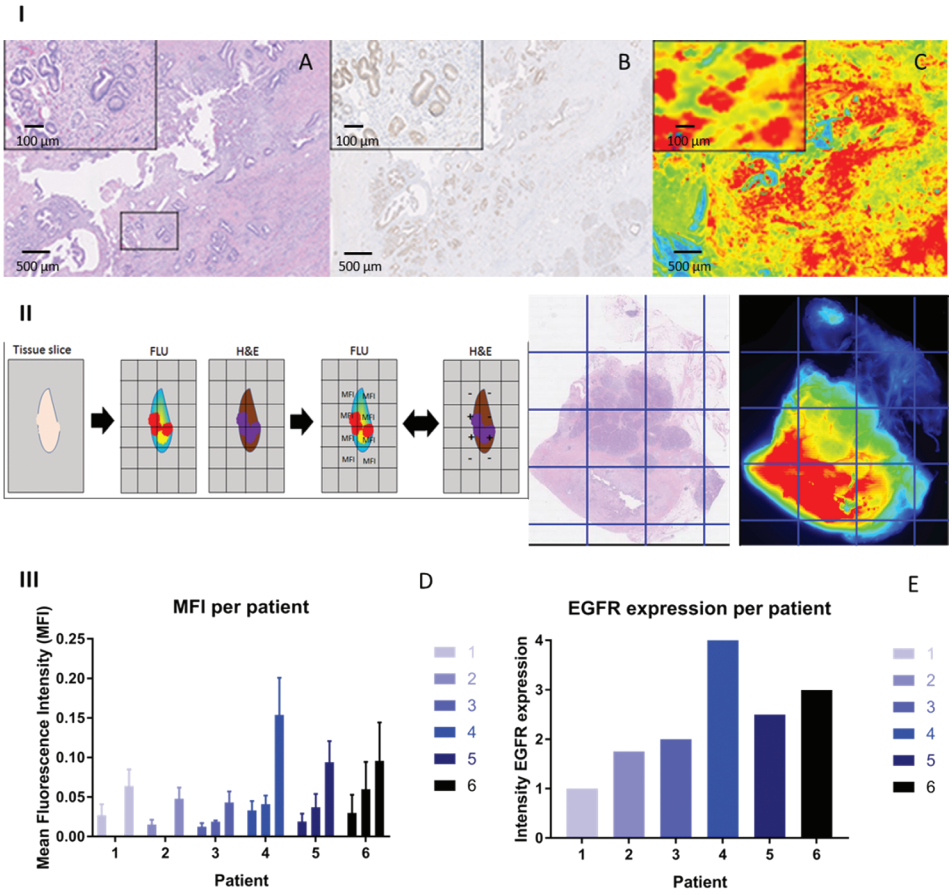



**Figure 5.** Histologic correlation with fluorescent signal. **Panel I:** Correlation between tumor in H&E section (**A**), EGFR expression (**B**), and fluorescence signal in heat-map (**C**) using Odyssey NIR Scanner (Li-COR Biosciences, Lincoln, NE). **Panel II:** The workflow to correlate histologic disease and fluorescence is shown here, a grid was overlayed on H&E and fluorescence slides to determine the tumor status and mean fluorescence intensity per area specific. **Panel III:** A graphic representation of the difference in MFI between patients in normal pancreatic tissue, pancreatitis, and PDAC, respectively (**D**), and the correlation with EGFR expression in PDAC in those patients (**E**). Intensity; 1-2 = low expression, 2-3 = moderate expression, and 4 = high expression.



panel II). The tumor could be identified with a sensitivity of 95% (CI 92.8-96.8%), specificity of 61% (CI 58.8-63.2%), AUC of 0.84 (CI 0.82-0.85), and a positive- and negative predicting values of 37.8% and 98.0%, respectively. MFI was also correlated with EGFR expression (Figure 5, panel III). In Figure 5D, the MFI per patient per tissue type is shown. A clear difference can be detected in MFI per patient. This is likely due to the heterogeneity of EGFR expression between

tumors. Patient 4 had relatively strong EGFR expression, patient 5 and 6 moderate EGFR expression and patient 1-3 low expression (Figure 5E). Although low EGFR expression in the tumor is seen in those patients, a clear difference in the MFI between tumor and surrounding pancreatic tissue could be detected (Figure 5D).

To localize cetuximab-IRDye800 within the tumor cells we used fluorescence microscopy. Figure S4 shows representative images of the 800 nm fluorescent signal at the tumor ducts but not adjacent stromal tissues. Importantly, fluorescent signal (serving as a surrogate for the antibody-dye bioconjugate) is identified within the tumor ducts, indicating the successful antibody penetration into the tumor.

## DISCUSSION

Here, we demonstrated for the first time the safety and efficacy of tumor-specific multimodality molecular imaging in the detection of pancreatic cancer using NIR fluorescently-labeled antibody. Current metabolic and anatomic imaging modalities often fail to detect small tumor lesions or tumor-bearing LN and as a result, intraoperative identification of the disease is critical to help guide decision making and precision surgery.

We found a significant difference in fluorescent signal between tumor-bearing and –negative LN at the lower dose (50 mg), however, at the higher dose (100 mg) we observed an increased number of false-positive fluorescent LN. We hypothesize this is caused by lymphatic drainage of excess antibody to the primary nodal basin, which is similar to findings with cetuximab-IRDye800 in head and neck cancer.[22] We have shown that this technique can guide tumor-bearing LN detection and removal when used at the optimal dose, which can be beneficial in patients with tumor-bearing LN in the first-echelon (N1).[23] Therefore, the optimal dose Cetuximab-IRDye800 established in this study is 50 mg, with a loading dose of 100 mg cetuximab. Due to variety of the infusion window in this study between cetuximab-IRDye800 infusion and surgery, no conclusion can be drawn if a specific timing is optimal. We can conclude that all

intervals in the infusion window, 2-5 days before surgery, provide clear tumor-to-background ratio's and are therefore sufficient for this purpose.

We have previously shown that EGFR has high levels of expression in the primary tumor and tumor-bearing LN,[15] a finding which is confirmed by the results of our current study using EGFR as a target. A difference in EGFR expression between neuro-endocrine tumors and PDAC was seen, as shown in figure S3D, with lower expression in neuro-endocrine tumors resulting in subsequent lower absolute fluorescence signal. Nevertheless, in both patients with neuro-endocrine tumors the background signal in normal pancreatic tissue was three times lower to provide sufficient TBRs for detection. High expression of EGFR in the stomach and duodenum resulted in high levels of background fluorescence in these organs. We hypothesize that this is located in normal luminal epithelium since fluorescence correlated with EGFR and Ki-67 expression at this position (Figure S5). Background fluorescence from these organs, however, did not interfere with detection of the primary tumor or LN during surgery, partly because the stomach and duodenum can be retracted away from the pancreatic tumor.

Furthermore, the potential of this technique to differentiate between PDAC and pancreatitis is crucial since this is a difficult distinction to make both before surgery and intraoperatively, leading to around 7% of pancreatic resections being performed for benign conditions.[24] Fluorescence imaging may also add value for margin assessment: in one patient, a positive pancreatic neck margin was evident during back-table imaging with clear fluorescence being visualized in the pancreatic neck, also confirmed by *ex vivo* imaging at pathology (Figure S6). This preliminary observation supports the notion that this technology may be useful for real-time identification of close or positive margins during resection, but future prospective studies are needed in this direction.



The observed negative contrast of tumor in the liver may be related to the intensity of fluorescence in the normal surrounding liver, since it is known that the amount of fluorescent dye coupled to EGFR targeting antibodies will influence the biodistribution of the conjugate. Our conjugate has a dye/protein ratio of 1.8, which indicates that some molecules will have 2 or more eq of dye coupled to the antibody.[17] Those are known to have the tendency for increased

liver uptake.[25] Another explanation can be the difference in EGFR expression in the metastases, which was clearly lower than surrounding hepatocytes.

It is worth noting that cetuximab-IRDye800 clearly penetrates the tumor and reaches the tumor cells. Limited success rates of phase II-III clinical trials on PDAC[26-30] is commonly attributed to the presence of dense desmoplastic stroma, consisting of cellular and acellular components.[31] This is thought to severely reduce the delivery of systemically administered therapies to the tumor and contribute the unresponsiveness of PDAC to systemic chemotherapy. Here we show at least to some extent that the EGFR monoclonal antibody can indeed reach the tumor successfully.

The main limitation of the study is the small sample size. However, while our sample size was small, it was sufficient for a proof-of-principle study investigating the safety and feasibility of multimodal molecular imaging in pancreatic cancer patients, and to identify significant results in the detection of tumor, and tumor-bearing LN. A second limitation is based on the limited depth penetration of NIR fluorescent imaging. For pancreatic cancer an imaging depth of 1 cm, achieved by fluorescence when used as single modality, is not enough to successfully capture spatial features of the tumor. The combination with photoacoustic imaging can overcome the limited depth penetration.

In conclusion, this is the first-in-human study evaluating the use of multimodality molecular imaging in patients undergoing surgical resection for pancreatic cancer. Our findings emphasize that the technique is safe and feasible for this pilot patient population. This type of tumor-specific imaging could be leveraged for a range of diagnostic techniques including detection of metastatic disease, identification of the primary tumor and tumor-bearing LN, assessment of resection margins, and identification of residual disease at the tumor bed after resection. Whether this additional information can change surgical management over commonly used, conventional methods remains to be determined in future prospective trials.

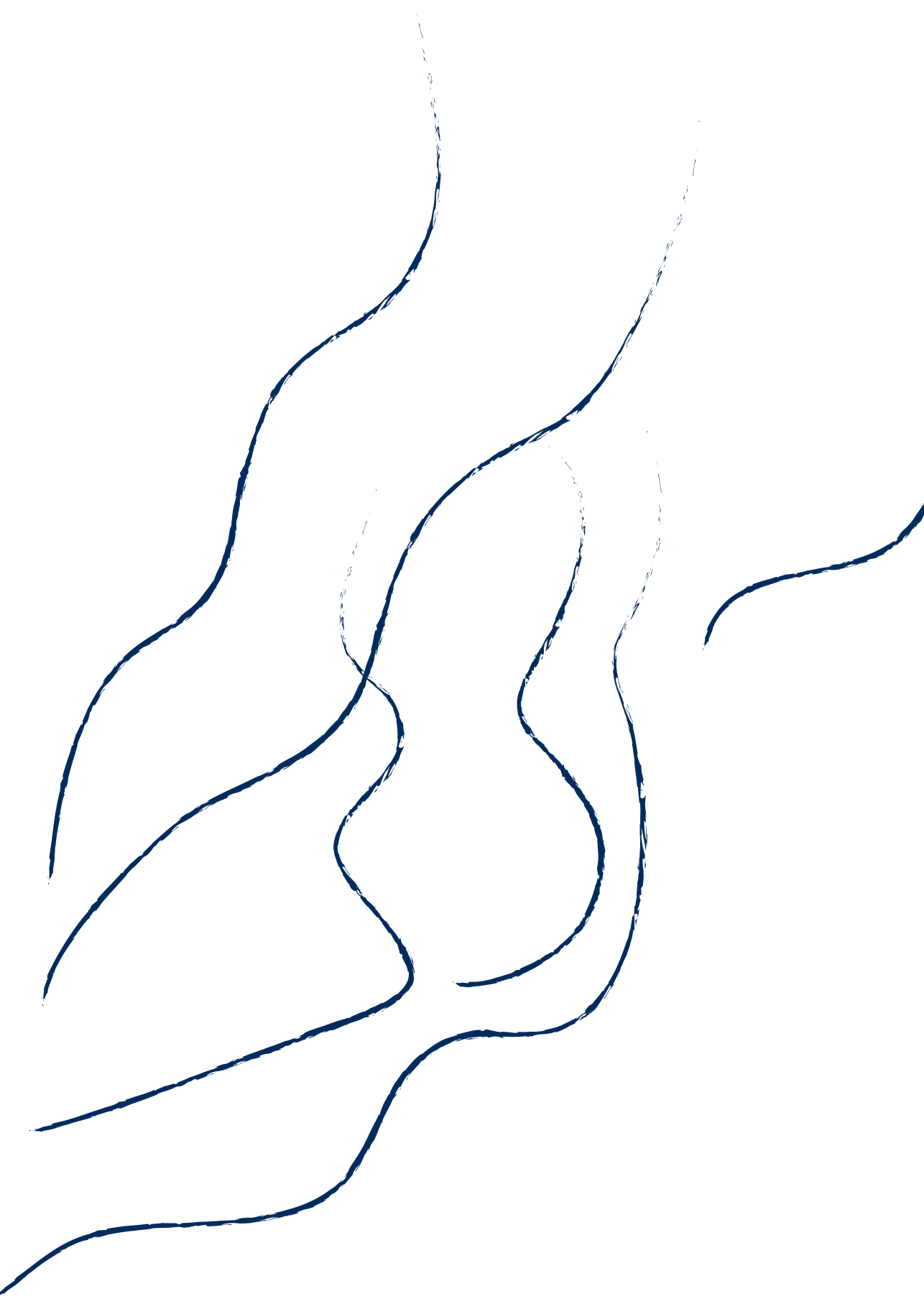
## ACKNOWLEDGMENTS

We would like to acknowledge support from Stanford Cancer Institute Translational Research Grant, and Intuitive Surgical Clinical Robotics Research Grant. Tummers WS contribution to this work was supported in part by Michaël-van Vloten Fonds, Lisa Waller Hayes Foundation, Jo Kolk Studiefonds, McKinsey Grant, and Ketel1 Studiefonds. Huland DM contribution to this work was supported in part by NCI training grant: T32 CA118681.

# REFERENCES


1. Christians, K.K., et al., Survival of patients with resectable pancreatic cancer who received neoadjuvant therapy. Surgery, 2016. 159(3): p. 893-900.
2. Roeder, F., Neoadjuvant radiotherapeutic strategies in pancreatic cancer. World J Gastrointest Oncol, 2016. 8(2): p. 186-97.
3. Bassi, C., et al., Value of regional lymphadenectomy in pancreatic cancer. HPB (Oxford), 2005. 7(2): p. 87-92.
4. Bachmann, J., et al., Pancreatic resection for pancreatic cancer. HPB (Oxford), 2006. 8(5): p. 346-51.
5. Tummala, P., T. Howard, and B. Agarwal, Dramatic Survival Benefit Related to R0 Resection of Pancreatic Adenocarcinoma in Patients With Tumor </=25 mm in Size and </=1 Involved Lymph Nodes. Clin Transl Gastroenterol, 2013. 4: p. e33.
6. Verbeke, C.S. and I.P. Gladhaug, Resection margin involvement and tumour origin in pancreatic head cancer. Br J Surg, 2012. 99(8): p. 1036-49.
7. Zhang, J.F., et al., Influence of perineural invasion on survival and recurrence in patients with resected pancreatic cancer. Asian Pac J Cancer Prev, 2013. 14(9): p. 5133-9.
8. Zackrisson, S., S.M. van de Ven, and S.S. Gambhir, Light in and sound out: emerging translational strategies for photoacoustic imaging. Cancer Res, 2014. 74(4): p. 979-1004.
9. Vahrmeijer, A.L., et al., Image-guided cancer surgery using near-infrared fluorescence. Nat Rev Clin Oncol, 2013. 10(9): p. 507-18.
10. Hutteman, M., et al., Clinical translation of ex vivo sentinel lymph node mapping for colorectal cancer using invisible near-infrared fluorescence light. Ann Surg Oncol, 2011. 18(4): p. 1006-14.
11. Rosenthal, E.L., et al., Safety and Tumor-specificity of Cetuximab-IRDye800 for Surgical Navigation in Head and Neck Cancer. Clin Cancer Res, 2015.
12. Bloomston, M., et al., Epidermal growth factor receptor expression in pancreatic carcinoma using tissue microarray technique. Dig Surg, 2006. 23(1-2): p. 74-9.
13. Uegaki, K., et al., Clinicopathological significance of epidermal growth factor and its receptor in human pancreatic cancer. Anticancer Res, 1997. 17(5B): p. 3841-7.
14. de Geus, S.W., et al., Selecting Tumor-Specific Molecular Targets in Pancreatic Adenocarcinoma: Paving the Way for Image-Guided Pancreatic Surgery. Mol Imaging Biol, 2016.
15. Tummers WS, F.S.A., Boonstra MC, Prevoo HA, Sier CF, Mioeg JS, Morreau J, van Eijck C, Kuppen P, van de Velde CJ, Bonsing BA, Vahrmeijer AL, Swijnenburg RJ Selection of optimal molecular targets for tumor-specific imaging in pancreatic ductal adenocarcinoma. Oncotarget, 2017. May.
16. Moore, L.S., et al., Effects of an Unlabeled Loading Dose on Tumor-Specific Uptake of a Fluorescently Labeled Antibody for Optical Surgical Navigation. Mol Imaging Biol, 2016.
17. Zinn, K.R., et al., IND-directed safety and biodistribution study of intravenously injected cetuximab-IRDye800 in cynomolgus macaques. Mol Imaging Biol, 2015. 17(1): p. 49-57.
18. Kothapalli, S.R., et al., Deep tissue photoacoustic imaging using a miniaturized 2-D capacitive micromachined ultrasonic transducer array. IEEE Trans Biomed Eng, 2012. 59(5): p. 1199-204.
19. Deeken, J.F., et al., Evaluation of the relationship between cetuximab therapy and corrected QT interval changes in patients with advanced malignancies from solid tumors. Cancer Chemother Pharmacol, 2013. 71(6): p. 1473-83.
20. Administration, U.S.F.a.D. ERBITUX® (cetuximab) injection, for intravenous infusion - label. 2004 2012 [cited 2017 July 27].
21. Kothapalli SR, e.a., Human Prostate Imaging Using a Novel Integrated Transrectal Ultrasound and Photoacoustic Instrument. Nature Communications, 2017. under review.
22. Rosenthal, E., et al., Sensitivity and Specificity of Cetuximab-IRDye800CW to Identify Regional Metastatic Disease in Head and Neck Cancer. Clin Cancer Res, 2017.

23. Buchler P, F.H., Müller M, AlKhatib J, Buchler MW, Survival benefit of extended resection in pancreatic cancer. The American Journal of Surgery, 2007. 194: p. S120-126.
24. Gerritsen, A., et al., Preoperative characteristics of patients with presumed pancreatic cancer but ultimately benign disease: a multicenter series of 344 pancreatoduodenectomies. Ann Surg Oncol, 2014. 21(12): p. 3999-4006.
25. Cohen, R., et al., Inert coupling of IRDye800CW to monoclonal antibodies for clinical optical imaging of tumor targets. EJNMMI Res, 2011. 1(1): p. 31.
26. Philip, P.A., Targeted therapies for pancreatic cancer. Gastrointest Cancer Res, 2008. 2(4 Suppl): p. S16-9.
27. Heinemann, V., et al., Meta-analysis of randomized trials: evaluation of benefit from gemcitabine-based combination chemotherapy applied in advanced pancreatic cancer. BMC Cancer, 2008. 8: p. 82.
28. Von Hoff, D.D., et al., Increased survival in pancreatic cancer with nab-paclitaxel plus gemcitabine. N Engl J Med, 2013. 369(18): p. 1691-703.
29. Moore, M.J., et al., Erlotinib plus gemcitabine compared with gemcitabine alone in patients with advanced pancreatic cancer: a phase III trial of the National Cancer Institute of Canada Clinical Trials Group. J Clin Oncol, 2007. 25(15): p. 1960-6.
30. Mitry, E., et al., Safety and activity of masitinib in combination with gemcitabine in patients with advanced pancreatic cancer. Cancer Chemother Pharmacol, 2010. 66(2): p. 395-403.
31. Adiseshaiah, P.P., et al., Nanomedicine strategies to overcome the pathophysiological barriers of pancreatic cancer. Nat Rev Clin Oncol, 2016. 13(12): p. 750-765.



Chapter | 11

# Detection of Visually Occult Metastatic Lymph Nodes Using Molecularly Targeted Fluorescent Imaging During Surgical Resection of Pancreatic Cancer

Willemieke S Tummers, MD [1 2], Sarah E Miller, B.S. [3], Nutte T Teraphongphom, Ph.D. [3], Nynke S. van den Berg, Ph.D. [3], Alifia Hasan, M.B.A. [3], Teri A Longacre, MD [4], George A Fisher, MD [5], Bert A Bonsing, MD, Ph.D. [2], Alexander L Vahrmeijer, MD, Ph.D. [2], Sanjiv S Gambhir, MD, Ph.D. [6], Rutger-Jan Swijnenburg MD, Ph.D. [2], Eben L Rosenthal, M.D., F.A.C.S. [3], George A Poultsides, MD [7].

[1] Department of Radiology, Molecular Imaging Program at Stanford (MIPS), Stanford University, Stanford, CA, 94305, USA. [2] Department of Surgery, Leiden University Medical Center, Albinusdreef 2, 2300 RC, Leiden, the Netherlands. [3] Department of Otolaryngology, Stanford University, Stanford, CA. [4] Department of Pathology, Stanford University, Stanford, CA. [5] Department of Medical Oncology, Stanford University, Stanford, CA. [6] Departments of Radiology, Bioengineering, and Materials Science & Engineering, Molecular Imaging Program at Stanford. Canary Center at Stanford for Early Cancer Detection. Stanford University, Stanford, CA, 94305, USA. [7] Department of Surgery, Stanford University, Stanford, CA.

## ABSTRACT

**Objective:** To examine the efficacy of molecularly targeted intraoperative fluorescent imaging in the detection of metastatic lymph nodes (LNs) during resection of pancreatic ductal adenocarcinoma (PDAC).

**Summary Background Data:** Although most patients with PDAC experience distant failure after resection, a significant portion still present with local recurrence. Intraoperative fluorescent imaging can potentially facilitate the visualization of involved peritumoral LNs and guide the locoregional extent of nodal dissection enabling staging and complete tumor clearance.

**Methods:** A dose-escalation prospective study was performed to assess the feasibility of tumor detection within peripancreatic LNs using cetuximab-IRDye800 in PDAC patients undergoing surgical resection. Patients received either 50 mg or 100 mg of cetuximab-IRDye800 2-5 days preoperatively. Fluorescent imaging of dissected LNs was analysed *ex vivo* macroscopically and microscopically and fluorescence was correlated with histopathology.

**Results:** A total of 144 LNs (72 in the low-dose and 72 in the high-dose cohort) were evaluated in 7 patients. Detection of metastatic LNs by fluorescence was better in the low-dose (50 mg) cohort, where sensitivity and specificity was 100% and 78% macroscopically, and 91% and 66% microscopically. More importantly, this method was able to detect occult foci of tumor (measuring < 5 mm) with a sensitivity of 88% (15/17 LNs).

**Conclusion:** This study provides proof of concept that intraoperative fluorescent imaging with cetuximab-IRDye800 can facilitate the detection of peripancreatic lymph nodes often containing subclinical foci of disease. This method holds promise in enhancing nodal tumor detection during surgery for PDAC, enabling more precise and targeted lymphadenectomy.

## INTRODUCTION

Pancreatic Ductal Adenocarcinoma (PDAC) represents a significant challenge in surgery and oncology. Autopsy studies have identified that although 70% of patients with pancreatic cancer die of widespread metastases, a significant portion (30%) die of locally destructive disease.[1] Therefore, although PDAC is largely considered a systemic disease at presentation, efforts to improve local therapies are very important. For patients with locally contained disease, surgery is the mainstay of management and the only chance for cure. Thus, maximizing the completeness of surgical resection in this setting is critical. However, even following what is felt to be a curative-intent resection, up to a third of patients with PDAC die from disease within a year from surgery.[2] This early failure is related mostly to unrecognized distant disease at the time of surgery, but also to residual disease left in situ at the resection bed. This occult residual disease is often below the threshold of detection by current intraoperative or radiologic imaging modalities. We have previously shown that tumor-specific imaging using a fluorescent dye targeting epidermal growth factor receptors (EGFR) on the tumor, especially in the form of intraoperative fluorescence imaging, has high sensitivity and specificity even for low-volume PDAC.[3-5]

The use of intraoperative fluorescence imaging can potentially improve the operative management of PDAC patients, since the extent of locoregional dissection can be expanded, to lymph node clearance. Sites of peritumoral lymphatics that can potentially be left behind after pancreatectomy, but are still considered locoregional sites of disease, are shown in Figure 1. The effect of additional lymph node resection remains subject to debate, as four previously published randomized trials have shown that extended lymphadenectomy for "all comers" undergoing PDAC resection does not provide therapeutic benefit.[6-10] However, these trials pertain to all presenting patients with resectable PDAC and it remains unclear whether precision surgery, (utilizing fluorescence guidance as part of the lymph node dissection to target occult nodes in the resection bed) could improve long-term surgical outcomes for this disease. To this end, we hypothesize that with intraoperative identification of occult metastatic lymph nodes using tumor-specific imaging, either a targeted lymph node dissection could be performed (should these nodes are considered regional), or

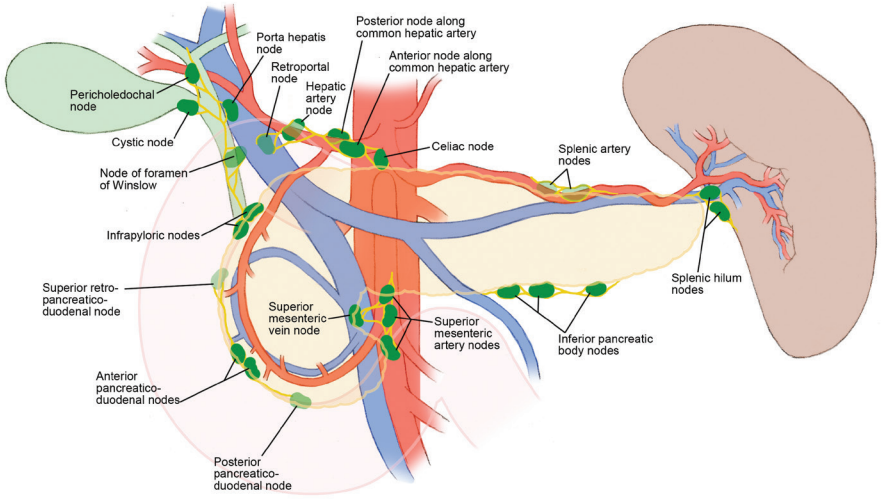



**Figure 1**. **Locoregional peripancreatic lymph nodes**. Involved lymph nodes in periaortic locations or high up in the hepatoduodenal ligament towards the liver would be considered distant metastatic disease during surgery for PDAC.

the resection could be aborted (if these nodes are considered M1 disease) if no oncologic benefit is anticipated from resection.

For tumor-specific molecular imaging, a biomarker is needed to be able to target tumor tissue. We have previously demonstrated in a cohort of 129 patients with different stages of PDAC that EGFR was abundantly expressed in up to 70% of cases.[11] To validate these results, we also tested the marker on tissues of patients with chronic pancreatitis and in lymph node metastases.[12] These experiments confirmed that EGFR is an appropriate pancreatic cancer-specific marker, also able to differentiate between benign and malignant pancreatic lesions, and detect tumor-positive lymph nodes. Interestingly, only low levels of EGFR expression are required for imaging,[13] which supports our hypothesis that small tumor burden in lymph nodes can be detectable by fluorescence.

We recently reported on the results of a prospective study utilizing EGFR-targeting cetuximab-IRDye800 for intraoperative fluorescent imaging of the pancreatic primary tumor during resection of PDAC.[5] In the current analysis, we

focus specifically on the diagnostic accuracy of this method for tumor-specific lymph node detection.

## MATERIALS AND METHODS

### Study design

The study was performed as a single-arm, open-label, dose-escalation study, with the main objective of determining the safety and feasibility of tumor-specific multimodal molecular imaging for detection of PDAC, as described previously.[5] Briefly, patients with suspected or biopsy-proven PDAC scheduled to undergo surgical resection at Stanford University Hospital were identified. A dose-escalation model using two doses (50 mg and 100 mg) of cetuximab-IRDye800 was chosen to identify the dose providing optimal tumor detection. The doses were determined based on previous findings by our group showing that a dose of 62.5 mg/m$^2$ provided the optimal tumor-to-background ratio (TBR) for head and neck cancer.[4] After informed consent, patients received a systemic infusion of the study drug 2-5 days before surgery. A pretreatment loading dose of 100 mg unlabeled cetuximab was administered before cetuximab-IRDye800 to differentiate between an infusion reaction to the parent compound (cetuximab) and a cetuximab-IRDye800 reaction, and also to preload the EGFR receptors in the liver.[14] After a 3-hour observation period, the patients were discharged and returned for surgery 2-5 days later.

### Investigational agent: cetuximab-IRDye800

The study drug (cetuximab-IRDye800) was produced under clinical Good Manufacturing Practice (cGMP) conditions at the University of Alabama (UAB) Vector Production Facility as previously described,[15] before shipment to Stanford University Hospital Pharmacy. During transit the temperature was monitored and kept stable. Briefly, cetuximab (ImClone LLC, Eli Lilly and Company) was concentrated and pH adjusted by buffer exchange to a 10mg/mL solution in 50 mmol/L potassium phosphate, pH 8.5. IRDye800CW NHS ester (LI–COR Biosciences) was conjugated to cetuximab for 2 hours at 20°C in the dark, at a molar ratio of 2.3:1.

## Optical imaging

### *Intraoperative near-infrared (NIR) imaging*

Intraoperative imaging of the operative field in real time was performed using the wide-field SurgVision Explorer (SurgVision BV, 't Harde, The Netherlands) at 3 time points: during preliminary inspection of the abdomen, after initial dissection but before tumor resection, and after tumor resection. The surgical specimen was processed by the pathologist according to standard clinical practice for inking, sectioning and margin evaluation. During this preliminary study, the findings of intraoperative imaging did not inform intraoperative management, which otherwise followed standard contemporary practice for patients with PDAC.

### *Closed-field near-infrared (NIR) ex vivo imaging*

Closed-field NIR *ex vivo* imaging was performed using The Pearl Impulse imaging platform (LI–COR Biosciences, Lincoln, NE) as previously described [5]. Briefly, the system was used to image fresh tissue obtained in the operating room prior to paraffin embedding. In addition, the system was used to measure mean fluorescence intensity (MFI) of the tumor and surrounding background tissue. MFI was defined as total counts/region of interest (ROI) pixel area, using integrated instrument software (ImageStudio, LI–COR Biosciences). After measuring the signal intensity from macroscopic images, the following formula was used to measure Tumor to Background Ratio (TBR) = MFI of the tumor/ MFI of the surrounding tissue.

## Pathologic assessment

All resected specimens were examined by a single dedicated gastrointestinal pathologist (TAL) with expertise in pancreatic disease. Formalin-fixed paraffin-embedded tumor tissues were sectioned at 4 μm thickness and fluorescence imaging was performed using the Odyssey NIR scanner (Li-COR Biosciences). The system was used to determine microscopic accuracy of fluorescence, correlated to standard hematoxylin-eosin (H&E) staining. NIR-fluorescence measurements were done following the same method as described above, using the integrated instrument software ImageStudio.

To confirm the presence of EGFR, additional sections underwent immunohistochemical (IHC) analysis for EGFR expression using anti-human EGFR

monoclonal antibodies (predilute, rabbit, clone 5B7, 790-4347, Ventana, Tucson, AZ). Automated immunohistochemical staining was performed with Ventana Benchmark XT (Ventana Medical Systems, Inc., Tucson, AZ, USA). Formalin fixed paraffin embedded (FFPE) tissue sections cut at 4 µm were deparaffinized and rehydrated. Antigen retrieval was performed by heat pretreatment at Standard Cell Conditioning 1 (Ventana Tris/ Borate/ EDTA-based buffer at pH 8.5) for 60 minutes. The slides were incubated with primary antibodies at 37°C for 32 minutes. After primary incubation, ultraView Universal DAB Detection system (Ventana) was used for single brown staining with 3,3'diaminobenzidine chromogen.

## Ethics approval

The described study is performed in accordance with the tenets established by the Helsinki Declaration of 1975 (as amended in Tokyo, Venice, Hong Kong, Somerset West, Edinburgh, Washington, and Seoul), ICH-GCP guidelines, and the laws and regulations of the United States. The Stanford University Institutional Review Board and the FDA approved the study protocol. All patients provided written informed consent. The study was registered in the Clinical Trials Database of the U.S. National Institutes of Health, under number NCT02736578.

## Statistical analysis

SPSS statistical software package (version 23.0, IBM Corp.) was used for statistical analyses, and GraphPad Prism 7 (version 7.02, GraphPad Sorftware, Inc.). Differences in fluorescent signal between tumor-positive and tumor-negative lymph nodes were tested separately and between different dose groups, with One-way ANOVA with posthoc Bonferroni correction. TBR is reported as the mean, SEM, and range. Graphical display was performed using box plot graphs, and Receiver Operating Characteristic (ROC) curves.

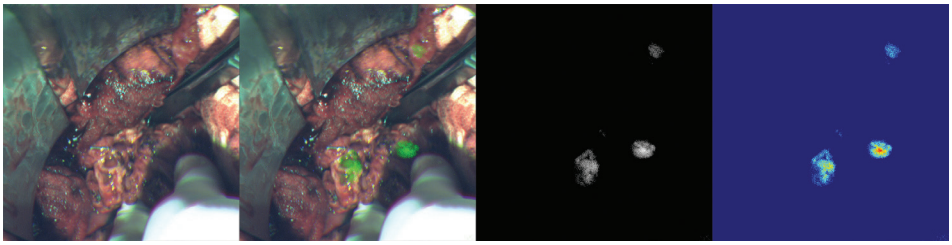


**Figure 2. Intraoperative lymph node detection**. Tumor-positive lymph nodes in the hepatoduodenal ligament during pancreaticoduodenectomy. Bright field image of wound bed (2A), overlay (2B), grayscale (2C), and heat-map (2D) fluorescence imaging provided clear contrast between tumor and surrounding tissue. Imaging was performed with wide-field SurgVision Explorer (SurgVision BV, 't Harde, The Netherlands).

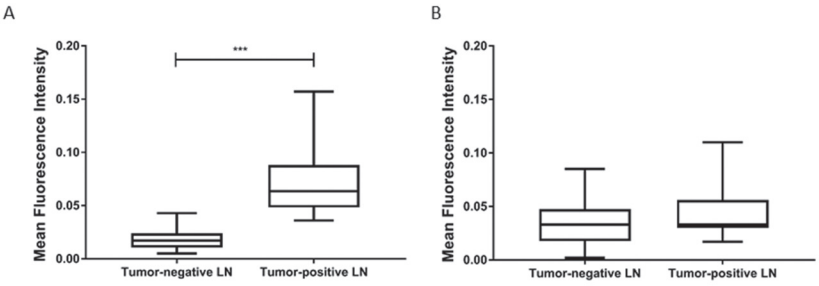
# RESULTS

## Metastatic lymph node detection using cetuximab-IRDye800

A total of 144 lymph nodes were evaluated in the 7 patients; in the low-dose cohort (50 mg), there were 72 nodes evaluated of which 64 were tumor-negative and 8 were tumor-positive. In the high-dose (100 mg) cohort, a total of 72 nodes was evaluated of which 56 were tumor-negative and 16 were tumor-positive. Examples of tumor-positive lymph nodes detected in real-time by fluorescence during surgery are shown in Figure 2.

For the entire cohort, tumor-positive lymph nodes could be detected *ex vivo* demonstrating significantly higher MFI (0.06±0.01) compared to tumor-negative lymph nodes (0.02±0.002) ($p<0.001$). This difference was more pronounced in the low-dose cohort, where MFI for tumor-positive lymph nodes was 0.071, compared to 0.018 for tumor-negative lymph nodes ($p<0.001$) (Figure 3A). In contrast, in the high-dose cohort, the difference in MFI between tumor-positive lymph nodes and tumor-negative lymph nodes was not significant (0.046 vs.0.035, $p=0.148$) (Figure 3B). The sensitivity to detect tumor-positive lymph nodes in the low-dose cohort was 100% (C.I. 73.5 – 100) and specificity 78% (C.I. 64.0 – 88.5), with a likelihood ratio of 4.55. In the high-dose cohort, the sensitivity was 88.2% (C.I. 63.6 – 98.5) and specificity decreased to 32.1% (C.I. 15.9 – 52.4), with a likelihood ratio of 1.30 (Figure 3C).

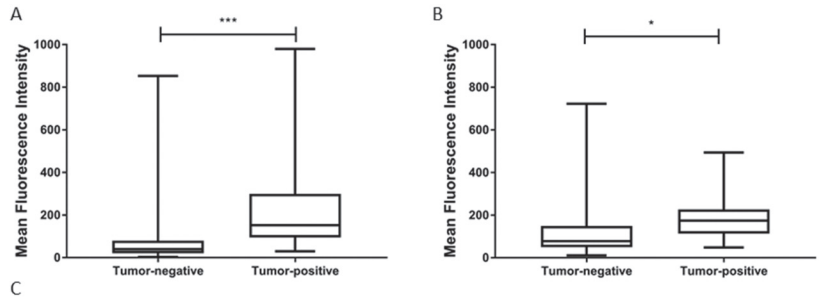
Fluorescence intensity of formalin-fixed paraffin-embedded tissue sections were evaluated to validate tumor targeting of the fluorescent agent. A significant




C

| | Low dose | High dose |
|---|---|---|
| Sensitivity (95% C.I.) | 100% (73.5 – 100) | 88.2% (63.6 – 98.5) |
| Specificity (95% C.I.) | 78% (64.0 – 88.5) | 32.1% (15.9 – 52.4) |
| AUC | 0.99 (0.98 – 1.00) | 0.58 (0.41 – 0.76) |
| Likelihood ratio | 4.55 | 1.30 |

**Figure 3. Detection of tumor-positive lymph nodes using fluorescence imaging of fresh tissue ex vivo**. Analyzing the low-dose cohort, MFI for tumor-positive lymph nodes was 0.071, compared to 0.018 for tumor-negative lymph nodes (p<0.001) (Figure 3A). In the high-dose cohort, the MFI for tumor-positive lymph nodes was 0.046, compared to 0.035 for tumor-negative lymph nodes (p=0.148) (Figure 3B). Images were obtained with The Pearl Impulse imaging platform (LI–COR Biosciences, Lincoln, NE), and MFI was determined with integrated software (ImageStudio, LI–COR Biosciences). Test characteristics of fluorescence for the detection of tumor-positive lymph nodes are shown in Figure 3C.




C

| | Low dose | High dose |
|---|---|---|
| Sensitivity (95% C.I.) | 91.4% (76.4 – 96.4) | 93.1% (77.2 – 99.2) |
| Specificity (95% C.I.) | 66.3% (61.6 – 70.8) | 34.8% (26.2 – 44.1) |
| AUC | 0.84 (0.79 – 0.89) | 0.73 (0.64 – 0.82) |
| Likelihood ratio | 2.64 | 1.43 |

**Figure 4. Detection of tumor-positive lymph nodes using fluorescent imaging of formalin-fixed paraffin-embedded tissue sections**. In the low-dose cohort, a significant difference was seen between the MFI of tumor-positive lymph nodes (250.4±33.9) and tumor-negative lymph nodes (76.4±5.1) (p<0.001) (Figure 4A). The same was true for the high-dose cohort, with the fluorescence in tumor-positive lymph nodes being 182.5±19.0 and in tumor-negative lymph nodes 126.9±11.9 (p=0.03) (Figure 4B). Images were obtained with the Odyssey NIR scanner (Li-COR Biosciences), and MFI was determined with integrated software (ImageStudio, LI–COR Biosciences). Test characteristics for the detection of tumor using fluorescence at the microscopic level per dose group are shown in Figure 4C.

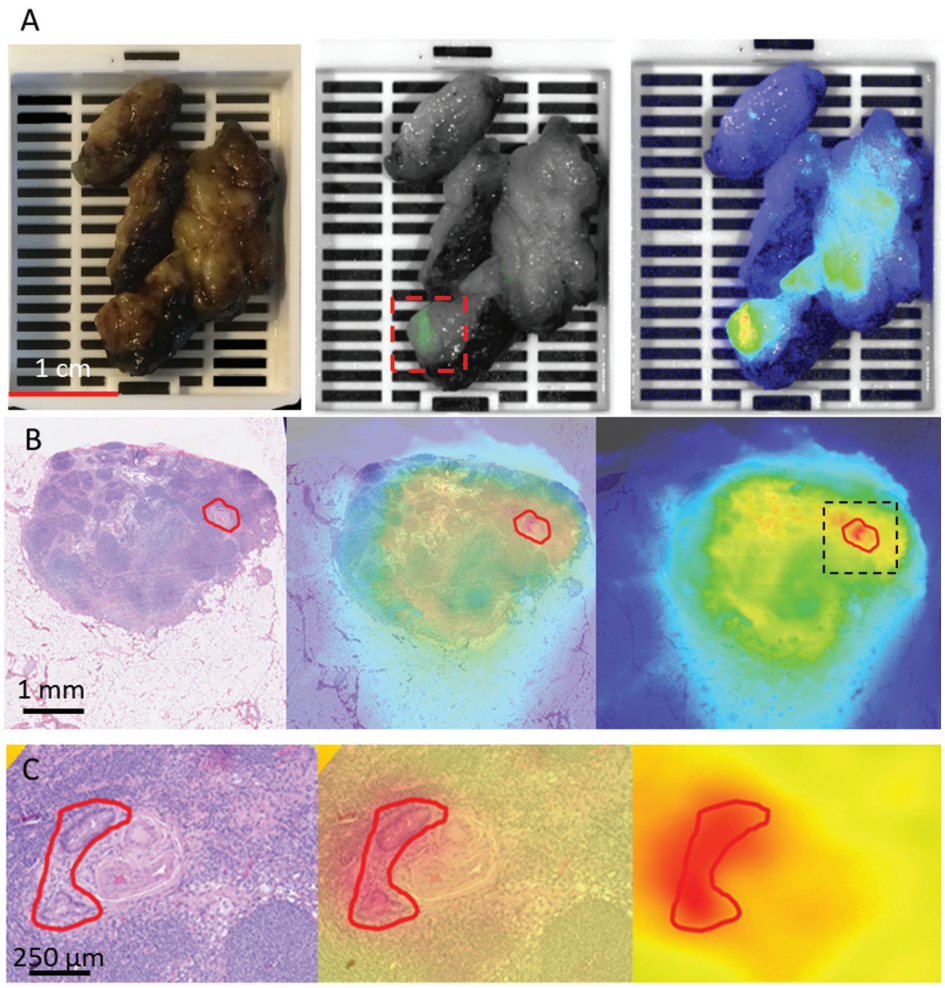



**Figure 5. Detection of occult tumor deposits within lymph nodes**. Figure 5A shows resected peripancreatic fat with an embedded lymph node ex vivo in bright light, overlay fluorescence mode, and heat-map fluorescence mode (respectively from left to right). In figure 5B the fluorescence part (red dotted box) is visualized at the microscopic level with the tumor section outlined. An overlay is created between the H&E and the fluorescence image in three steps showing high fluorescence only at the location of the occult tumor (black dotted box). In figure 5C, the two tumor foci are visualized in more detail with the same method of overlaying the H&E and fluorescence image, demonstrating the ability of fluorescence to detect tumor deposits of only 0.5 x 0.25 mm in size.

difference in MFI was seen in the low-dose cohort between tumor-positive lymph nodes (250.4±33.9) and tumor-negative lymph nodes (76.4±5.1) ($p<0.001$) (Figure 4A). The same was true for the high-dose cohort, but a smaller difference in MFI between tumor-positive and tumor-negative lymph nodes (182.5±19.0 and

126.9±11.9, respectively) was noted (p=0.03) (Figure 4B). The test characteristics for the microscopic detection of tumor using targeted fluorescence imaging for the low-dose cohort included sensitivity of 91.4% (C.I. 76.4 – 96.4) and specificity of 66.3% (C.I. 61.6 – 70.8). In the high-dose cohort, the specificity was relatively low due to high frequencies of false-positive detection in the lymph nodes (34.8%, C.I. 26.2 – 44.1), though sensitivity was higher (93.1%, 77.2 – 99.2) (Figure 4C).

### *Imaging of occult tumor in lymph nodes*

For intraoperative fluorescence to augment current intraoperative techniques used by the surgeon (palpation, inspection), it should allow for the detection of subclinical/occult tumors. Therefore, it is important that even lymph nodes that contain "microscopic" amounts of tumor can be detected by fluorescence (Figure 5A). When analyzing the fluorescence data at the microscopic level, even sub-millimeter tumor lesions of 0.25 by 0.5 mm (e.g. 2 tumor glands in close proximity) were detected using fluorescence (Figure 5B and 5C). Of the 17 lymph nodes with "occult" tumor (defined as tumor foci < 5 mm in size), 15 were detected by fluorescence, and 2 were not, resulting in a sensitivity of 88.2%. The amount of tumor in the two non-fluorescent lymph nodes was comparable to the fluorescent lymph nodes (0.83 mm vs 1.98 mm, p = 0.425).

### *Non-specific drainage of fluorescent agent*

In the high dose cohort, a significant amount of false-positive lymph nodes were seen. Additional sectioning and pathologic analysis of these false-positive nodes did not reveal occult tumor not identified at initial pathological review. We, therefore, hypothesized that this was due to the tumor-bound cetuximab-IRDye800 leaking non-specifically out of the tumor, into the regional lymphatic nodal basin. To examine this hypothesis, we looked into the localization of fluorescence within these false-positive lymph nodes and the relationship with D2-40 immunostaining (a marker of lymphatic endothelium). We identified that areas of high (false-positive) fluorescence corresponded to enlarged lymphatics, as highlighted by D2-40 staining (Figure 6).

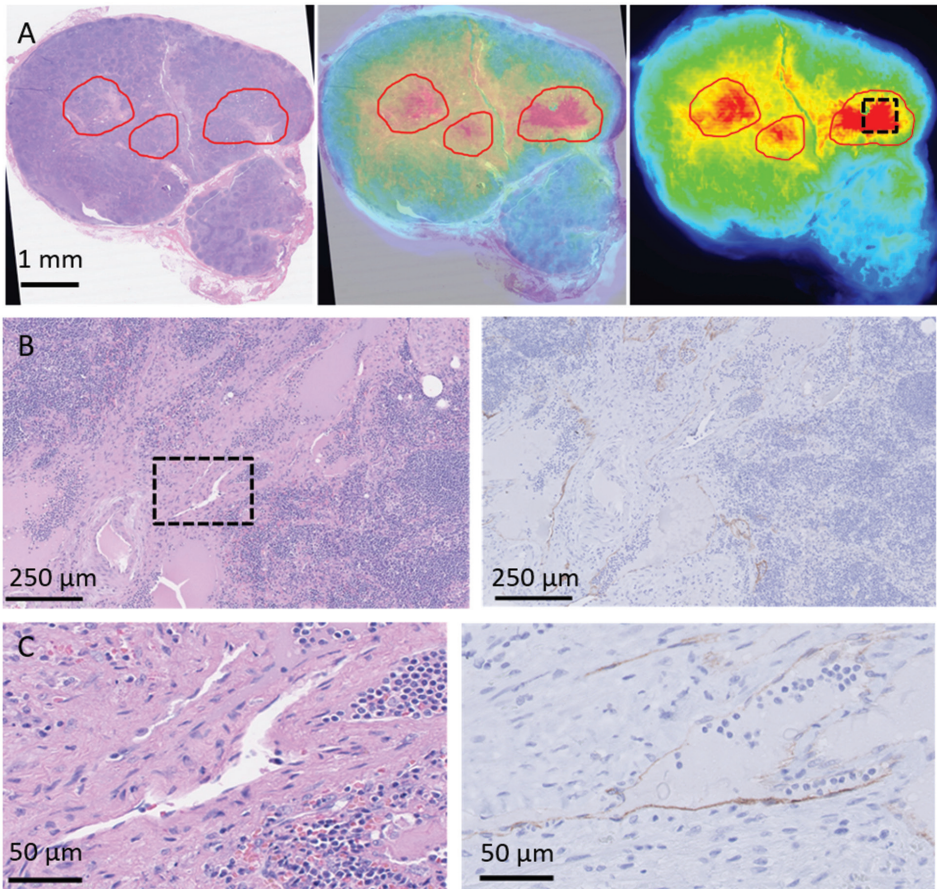



**Figure 6. Non-specific drainage pattern in false-positive lymph nodes**. Fluorescence and H&E overlays are shown with high fluorescence at position of lymphatic vessels (Figure 6A) in a patient who received the high-dose (100 mg) of cetuximab-IRdye800. In Figure 6B, a magnification of an area with high fluorescence (black dotted box) is shown, together with a D2-40 immunostain, which is a marker of lymphatic epithelium. In figure 6C this area is magnified further to shown co-localization of D2-40 staining (Figure 6C).

## DISCUSSION

In this prospective dose escalation study of patients undergoing pancreatectomy for PDAC, we showed that in the low-dose cohort (50 mg of cetuximab-IRDye800) tumor-targeted fluorescent imaging identified tumor-positive lymph nodes *ex vivo* with a sensitivity of 100% and specificity of 78%. At the microscopic level, the sensitivity of the method was 91% and specificity was 66%. If the

high-sensitivity of this method can be replicated *in vivo* with improved surgical imaging equipment, this information can be used to improve intraoperative management and decision making. Specifically, if the fluorescently detected (but otherwise occult) node is located at distant site (and is conformed to be involved on frozen section), the resection can be aborted. Alternatively, if the detected node is considered locoregional, the resection can be extended to include this nodal basin and achieve a more complete resection.

Four prospective randomized trials, two from the US,[6-8] one from Europe[10] and one from Asia[9] have previously tried to answer the question of whether an extended lymph node dissection - including periaortic, renal hilum, upper hepatoduodenal, celiac, and superior mesenteric artery (N2) nodes – for all patients undergoing surgery for PDAC is associated with oncologic benefit. In aggregate, these studies included 424 patients and showed that the number of resected lymph nodes was significantly higher in the pancreaticoduodenectomy with extended lymphadenectomy group compared with the standard lymph node dissection group. Morbidity and mortality rates were comparable. In none of these trials, however, was a benefit in long-term survival demonstrated with extended lymphadenectomy. In accordance with these studies, we do not advocate routine performance of extended lymph node dissection in patients undergoing resection of PDAC. However, we view intraoperative molecularly targeted fluorescent imaging as a tool to identify the subset of patients with tumor-positive nodes remaining in the resection bed. The surgeon can proceed with their resection if they are felt to be locoregional sites of disease. In two of the aforementioned trials,[6-8] metastasis was noted in 15% and 29% of these second-order (N2 nodes) in the extended lymphadenectomy group. We feel that intraoperative fluorescent imaging may be a promising tool that can identify this exact subset of patients where disease would have otherwise been left in situ in the resection bed after a standard resection/lymphadenectomy, and where additional nodal dissection may ensure a more complete resection. Along the same lines, this “extended” lymphadenectomy does not have to be comprehensive to include all aforementioned N2 lymph node stations, but selective and targeted to include only the fluorescent nodes, thereby minimizing the potential complications and adverse events associated with more aggressive lymph node dissections. We envision this tool as a step closer to precision medicine in pancreatic cancer surgery. Whether this approach of

"precision lymphadenectomy" will be associated with improved long-term survival remains to be determined, however, it is interesting to note that the study of Pedrazzoli et al. showed improved survival for patients undergoing extended lymphadenectomy in an a *posteriori* subset analysis of patients with positive lymph nodes.[10]

Our method of molecularly-targeted fluorescent intraoperative imaging had relatively high sensitivity, but lower specificity for PDAC. Since fluorescent lymph nodes (in M1 sites) would routinely be checked with frozen section analysis during surgery to confirm the presence of cancer before further management decisions are made intraoperatively, we feel that the high number of false-positive lymph nodes is preferred to prevent the possibility of missing occult disease. In addition, one can hypothesize that these nodes may serve as sentinel lymph nodes (the first echelon of lymph nodes to which the tumor drains) in pancreatic cancer surgery with several clinical applications down the line. On the other hand, our method's high sensitivity is extremely important for any intraoperative guidance tool, as the lack of fluorescence in the resection bed (or other distant sites) would be highly reassuring for the absence of residual tumor in these areas.

Perhaps the most novel finding of this study is the demonstrated ability of our method to detect subclinical, occult foci of tumor within a lymph node that macroscopically appears normal. The fact that this technique could readily identify tumor deposits of 0.5 x 0.25 mm *ex vivo* could potentially have significant implications in the surgical management of patients with PDAC. Obviously, the sensitivity of this method to detect such occult foci of disease *ex vivo* should be replicated *in vivo* before one can definitively comment on the potential clinical utility of this tool intraoperatively.

As noted above, the main limitation of this study is that all analyzed images to determine the detection threshold for tumor-positive lymph nodes were obtained *ex vivo*. In our previous study, we have shown that it is possible to detect PDAC intra-operatively using clinically available cameras.[5] The smallest tumor size we could detect *in vivo* was a lymph node of 3.0 x 1.2 x 1.0 cm, containing several tumor lesions of different sizes on H&E with the largest focus being 6.8 x 5.6 mm. At this point, the intra-operative fluorescence cameras are not sensitive

enough to detect small amounts of tumor like those used *ex vivo*. The closed-field fluorescent PEARL camera is a highly sensitive camera for imaging of fresh tissue *ex vivo*, and together with the Odyssey NIR fluorescence scanner, these modalities were able to detect minimal amounts of tumor in surgical specimens. There is an obvious need to develop intraoperative cameras that can also reach this degree of sensitivity. Therefore, future development is warranted to improve the performance of intraoperative cameras, and to develop new imaging agents with higher quantum yields resulting in a more intense fluorescent signal. In the future, we hope to reach the aforementioned detection limits with *in vivo* imaging. An additional limitation is the small sample size of this prospective study. However, even though the number of patients was limited, the number of lymph nodes, both positive and negative, was sufficient to show statistically significant and clinically relevant differences.

## CONCLUSION

In conclusion, this study provides proof of concept that molecularly targeted fluorescence imaging can detect tumor-positive peripancreatic lymph nodes *ex vivo* with high sensitivity, even in the case of visually occult microscopic disease. Therefore, we believe that this technique, if implemented *in vivo,* has the potential to enhance the surgeon's intraoperative "visibility", thereby enabling better intraoperative staging, and perhaps leading to a more precise and targeted lymph node dissection. Having proven the feasibility and efficacy of intraoperative EGFR-directed molecular fluorescence imaging on patients undergoing resection of pancreatic cancer with this study, and a previous study focusing on detection of the main tumor,[5] our group is in the process of initiating a larger prospective study utilizing EGFR-targeted fluorescent imaging, with the main objective of assessing the frequency by which this intervention can change intraoperative management both in terms of expanding the extent of resection or aborting the resection due to metastatic disease.

## FUNDING

We would like to acknowledge support from Stanford Cancer Institute Translational Research Grant, and Intuitive Surgical Clinical Robotics Research Grant. Tummers WS contribution to this work was supported in part by Michaël-van Vloten Fonds, Lisa Waller Hayes Foundation, Jo Kolk Studiefonds, McKinsey Grant, and Ketel1 Studiefonds.

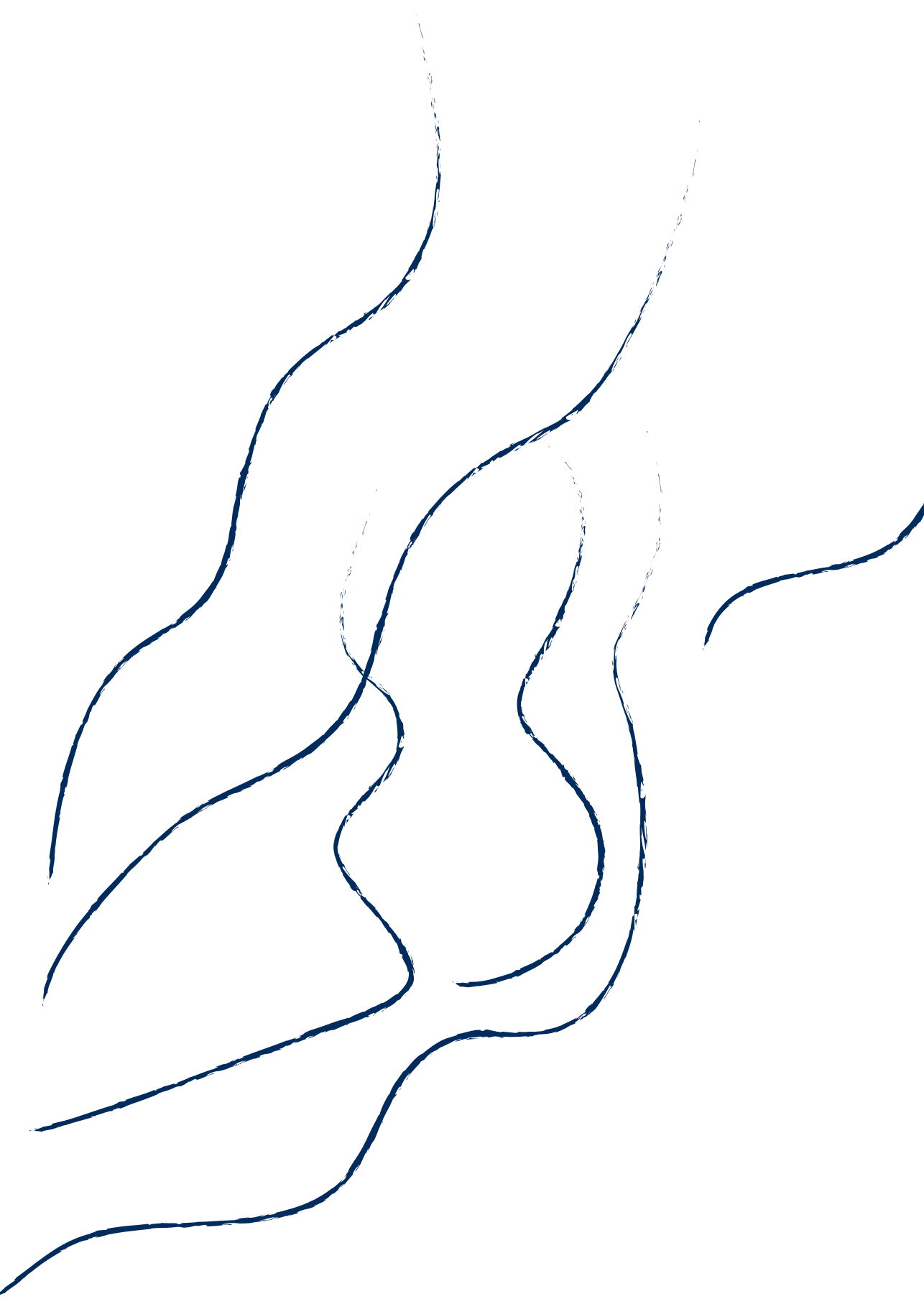
# REFERENCES


1. Iacobuzio-Donahue, C.A., et al., DPC4 gene status of the primary carcinoma correlates with patterns of failure in patients with pancreatic cancer. J Clin Oncol, 2009. 27(11): p. 1806-13.
2. Winter, J.M., et al., Survival after resection of pancreatic adenocarcinoma: results from a single institution over three decades. Ann Surg Oncol, 2012. 19(1): p. 169-75.
3. Warram, J.M., et al., Fluorescence imaging to localize head and neck squamous cell carcinoma for enhanced pathological assessment. J Pathol Clin Res, 2016. 2(2): p. 104-12.
4. Rosenthal, E.L., et al., Safety and Tumor-specificity of Cetuximab-IRDye800 for Surgical Navigation in Head and Neck Cancer. Clin Cancer Res, 2015.
5. Tummers, W.S., et al., Intraoperative Pancreatic Cancer Detection Using Tumor-Specific Multimodality Molecular Imaging. Ann Surg Oncol, 2018. in press.
6. Yeo, C.J., et al., Pancreaticoduodenectomy with or without distal gastrectomy and extended retroperitoneal lymphadenectomy for periampullary adenocarcinoma, part 2: randomized controlled trial evaluating survival, morbidity, and mortality. Ann Surg, 2002. 236(3): p. 355-66; discussion 366-8.
7. Yeo, C.J., et al., Pancreaticoduodenectomy with or without extended retroperitoneal lymphadenectomy for periampullary adenocarcinoma: comparison of morbidity and mortality and short-term outcome. Ann Surg, 1999. 229(5): p. 613-22; discussion 622-4.
8. Farnell, M.B., et al., A prospective randomized trial comparing standard pancreatoduodenectomy with pancreatoduodenectomy with extended lymphadenectomy in resectable pancreatic head adenocarcinoma. Surgery, 2005. 138(4): p. 618-28; discussion 628-30.
9. Nimura, Y., et al., Standard versus extended lymphadenectomy in radical pancreatoduodenectomy for ductal adenocarcinoma of the head of the pancreas: long-term results of a Japanese multicenter randomized controlled trial. J Hepatobiliary Pancreat Sci, 2012. 19(3): p. 230-41.
10. Pedrazzoli, S., et al., Standard versus extended lymphadenectomy associated with pancreatoduodenectomy in the surgical treatment of adenocarcinoma of the head of the pancreas: a multicenter, prospective, randomized study. Lymphadenectomy Study Group. Ann Surg, 1998. 228(4): p. 508-17.
11. de Geus, S.W., et al., Selecting Tumor-Specific Molecular Targets in Pancreatic Adenocarcinoma: Paving the Way for Image-Guided Pancreatic Surgery. Mol Imaging Biol, 2016. 18(6): p. 807-819.
12. Tummers, W.S., et al., Selection of optimal molecular targets for tumor-specific imaging in pancreatic ductal adenocarcinoma. Oncotarget, 2017. 8(34): p. 56816-56828.
13. Rosenthal, E.L., et al., Safety and Tumor Specificity of Cetuximab-IRDye800 for Surgical Navigation in Head and Neck Cancer. Clin Cancer Res, 2015. 21(16): p. 3658-66.
14. Moore, L.S., et al., Effects of an Unlabeled Loading Dose on Tumor-Specific Uptake of a Fluorescently Labeled Antibody for Optical Surgical Navigation. Mol Imaging Biol, 2016.
15. Zinn, K.R., et al., IND-directed safety and biodistribution study of intravenously injected cetuximab-IRDye800 in cynomolgus macaques. Mol Imaging Biol, 2015. 17(1): p. 49-57.



Part | V

# Future Directions for Targeted Molecular Imaging



Chapter | 12

# Recommendations for reporting on emerging optical imaging agents to promote clinical approval

Willemieke S. Tummers [1 2], Jason M Warram [3], Nynke S. van den Berg [4], Sarah E. Miller [4], Rutger-Jan Swijnenburg [2], Alexander L. Vahrmeijer [2], Eben L. Rosenthal [4]

[1] Department of Radiology, Molecular Imaging Program, Stanford University, Stanford, CA.
[2] Department of Surgery, Leiden University Medical Center, Leiden, Netherlands.
[3] Department of Otolaryngology, University of Alabama at Birmingham, AL
[4] Department of Otolaryngology, Stanford University, Stanford, CA.

*Theranostics, Accepted, August 2018*

## ABSTRACT

Intraoperative fluorescence imaging is particularly well-suited for surgical applications due to its inherently high sensitivity, resolution, and ability to provide images in real-time. To date, the intraoperative observation of fluorescence has largely been subjective. With the need to show objective evidence in order to demonstrate the benefit of this technique, quantitative data needs to be provided to the overseeing regulatory bodies. Standardization in fluorescent imaging protocols would improve reproducibility and minimize inter- and intra-institution variance. This would allow studies to be conducted using the same injection techniques, imaging times, reconstruction methods, and analyses. Here, we provide recommendations for standardized methodologies with the goal of setting a minimum requirement for reporting fluorescence-guided surgery results based on both qualitative and (semi-) quantitative data collection. Clinical trials using fluorescence-guided surgery should present results of three critical elements; 1) intra-operative imaging, 2) specimen mapping and pathology correlation, and 3) target validation. Qualitative analyses should consist of a bright field image, black-and-white fluorescent image, pseudo-colored fluorescent overlay image, and/or heat-map whereby fluorescent signal intensity differences are displayed on a color spectrum. Quantitative analyses should include 1) intraoperative data (consisting of images or video, raw numeric values and ratios); 2) specimen mapping, for correlation of fluorescence with the presence of disease (performed using fresh tissue); and 3) target validation (designed to determine fluorescent intensity relative to receptor density of a specific area). Including the aforementioned methods of both qualitative and quantitative analyses will ensure that trial results are comparable and could be collated in future studies to expedite FDA approval.

## INTRODUCTION

An incremental improvement in oncologic surgical outcomes can be obtained by successful identification of visually occult disease and tumor-positive margins during surgery, which will have a significant impact on overall cancer survival. Interest in cancer-specific intraoperative molecular imaging has undergone rapid growth. This substantial interest is not surprising considering the robust potential of the technique to achieve subclinical tumor-detection and improved surgical guidance. Fluorescence-guided surgery (FGS) is particularly well-suited for surgical applications due to its inherently high sensitivity, resolution, and ability to provide images in real-time.[1] In recent years, the number of early phase clinical trials using FGS has drastically risen, and shifted towards the use of dyes emitting in the near-infrared fluorescent rather than in the visible part of the light spectrum. An example of a commonly used near-infrared fluorescent (NIRF) dye is indocyanine green (ICG). ICG achieves its tumor-targeting through "second window imaging," which is based on the enhanced permeability and retention (EPR) effect.[2, 3] While safe, ICG is a non-specific agent that is rapidly cleared by the liver and excreted in bile. Currently, most strategies use a NIRF dye which is conjugated to a targeting vehicle directed against a tissue of interest, such as a tumor-specific agent, and this combination permits optimal cancer-specific detection.[4, 5] However, human testing using such novel NIRF-guided surgical agents has thus far only been conducted in early phase trials to establish safety and efficacy.[6-13] These trials are unable to show benefit over the current standard-of-care; larger phase II/III trials are needed to demonstrate superiority prior to obtaining regulatory approval and wide-spread adoption into practice. Early stage clinical trials are crucial to providing data to support *in vivo* application, surgical specimen mapping, and target validation. These three elements should be evaluated using a standardized methodology that can be used to advance these technologies through regulatory pathways into routine clinical use.

Positron emission tomography (PET) imaging represents a clear precedent for the introduction of standardization into FGS. Since its establishment in 1984, numerous articles have been published describing the need for standardization of the technology with regards to clinical application.[14-16] These studies showed that strict standardization of all aspects of imaging and data analysis is required

to obtain quantitative, accurate, reliable, precise and reproducible results. Similarly, multiple studies have been performed investigating the concordance of PET results obtained at different institutions.[15, 17, 18] Developing a standardized approach will minimize variability between studies in addition to facilitating the development of multicenter studies, thus allowing for direct comparison of results within and between clinical trials. Moreover, it can potentially allow for future direct translation of results to other centers.

Although often difficult to test in clinical trials, the qualitative representation of fluorescence imaging data is critical, as surgeons make intraoperative decisions based on their own interpretation of images generated and displayed by the imaging device. To be valuable, high-resolution images need to be generated in real-time, without delayed image processing. In many cases, the value and objectivity of qualitative data is questioned, though in the case of FGS its representation is of the utmost importance to the technology's implementation and utility.

Simultaneously, quantitative data plays a key role in the analysis of FGS clinical trials. Currently, quantitative data is difficult to generate as compared to qualitative data, and since FGS is primarily a visual tool for the surgeon, the use of quantitative data has been less emphasized in the first early phase clinical trials. However, with the need to show objective evidence to demonstrate the superiority of FGS techniques, quantitative data should also be provided to the regulatory bodies.

Here, we propose a methodology for reporting results from fluorescence-guided oncologic surgery studies (Figure 1). Our proposed method is based on the minimum requirements for the presented data from all phases of a clinical trial, including intraoperative imaging, *ex vivo* imaging, and pathologic correlation, which should be represented using both qualitative and quantitative data.

## QUANTITATIVE DATA

*In vivo* fluorescence quantification is challenging, since the measured fluorescence depends not only on the concentration of the imaging agent,

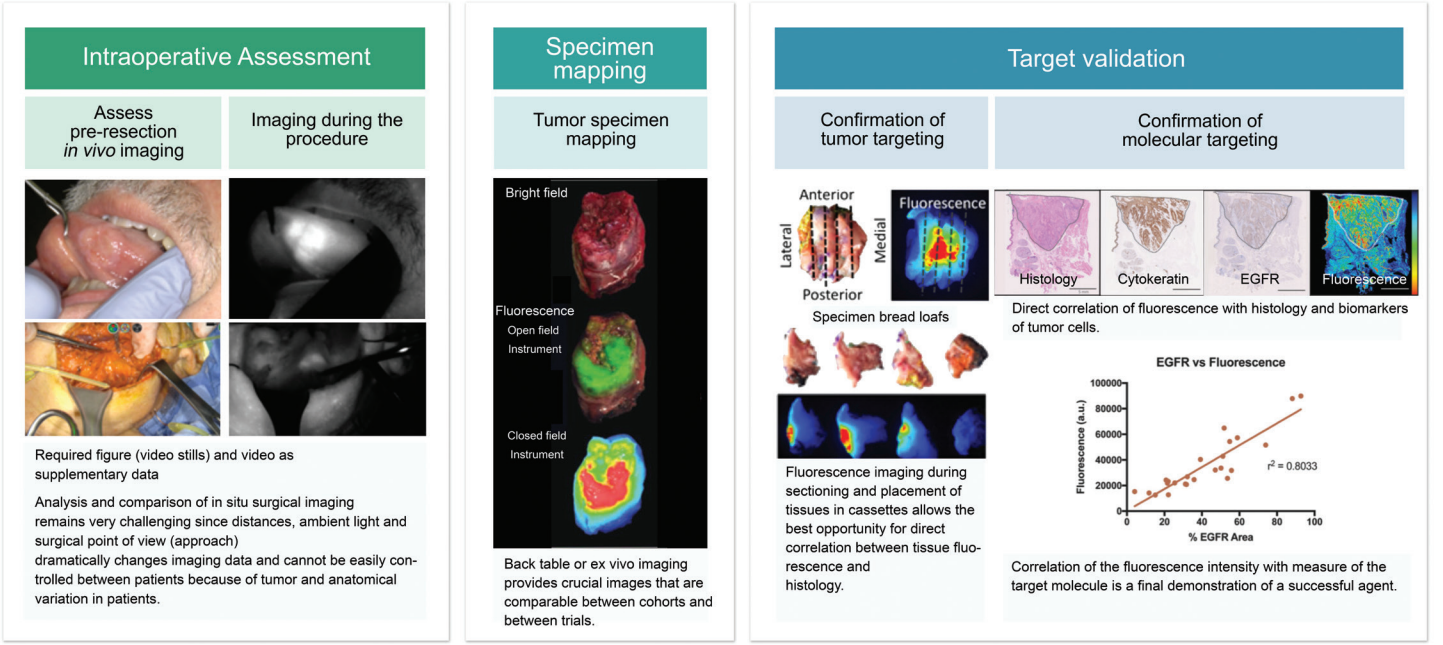



**Figure 1.** Standardized assessment of reporting results in fluorescence-guided oncologic surgical trials for all aspects of the clinical trial; intraoperative imaging, *ex vivo* imaging and pathologic assessment. During the intraoperative assessment, focus should remain on imaging at predetermined timepoints intraoperatively. *Ex vivo* imaging will ensure exact tumor mapping to correlate imaging results to pathology. During pathologic assessment the focus should be on confirmation of fluorescence targeting to tumor tissue [adapted from Gao RW et al. Cancer Res. 2018 Jul 2]

but on multiple parameters, such as intrinsic autofluorescence of tissue, the sensitivity of the imaging device, the absorption and scattering properties of the tissue, and photobleaching. All these parameters can influence the accuracy of quantification.[19-21] Standardization of quantification in fluorescence imaging protocols would improve reproducibility and minimize inter- and intra-institution variance, and studies should be conducted using the same injection technique, imaging time, reconstruction method, and analysis.[14] Such strategies are critical for reproducibility in multi-institutional clinical trials but are not easy to achieve. Use of phantoms will be beneficial to determine how well individual cameras and centers perform in the technical aspects of image acquisition, data processing, and analysis.[22] In multicenter studies using PET imaging, the submission of a phantom scan is usually required periodically for scanner calibration and reproducibility.[23]

Perhaps the largest research effort to quantify fluorescence *in vivo* has been focused on the measurement of photosensitizer concentration prior to and during photodynamic therapy (PDT).[20, 21, 24, 25] Because the effect of PDT depends directly on the concentration of sensitizer used, there is a high need for measuring this quantity quickly and noninvasively.[20] Kim et. al describe a noninvasive *in vivo* method to determine fluorophore concentration in neurosurgery using 5-ALA.[19] Using a fiber-optic probe, the fluorophore concentration is calculated from the quantitative fluorescent spectrum, which is the fluorescent emission spectrum corrected for optical attenuation of the tissue, thus quantifying the observed fluorescence.[19] These handheld fiber-optic probes need to simultaneously collect tissue fluorescence and diffuse reflectance spectra *in vivo*.[26] The method is performed using specific fiber-optic probes that touch the tissue, which requires a separate device in combination with the fluorescent camera for intra-operative navigation. Another complicating factor of this method is the need to identify the optical properties of tissues and the variation of these properties which are mostly unknown.[26]

Achieving absolute *in vivo* quantification is unlikely, since the current fluorescence imaging systems are not equipped to generate quantified imaging data, but a semi-quantification of the fluorescent signal should be possible. Similar as to in PET imaging, where maximum standard uptake values ($SUV_{max}$) are calculated based on the administered radioisotope dose and the patient

weight, one can also calculate fluorescent signal uptake values by correcting for tissue surface area.[10] In fluorescence imaging, only fluorescence arising from <1 cm depth will contribute to the measured signal. Therefore, signal should be corrected for surface area since corrections either for weight or volume will not necessarily generate a representative value. Consequently, it is recommended for fluorescence imaging to provide standardized reports on surface area-adjusted values where feasibly measured by *ex vivo* imaging. For example, adjusted from the formula for SUV values, mean fluorescence intensity (MFI) could be calculated as $MFI_{corrected}$ = fluorescence intensity of tissue of interest / (injected dose/surface area of the tissue).[27]

As described above, quantification of fluorescent signal is still in its infancy. Ultimately, it is expected that this objective measure is going to play a major role in providing evidence of patient benefit. Next to the extensive investments in novel agents and clinical cameras, innovative solutions are being developed for the quantification of fluorescent imaging signals in the *ex vivo* setting. Several groups are working on the real-time detection of the actual amount and concentration of the fluorescent agent that accumulates in tissues. By scanning part of the tissue or by taking point measurements, the concentration can be determined leading to exact quantification.[19, 28] Another method to objectify and automate quantification is by machine learning. Here, the software can be trained to identify the fluorescent cut-off value for true-positive fluorescence and true-negative fluorescence. With a learning set, these values can be validated and applied to the all patients injected with the same agent and dose.[29] For now, these methods are not commercially available, and further research is required to validate their applicability, but semi-quantification of the fluorescent signal is already possible without these novel devices using methods described below.



## QUALITY CONTROL PROCEDURES

FGS is intrinsically linked to the sensitivity of the imaging device used. Currently, various imaging systems, ranging from large open-field cameras to minimally-invasive endoscopic cameras, are available for NIRF excitation and emission signal detection during surgery and *ex vivo*. Consequently, results from different imaging systems are hard to compare. This is one of the main reasons

that the FDA primarily reviews combination products, instead of an imaging agent and device separately.[30] This is in contrast to PET agents and scanners, where the implementation of quality control (QC) procedures have led to an established method to verify consistency, linearity, and safety functions of PET scanners. For PET imaging, the National Electrical Manufacturers Association (NEMA) has formulated performance standards, to which manufacturers need to adhere.[31] For fluorescent imaging devices, this is still far from standard practice, with only safety standards currently available. Incorporating documentation on performance testing can help to identify relevant characteristics (e.g., spatial resolution, uniformity, sensitivity, dynamic range), provide guidelines for testing (e.g., phantom material property range/geometry, methods for calculating metrics), and describe viable test methods for the validity of performance characteristics.[30]

## GENERAL ASPECTS OF FLUORESCENT DATA ANALYSIS

Ideally, all acquired FGS data should be analyzed for the correlation between imaging results and pathology using a quantitative and qualitative approach.

### Detection threshold

Targeted agents are usually present in the tissue of interest at nanomolar concentrations, which requires sensitive cameras with low detection thresholds. Analysis of this threshold for different imaging systems and agents is important when evaluating agents for their intended use. If one aims to detect micrometastases, the sensitivity of the camera and the specificity of the agent should both be extremely high. DSouza et al. performed a study to determine the detection limit of various fluorescent imaging systems using dye concentrations in a phantom and showed that devices with higher bit depths, variable electronic gain settings, and background-light correction during acquisition, had the highest sensitivities.[32] Previously, we have shown that small amounts of cancer cells can be detected in optimized *ex vivo* settings both preclinically (2.4 × 104 cells) and clinically (<5mm).[33]

## Quantification parameters

Significant variations can occur when reporting on fluorescent signal intensities since the value remains dependent on the way the images are analyzed. Below we discuss various methods to quantify fluorescent imaging data.

### *Mean fluorescence intensity*

The mean fluorescence intensity (MFI) is a measurement of the fluorescent signal in a region of interest (ROI) divided by the area within that ROI (either in pixels or $cm^2$). The MFI is typically shown in arbitrary units of fluorescence (AU) or total number of photons detected by the device for each pixel, or per $cm^2$. Arbitrary values are generally used for relative, ratiometric quantification to determine the fold difference or change between various samples that are analyzed in parallel. Devices that use a scaled algorithm for determining fluorescent signal also use AU. The MFI can also be shown in relative fluorescent units (RFU), which is a relative unit of measurement compared to a reference measurement using the same ROI area. In PET imaging a defined background is determined to compare to the SUVmax value, in order to determine the presence of increased uptake. As with PET imaging, it may be recommended to use the maximum fluorescent value, since this is independent from an ROI, less observer-dependent, and more reproducible compared to the mean value. The primary disadvantage is that a maximum value is more susceptible to noise. Comparing the maximum fluorescent value to that of a set background (Table 1), may be used to correct for this noise.

### *Tumor-to-background ratio*

When addressing the quality of an imaging agent to provide tumor-specific contrast, it has generally been related to a ratio such as tumor-to-background ratio (TBR), signal-to-noise ratio (SNR) or contrast-to-noise ratio (CNR). In the past, studies aimed for a TBR of >2.5, since it was thought that any lower rate was insufficient to identify cancerous tissue intraoperatively.[2, 34] However, an intraoperative TBR of >2.5 is relatively hard to achieve in a clinical setting with currently available agents and imaging systems, although at this TBR the tumor can be clearly distinguished from the surrounding tissue. While a higher signal in the tumor when compared to surrounding tissue is preferred, there are many other variables that contribute to an agent's ability to differentiate normal from diseased tissues. Therefore, it may not be appropriate to identify a specific

**Table 1**. Suggestions for tissue to appoint as background for quantitative fluorescent imaging analysis

| Cancer type and location | Ideal background | Appropriate background |
|---|---|---|
| **Breast** | Uninvolved breast tissue | Adipose tissue |
| **Head and neck** | Muscle | Skin or mucosa |
| **Colorectal** | Uninvolved bowel serosa | Normal bowel mucosa |
| **Pancreas** | Peritumoral inflammation | Normal pancreatic tissue |
| **Lung** | Uninvolved lung tissue | Skin |
| **Brain** | Uninvolved brain tissue | Uninvolved brain tissue |
| **Hepatocellular and CRLM** | Immature hepatocytes | Uninvolved liver tissue |
| **Prostate** | Uninvolved prostate tissue | Connective tissue |
| **Parathyroid** | Thyroid tissue | Muscle |

number as a minimum value before one can determine there is "sufficient contrast". At a minimum, the difference in signal needs to be high enough for the surgeon to differentiate tumor from normal tissue – in our experience a TBR >3.0 in preclinical studies and >1.5 in clinical studies would be appropriate for further studies.

Another important note is that TBR is highly dependent on the dynamic range of the imaging devices used in addition to the variability in properties of the chosen background tissue. The background will greatly influence the TBR value, and currently no guidelines exist regarding an appropriate background for various cancer types. If unrealistically high values of TBR are set as a standard, it is likely that only surrounding tissues with virtually no fluorescence will be candidates for employing these techniques. However, to ensure clinical applicability of the technique, the background tissue is inherently in close proximity of the tumor even when this tissue displays some intensity of fluorescence. For example, in pancreatic cancer surgery, muscle would not be an appropriate background, whereas for head and neck cancer, muscle would be appropriate based on the surgical field of view (Table 1).

### *Signal-to-noise ratio (SNR)*

The SNR is the quotient of the MFI measured in a ROI and the standard deviation (SD) of the signal intensity in a region outside the boundaries of the object being imaged (i.e. a region from which the tissue's fluorescent signal is zero).[35] There are two forms of noise in images: random and structured. Random noise (or statistical noise) is directly related to the number of signals coming from the imaging agent. Structured noise refers to non-random variations in counting rates. The latter will adversely affect the interpretation and analysis of the images. Examples of structured noise are organ motion, and imaging instrument non-uniformities.[36]

### *Contrast-to-noise ratio (CNR)*

To ensure only contrast through targeted uptake is measured, and contrast through non-specific enhanced-permeability effect (EPR) is excluded, contrast can be quantified by calculating the average signal in the tumor and subtracting the average signal in the selected background tissue. This value can be divided by the standard deviation of the background to estimate the CNR.[37] This technique may be particularly helpful to assess off-target accumulation in non-cancerous tissues that express the biomarker of interest. CNR is especially useful in situations where the background and tumor signals fluctuate widely. In these cases, the TBR value could be the same as compared to a situation with a more constant signal profile. However, the tumor would be more consistently clearly visible in case of a constant pattern. In situations with more fluctuation, CNR would show a difference in value, providing a more representative value that assists in distinguishing true contrast from noise.[37]

When detecting lesions in the body, a high SNR alone will not guarantee that sufficient contrast exists to make the lesion detectable. Therefore, SNR should be used to assess one single image. CNR on the other hand can be used to identify fluctuations within one patient over time as it compares a measure of signal fluctuations to noise. In summary, SNR is a good measure to assess data quality of a single image, and CNR provides knowledge regarding how easy or hard it is to detect signal fluctuations over time.[35]

### Sensitivity and Specificity

A topic of constant debate in the field of FGS is the reporting of test characteristics. Certain groups choose not to report sensitivities and specificities in early phase clinical trials, since the number of patients is insufficient for a powered calculation. Some groups use multiple separate specimens from each patient to generate a sufficient sample size for determining test characteristics. We believe that reporting on sensitivity and specificity in early trials is important in order to determine the potential of the fluorescent imaging agent for FGS. In larger clinical trials in later phases, the additional benefit of sensitivity and specificity should focus on improving or complementing the surgeon's assessment.

## DEMONSTRATION OF VALUE IN EARLY PHASE CLINICAL TRIALS: THREE CRITICAL ELEMENTS

### I. Intraoperative data collection

Real-time fluorescence tumor imaging should demonstrate sufficiently higher contrast enhancement in the tumor relative to surrounding normal structures in order to augment the current standard of care. During minimally-invasive and robotic surgery, this real-time detection of fluorescence is easily integrated as the current technology requires the surgeon to operate using a screen to visualize the surgical field. However, to properly interpret a positive fluorescent signal that will subsequently affect clinical decision-making, consensus should be reached regarding validation of fluorescent markers and imaging devices designed to differentiate tumor from peri-tumoral tissue. To date, an insufficient number of standardized studies have been performed to reach this type of consensus.

Developers of strategies for intraoperative imaging should recognize that the surgical approach varies significantly by tumor type, and that each approach has a unique workflow. The incorporation of intraoperative FGS into the surgical workflow will be individualized to the type of procedure being performed, and the type of cancer being resected. For example, in the case of ovarian cancer, brain cancer or peritoneal metastases during a cytoreduction and hyperthermic intraperitoneal chemotherapy procedure (HIPEC), the primary goal is a more

complete debulking.[38] In these cancer types, it is known that extensive debulking leads to prolonged survival for patients.[39] Here, FGS has the potential to be beneficial in identification of subclinical disease, or occult tumor deposits.[12] For other tumor types, complete resection is the key to prolonged survival. In these situations, FGS will play a crucial role in assessing the resection bed for residual tumor after initial resection or to assess the margins of the specimen.[6, 9, 11, 13] Next steps in treatment could be informed by the presence of residual fluorescence, warranting either further resection or, for example, novel techniques such as applying PDT to the resection bed.[40]

Intraoperatively, FGS is particularly important for: 1) Identification of tumor; 2) Assessment of resection margins, both before the resection for operative planning and after to assess the wound bed; and 3) Detection of tumor-positive lymph nodes, especially in locations that would suggest metastatic disease. In this case, for example, FGS could inform clinical decision making by aborting a surgery when there is no oncologic benefit.

### *Margin assessment in the OR*

One of the biggest gaps in oncologic surgery remains the high rate of positive margins following surgical resections, which directly correlates with poor survival and locoregional recurrence.[41-43] Both the *in vivo* assessment of the resection bed and the *ex vivo* assessment of the specimen are critical to ensure negative margins. The current approach to margin assessment in most tumor types is circumferential analysis of the resected specimen using frozen sections.[44] Therefore, only a fraction of the tumor mass can be analyzed due to the limited sampling that is feasible with frozen sectioning. A tumor-specific fluorescent contrast agent can be leveraged to perform fluorescent mapping of the surgical specimen. Fluorescent 'hot spots' could be used to direct clinicians toward suspicious regions, and thereby reduce sampling error. The detection of a fluorescent signal using back-table benchtop devices could also result in reduction of time needed for specimen analysis, since sampling can be performed based on fluorescent positive areas, as opposed to sampling all surfaces of a large tumor specimen (i.e. hepatic tumor resections).

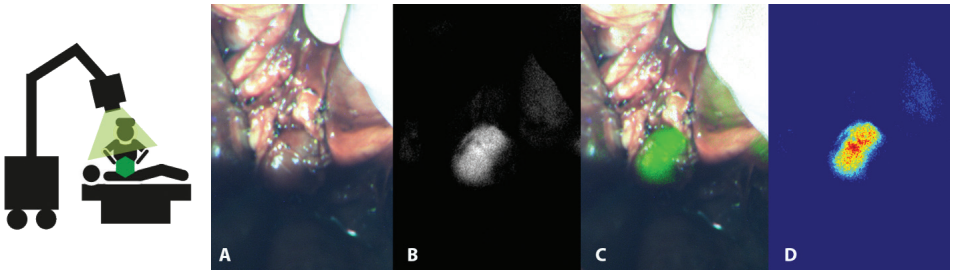



**Figure 2.** Suggested method of reporting intra-operative imaging results. This includes a bright field image (A), black-and-white fluorescent image (B), fluorescent overlay image (C), and fluorescent heat-map (D). In this case, an example of a tumor-positive lymph node during abdominal surgery is shown.

### *Data representation from intraoperative imaging*

During surgery, fluorescence imaging should be performed at multiple fixed time points as outlined in the clinical trial protocol and standard operation procedure (SOP). For example, one can identify three imaging time points to be used in most trials; first, while scanning the area of interest for the localization of the primary tumor and/or detection of metastases prior to excision. Second, once the tumor has been exposed while still *in situ*, with surrounding normal tissue in the field of view. And third, after resection of the primary tumor for assessment of the wound bed. During surgery, both endoscopic and open-field imaging systems can be used. In some operative cases, such as an abdominal laparotomy that is converted to an open procedure, both systems can be used at different timepoints. Since the two devices will generate data that is not necessarily comparable, it is important to clearly state which device's data will be used in a clinical trial and document this in the SOP. Depending on the capabilities of the fluorescent camera, multiple images should be obtained in each setting; a bright field image, a black-and-white fluorescent image, a pseudo-colored fluorescent overlay image, and/or a heat-map whereby fluorescent signal intensity differences are displayed in different colors (Figure 2). *Ex vivo* imaging of fresh tissue should be presented in a similar manner. Quantitative data of intraoperative images should consist of a numeric value representing fluorescent signal. This can either be reported in MFI values or in a ratio such as TBR.

The development process of an optimal intraoperative imaging strategy should keep in mind the specific nature of the surgical workflow in order to minimize

interruptions and facilitate the adoption of this technology. Early phase clinical trials are designed to demonstrate the safety, appropriate dose and tumor specificity of experimental agents. For these trials, the secondary outcomes primarily focus on the tumor-specific contrast that is generated between tumor tissue and background tissue using the agent-device combination. Regulatory standards ensure the workflow of these early phase trials maintain the standard of care, which makes it difficult to objectively assess the potential clinical value and patient benefit of FGS. For larger clinical trials, clinically relevant endpoints that necessitate experimental assessment will be needed to demonstrate superiority to the current standard of care. Examples of secondary endpoints include improved detection of tumor-positive margins, decreased morbidity, reduced local recurrence, or increased efficiency in the operating room.[30] These endpoints can be directly correlated with known statistics pertaining to survival, thereby demonstrating clinical benefit.

It is important to recognize that the success of these trials will be influenced by the parameters of the clinical imaging devices employed. Not all imaging devices are able to show a TBR in real-time, and the significant differences in sensitivity among the various devices will make it challenging to achieve consistency and compare results regarding the clinical utility of tumor-specific contrast agents. Another limitation that should be recognized is the inability to directly correlate intraoperative images with pathology results in real-time. Therefore, dependence on *ex vivo* imaging to confirm tumor status will remain a critical component of FGS validation, especially in early phase clinical trials where confirmation of tumor specificity is critical. To circumvent this limitation, *ex vivo* imaging can be done in the form of back-table fluorescence imaging in the operating room using either a clinical camera, or a bench-top device, developed for this purpose. These results can later be directly correlated to the pathological assessment.[6-13]



## II. Specimen Mapping

An important stage in the validation of FGS is the correlation of the fluorescent imaging-based results with the pathologic findings, which is used to determine if the fluorescent signal is specifically localizing to the tumor. It is recommended that the correlation be performed in a standardized and rigorous method as described in Figure 3. After analysis of the resected fresh tissue, the surgical

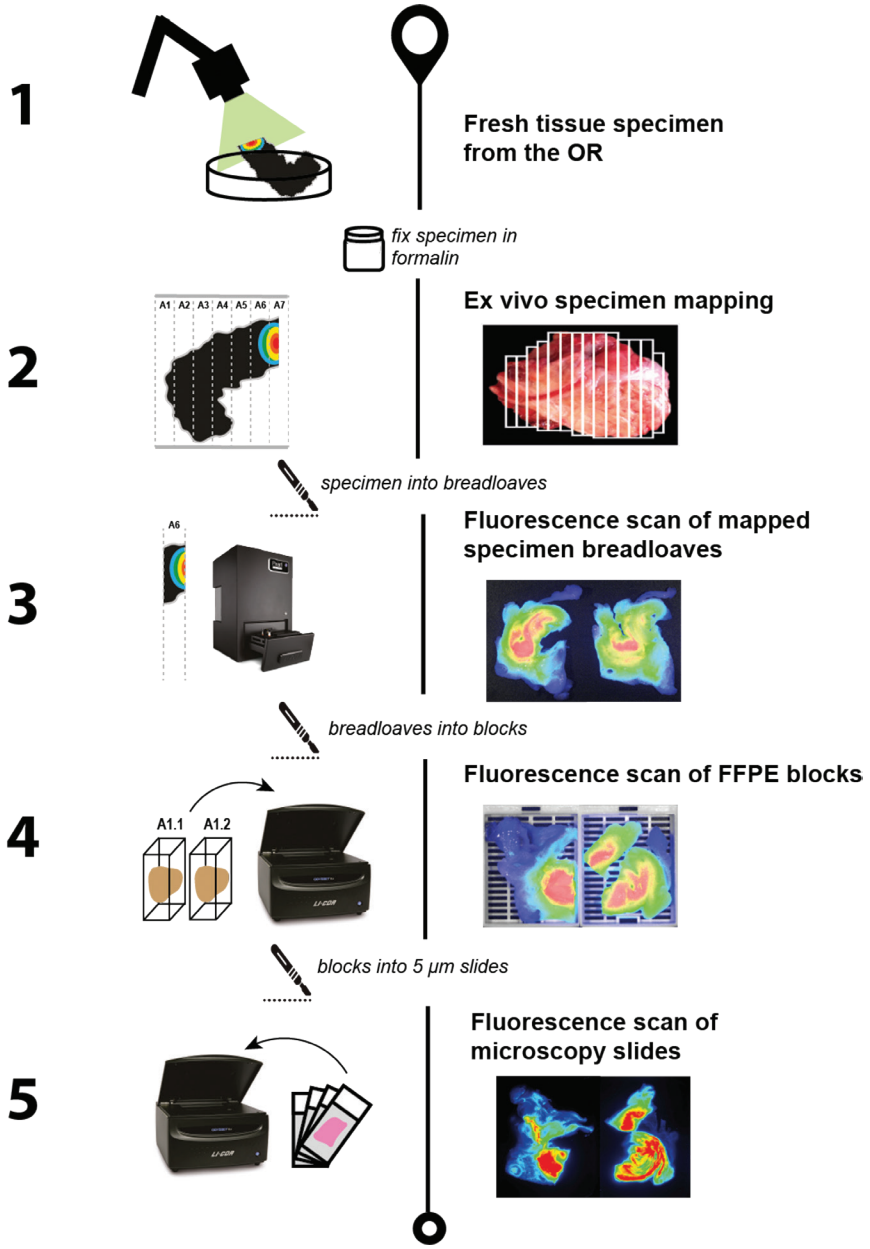



**Figure 3**. Detailed overview using a clinical example of the *ex vivo* mapping process of a surgical specimen to ensure exact correlation of the surgical specimen with pathologic assessment. During step 1 the fresh tissue specimen is imaged *ex vivo* to ensure images from all angles. After formalin fixation, the specimen is mapped and sliced into bread loaves in step 2. Fluorescence imaging is subsequently performed of the bread loaves separately. In step 4 cassettes are made that include one bread loaf each and are imaged either on a fluorescence scanner or in a closed-field imaging system. The cassettes are then paraffin-embedded and sectioned to produce microscopy slides. In step 5, these slides are used for pathologic assessment and fluorescence scanning.

specimen is processed into bread loaves (either before or after formalin-fixation) and later into blocks to be placed in cassettes (Figure 3). These cassettes are then imaged on a fluorescent scanner both before and after paraffin embedding. Finally, these cassettes are processed into microscopy slides where fluorescence can then be correlated with hematoxylin and eosin (H&E) histopathology. These steps are possible when the fluorescent capabilities of the probe are maintained after formalin-fixation. Additional immunohistochemical correlation of the target of interest and H&E should be performed to determine co-localization of the target and fluorescence, which will be discussed later.

### *Mapping process of the gross surgical specimen*

To facilitate the processing of the specimen, a bright-field image of the gross surgical specimen can be acquired and used as a reference map as the specimen is sectioned and placed into cassettes. The origin of the cassette-specific sections can be drawn on a printed or digital image of the primary specimen and saved for later correlation at the time of histopathologic study. This methodology is commonly employed during pathological processing of large surgical specimens. Precise imaging of the gross specimen and close correlation with histopathologic sections increases the efficiency and accuracy of pathologic assessment and enables consistent and accurate interpretation of the technique's specificity. This method is anecdotally used during Mohs surgery and is also described in the standardized pathologic assessment of breast cancer specimens.[45] It is important to maintain the specimen orientation relative to the patient so that the slide-mounted section can be registered back to the primary specimen, and ultimately to the wound bed. This approach will allow the clinician to determine if fluorescence observed on either the resected specimen or in the wound bed is clinically relevant and a source of potential recurrence.



### *Data representation of ex vivo imaging*

After removal from the patient, the fresh specimen is imaged at the back-table using a benchtop device or the surgical camera. Fresh tissue should be imaged when possible and fluorescent intensity should be expressed relative surface area of the specimen.

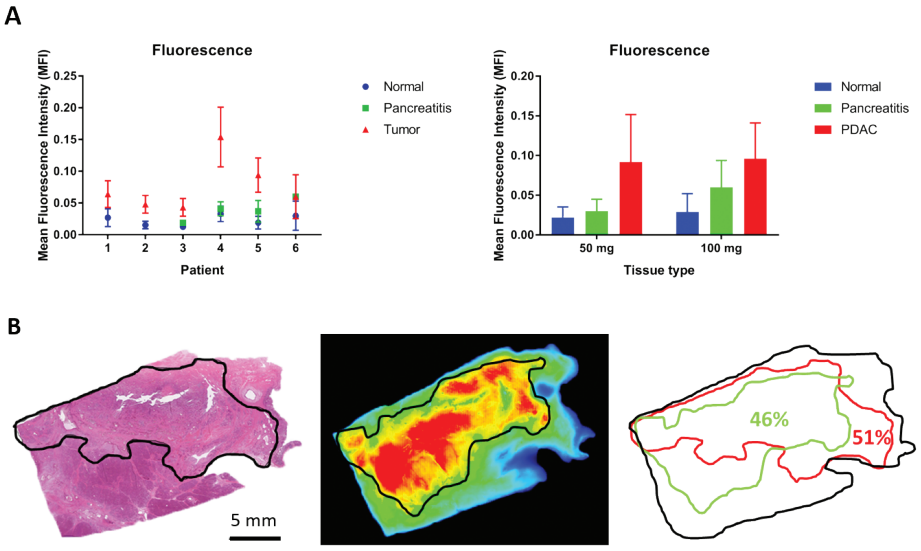



**Figure 4.** Quantitative analysis of *ex vivo* imaging. Quantitative analysis of formalin-fixed tissue can be performed in several ways. Two examples are shown here. (A) a quantitative comparison using the calculated MFI could be performed between tumor tissue and normal surrounding tissue, either per patient or per dose cohort. (B) a semi-quantitative scoring method could be used to determine the percentage of fluorescent tissue, compared to the percentage of tumor tissue per tissue block.

After imaging the fresh surgical specimen, the tissue should be formalin-fixed prior to being processed into bread loaves. Formalin-fixed tissue can still be used for qualitative and quantitative analysis of fluorescent imaging signal, in contrast to paraffin-embedded tissue which is more suitable for qualitative data analysis. Cassetted, formalin-fixed tissues are ideal for identification of complex tumor-containing tissues since both the orientation and size are matched to the hematxoylina and eosing (H&E) stained slide of that specific block after paraffin embedding.

Quantitative analysis of formalin-fixed tissue can be performed in two ways. First, an absolute quantitative comparison of MFI from the raw data can be performed between tumor tissue and normal surrounding tissue, either per patient or per dose cohort, as demonstrated by an example in pancreatic cancer in Figure 4A. Alternatively, a semi-quantitative scoring method could be used to determine the percentage of fluorescent tissue, compared to the percentage of tumor tissue per tissue block (Figure 4B). The amount of tumor tissue can be assessed on the H&E slide from a particular block, while fluorescence can be

measured either with a fluorescent scanner or a closed-field imaging device of a deparaffinized slide.Qualitative representation of *ex vivo* imaging preferably includes images of the *ex vivo* specimen, a bread loaf slice and the corresponding cassette to ensure correlation, as also shown in Figure 3. In this context, the bright field image, a black-and-white fluorescent image, and fluorescent overlay image should be shown of each specimen, and ideally also a fluorescent heat-map image.

### III. Target validation

After paraffin-embedding of the tissue, the fluorescent signal will be attenuated. This influences the quantification properties of the signal. This, on the other hand, does not influence two other key aspects of data analysis in FGS trials. In the pathologic assessment one should focus on (1) confirmation of tumor targeting using histology, and (2) confirmation of molecular targeting of the biomarkers to the tumor cell. Lastly, correlation of fluorescent intensity with the density of the target molecule can be performed (Figure 1, panel III). Other key factors associated with delivery of the agent can also be assessed in this stage including vascular density, the presence or absence of lymphatic vessels, and the amount of cell proliferation.

#### *Confirmation of tumor cell targeting*

As discussed above, this step allows for direct correlation between tissue fluorescence and tumor status on H&E. In early phase trials, this step is critical to ensuring the agent is indeed targeting the tumor. Confirmation of tumor status on the H&E slides should be performed in close collaboration with a trained pathologist, who is preferably blinded to the fluorescent imaging results. With the use of a fluorescent scanner, the location of fluorescence can be detected with a µm resolution. Because the tumor is often composed of stromal elements, it will be necessary to distinguish between tumor/cancer cell targeting and targeting of other structures within the tumor mass.



If the mapping process (as described above) is performed in a rigorous manner, the correlation generated at this step can be traced back to the images of the intact gross surgical specimen acquired during back-table imaging. It is even possible to apply this correlation back to the intraoperative findings; however, this is complicated by the necessary preservation of the specimen's orientation

at each step in addition to the influence of ambient light on intraoperative fluorescence.

### *Confirmation of molecular targeting*

In the case of a targeted agent, the confirmation of precise tumor targeting should be a required step of the data analysis. Here, co-localization of the target of interest and fluorescent signal shows that the agent truly targets the biomarker, as compared to fluorescent signal seen in the tumor as a result of the EPR effect. A (semi-) quantitative analysis can be performed to analyze the fluorescent intensity relative to the receptor density of a specific tissue section (Figure 1). Co-localization can be performed using serial tissue sections, where one slide is used for immunohistochemistry (IHC) to confirm the target biomarker and one is used for fluorescent scanning. Additional IHC may be performed to gain a better understanding of the behavior of the factors influencing the tissue target; for example, for markers that influence delivery of the agent such as vascular density, the presence of lymphatic vessels, and the amount of cell turnover. Therefore, this staining will uniquely be performed during early phase trials when this information is relevant to advancing the agent and further characterizing its potential as a fluorescent biomarker. In later phase trials, one could choose to perform additional staining if the imaging results of a patient are out of the range of what is expected but would not necessarily be performed routinely. Fluorescent microscopy may be introduced into future analyses in FGS clinical trials in order to determine the position of the imaging agent in the tumor, e.g. membrane-bound, internalized, or in stroma.

## SUMMARY AND CONCLUSION

To ensure wide-spread use and FDA approval of FGS, the quality and standardization of reporting is paramount. Therefore, we present here recommendations for standardized reporting with the goal of establishing a set of minimum requirements for reporting FGS clinical trial results. In this approach, both qualitative and quantitative data play a major role. Three critical elements of early phase clinical trials can be identified and should be reported:

**1) Intra-operative data collection:** FGS has the potential to play a unique role in the identification of tumor tissue, assessment of resection margins, and

detection of tumor-positive lymph nodes, especially in locations that would suggest metastatic disease. In early phase trials, qualitative data should consist of multiple images obtained in each setting which include a bright field image, a black-and-white fluorescent image, a pseudo-colored fluorescent overlay image, and/or a heat-map. Quantitative data should consist of numerical values reporting fluorescence, preferably both raw MFIs and a ratio such as TBR.

**2) Specimen mapping**: This is critical to the validation of FGS to correlate fluorescent imaging-based results with the pathologic findings, preferably using fresh tissue. After imaging the fresh surgical specimen, the specimen should be formalin-fixed. Formalin-fixed tissue can be used for qualitative and quantitative analysis of fluorescent signal, in contrast to paraffin-embedded tissue which is more suitable for qualitative data analysis.

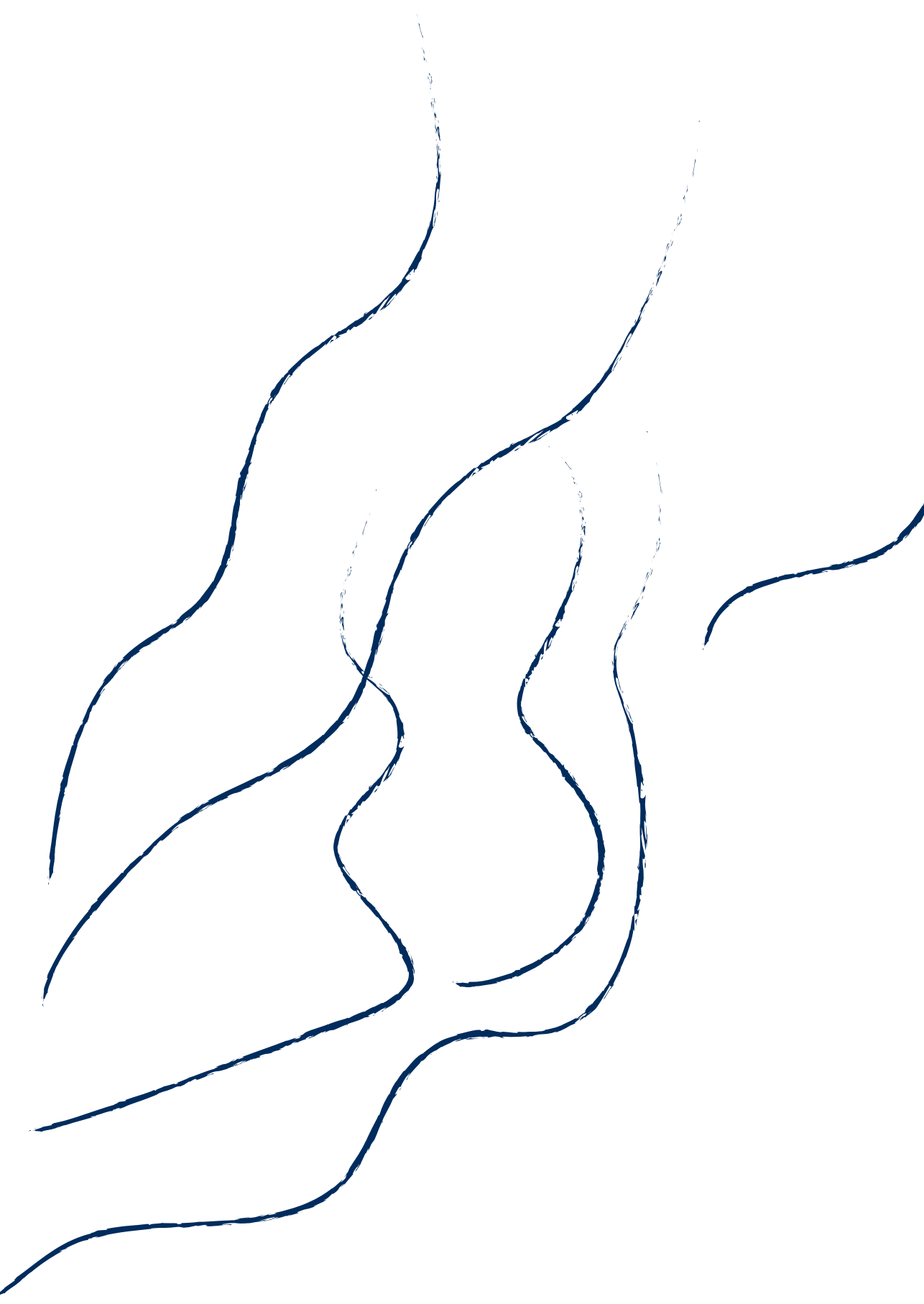
**3) Target validation**: Co-localization of the target of interest and fluorescent signal needs to demonstrate that the agent truly targets the biomarker. A semi-quantitative analysis can be performed to analyze the fluorescent intensity relative to the receptor density of a specific area. In summary, if these guidelines are widely accepted, trial results could be comparable and collated to expedite future FDA approval.

# REFERENCES


1. Vahrmeijer AL, Hutteman M, van der Vorst JR, van de Velde CJ, Frangioni JV. Image-guided cancer surgery using near-infrared fluorescence. Nature reviews Clinical oncology. 2013; 10: 507-18.
2. Jiang JX, Keating JJ, Jesus EM, Judy RP, Madajewski B, Venegas O, et al. Optimization of the enhanced permeability and retention effect for near-infrared imaging of solid tumors with indocyanine green. American journal of nuclear medicine and molecular imaging. 2015; 5: 390-400.
3. Madajewski B, Judy BF, Mouchli A, Kapoor V, Holt D, Wang MD, et al. Intraoperative near-infrared imaging of surgical wounds after tumor resections can detect residual disease. Clinical cancer research : an official journal of the American Association for Cancer Research. 2012; 18: 5741-51.
4. Zhang RR, Schroeder AB, Grudzinski JJ, Rosenthal EL, Warram JM, Pinchuk AN, et al. Beyond the margins: real-time detection of cancer using targeted fluorophores. Nature reviews Clinical oncology. 2017; 14: 347-64.
5. Rosenthal EL, Warram JM, Bland KI, Zinn KR. The status of contemporary image-guided modalities in oncologic surgery. Annals of surgery. 2015; 261: 46-55.
6. Rosenthal EL, Warram JM, de Boer E, Chung TK, Korb ML, Brandwein-Gensler M, et al. Safety and Tumor Specificity of Cetuximab-IRDye800 for Surgical Navigation in Head and Neck Cancer. Clinical cancer research : an official journal of the American Association for Cancer Research. 2015; 21: 3658-66.
7. Burggraaf J, Kamerling IM, Gordon PB, Schrier L, de Kam ML, Kales AJ, et al. Detection of colorectal polyps in humans using an intravenously administered fluorescent peptide targeted against c-Met. Nature medicine. 2015; 21: 955-61.
8. Hoogstins CE, Tummers QR, Gaarenstroom KN, de Kroon CD, Trimbos JB, Bosse T, et al. A Novel Tumor-Specific Agent for Intraoperative Near-Infrared Fluorescence Imaging: A Translational Study in Healthy Volunteers and Patients with Ovarian Cancer. Clinical cancer research : an official journal of the American Association for Cancer Research. 2016; 22: 2929-38.
9. Boogerd LSF, Hoogstins CES, Schaap DP, Kusters M, Handgraaf HJM, van der Valk MJM, et al. Safety and effectiveness of SGM-101, a fluorescent antibody targeting carcinoembryonic antigen, for intraoperative detection of colorectal cancer: a dose-escalation pilot study. The lancet Gastroenterology & hepatology. 2018.
10. Miller SE, Tummers WS, Teraphongphom N, van den Berg NS, Hasan A, Ertsey RD, et al. First-in-human intraoperative near-infrared fluorescence imaging of glioblastoma using cetuximab-IRDye800. Journal of neuro-oncology. 2018.
11. Tummers WS, Miller SE, Teraphongphom NT, Gomez A, Steinberg I, Huland DM, et al. Intraoperative Pancreatic Cancer Detection using Tumor-Specific Multimodality Molecular Imaging. Annals of surgical oncology. 2018.
12. van Dam GM, Themelis G, Crane LM, Harlaar NJ, Pleijhuis RG, Kelder W, et al. Intraoperative tumor-specific fluorescence imaging in ovarian cancer by folate receptor-alpha targeting: first in-human results. Nature medicine. 2011; 17: 1315-9.
13. Lamberts LE, Koch M, de Jong JS, Adams ALL, Glatz J, Kranendonk MEG, et al. Tumor-Specific Uptake of Fluorescent Bevacizumab-IRDye800CW Microdosing in Patients with Primary Breast Cancer: A Phase I Feasibility Study. Clinical cancer research : an official journal of the American Association for Cancer Research. 2017; 23: 2730-41.
14. Shankar LK, Hoffman JM, Bacharach S, Graham MM, Karp J, Lammertsma AA, et al. Consensus recommendations for the use of 18F-FDG PET as an indicator of therapeutic response in patients in National Cancer Institute Trials. Journal of nuclear medicine : official publication, Society of Nuclear Medicine. 2006; 47: 1059-66.
15. Barrington SF, Qian W, Somer EJ, Franceschetto A, Bagni B, Brun E, et al. Concordance between four European centres of PET reporting criteria designed for use in multicentre trials in Hodgkin lymphoma. European journal of nuclear medicine and molecular imaging. 2010; 37: 1824-33.

16. Boellaard R, Krak NC, Hoekstra OS, Lammertsma AA. Effects of noise, image resolution, and ROI definition on the accuracy of standard uptake values: a simulation study. Journal of nuclear medicine : official publication, Society of Nuclear Medicine. 2004; 45: 1519-27.
17. Antunovic L, Rodari M, Rossi P, Chiti A. Standardization and quantification in PET/CT imaging: tracers beyond FDG. PET clinics. 2014; 9: 259-66.
18. Kinahan PE, Fletcher JW. Positron emission tomography-computed tomography standardized uptake values in clinical practice and assessing response to therapy. Seminars in ultrasound, CT, and MR. 2010; 31: 496-505.
19. Kim A, Khurana M, Moriyama Y, Wilson BC. Quantification of in vivo fluorescence decoupled from the effects of tissue optical properties using fiber-optic spectroscopy measurements. Journal of biomedical optics. 2010; 15: 067006.20. Weersink R, Patterson MS, Diamond K, Silver S, Padgett N. Noninvasive measurement of fluorophore concentration in turbid media with a simple fluorescence /reflectance ratio technique. Applied optics. 2001; 40: 6389-95.
21. Pogue BW, Burke G. Fiber-optic bundle design for quantitative fluorescence measurement from tissue. Applied optics. 1998; 37: 7429-36.
22. Westerterp M, Pruim J, Oyen W, Hoekstra O, Paans A, Visser E, et al. Quantification of FDG PET studies using standardised uptake values in multi-centre trials: effects of image reconstruction, resolution and ROI definition parameters. European journal of nuclear medicine and molecular imaging. 2007; 34: 392-404.
23. Scheuermann JS, Saffer JR, Karp JS, Levering AM, Siegel BA. Qualification of PET scanners for use in multicenter cancer clinical trials: the American College of Radiology Imaging Network experience. Journal of nuclear medicine : official publication, Society of Nuclear Medicine. 2009; 50: 1187-93.
24. Wu J, Feld MS, Rava RP. Analytical model for extracting intrinsic fluorescence in turbid media. Applied optics. 1993; 32: 3585-95.
25. Patterson MS, Pogue BW. Mathematical model for time-resolved and frequency-domain fluorescence spectroscopy in biological tissues. Applied optics. 1994; 33: 1963-74.
26. Huang Z, Shi S, Qiu H, Li D, Zou J, Hu S. Fluorescence-guided resection of brain tumor: review of the significance of intraoperative quantification of protoporphyrin IX fluorescence. Neurophotonics. 2017; 4: 011011.
27. Tahari AK, Chien D, Azadi JR, Wahl RL. Optimum lean body formulation for correction of standardized uptake value in PET imaging. Journal of nuclear medicine : official publication, Society of Nuclear Medicine. 2014; 55: 1481-4.
28. Valdes PA, Angelo JP, Choi HS, Gioux S. qF-SSOP: real-time optical property corrected fluorescence imaging. Biomedical optics express. 2017; 8: 3597-605.
29. Choi H. Deep Learning in Nuclear Medicine and Molecular Imaging: Current Perspectives and Future Directions. Nuclear medicine and molecular imaging. 2018; 52: 109-18.
30. Tummers WS, Warram JM, Tipirneni KE, Fengler J, Jacobs P, Shankar L, et al. Regulatory Aspects of Optical Methods and Exogenous Targets for Cancer Detection. Cancer research. 2017; 77: 2197-206.
31. Daube-Witherspoon ME, Karp JS, Casey ME, DiFilippo FP, Hines H, Muehllehner G, et al. PET performance measurements using the NEMA NU 2-2001 standard. Journal of nuclear medicine : official publication, Society of Nuclear Medicine. 2002; 43: 1398-409.
32. Souza AV, Lin H, Henderson ER, Samkoe KS, Pogue BW. Review of fluorescence guided surgery systems: identification of key performance capabilities beyond indocyanine green imaging. Journal of biomedical optics. 2016; 21: 80901.
33. Prince AC, Jani A, Korb M, Tipirneni KE, Kasten BB, Rosenthal EL, et al. Characterizing the detection threshold for optical imaging in surgical oncology. Journal of surgical oncology. 2017; 116: 898-906.
34. Zhang C, Liu T, Su Y, Luo S, Zhu Y, Tan X, et al. A near-infrared fluorescent heptamethine indocyanine dye with preferential tumor accumulation for in vivo imaging. Biomaterials. 2010; 31: 6612-7.
35. Welvaert M, Rosseel Y. On the definition of signal-to-noise ratio and contrast-to-noise ratio for FMRI data. PloS one. 2013; 8: e77089.

36. Weissleder RR, B. D.; Rehemtulla, A.; Gambhir, S, S,. Molecular Imaging: Principles and Practice. 1st ed: People's Medical Publishing House--USA LTD; 2010.
37. Tichauer KM, Holt RW, Samkoe KS, El-Ghussein F, Gunn JR, Jermyn M, et al. Computed tomography-guided time-domain diffuse fluorescence tomography in small animals for localization of cancer biomarkers. Journal of visualized experiments : JoVE. 2012: e4050.
38. Tipirneni KE, Warram JM, Moore LS, Prince AC, de Boer E, Jani AH, et al. Oncologic Procedures Amenable to Fluorescence-guided Surgery. Annals of surgery. 2017; 266: 36-47.
39. Stummer W, Novotny A, Stepp H, Goetz C, Bise K, Reulen HJ. Fluorescence-guided resection of glioblastoma multiforme by using 5-aminolevulinic acid-induced porphyrins: a prospective study in 52 consecutive patients. Journal of neurosurgery. 2000; 93: 1003-13.
40. Dolmans DE, Fukumura D, Jain RK. Photodynamic therapy for cancer. Nature reviews Cancer. 2003; 3: 380-7.
41. Sadot E, Groot Koerkamp B, Leal JN, Shia J, Gonen M, Allen PJ, et al. Resection margin and survival in 2368 patients undergoing hepatic resection for metastatic colorectal cancer: surgical technique or biologic surrogate? Annals of surgery. 2015; 262: 476-85; discussion 83-5
.42. Pawlik TM, Scoggins CR, Zorzi D, Abdalla EK, Andres A, Eng C, et al. Effect of surgical margin status on survival and site of recurrence after hepatic resection for colorectal metastases. Annals of surgery. 2005; 241: 715-22, discussion 22-4.
43. O'Kelly Priddy CM, Forte VA, Lang JE. The importance of surgical margins in breast cancer. Journal of surgical oncology. 2016; 113: 256-63.
44. Black C, Marotti J, Zarovnaya E, Paydarfar J. Critical evaluation of frozen section margins in head and neck cancer resections. Cancer. 2006; 107: 2792-800.
45. Provenzano E, Bossuyt V, Viale G, Cameron D, Badve S, Denkert C, et al. Standardization of pathologic evaluation and reporting of postneoadjuvant specimens in clinical trials of breast cancer: recommendations from an international working group. Modern pathology : an official journal of the United States and Canadian Academy of Pathology, Inc. 2015; 28: 1185-201.



Chapter | 13

# General discussion and future perspectives

In the field of molecular imaging, significant progress has been made over the last years. Tumor-specific optical imaging has entered clinical trials, and safety and feasibility has been shown for several cancer types. This thesis shows the complete roadmap from preclinical development and validation to clinical translation in a phase I trial for pancreatic cancer patients. Now, next steps need to be taken by the field to move this technique from Phase I trials to more wide-spread use and larger clinical trials. To be able to achieve wide-spread use, more specific aspects of tumor biology need to be taken into account, especially the effects of neoadjuvant therapy, before tumor-specific imaging can be applicable in all patients. Also, inter- and intrapatient tumor heterogeneity is a known complicating factor in the search for optimal biomarkers for tumor detection.

## The search for the ideal biomarker

In pancreatic cancer, it is known that tumor cells are selected by means of fitness and growth advantages.[1] Cells that enter the blood stream from the site of the primary tumor and lead to metastases, are probably the cells that have achieved the highest fitness in the primary site. These have the greatest chance of homing in new microenvironments, such as the liver, lung or peritoneum, which are the common sites of metastasis in pancreatic cancer.[1] Homing of tumor cells into new microenvironments will lead to novel mutations, and consequently further heterogeneity, both between the primary lesions and metastases, and between different metastases. This heterogeneity will make it almost impossible to identify a single biomarker that would allow, tumor-specific imaging for each tumor in each patient. To solve this issue, one could imagine that in the future multiple imaging agents directed against different biomarkers are available, and that prior to surgery the most optimal agent is chosen, based on biomarker expression from biopsy tissue. This would, on the other hand, not solve the problem of heterogeneity within the primary tumor, or between primary tumor and potential metastatic sites. An additional complicating factor in pancreatic cancer is that some patients do not receive a biopsy prior to surgery, and if a biopsy is taken, the material is not always representative for the suspected tumor. In those cases, it could be preferred to use a cocktail with different imaging agents, targeting a set of the most common biomarkers.[2, 3]

Another complicating factor in the identification of the ideal biomarker, is the use of (neo)adjuvant therapy. This form of therapy undoubtly influences the biomarker expression on tumor cells. This phenomena is extensively studied in breast cancer patients, but little is known of the effect in pancreatic cancer patients.[4, 5] In Chapter 4, we assessed the effect of neoadjuvant therapy on CEA and αvβ6 expression. There, we have shown the importance of a separate analysis on neoadjuvant treated tumor tissue. If neoadjuvant treated patients were not included in this IHC analysis. We would have concluded that CEA was the optimal target for pancreatic cancer, However, it was seen that CEA expression almost disappeared after neoadjuvant therapy, while tumor cells remained vital, making it impossible to target that receptor in neoadjuvant treated pancreatic cancer patients. Taking this into account, it was concluded that αvβ6 was the most ideal biomarker in all clinical relevant situations.

In this thesis we mainly focused on tumor-specific imaging directed against the cancer cell, while in chapter 2, we have also described the possibility to target the micro-environment in pancreatic cancer. It is recognized that pancreatic cancer for a large part consists out of stroma tissue compared to actual tumor cells. Since the micro-environment plays an important role in tumor development and progression, it could be of additional value and potentially more complete targeting of the tumor could be achieved, when choosing this route.[6] Since there is currently no experience with targeting only the stroma cell compartment in patients, we have chosen to focus on the tumor cells in this early phase work for pancreatic cancer. However, in the future, it could be recommended to use a cocktail of agents targeting both the tumor, and it's micro-environment.

### Early detection of pancreatic cancer

As described in this thesis, pancreatic cancer has a dismal prognosis, mainly due to late onset of symptoms when disease is already spread to other organs, either distant or locally. This stresses the need for early detection. Fluorescence-guided surgery as described in this thesis will not be beneficial for early detection of pancreatic cancer, but early detection of this and other types of cancer could be performed in various ways; first, one could focus on identifying and validating a biomarker which may likely be very different compared to those of late stage disease. Identification of these kind of early biomarkers could be done in studies

like the baseline study recently initiated by Verily Life Sciences, performed in 10.000 healthy volunteers who will be monitored daily (NCT03154346). These studies will generate invaluable data regarding early signs of disease, and the time until development of symptoms. Another method for the early detection of pancreatic cancer could be to develop a standardized bio-repository with longitudinal follow-up, established in patients with pancreatic cancer precursor lesions such as IPMN or with high risk for pancreatic cancer based on family history and established genetic risk factors. By the collection of tissues, cystic fluids, serum and plasma, captured prior to pancreatic cancer onset, predictive and early detection biomarkers can be identified. The next challenge after identification of biomarkers associated with early onset of disease, is the method to detect these markers. This can be performed in bodily fluids, such as the FOPT test in colon cancer, or by using imaging, such as breast cancer screening. In the thesis, we have focused on the improved detection of pancreatic cancer by targeted imaging. Both targeted ultrasound, in form of photoacoustic imaging, and targeted PET-CT could be used for this purpose. Photoacoustic imaging with targeted agents, such as microbubbles, could be a non-invasive way to image the pancreas for screening purposes.[7, 8] Due to the costs and radiation used for targeted PET-CT imaging, this would not be a imaging method used in the general population for screening, but could be used in high-risk patients during periodical screening.

### Other novel molecular imaging techniques

In addition to fluorescence and photoacoustic imaging, other potential novel molecular imaging techniques could be beneficial during surgery. In chapter 2 of this thesis, Raman imaging is shortly addressed, together with the advantages and disadvantages. Raman and Cherenkov luminescence imaging (CLI) are molecular imaging techniques that receive tremendous attention in preclinical research, but currently, clinical applications are limited. In CLI, the visible photons emitted by Cherenkov radiation are captured, resulting in optical imaging of radiotracers, which could be used for intraoperative guidance in a way SPECT is used now in clinical trials.[9] CLI could overcome the depth limitation of fluorescence-guided surgery, since it used radiation for visualization instead of emitted light. Thorek and colleagues described the successful use of CLI in patients undergoing FDG-PET in 2014,[10] but since then no clinical studies are performed. The main advantage of Raman imaging is that it could be used

for multiplexing. The advantage of multiplexing is that it allows simultaneous detection of multiple biomarkers which is ideal in case of heterogenic tumors. By varying the Raman active layer, different Raman particles can be created, each emitting a characteristic spectrum. Since each type of particles has a unique spectral signature they can be used for multiplexing when functionalized for different targets.[11] For now, a disadvantage of Raman imaging is the duration it takes to scan a tissue surface, limiting the clinical applicability. To overcome this limitation, Garai and colleagues developed a clinical endoscopic Raman system able to rapidly scan large tissue surfaces such as colon.[11]

### A standard method to assess novel imaging agents

As described in this thesis, multiple early phase clinical trials are performed in the field of fluorescence-guided surgery. In Chapter 12, we described the need for a uniform set-up of these clinical trials. Currently, most trials are designed just to show feasibility of the technique. By now, enough proof is generated showing the capability of targeting tumors in a tissue-specific manner using optical imaging agents. At this point, the field should move one step further and show the world this technique helps to improve surgical care for the patient otherwise wide-spread use will not be reached. Furthermore, to get novel imaging agents approved by regulatory bodies, large trials showing patient benefit have to be performed. To execute these large clinical trials, extensive resources are needed which are mostly only possible when supported by industry. However, if the clinical trials would be designed in a similar manner and shared endpoints are chosen, results of different trials could be put together and collective conclusions could be drawn, leading to a more cost-efficient and less time-consuming strategy as described in chapter 8.

### Quantification in fluorescence imaging

Another crucial aspect which is still in its infancy in fluorescence-guided surgery is quantification of the signal. At this point, the intra-operative use of fluorescence is based on binary “fluorescence yes or no”, instead of the numerical intensity of the signal. The problem with this way of interpreting fluorescence is that most imaging systems have an incorporated method to enhance the imaging signal even when it is weak, and therefore it is not clear for the surgeon how intense the signal actually is. This is important because depending on the imaging agent, normal tissue could express the biomarker

and therefore some fluorescence signal as well. In these cases, the intensity of the signal provides information on how likely it is that the fluorescent tissue is actual tumor. Although the potential of tumor-specific optical imaging is yet to be realized, tumor-specific intraoperative optical imaging is likely to play an important role in the identification and treatment of cancer in the near future. Therefore, real-time quantification should be available to provide better understanding of the signal to the surgeon and increasing the sensitivity and specificity of this technique, to allow clinical decision-making based on this technique.

## FUTURE PERSPECTIVES

### The future of cancer treatment

This thesis shows the great potential of tumor-specific imaging and it is expected that it's use both in the diagnostic process and for intra-operative use will increase in the future. In the past, treatments in general, but specifically in oncology were based on a "one-size fits-all"-strategy undervaluing all the different characteristics disease and patients can have. Later on, this was optimized by stratification of patients by disease subtypes, clinical features and demographics. This method still did not lead to the preferred results in patient outcome, and therefore at this point there is a need to further specialize care based on precision medicine. Here, a doctor needs to look at the individual patient and has to take patient preferences, demographics, medication history, clinical features of the disease, biomarkers and behavior into account when deciding on the most optimal treatment. The call for precision medicine will require the need to search for treatment strategies that are focused on these specific characteristics of the tumor and the patient. Since the results of early phase clinical trials in the field of tumor-specific imaging are promising, this modality could help to fill part of that need.

### The future of surgery

Besides the need for precision medicine, the increasing use of minimally-invasive surgery (MIS), such as robotic-assisted and laparoscopic surgery, requires a method to substitute the lack of tactile information for the surgeon. During open surgery the consistency of tissue gives the surgeon tremendous

information regarding the potential benign or malignant nature of the tissue. To substitute this information in MIS, novel methods are needed providing visual feedback to the surgeon regarding the tissue status. This visual feedback could come from a fluorescent imaging signal in case of tumor-specific imaging. For photoacoustic imaging, the second intraoperative optical imaging modality discussed in this thesis, this becomes more challenging. Photoacoustic imaging requires an ultrasound probe able to enter the abdominal cavity through laparoscopic trocars. At this point, such photoacoustic imaging probes are not available yet, however certain groups are working on this feature. Also, the photoacoustic signal cannot be projected on the screen already used by the surgeon to perform the surgery, so an additional device and screen are needed in the operating room.

### The future of pancreatic cancer diagnostics

Precision medicine will not only change the way surgery is performed nowadays, also the diagnostic process needs to implement this phenomena. In this thesis the first steps of this transition are shown in chapter 9 using tumor-specific PET-CT imaging to diagnose pancreatic cancer. In the case of pancreatic cancer, tissue-specific diagnostics could help differentiating between tumor and inflammation prior to resection and/or to determine resectability. Also, this method could potentially be used to monitor response to neoadjuvant therapy. A large clinical trial is about to start in the LUMC investigating this specific aspect. Another area of development for both diagnostic and intra-operative tissue-specific imaging is hybrid imaging were one agent is conjugated to both a radioactive label for diagnostics and a fluorescent label for intra-operative use. The main benefits of this method are the fact that a patient has to undergo only one injection with the agent, the high probability that the same lesions are found both on the diagnostic modality as during surgery, and the possibility to perform radioguided surgery together with fluorescence. In this case, both the fluorescent and the radioactive signal can be used during the surgery with a Gamma counter and a fluorescent camera. The radioactive signal can be used to direct the surgeon to the area of interest and the high sensitivity of the fluorescence for the actual resection or identification of the tumor.[12] Besides these important benefits of a hybrid agent, the use of two separate agents should be preferred looking at the logistics in a hospital. In case of a hybrid agent, the diagnostic imaging and the surgery should be performed

within a few days to be able to use both the radioactive and the fluorescent signal since both will decay after a certain amount of time. In addition, the radioactive signal cannot be too high during surgery, exposing the surgeon and the OR team to radioactivity. Therefore, a hybrid agent is an interesting idea for research purposes, but it remains questionable how feasible this is for actual patient care.

## The future of fluorescence guided surgery

When looking at the future of fluorescence guided surgery, not only the NIR window from 700-900 nm has become of interest to the field, also the wavelengths in the second near-infrared window (NIR II) of 900 nm and above seem promising.[13, 14] Preclinical research using these wavelengths show diminished tissue autofluorescence, reduced photon scattering, and low levels of photon absorption allowing centimeters imaging depth at low resolution and micron-scale resolution at low depths.[13] Until recent, all NIR-II fluorophores were inorganic nanomaterials, which are excreted slowly and are largely retained within the reticuloendothelial system, making clinical translation nearly impossible due to unknown long-term toxicity concerns.[15] In 2015, Antaris and colleagues published a study developing a small molecule dye for the NIR-II window of 8.9 kDa with renal excretion.[16] The agent outperformed ICG on several levels in mouse models. The disadvantage of this small molecule dye is the labor-intensive and expensive synthesis, making large scale synthesis for human use impossible. Thus far, no clinical results using NIR-II imaging are shown and no clinical imaging systems are available. As seen in the past, it is hard to translate successful preclinical results into the human situation, therefore the potential benefit of NIR-II imaging for patient care with clinically available agents is still something that needs to be investigated in the future.

## The future of organ-sparing strategies in cancer treatment

Especially in rectal and breast cancer, another aspect that becomes increasingly important in the way medicine is practiced today, is the trend towards organ-sparing treatment. For pancreatic cancer this is not a feasible treatment option for now, since successful neoadjuvant regimens have just been initiated in this disease and long term effects still need to be investigated. Studies have been suggesting that “organ preservation” strategies might be appropriate alternatives to standard resection in patients with a clinical complete response (cCR) on

neoadjuvant therapy.[17, 18] In a so-called "Watch-and-Wait" (W&W) strategy, surgery is omitted and instead, patients are closely monitored with intensive clinical and imaging follow-up. Although several successful small cohort studies have been conducted in the last years, W&W is not widely adopted yet. One of the main reasons is because the accuracy of conventional imaging modalities is insufficient, resulting in reported 2-year local tumor regrowth rates of 15-33%.[19] With tumor-specific targeted imaging, a non-invasive imaging approach can be implemented to help improve the response monitoring during diagnostic imaging in these patients. This specific use of tumor-specific imaging also increases the need to identify a biomarker which is present on viable tumor cells, but not on chemotherapy-induced necrosis and fibrosis.

In the future, molecular imaging could not only be used to diagnose and treat patients directly. Also for the development of novel drugs molecular imaging could play an important role. Imaging could be used to inform physicians and researcher and lead to better understanding for the most optimal implementation of novel drugs. In drug development, imaging could provide information on biodistribution, the difference between individuals on pharmacodynamic and -kinetic level, and it could determine disease progression to verify for example an indication.[20]

## GENERAL CONCLUSIONS

Pancreatic cancer remains an extremely challenging disease for a surgeon to tackle. Since most of the patients will not benefit from surgical resection, it is essential to be able the select only those patients that will benefit. Implementing tumor-specific imaging, both in the diagnostic process and during surgery will improve the detection of small lesions, assess resection margins, and help to identify a non-curative resection. In this thesis, we have identified integrin αvβ6 as the most optimal target for pancreatic cancer, to distinguish cancer from normal pancreatic tissue and inflammation. Also, expression is retained after neoadjuvant therapy in vital tumor cells compared to chemotherapy-induced necrosis and fibrosis. In preclinical mouse models, we have shown the potential to target αvβ6 using a fluorescent agent, and in healthy volunteers and patients the possibility is shown to diagnose pancreatic cancer targeting αvβ6 with

PET-CT imaging. In addition, we have proven the safety and feasibility of tumor-specific fluorescence imaging using cetuximab-IRDye800 for the intraoperative detection of pancreatic cancer, even in the case of subclinical disease.

Now that practicing medicine has changed to a more precision-type approach, tailored for each patient, tumor-specific optical imaging is likely to get an important role. Before this role can be claimed by the field, we have stressed the need to proof of patient benefit by showing improved survival and reduced morbidity. This can be achieved by performing large, randomized controlled, clinical trials, by developing a standardized way clinical trials are performed, and by choosing relevant clinical endpoints. Hopefully this can lead to wide-spread implementation of this technique in the near future, and eventually to improved prognosis for patients with pancreatic cancer.

# REFERENCES


1. Makohon-Moore, A. and C.A. Iacobuzio-Donahue, Pancreatic cancer biology and genetics from an evolutionary perspective. Nat Rev Cancer, 2016. 16(9): p. 553-65.
2. Campbell, P.J., S. Yachida, L.J. Mudie, et al., The patterns and dynamics of genomic instability in metastatic pancreatic cancer. Nature, 2010. 467(7319): p. 1109-13.
3. Yachida, S., S. Jones, I. Bozic, et al., Distant metastasis occurs late during the genetic evolution of pancreatic cancer. Nature, 2010. 467(7319): p. 1114-7.
4. Zhou, X., J. Zhang, H. Yun, et al., Alterations of biomarker profiles after neoadjuvant chemotherapy in breast cancer: tumor heterogeneity should be taken into consideration. Oncotarget, 2015. 6(34): p. 36894-902.
5. Gahlaut, R., A. Bennett, H. Fatayer, et al., Effect of neoadjuvant chemotherapy on breast cancer phenotype, ER/PR and HER2 expression - Implications for the practising oncologist. Eur J Cancer, 2016. 60: p. 40-8.
6. Boonstra, M.C., J. Prakash, C.J. Van De Velde, et al., Stromal Targets for Fluorescent-Guided Oncologic Surgery. Front Oncol, 2015. 5: p. 254.
7. Abou-Elkacem, L., H. Wang, S.M. Chowdhury, et al., Thy1-Targeted Microbubbles for Ultrasound Molecular Imaging of Pancreatic Ductal Adenocarcinoma. Clin Cancer Res, 2018. 24(7): p. 1574-1585.
8. Valluru, K.S., K.E. Wilson, and J.K. Willmann, Photoacoustic Imaging in Oncology: Translational Preclinical and Early Clinical Experience. Radiology, 2016. 280(2): p. 332-49.
9. Bugby, S.L., J.E. Lees, and A.C. Perkins, Hybrid intraoperative imaging techniques in radioguided surgery: present clinical applications and future outlook. Clin Transl Imaging, 2017. 5(4): p. 323-341.
10. Thorek, D.L., C.C. Riedl, and J. Grimm, Clinical Cerenkov luminescence imaging of (18)F-FDG. J Nucl Med, 2014. 55(1): p. 95-8.
11. Garai, E., S. Sensarn, C.L. Zavaleta, et al., A real-time clinical endoscopic system for intraluminal, multiplexed imaging of surface-enhanced Raman scattering nanoparticles. PLoS One, 2015. 10(4): p. e0123185.
12. Hekman, M.C.H., M. Rijpkema, D.L. Bos, et al., Detection of Micrometastases Using SPECT/Fluorescence Dual-Modality Imaging in a CEA-Expressing Tumor Model. J Nucl Med, 2017. 58(5): p. 706-710.
13. Hong, G., J.C. Lee, J.T. Robinson, et al., Multifunctional in vivo vascular imaging using near-infrared II fluorescence. Nat Med, 2012. 18(12): p. 1841-6.
14. Hong, G., J.T. Robinson, Y. Zhang, et al., In vivo fluorescence imaging with Ag2S quantum dots in the second near-infrared region. Angew Chem Int Ed Engl, 2012. 51(39): p. 9818-21.
15. Choi, H.S., W. Liu, P. Misra, et al., Renal clearance of quantum dots. Nat Biotechnol, 2007. 25(10): p. 1165-70.
16. Antaris, A.L., H. Chen, K. Cheng, et al., A small-molecule dye for NIR-II imaging. Nat Mater, 2016. 15(2): p. 235-42.
17. Glynne-Jones, R., M. Wallace, J.I. Livingstone, et al., Complete clinical response after preoperative chemoradiation in rectal cancer: is a "wait and see" policy justified? Dis Colon Rectum, 2008. 51(1): p. 10-9; discussion 19-20.
18. Appelt, A.L., J. Ploen, H. Harling, et al., High-dose chemoradiotherapy and watchful waiting for distal rectal cancer: a prospective observational study. Lancet Oncol, 2015. 16(8): p. 919-27.
19. Habr-Gama, A., J. Gama-Rodrigues, G.P. Sao Juliao, et al., Local recurrence after complete clinical response and watch and wait in rectal cancer after neoadjuvant chemoradiation: impact of salvage therapy on local disease control. Int J Radiat Oncol Biol Phys, 2014. 88(4): p. 822-8.
20. Willmann, J.K., N. van Bruggen, L.M. Dinkelborg, et al., Molecular imaging in drug development. Nat Rev Drug Discov, 2008. 7(7): p. 591-607.



## Appendices

# Summary

# Nederlandse samenvatting

# List of publications

# Curriculum Vitae

# Dankwoord

## Appendices

# Summary

For years, pancreatic cancer had a dismal prognosis with a long term survival of around 5%. Since the centralization of pancreatic cancer surgery and the introduction of systemic chemotherapy with FOLFIRINOX, the median overall survival increased from 6-13%, after gemcitabine therapy, to around 20%. However, even with the introduction of these novel treatment regimens, the achieved survival rates remain disappointing compared to other cancer types. Consequently, radical tumor-margin free resection provides the patient with the best potential chance for cure. However, due to late onset of symptoms, the majority of patients present with inoperable disease. These patients can benefit from neoadjuvant therapy, or palliative chemotherapy. During clinical practice, this means that decision-making before and during surgery is critical to select the most optimal primary treatment modality for the patient. Currently, conventional imaging modalities lack sensitivity to detect small metastatic lesions, and are unable to visualize treatment response on neoadjuvant therapy.

Tumor-specific molecular imaging in the form of fluorescence and photoacoustic imaging aids the surgeon to accurately recognize and resect malignant tissues in real-time during surgery. The other form of this kind of imaging, PET-CT using radioactive signal, can be used in the perioperative process to assess tumor spread and help in the surgical planning. This thesis focuses on the challenges a surgeon faces during pancreatic cancer treatment, and the potential improvements that could be achieved by the use of tumor-specific imaging. In addition, the regulatory aspects of clinical translation of tumor-specific optical imaging agents are addressed.

### Part 1: Development of Targeted Molecular Imaging for Pancreatic Cancer

**Chapter 2** describes the current clinical imaging applications for the detection of pancreatic cancer, and the upcoming molecular imaging strategies with emphasize on tumor-specific intra-operative imaging. This technique has shown great potential in order to bridge the gap between diagnostic and intra-operative imaging for pancreatic cancer treatment. In this chapter the need for an optimal biomarker to perform tumor-specific imaging is described together with the advantages and disadvantages of several biomarkers.

To be able to implement a novel technique, such as tumor-specific imaging, in patient care and achieve actual improvement in outcomes, one needs to know

where this technique needs to make a difference. This element is describes in **chapter 3**, where a retrospective study is reported showing that a margin-positive (R1) resection is a major contributor to reduced survival and early recurrence, especially in patients with lymph node negative (N0) disease.

As stressed before, a biomarker is needed to be able to perform tumor-specific imaging. Idealy, this biomarker is able to discriminate between pancreatic cancer and inflammation since this is challenging both at preoperative imaging and during surgery. In **chapter 4** of this thesis an immunohistochemistry study is performed identifying such a biomarker, which is also overexpressed on associated lymph node metastases and on vital tumor cells after neoadjuvant therapy. It was concluded that both integrin αvβ6 and carcinogenic embryonic antigen (CEA) are promising candidates, especially when used in combination. Integrin αvβ6 has the advantage over CEA that this biomarker retains expression after neoadjuvant radiochemotherapy.

### Part 2: Validation of Targeted Molecular Imaging for Pancreatic Cancer

In **chapter 5** a novel fluorescent imaging agent is developed targeting integrin αvβ6. This agent consists of an existing cysteine knottin peptide, R01-MG, conjugated to the near-infrared (NIR) fluorescent dye IRDye800. This agent is validated extensively in preclinical mouse models, showing specific targeting to αvβ6 and a significantly higher tumor-to-background ratio (TBR) compared to normal pancreatic tissue in transgenic mouse models. **Chapter 6** focusses on early detection of cancer in preclinical models, using activatable agents. These agents can be used for early detection because the agent is only "turned-on" in the tumor microenvironment, which dramatically improves sensitivity of cancer detection.

### Part 3: Clinical Translation of Targeted Molecular Imaging

Targeted molecular imaging is a novel technique which requires regulatory approval before this technique can have wide-spread use in patient. Targeted molecular imaging is unique in its ability to provide real-time feedback to the surgeon in the case of intra-operative imaging, complicating the approval process. In addition, this technique requires the use of both an agent and an imaging device, which are important considerations in this process. **Chapter 7** describes the regulatory hurdles in detail. Important here is that the proposed

"indication for use" will direct all future studies needed for approval, and therefore, should be chosen carefully. Success or failure of optical imaging agents will critically depend on the design of clinical trials and the chosen endpoints. In **chapter 8** insight is given into the process of engaging the FDA in the evaluation of tumor-specific imaging agents, and a guide for designing optimal optical imaging clinical trials.

### Part 4: Clinical Application of Targeted Molecular Imaging for Pancreatic Cancer

This part is focused on the clinical use of this novel technique describing early phase clinical trials performed in pancreatic cancer patients. In the diagnostic process, tumor-specific PET-CT imaging could improve the detection of pancreatic cancer and aid the perioperative process to assess tumor spread and help in the surgical planning as shown in chapter 9. Targeting αvβ6 using [18F] FP-R01-MG-F2, provided an elevated imaging signal in the tumor compared to normal pancreas. In chapter 10, the first-in-human use of multimodality molecular imaging for the intra-operative detection of pancreatic cancer is reported using cetuximab-IRDye800 that binds to epidermal growth factor receptor (EGFR). Fluorescent imaging successfully identified tumor with a significantly higher mean fluorescence intensity (MFI) compared to normal pancreatic tissue and inflammation, with a sensitivity of 96.1% and specificity of 67.0%. In addition, the mean photoacoustic signal in the tumor was 3.7-fold higher than surrounding tissue. In chapter 11 a more in-depth analysis is performed on the ability of tumor-specific fluorescent imaging to detect visually occult tumor-positive lymph nodes during surgical resection of pancreatic cancer. With the use of cetuximab-IRDye800 peritumoral lymph nodes were detected with a sensitivity of 100% and specificity of 78% macroscopically. Also, this method was able to detect occult foci of tumor (< 5mm) with a sensitivity of 88%.

### Part 5: Future Directions for Targeted Molecular Imaging

In **chapter 12** of this thesis the future of tumor-specific optical imaging is discussed. To eventually achieve wide-spread use of this novel technique patient benefit needs to be shown as discussed in this thesis. Therefore, larger trials are needed with correctly chosen endpoints. To put the results of different studies into a broader perspective, results of different clinical trials should be

comparable. In chapter 12, a format is presented to standardize the way results of tumor-specific imaging trials are reported, which will hopefully lead to a more generalized method in which results can be better appreciated. Eventually, this will ensure that results of different trials can be pooled and hopefully used together in the approval process for novel imaging agents and devices.

Appendices

# Nederlandse samenvatting

Tot op heden had pancreascarcinoom een zeer slechte prognose met een lange termijn overleving van ongeveer 5%. Door de centralisering van de chirurgie voor pancreascarcinoom en de introductie van het nieuwe chemotherapie schema FOLFIRINOX, is de mediane overleving verbeterd van 6-13% na gemcitabine behandeling, naar ongeveer 20%. Ondanks deze nieuwe behandelmethoden, blijven de behaalde sterftecijfers achter bij andere vormen van kanker. Hierdoor is het nog steeds zo dat radicale resectie met tumor-vrije (R0) resectie marges de patient de beste kans op genezing biedt. Echter, gezien het feit dat de symptomen van pancreascarcinoom zich pas in een laat stadium manifesteren, presenteert het grootste deel van de patiënten zich met inoperabele ziekte. Deze patiënten kunnen wel gebaat zijn bij neoadjuvante therapie, of palliatieve chemotherapie. Dit betekent dat het gedurende het diagnostische proces en de operatie van cruciaal belang is om onderscheid te kunnen maken tussen deze patiënten groepen, om de meeste optimale primaire behandelmodaliteit te selecteren voor de individuele patiënt. Op dit moment kan dat niet gerealiseerd worden aangezien de conventionele beeldvormingsmodaliteiten niet sensitief genoeg zijn om kleine metastasen te identificeren en om het behandeleffect na neoadjuvante therapie te monitoren.

Tumor-specifieke optische beeldvorming, zoals fluorescentie beeldvorming en foto-akoestische echo, heeft de potentie dit gat op te vullen. Deze techniek kan de chirurg tijdens de operatie helpen bij het herkennen en reseceren van tumor weefsel. Een andere vorm van tumor-specifieke beeldvorming is PET-CT, welke een radioactief signaal gebruikt voor het in beeld brengen van het beoogde weefsel. Dit kan gebruikt worden in het perioperatieve proces om verspreiding van ziekte te detecteren, zowel lokaal als op afstand, en om te helpen bij het bepalen van een chirurgische strategie. In dit proefschrift word de focus gelegd op de uitdagingen waar een chirurg mee geconfronteerd wordt bij de behandeling van pancreascarcinoom, en de mogelijke verbeteringen die gerealiseerd kunnen worden door het gebruik van tumor-specifieke beeldvorming.

## Deel 1: Ontwikkeling van tumor-specifieke moleculaire beeldvorming voor pancreascarcinoom.

Hoofdstuk 2 beschrijft de huidige stand van zaken rond de beeldvormingsmodaliteiten die worden gebruikt bij de detectie van pancreascarcinoom, en de nieuw ontwikkelde moleculaire beeldvormingstechnieken met focus op tumor-specifieke intra-operatieve beeldvorming. Deze techniek heeft de potentie om een brug te slaan tussen diagnostische en intra-operatieve beeldvorming bij de behandeling van pancreascarcinoom. In dit hoofdstuk wordt ook het belang van een optimale biomarker besproken voor het gebruik van tumor-specifieke beeldvorming, samen met de voor- en nadelen van enkele biomarkers.

Om te zorgen dat een nieuwe techniek, zoals tumor-specifieke beeldvorming, geïmplementeerd wordt in het huidige behandeltraject en te zorgen dat het tot verbetering leidt voor patiënten, is het van het grootste belang dat men beseft waar een dergelijke nieuwe techniek het verschil kan maken. Om dit te onderzoeken is in **hoofdstuk 3** een retrospectieve database studie gedaan naar het effect van tumor-positieve (R1) resectie marges op overleving en kans op recidief. Hierin is aangetoond dat een R1 resectie negatieve invloed heeft op overleving en recidief van de ziekte, vooral als de ziekte zich nog niet heeft verspreid tot in de lymfeklieren (N0).

Zoals reeds eerder werd aangegeven is een goede biomarker van essentieel belang als het gaat om tumor-specifieke beeldvorming. Voor pancreascarcinoom bestaat een ideale biomarker uit een marker die wel voorkomt op pancreascarcinoom, maar niet op ontstekingsweefsel of gezond pancreas weefsel. Dit is van belang aangezien het voorafgaand aan de operatie met de huidige beeldvorming niet mogelijk is dit onderscheid te maken, net als gedurende de operatie. In **hoofdstuk 4** van dit proefschrift worden de resultaten van een immunohistochemie studie gepresenteerd waar een dergelijke biomarker is geselecteerd, die ook tot overexpressie komt op tumor-positieve lymfeklieren en op vitale tumorcellen na neoadjuvante behandeling. In dit onderzoek is geconcludeerd dat zowel integrine αvβ6 als carcinogeen embyronaal antigeen (CEA) veelbelovende biomarkers zijn, vooral wanneer deze in combinatie worden gebruikt. Het voordeel van het gebruik van integrine αvβ6 als biomarker ten opzichte van CEA is dat expressie behouden blijft na neoadjuvante chemo-radiotherapie.

## Deel 2: Validatie van tumor-specifieke moleculaire beeldvorming voor pancreascarcinoom.

In **hoofdstuk 5** is een nieuwe fluorescente tumor-specifieke contraststof ontwikkeld gericht tegen integrine αvβ6. Deze contraststof bestaat uit een peptide, de cysteine knoop R01-MG, welke is gekoppeld aan de nabij-infrarode fluorescente stof IRDye800. De nieuwe contraststof is gevalideerd is verschillende muismodellen waarbij specifieke binding aan αvβ6 is aangetoond en een significant hoger signaal in de tumor werd gezien vergeleken met de gezonde pancreas in een genetisch gemodificeerd muismodel. In **hoofdstuk 6** wordt de mogelijkheid tot vroege detectie van kanker besproken door middel van activeerbare contraststoffen in preklinische modellen. Deze stoffen kunnen gebruikt worden bij vroege detectie omdat deze pas een signaal genereren als ze zich in de nabije omgeving van de tumor bevinden, wat leidt tot een dramatische verhoging van het signaal en daarmee de sensitiviteit van de techniek.

## Deel 3: Klinische translatie van tumor-specifieke beeldvorming

Tumor-specifieke beeldvorming is een veelbelovende nieuwe techniek die goedkeuring vereist van overheidsinstanties zoals de FDA en EMA, voordat deze techniek in algemeen gebruik kan worden genomen. In het geval van intra-operatieve tumor-specifieke moleculaire beeldvorming is een uniek aspect de mogelijkheid om in real-time feedback te geven aan de chirurg tijdens de operatie. Dit zorgt ervoor dat goedkeuring van deze techniek gecompliceerd is. Daarnaast is het een feit dat voor deze vorm van beeldvorming zowel een contraststof als een camera of echo apparaat nodig zijn, wat belangrijke overwegingen met zich meebrengt in het proces tot goedkeuring van zowel de contraststof als de camera. In **hoofdstuk 7** worden de uitdagingen die komen kijken bij het goedkeuringsproces in detail besproken. Van belang hierbij is de indicatie die wordt toegekend aan de camera of de stof aangezien die indicatie richting geeft aan alle vervolgstudie die moeten worden verricht. Daarnaast hangt het succes van een contraststof af van de uitgevoerde klinische studies en de gekozen primaire en secundaire eindpunten. Om die reden is het van groot belang kritisch te kijken naar een studie design en zal men zich gedurende het proces bij elke stap moeten afvragen of de uitgevoerde klinische studies het juiste doel dienen. In **hoofdstuk 8** wordt inzicht verschaft in het evaluatie proces van een nieuwe contraststof door de FDA en worden adviezen gegeven

over het optimale design voor een klinische studie met nieuwe tumor-specifieke contraststoffen.

### Deel 4: Klinische toepassing van tumor-specifieke moleculaire beeldvorming voor pancreascarcinoom.

Dit deel van het proefschrift richt zich op het klinische gebruik van tumor-specifieke beeldvorming en beschrijft de eerste klinische studies in pancreascarcinoom patiënten. In de diagnostische fase kan tumor-specifieke PET-CT de detectie van pancreascarcinoom verbeteren en kan het gebruikt worden in het perioperatieve proces om verspreiding van ziekte te detecteren, zowel lokaal als op afstand, en voor het bepalen van een chirurgische strategie zoals getoond in **hoofdstuk 9**. Met gebruik van [18F]FP-R01-MG-F2, gericht tegen integrine αvβ6, werd een verhoogd PET signaal in de tumor verkregen vergeleken met het omliggende pancreasweefsel. In **hoofdstuk 10** worden de resultaten getoond van een klinische studie die gebruikt maakt van multimodale moleculaire beeldvorming voor de intra-operatieve detectie van pancreascarcinoom door gebruik te maken van cetuximab-IRDye800, dat is gericht tegen de epidermale groei factor receptor (EGFR). Door middel van fluorescentie beeldvorming kon tumor worden geïdentificeerd met een significant hoger fluorescentie signaal (MFI) vergeleken met gezonde omliggende pancreasweefsel en ontsteking, met een sensitiviteit van 96.1% en een specificiteit van 67.0%. Daarnaast was het foto-akoestische echo signaal in de tumor 3.7x hoger dan in het omliggende weefsel. In **hoofdstuk 11** is een diepte analyse verricht omtrent de mogelijkheid om tumor-specifieke fluorescentie beeldvorming te gebruiken voor de detectie van micrometastasen in lymfeklieren bij pancreascarcinoom. Met het gebruik van cetuximab-IRDye800 konden peritumorale lymfeklieren macroscopisch worden geïdentificeerd met een sensitiviteit van 100% en een specificiteit van 78%. Daarnaast was het met deze techniek ook mogelijk om occulte tumor foci (< 5 mm) te detecteren met een sensitiviteit van 88%.

### Deel 5: Toekomstige perspectieven van tumor-specifieke beeldvorming

**Hoofdstuk 12** van dit proefschrift richt zich op de toekomst van tumor-specifieke beeldvorming. Om ervoor te zorgen dat deze techniek wijdverbreid zal worden, zal er moeten worden aangetoond dat de patiënt baat heeft bij het gebruik, zoals besproken in dit proefschrift. Om dit te bereiken zijn er grote studies nodig met zorgvuldig gekozen eindpunten. Daarnaast is het van

belang dat de resultaten van verschillende klinische studies vergelijkbaar zijn zodat deze in een breder perspectief geplaatst kunnen worden. In hoofdstuk 12 wordt een gestandaardiseerde manier gepresenteerd voor het beschrijven van de resultaten van klinische studies wat hopelijk zal leiden tot een meer gegeneraliseerde manier van rapporteren. In de toekomst kan dit ervoor zorgen dat de resultaten van verschillende klinische studies samengevoegd kunnen worden en op die manier kunnen bijdragen aan de goedkeuring van nieuwe contraststoffen en camera's.

## Appendices

# List of Publications

**Tummers WS**, Warram JM, van den Berg NS, Miller SE, Swijnenburg RJ, Vahrmeijer AL, Rosenthal EL. Recommendations for reporting on emerging optical imaging agents to promote clinical approval. *Theranostics*. 2018, Accepted.

**Tummers WS**, Willmann JK, Bonsing BA, Vahrmeijer AL, Gambhir SS, Swijnenburg RJ Advances in Diagnostic and Intraoperative Molecular Imaging of Pancreatic Cancer. *Pancreas. 2018 Jul;47(6):675-689*. PMID: 29894417

Gao RW, Teraphongphom NT, van den Berg NS, Martin BA, Oberhelman NJ, Divi V, Kaplan MJ, Hong SS, Lu G, Ertsey R, **Tummers WS**, Gomez AJ, Holsinger FC, Kong CS, Colevas AD, Warram JM, Rosenthal EL. Determination of Tumor Margins with Surgical Specimen Mapping Using Near-Infrared Fluorescence. *Cancer Res. 2018 Jul 2*. PMID: 29967260

Miller SE*, **Tummers WS***, Teraphongphom N, van den Berg NS, Hasan A, Ertsey RD, Nagpal S, Recht LD, Plowey ED, Vogel H, Harsh GR, Grant GA, Li GH, Rosenthal EL. First-in-human intraoperative near-infrared fluorescence imaging of glioblastoma using cetuximab-IRDye800. *J Neurooncol. 2018 Apr 6*. PMID: 29623552

**Tummers WS**, Miller SE, Nutte T Teraphongphom, Adam Gomez, Idan Steinberg, David M Huland, Steve Hong, Sri-Rajasekhar Kothapalli, Alifia Hasan, Robert Ertsey, Bert A Bonsing, Alexander L Vahrmeijer, Rutger-Jan Swijnenburg, Teri A Longacre, George A Fisher, Sanjiv S Gambhir, Poultsides GA, Rosenthal EL. Intraoperative Pancreatic Cancer Detection Using Tumor-Specific Multimodality Molecular Imaging. *Ann Surg Oncol. 2018 Apr 17*. PMID: 29667116

**Tummers WS**, Kimura R, Abou-Elkacem L, Vahrmeijer AL, Swijnenburg RJ, Willmann JK, Gambhir. Preclinical development and validation of multimodal probe for the tumor-specific imaging of pancreatic cancer. *Clin Cancer Res; 2018 Apr 1;24(7):1667-1676*. PMID: 29298796

**Tummers WS**, Farina Sarasqueta AF, Boonstra MC, et al. Selection of optimal molecular targets for tumor-specific imaging in pancreatic ductal adenocarcinoma. *Oncotarget 2017, May 2017*. PMID: 28624798

**Tummers WS*,** Warram JM*, Tipirneni K, et al. Regulatory Aspects of Optical Methods and Exogenous Targets for Cancer Detection. *Cancer Research 2017; 77 (9); 1-10.* PMID: 28428283

Hori SS*, **Tummers WS*,** Gambhir SS. Activatable, Amplifiable Diagnostics for Earlier Cancer Detection. *Nature Biomedical Engineering 2017; Apr 12. News and Views.*

**W Tummers**, J van Schuppen, H Langeveld, J Wilde, E Banderker, A van As. Role of focused assessment with sonography for trauma as a screening tool for blunt abdominal trauma in young children after high-energy trauma. *S Afr J Surg 2016;54(2).* PMID: 28240501

de Geus SW, Boogerd LS, Swijnenburg RJ, Mieog JS, **Tummers WS**, Prevoo HA, Sier CF, Morreau H, Bonsing BA, van de Velde CJ, Vahrmeijer AL, Kuppen PJ. Selecting Tumor-Specific Molecular Targets in Pancreatic Adenocarcinoma: Paving the Way for Image-Guided Pancreatic Surgery. *Mol Imaging Biol. 2016 Apr 29.* PMID: 27130234

**Tummers WS**, van der Vorst JR, Swank DJ. Traumatic rupture of Meckel's diverticulum following blunt abdominal. *Int J Surg Case Rep. 2016;19:8-10.* doi: 10.1016/j.ijscr.2015.12.002. PMID: 26701844

**Tummers WS**, Isaacs S, van As AB. Total body imaging evaluation after initial resuscitation in paediatric trauma. *Injury Extra 44 (2013) 37-38*

## Appendices

# Curriculum vitae

Willemieke Tummers werd op 9 juni 1989 geboren te Enschede. In 2007 behaalde zij cum laude haar eindexamen aan het Gymnasium van het Bonhoeffer College te Enschede, waarna zij Geneeskunde ging studeren aan de Universiteit Leiden. Gedurende haar studie was zij onder andere werkzaam als allocatie medewerker bij Stichting Eurotransplant International. Daarnaast was zij actief lid van de Leidse Studenten Vereniging 'Minerva'.

Voorafgaand aan haar co-schappen verbleef zij 6 maanden in het Red Cross War Memorial Children's Hospital in Kaapstad, Zuid-Afrika. Hier deed zij een klinische stage bij de kinderchirurgie en verrichtte ze haar wetenschapsstage naar de rol van echo FAST bij stomp abdominaal trauma bij kinderen onder begeleiding van prof. dr. A.B. van As en dr. J.C.H. Wilde. Op 24 april 2015 behaalde Willemieke cum laude haar artsexamen. Daarna begon zij als arts-onderzoeker in the Image-Guided Surgery onderzoeksgroep onder leiding van dr. A.L. Vahrmeijer en prof. dr. C.J.H. van de Velde, waarvan de resultaten zijn beschreven in dit proefschrift. Tijdens deze periode verbleef zij 18 maanden op Stanford University in de Verenigde Staten, om onderzoek te doen in het Multimodality Molecular Imaging Lab van prof. S.S. Gambhir.

In december 2017 startte zij als arts-assistent niet in opleiding (ANIOS) bij de afdeling chirurgie van het Groene Hart Ziekenhuis te Gouda. Naast haar promotieonderzoek en werkzaamheden als ANIOS chirurgie heeft zij zich de afgelopen jaren verder verdiept in de organisatorische kant van de zorg door deel te nemen aan de Summer Academy van Medical Business Education, door een optimalisatie project uit te voeren op de polikliniek Vrouwenzorg bij AMC/VUmc met Medical Business Projects en door zich in te spannen als ambassadeur Doelmatigheid van Zorg in het Groene Hart Ziekenhuis.

Appendices

# Dankwoord

Dit proefschrift is het resultaat van een zeer bijzondere en leerzame ervaring. Promoveren doe je niet alleen en ik wil dan ook iedereen die hieraan bijgedragen heeft, in het bijzonder alle coauteurs, hartelijk danken.

First, I want to thank all the patients who participated in the clinical trial at Stanford University, who despite their illness were willing to participate in medical research. Without them, this thesis would not exist.

Prof. van de Velde, beste Professor, dank voor het vertrouwen dat u in mij heeft gehad en het feit dat ik onder uw leiding promotieonderzoek heb mogen doen. Uw uitgebreide staat van dienst is een inspiratie en maakt het een eer om onder u te mogen promoveren. Beste Xandra en Lilian, dank voor alle hulp en ondersteuning die horen bij de praktische kant van promoveren en met name bij Converis.

Dr. Vahrmeijer, beste Lex, dank voor alles! Zonder jou zou onze onderzoeksgroep niet zijn wat het nu is en hadden we nooit zoveel bereikt. Dank voor al het vertrouwen dat je in me hebt gehad en het feit dat je me ook op Stanford altijd gesteund hebt. Ik heb zeer veel bewondering voor hoe jij leiding geeft aan de groep en hoe je altijd van alles op de hoogte bent.

Dr. Swijnenburg, beste RJ, ik ben zeer trots dat ik je eerste promovendus ben en ik weet zeker dat er nog velen zullen volgen. Dank voor onze eindeloze vergaderingen, je geduld, je enthousiasme, de vrijheid die je me gaf en jouw gave om me altijd weer te motiveren! Ik vind onze samenwerking zeer bijzonder en waardeer het heel erg.

Prof. Gambhir, dear Sam, it was a privilege to be part of your lab. I admire your impressive record, and your drive to improve the world for cancer patients is admirable. During our meetings and the labmeetings on Tuesday I have learned so much, and I hope I will always remember and stay inspired by your drive to improve healthcare.

Prof. Rosenthal, dear Eben, thank you for your trust in me and for letting me participate in the Rosenthal Lab. Without you, I would never have been able to perform a clinical trial at Stanford. I admire your motivation, critical view on results and drive to improve the field of fluorescence-guided surgery. Special thanks to Jason, Sarah and Tarn.

Dear George, it was amazing to work with you in the OR. I'm glad we transformed you into a Fluorescent-Believer!

Dear Gambhir Lab, thanks to everyone for making me feel at home. Thanks for the patience when explaining something new, the interesting discussions and for all the help I got from all of you. Special thanks to Richard, Corinne, Aimen and Lotfi.

Green Team, te groot om allemaal te noemen, dank voor een hele mooie tijd. Ik heb zeer veel geleerd en genoten van de samenwerking. Hein, jou wil ik in het bijzonder bedanken voor al je hulp, zelfs toen ik op Stanford zat. Daarnaast natuurlijk mijn J3; Babs, Kim, Marion, Friso, Thomas, en Ruben, heel veel dank voor de gezelligheid! Friso, dank dat je het aandurfde om naar Stanford te gaan en daar al het moois voort te zetten.

Gouden Jaren, ooit begonnen in Leiden als huisgenoten en nu zoveel meer dan dat! Jullie wil ik bedanken voor alle steun, het informeren en het meeleven met mijn promotietraject.

Clubje Chaos, al het plezier dat wij met elkaar hebben gehad en nog steeds hebben, zorgt voor een goede balans tussen plezier en hard werken! Dank daarvoor!

Lieve Alexandra, paranimf Aal, wat ben ik blij dat ik jou in Den Haag heb leren kennen en dat je opeens tegelijk met mij in San Francisco zat! Ik vind het bijzonder dat ik dit feest met jou kan delen.

Lieve mam, dank voor je onvoorwaardelijke steun, je eeuwig luisterend oor en je vertrouwen in alles wat ik doe. Zonder jou was dit nooit gelukt! Lieve pap, dank voor al je interesse en trots bij mijn promotietraject. Jullie hebben samen de basis gelegd voor alles wat ik nu doe.

Lieve Quirijn, Johanneke en Fokkedien, met z'n vieren drijven wij elkaar tot grote hoogte en zonder jullie was ik nooit zo ver gekomen! Dank voor al jullie steun en ik geniet van alles wat we samen doen en hoe we er altijd voor elkaar zijn.

Lieve Twan, als ik iemand veel dank verschuldigd ben, ben jij het wel! Jouw eeuwige steun, je kalmte, liefde, geduld en no-nonsense houding hebben mij vaak geholpen. Ook voor jou was dit promotietraject niet altijd makkelijk maar je bent er altijd voor me geweest, ook toen ik ver weg zat! Heel veel dank!

